Feasibility of applications of waste driven composite for the treatment of paper and pulp industry wastewater

Thesis

Submitted in partial fulfilment of the requirement of the degree of

DOCTOR OF PHILOSOPHY

In

ENVIRONMENTAL SCIENCE & TECHNOLOGY

By:

Sonali

(Roll No. - 901914008)

Under the supervision of:

Dr. Anoop Verma

Professor

Department of Energy and Environment, Thapar Institute of Engineering &Technology
Patiala, India

Department of Energy and Environment

Thapar Institute of Engineering and Technology

Patiala-147004, Punjab, India

Certificate

This is to certify that the thesis entitled "**Feasibility of applications of waste driven composite for the treatment of Paper and Pulp industry wastewater"** that is being submitted by Mrs. Sonali, in the Department of Energy and Environment, Thapar Institute of Engineering and Technology (Deemed to be University), Patiala, India, for the award of the degree of ' **Doctor of Philosophy** ', is a record of the candidate's own independent and original research work carried out by her under my supervision and guidance. The matter embodied in this thesis has not been submitted, in part or full, to any other institute for the award of any degree in other University or Institute.

Supervisor

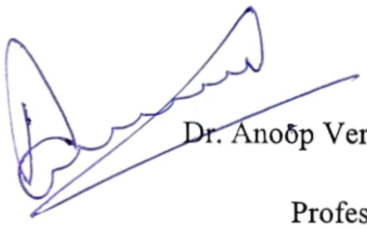

Dr. Anoop Verma

Professor

Department of Energy and Environment

Thapar Institute of Engineering

and Technology, Patiala (147004),

Punjab, India

Declaration

This is to declare that the research work which is being presented in this thesis entitled '**Feasibility of applications of waste driven composite for the treatment of Paper and Pulp industry wastewater**' in partial fulfilment of requirement of the degree of 'Doctor of Philosophy' in Department of Energy and Environment, Thapar Institute of Engineering and Technology, Patiala, India, is an authentic record of my own research work carried out under the supervision of Dr. Anoop Verma (Professor and Head, Department of Energy and Environment, TIET, Patiala, India). Documents, embodied in this thesis, from other researchers' works are duly listed in the reference section. The matter presented in this thesis has not been submitted, in part or full, to any other institute for the award of any degree.

Sonali

(Reg. No. 901914008)

Acknowledgment

I feel truly fortunate to have been surrounded by an abundance of inspiration, guidance, support, and care throughout this academic journey. Reflecting on the many individuals who have helped me along the way is one of the most gratifying aspects of completing this endeavour. I realize that I might not have achieved my goals, at least not so effectively, without their assistance. Looking back on the past five years of my PhD fills me with emotion, and I find it challenging to express my gratitude adequately to everyone who has played a part in this journey.

I would like to express my deepest gratitude to my supervisor, ***Dr. Anoop Verma****, Professor and Head, Department of Energy and Environment, TIET, Patiala, India, for his invaluable guidance throughout my research journey. From helping me select the research title to steering me towards meaningful results, his vast knowledge, motivation, and patience have been instrumental in my progress. His support has empowered me to excel in my research writing, making the study of such a complex topic far more manageable. Dr. Verma has been an outstanding mentor and advisor for my doctoral studies, exceeding all expectations.*

I would like to extend my heartfelt thanks to ***Prof. Padmakumar Nair****, Director of Thapar Institute of Engineering and Technology, Patiala, for providing the necessary infrastructure and support that facilitated the smooth and timely completion of my research work. I also express my sincere gratitude to* ***Prof. N. Tejo Prakash****, Dean of the Research and Development Cell at Thapar Institute of Engineering and Technology, Patiala, for his continuous encouragement and support throughout my research journey at the Institute. I would like to extend my thanks to* ***Prof. Amit Dhir****, of Department of Energy and Environment, TIET who gave access to the laboratory and research facilities. Without his precious support, it would not be possible to conduct this research*

I express my deepest gratitude to my doctoral committee members ***Dr. Shilpi Verma****,* ***Dr. Gaurav Goel, and Dr. Neetu Singh*** *for their constant encouragement, insightful comments, and a keen interest in me at every stage of my research work. I am also thankful to* ***Mr. Suhail*** *and* ***Mr. Gurpreet Singh*** *from the Department of Energy and Environment for their constant cooperation and kind help throughout my Ph.D. work. This research work would have not been completed without the help received from SAI Labs, and CEEMS Patiala.*

My heartfelt thanks to my seniors ***Dr. Palak Bansal***, ***Dr. Jayishnu Singla***, ***Dr. Steffi Talwar***, ***Dr. Ina Thakur, Dr. Rajesh Kondabala*** *for their support and guidance. I would also like to thank my colleagues* ***Mrs. Sheetal Thakur*** *and* ***Mr. Bimalpreet Singh*** *for their cheerful discussion and help. I will cherish all the warmth shown by them.*

I would always remember my fellow lab-mates, ***Ms. Shelly Tiwari***, ***Mr. Gursimranjot Singh Mavi, and Mr. Aman*** *for the fun time we spent together, the sleepless nights that gave us the courage to complete tasks before deadlines, and for stimulating the discussions.*

Life is definitely not always easy, and there are times when challenges seem to come from every direction, but true friends make the journey much smoother. I want to highlight and express my deepest gratitude to my dear friends, ***Mrs. Sheetal Thakur***, ***Dr. Anushka Garg***, *and* ***Mr. Tanveer***, *whose unwavering support has been a cornerstone of my success. Their encouragement, assistance, and companionship helped me navigate numerous obstacles that could have posed major challenges to my research. I also extend my heartfelt thanks to* ***Ms. Diksha Sharma***, ***Ms. Navneet Kaur Ghuman***, ***Ms. Harmeet Kaur***, *and* ***Ms. Anjali Goswami*** *for their invaluable contributions. I would not have reached this point without the selfless support and help of these incredible individuals.*

I want to take a moment to acknowledge the most important part of my journey and my life: my family. My father, ***Mr. Ashwani Kumar***, *my mother,* ***Mrs. Asha Puri*** *and, my brother* ***Mr. Rohan Puri*** *are the true pillars of my strength. Their unwavering support and endless love have shaped who I am today, and I am forever grateful for all they have done. I owe them not only my wonderful present but also the dreams that fill my future. I also want to extend my heartfelt gratitude to my father-in-law,* ***Mr. Kamal Attri***, *my mother-in-law, Mrs.* ***Monika Attri*** *and, my brother-in-law* ***Mr. Ishaan Attri*** *whose unconditional love and support have been a constant source of comfort and encouragement.*

It is hard to find words to fully express the profound sense of gratitude I feel towards my husband, ***Er. Abhishek Attri***. *He has been my rock, my constant source of strength, and the one who believed in me even before I believed in myself. Throughout this journey, his unwavering faith in my abilities has been the light that guided me through the darkest moments. When my enthusiasm faltered, it was his love and encouragement that lifted me up, reminding me of my potential and pushing me to keep going.* ***Abhi***, *you have been my greatest support and my most*

cherished companion, and I am forever grateful for your boundless love, patience, and belief in me. Without you, this journey would have been incomplete.

My deepest gratitude and heartfelt thanks go to my sister, ***Mrs. Neha Kaushal****, for her unwavering love, support, and guidance. She has been a constant source of strength and inspiration, filling my life with countless beautiful memories that I will cherish forever. Her presence has made this journey more meaningful, and I am endlessly thankful for everything she has done for me.*

Above all, I want to express my deepest gratitude to ***Lord Krishna****, whose divine teachings of perseverance, righteousness, and unwavering faith have guided me through the challenges of this journey. His wisdom has been a source of strength and inspiration, helping me stay grounded and focused on my path.*

Lastly, I would like to extend my heartfelt thanks to everyone who, though are not mentioned by name, have supported me in any way throughout this journey. Your contributions, big or small, have been invaluable, and I am truly grateful for each and every one of you.

Sonali

(901914008)

Abstract

The agro-based pulp and paper (P&P) industry produces wastewater with persistent color due to lignin derivatives and other organic compounds, which conventional treatment methods have failed to address effectively. This study explores Advanced Oxidation Processes (AOPs) for decolorizing real industrial effluents. Following circular economy principles, industrial discards such as furnace blast sand (FBS) and foundry sand (FS) were repurposed as substitutes for iron in the synthesis of Fe-TiO_2 composites used in the treatment process. The results highlight AOPs and material reuse as promising strategies for enhancing environmental sustainability in wastewater management.

The present study aimed to reduce the residual color in real wastewater streams from an agro-based P&P industry. Wastewater samples were collected from three distinct stages: the first, known as the UASB stream, which has highest amount of color was sourced from the initial stage involving straw washing and pulping; the second, the I/L or alkali stream, was obtained from the paper-making, chemical recovery, and bleaching stages; and the third, the O/L or outlet stream, was collected after secondary treatment, though it still exhibited significant color. Due to the varying properties and color intensities of these streams, different treatment methods were employed. A two-step process combining coagulation/flocculation, followed by a simultaneous dual process of simultaneous photocatalysis and photo-Fenton, was employed to treat both the UASB and I/L streams effectively. For O/L stream direct application of dual process was successful. Coagulation-flocculation was applied as a pretreatment to reduce the color load that hindered light penetration, making direct application of the dual process (photocatalysis and photo-Fenton) impractical for the UASB and I/L streams. This pretreatment step was necessary to address persistent organics like phenols and lignin derivatives, which were not effectively removed in the initial stage, allowing for enhanced color removal.

For implementation of dual process, a visibly active and low-cost composite was prepared using industrial waste materials, such as FS, FBS and clay mixed in the ratio 1:1:2 respectively. A thin film of TiO_2 was coated on spherical composite beads, enabling photocatalysis, while iron leaching from the composite triggered the photo-Fenton process, effectively combining both effects within a single system.

The study utilized three different reactors Batch, Recirculation, and Once-through to treat three distinct wastewater streams (UASB, I/L, and O/L). Initially, batch-scale experiments were conducted for all streams, optimizing variables such as pH, coagulant dose, bead surface area coverage, and oxidant dose. Under optimized conditions, the dual process achieved 90.62% color removal for the UASB stream in 90 min. 87.17% for the I/L stream in 120 min. and 91.6% for the O/L stream in 60 min.

Further adjustments were made in the recirculation reactor by varying factors such as bead size and flow rate, alongside the previously mentioned parameters. Treating 5L of effluent per stream yielded 89.74% color removal for the UASB stream in 90 min. 84.5% for the I/L stream in 90 min. and 75% for the O/L stream in just 45 min. To optimize the process more efficiently, Design Expert software with Box-Behnken Design (BBD) was used for the I/L and O/L streams. The results showed a close match between predicted and experimental values, confirming the software's effectiveness. Both streams achieved high R^2 values (>0.8), validating the reliability of the model.

The color removal study was also conducted using a once-through reactor approach for all three streams, employing similar operating parameters. Optimized conditions resulted in color removal efficiencies of 94.4% for the O/L stream, 88% for the I/L stream, and 84% for the UASB stream within just 45 minutes. To identify the primary reactive species responsible for color removal, different scavengers were used. The significant reduction of ~40-50% in color removal upon the addition of TBA quencher indicated that hydroxyl radicals ($OH^{\bullet}$) played a major role in the process.

Various characterizations, including SEM, EDS, UV-DRS, and FT-IR, HRTEM, XPS etc. were conducted to verify the catalyst's integrity, confirm the presence of elements, and identify the complexes formed. A key challenge in using composite beads is maintaining the hybrid effect over multiple recycles, which requires continuous iron extraction from the support material while preserving the surface activity of TiO_2. In this study, the composite beads were successfully recycled for over 100 recycles with minimal reduction in color removal efficiency. The hybrid effect, encompassing both iron leaching and TiO_2 activity, remained consistently effective throughout these recycles. Mineralization study was also performed in terms of % COD reduction. Cost analysis was also performed in scale-up trials employing once through reactor.

This study is the first to report the successful implementation of a fixed-bed in-situ dual process using industrial waste materials, along with scale-up trials, for the treatment of real agro-based P&P industry wastewater.

List of Tables

List of Figures

Table of contents

Chapter 1a

Introduction

1.1 a General

The potential for wastewater to contaminate land, groundwater, and surface water resources has increased in recent years, making it a critical and multidimensional environmental concern (Banerjee et al. 2006; Khalid et al. 2018). Recent years have seen a significant increase in the volume and complexity of wastewater generated across various sectors have reasonably increased (Kaur et al. 2017; Kesari et al. 2021). This increased generation of effluents, which consist of a complex mixture of pollutants and chemicals, has emphasized the necessity for a thorough evaluation, proactive control, and inventive remediation approaches (Rashid et al.; Pronina et al. 2015).

The effects of water pollution, stemming from treated and untreated sewage along with industrial effluents have profound effects across a spectrum of vital water sources, including land, groundwater, and surface water (Giri 2021). Sewage, which emanates from residential dwellings and urban areas, frequently transports a combination of various pollutants, including microbes, organic substances, and nutrients (Sidhu et al. 2013). Sewage can cause a chain reaction of ecological problems when it is not handled well or when it is dumped into water bodies without being treated. Microorganisms can grow in number, which can cause oxygen levels to drop, diseases to spread through water, and damage to aquatic environments (Wallender et al. 2014).

In contrast, industrial wastewater presents a more complex and sophisticated problem owing to its varied composition. Various industries emit a diverse range of pollutants, including heavy metals, chemicals, and synthetic compounds, which have the potential to cause significant damage to aquatic environments (Rebelo et al. 2014; Carolin et al. 2017). The repercussions manifest themselves across various levels, encompassing both immediate harmful impacts on aquatic organisms and the process of bioaccumulation within the food chain, ultimately affecting human well-being and entire ecological systems (Ebele et al. 2017; Saravanan et al. 2017).

Wastewater is a complex mixture of residuals from numerous industrial sectors, each leaving an impression on the aquatic environment (Rodriguez-Narvaez et al. 2017; Saravanan et al. 2017). The pharmaceutical sector releases many pharmaceutical chemicals into wastewater, demonstrating our dependency on medical developments (Gadipelly et al. 2014). Textile and paper industries contribute with dyes, solvents, and pulp by-products, adding

vibrant hues and fibrous remnants to the water tapestry (Tarlan et al.; Pang and Abdullah 2013; Haile et al. 2021). Organic matter and nutrients are discharged by food processing plants, disrupting the balance of aquatic ecosystems(Carey and Migliaccio 2009). Meanwhile, mining activities discharge minerals and silt, altering the quality and composition of the water. Various industries shape the complex composition of wastewater in this dynamic interplay, emphasizing the importance of sustainable practices and technical advancements to reduce their environmental footprint (Younger and Wolkersdorfer; Banerjee et al. 2020)

Particularly textile and P&P industries are a major cause of concern in terms of freshwater consumption & wastewater generation (Abd El-Sayed et al. 2020; Kishor et al. 2021). Concerns about treated wastewater from the P & P industry include chemical residues, high organic matter that depletes oxygen, nutrient imbalances that lead to eutrophication, suspended solids that harm marine life, and color/turbidity that affect the aesthetic look of water (Thompson et al.; Kamali and Khodaparast 2015). In the same way, treated wastewater from the textile industry raises concerns about dye and chemical residues that stay in the water, the color of the water and how it looks, the presence of heavy metals, pH imbalances that hurt aquatic life, and the amount of salt in the water and land (Holkar et al. 2016; Islam and Mostafa 2018).

In the textile industry, dyes are the chemical molecules that give clothes their color. These dyes are frequently complex organic compounds with specialized chemical structures that enable them to bind with textile fibers. Azo dyes, anthraquinone dyes, and phthalocyanine dyes are some of the most commonly used dye groups in the textile industry. Azo dyes containing nitrogen-nitrogen double bonds (azo groups) are frequently utilized for their vibrant and diverse colors (Alinsafi et al. 2007; Harrelkas et al. 2008). However, they can be hazardous since they degrade into aromatic amines, some of which are known to be carcinogenic. Anthraquinone dyes, derived from anthraquinone molecules, are known for their excellent colorfastness' but can be challenging to remove from wastewater. Phthalocyanine dyes, based on phthalocyanine complexes, are valued for their intense blue and green colors but can also pose environmental challenges due to their complex chemical structures (Tanaka et al.; Can et al. 2016).

In the P&P industry, lignin is a significant contributor to the residual color in wastewater (Dixit et al. 2019). Lignin is an essential constituent of wood and a complex organic polymer that provides structural support to plant cell walls. During the pulping process, which is used to separate the cellulose fibers for papermaking, lignin is partially removed from the

wood fibers. However, some lignin remains in the pulp and can impart a dark color to the paper product (Veluchamy and Kalamdhad 2017). The remaining lignin undergoes more degradation, forming colored molecules referred to as chromophores when the pulp is bleached to produce white paper. The dark brown water coloring from these chromophores is unattractive aesthetically and unacceptable environmentally. Moreover, if untreated, they may lead to the death of aquatic organisms through toxicity and cause oxygen depletion in water bodies. Various methods are employed in dealing with lignin-related color in wastewater from the pulp and paper industry. One such method is biological treatment whereby microorganisms are used to decompose organic compounds including lignin into simpler less colored materials. Chemical treatment is also a viable option which entails the use of chemicals like hydrogen peroxide or ozone to break down and oxidize chromophores thus reducing wastewater coloration (Hubbe et al. 2016a; Abhishek et al. 2017). Enzymatic treatment like (lignin peroxidase, manganese peroxidase, and Laccase) have shown its ability to degrade lignin and its derivatives under milder conditions than typical treatment (Sigoillot et al. 2012; Cagide and Castro-Sowinski 2020).

In addition to the color problem, the P&P industry has a major cause for concern due to its substantial water consumption. As much as 40-60 cubic meters are used for every metric ton of paper produced by this sector (Sridhar et al. 2011). This can exhaust local water sources thereby resulting in huge amounts of wastewater, which needs to be treated. To deal with this challenge, industries are implementing closed-loop systems, water-saving technologies, and sustainable pulping processes to minimize the amount of water used and its impact on the environment (Pokhrel and Viraraghavan 2004; Asaithambi 2016).

Keeping this in view, the present study is oriented toward the treatment of selected wastewater streams from the P&P industry using advanced techniques. The sole purpose is to explore the feasibility of recycling any one of these waste streams to visualize the zero liquid discharge mandate of the selected paper industry. Almost all the wastewater streams in the selected P&P industry had light to intense color present in them. Thus, based on the inputs from the industry, three different streams were targeted for the study i.e., the Up-flow anaerobic sludge bioreactor (UASB) stream, Alkali (I/L) stream, and, the outlet (O/L) stream. UASB is a highly colored but low volume stream whereas I/L has less color than UASB but more in volume whereas O/L has much lesser color but very high wastewater volume. We proposed different schemes for different streams like UASB and I/L have very intense colors so the Advanced Oxidation Process (AOP) cannot be applied directly as the dense color hinders the

light entrance inside the rector. So UASB and I/L have gone through a pre-treatment to remove some amount of color i.e., coagulation/flocculation followed by AOP. A detailed explanation of the whole process is given in Chapter 1b.

1.2 a Scenario of the P&P industry worldwide:

The P&P industry is one of the biggest in the world, which helps the world economy in a big way. It has a stronghold in North America, Northern Europe, and East Asia, where strong donations from companies are especially noticeable. Also, Latin America and Australasia have become important hubs for many P&P industries. The amount of paper and paperboard made around the world has risen to more than 400 million tonnes (Chauhan and Meena 2021). There is an interesting trend in how different fibers are used to make paper: 55% come from recovered fibers, 42% come from virgin fibers, and 3% come from other fibers (Monte et al. 2009). At the same time, the Per Capita Consumption number, which measures how much paper each person uses in kilograms per person per year, becomes an important way to measure how society is changing. Fig. 1.1a vividly outlines the per capita consumption of paper in different regions (Chauhan and Meena 2021).

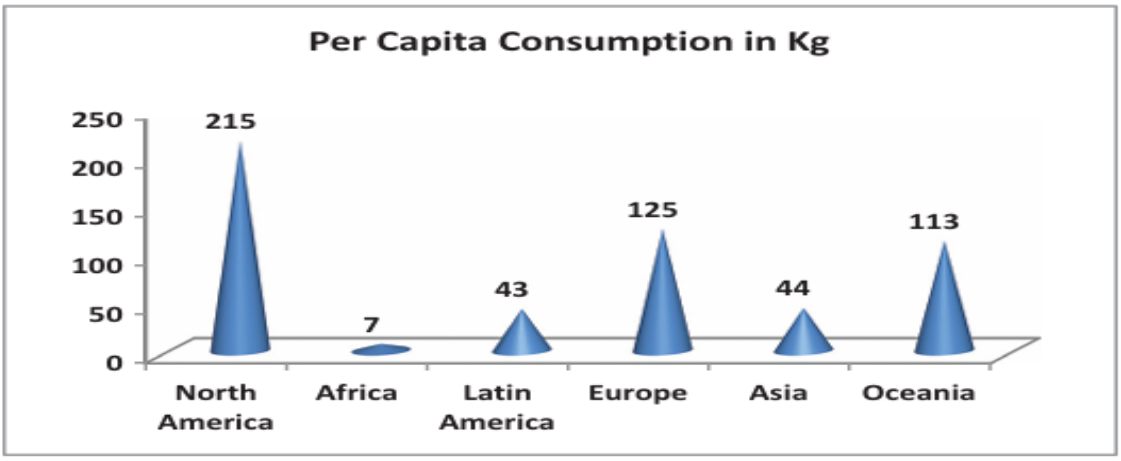

Fig. 1. 1 a Per capita consumption of paper by region (Chauhan et, al., 2020)

1.3 a History and Scenario of the P&P industry in India:

The Indian P&P industry has emerged as a versatile and specialized participant, giving rise to a variety of paper variations specifically designed for a wide range of applications. These include watermark paper, filter paper, drawing sheets, and various more specialized forms. The paper industry comprises a diverse array of products, including paper bags, paper diaries, handmade paper boxes, paperboard, and newsprint. 3.7% of global paper production is contributed by the Indian paper industry. With over 600 paper mills with a capacity of 22

million tonnes and a utilization rate of 80%, India's market grew at a compound annual growth rate of 8% from 2011 to 2016, outpacing global competitors by 1%. The utilization of raw materials consists of 88% recycled fiber (RCF), 23% wood fiber, and 9% agro-based fiber. 53% of the sector's produce is packaging-grade, 38% is waste-grade, and 8% is newsprint-grade. Notable elements include writing/printing paper and paperboard. India's market is significantly more fragmented than those of the United States, Indonesia, and China, with ITC holding 4.1%, JK Paper 2.6%, and TNPL 2.4% of the market. (Kujur and Kumar Kujur; Hubbe et al. 2009; Abdul Khalil et al. 2014; Lieder and Rashid 2016).

1.4 a Classification of the Pulp and Paper Industry

Based on raw materials the Indian P & P industry is divided into 3 major categories i.e., wastepaper-based, wood-based, and agro-based accounting for 30%, 37%, and 33% respectively (Kong et al. 2016; Rogers et al. 2018) as shown in Fig. 1.2a.

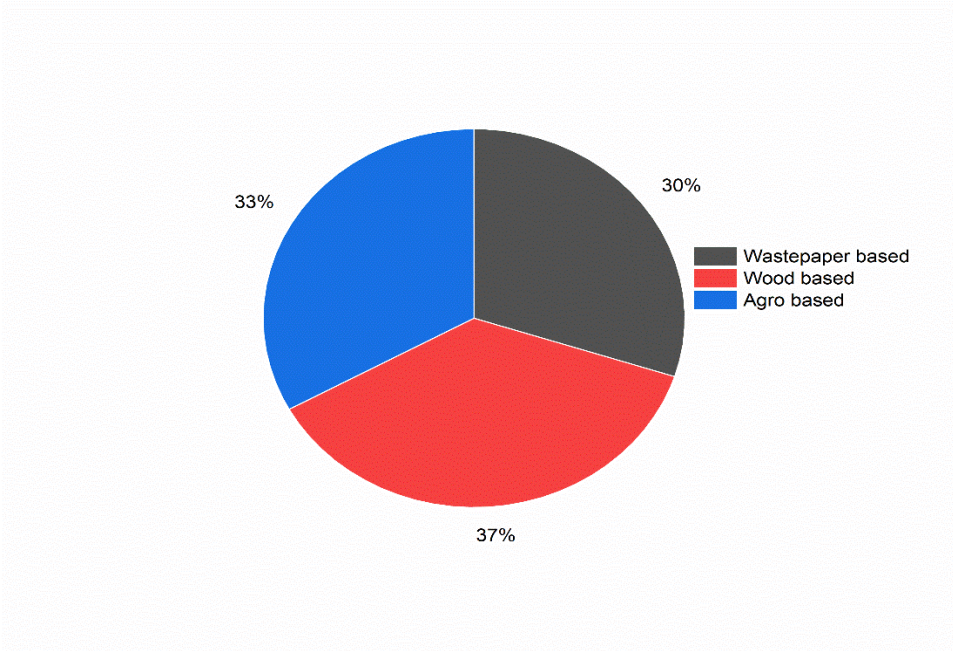

Fig. 1. 2 a Different category of the paper industry based on raw material

1.5 a Raw material for paper-making

Mainly two types of sources are used for papermaking i.e., wood-based and agro-based.

1.5.1 a Wood-based large sources

- **Softwoods** like Pine, spruce, and fir are used commonly due to their long fibers and strong properties making them suitable for products like packaging materials and printing papers.

- **Hardwoods** like eucalyptus, birch, and maple are ideal for fine sheets and tissues because of their smoother surface and shorter fibers.

1.5.2 a Agro-based sources

Plant leftovers that are not intended for consumption, such as sugarcane bagasse, wheat straw, rice husks, and maize stalks, have the potential to be utilized in the production of pulp (Ioannidou et al. 2009; Rajput et al. 2016). Agro-based fibers offer a viable alternative to conventional wood-based sources, hence facilitating the promotion of sustainable resource use (Loh et al. 2013; Quereshi et al. 2022).

1.6 a Paper manufacturing processes

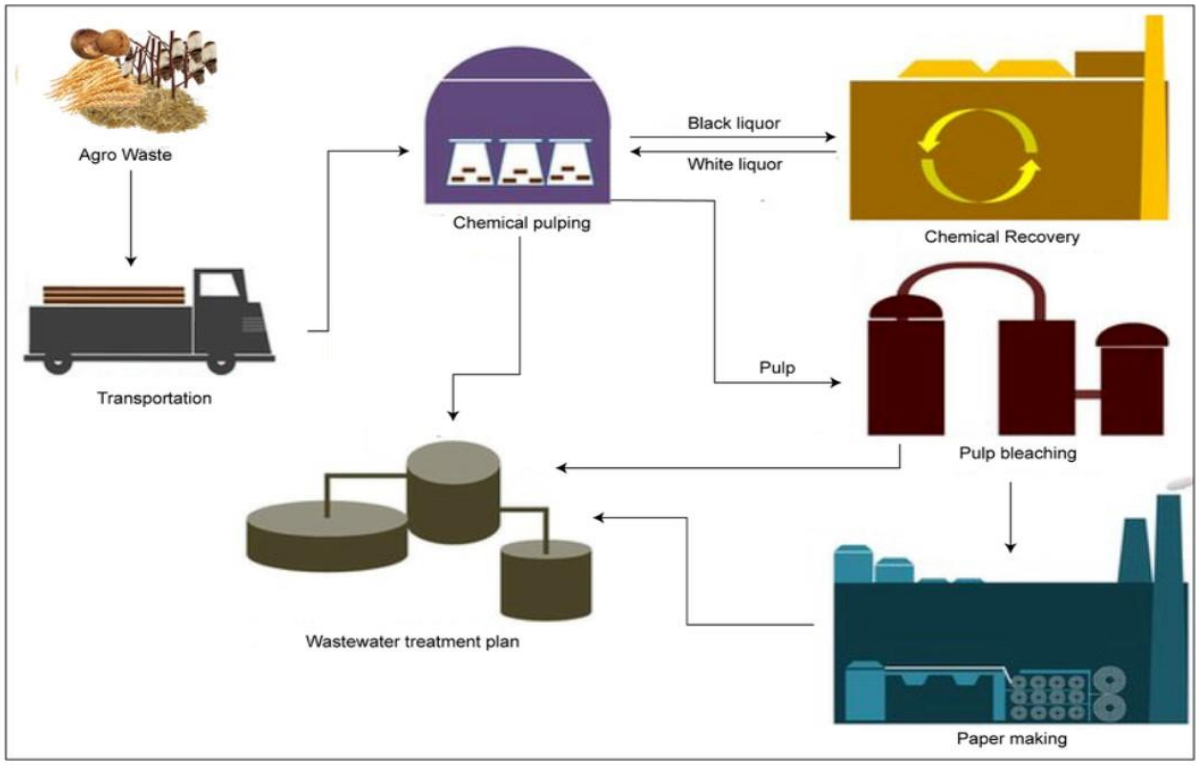

Fig. 1. 3 a Process of Pulp processing and paper making in the P&P industry (Gupta et al. 2022)

In the realm of paper production, the path begins with the preparation of raw materials, continues with the creation of pulp, and concludes with the complex process of paper manufacturing. This intricate procedure begins with pulping, a stage that can be accomplished mechanically or chemically. Pulp preparation involves a variety of processes, including slushing, preliminary mechanical treatments, amalgamation of pulps with varying properties,

and the addition of additives and fillings to achieve the desired paper qualities. The precise techniques employed are tailored to the intended paper quality. Pulping is the key step in transforming timber and other lignocellulosic materials into a fibrous mass. This phase entails debarking, a process that eliminates contaminants such as soil, dirt, and bark from the initial timber materials, resulting in smaller plant fibre-containing chips (Ali and Sreekrishnan 2001). Pulping is the first stage in the papermaking process and the source of the raw material as shown in Fig. 1.3a. Sadly, it is also a significant source of contamination in the overall paper production procedure (Gavrilescu et al. 2008).

1.6.1 a Pulping techniques

Let's now explore some of the various pulping techniques that are widely used in the sector:

- **Mechanical Pulping:** With this method, wood fibers are physically broken down by machines, like grinding or polishing. The main goal is to separate the fibers while keeping the length of each one. But mechanical pulping makes the fibers shorter, which can make the paper less strong. Groundwood mechanical pulping and refiner mechanical pulping are two popular types of mechanical pulping.
- **Pulping by chemicals:**
- **Kraft Pulping:** In this process, chemicals, heat, and pressure are used to separate the lignin from the wood fibers. It makes strong fibers that can be used in a wide range of types of paper.
- **Sulphite Pulping:** Like Kraft pulping, sulphite pulping uses chemicals to get rid of lignin, just like Kraft pulping. It makes brighter pulp, which is often used to make specialty papers.
- **Soda Pulping:** In this method, lignin is broken down with a solution of sodium hydroxide (soda). It makes pulp that isn't very strong, but it can be used to make some kinds of paper.
- **Chemi-Thermo-Mechanical Pulping (CTMP):** To break down fibers, this method uses a combination of chemical treatments, heat, and mechanical refining. It finds a middle ground between mechanical and chemical pulping to make stronger fibers.
- **Organosolv Pulping:** This method is good for the environment because it uses organic solvents to break up the lignin and split the fibers. Compared to other chemical methods, it gives you more power over the process.
- **Hybrid Pulping:** This method uses different ways of pulping to get the best fiber properties for different types of paper. It tries to find a good mix between strength, quantity, and quality.

- **Non-Wood Pulping:** Paper can also be made from things other than wood, like bamboo, bagasse, and straw. Depending on how these materials are made, there may be different ways to turn them into pulp.

These diverse pulping processes accommodate diverse paper needs by harmonizing factors such as fiber strength, paper quality, and environmental concerns. The industry must select the optimal pulping method based on the desirable paper characteristics and the overall sustainability objectives (Amândio et al. 2022).

1.7 a Wastewater scenario of the P&P industry

P&P industries contribute significantly to the economics of numerous nations, including the United States, Canada, India, and Portugal. Nonetheless, the P&P industry is widely acknowledged as one of the most environmentally polluting industries (Sattler et al. 2004). These mills primarily engage in tasks including preparing raw materials, pulping, bleaching, and manufacturing paper, all of which require a lot of water and energy. Among these processes, pulping, which involves removing lignin and fibers to produce paper is particularly considered the most polluting stream in paper making. The bleaching processes used in paper mills are intended to whiten the pulp and improve its brightness. These P&P manufacturing processes consume a lot of water, which causes wastewater to be produced that is then contaminated with organic substances. This pollution further highlights the ecological challenges posed by the industry(Han et al. 2021).

The P&P mill, which ranks third globally in terms of water use, produces a variety of wastewater types with varying properties, depending on the method used to make the P&P and the raw materials used. According to (P. Ravichandran et. al., 2018), this sector produces roughly 40 m^3 of wastewater for every ton of paper produced, with significant pollutant loadings of 90–240 kg of suspended particles per ton of paper, 85–370 kg of biochemical oxygen demand per ton of paper, and 500–1100 kg of chemical oxygen demand per tonne of paper. Paper-making processes have different shares of water consumption as shown in Fig. 1.4 a.

1.7.1a Water consumption in the Pulp and Paper Industry for various processes:

- **Pulping:** Water is used to break down wood fibers and separate them from other parts like lignin and chemicals. Different ways of making pulp, like kraft, sulphite, and mechanical, need different amounts of water.

- **Bleaching:** The bleaching process uses water to remove color and contaminants from the pulp. This procedure may entail several phases, each of which requires a substantial volume of water.
- **Papermaking:** Pulp needs water to make paper sheets. Papermaking requires water for dewatering, pressing, and drying.
- **Cooling and Heating:** Water is utilized for heating during some production steps as well as cooling machinery and equipment.

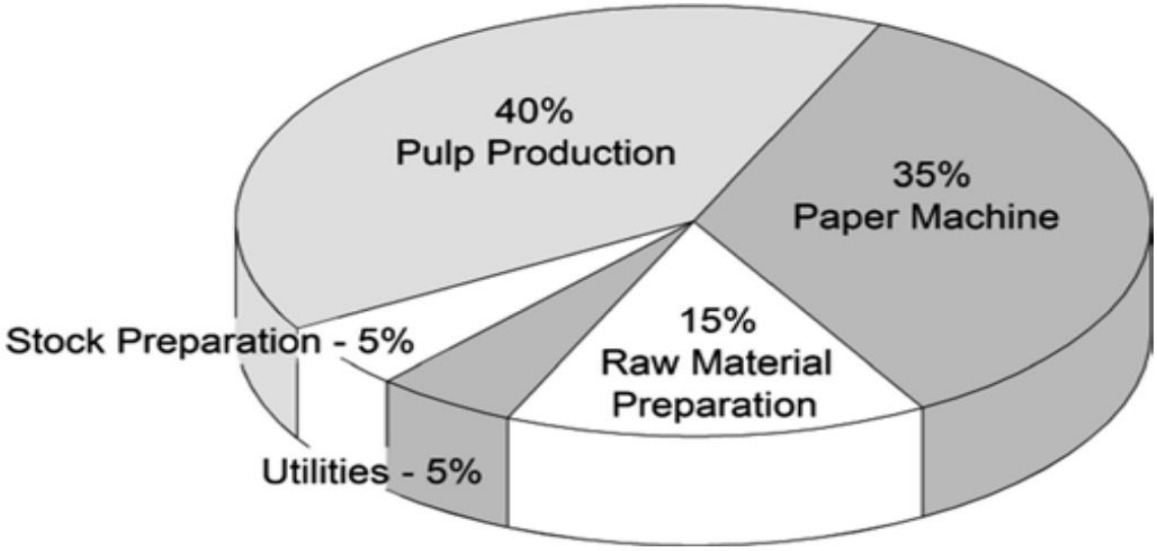

Fig. 1. 4 a % water consumption by various paper-making processes (Olejnik 2011)

1.7.2 a Wastewater generation:

The pulping process produces a lot of black liquor or wastewater. This effluent contains pulping by-products like lignin and chemicals. After that the bleaching process, dewatering, and washing also release wastewater. Effluents from cooling and cleaning machinery may contain oils and greases. The detailed flow chart of wastewater discharge from different processes is given in Fig. 1.5 a. Table 1.1 a shows discharge norms/standards acc. to CPCB for large-scale P&P industry.

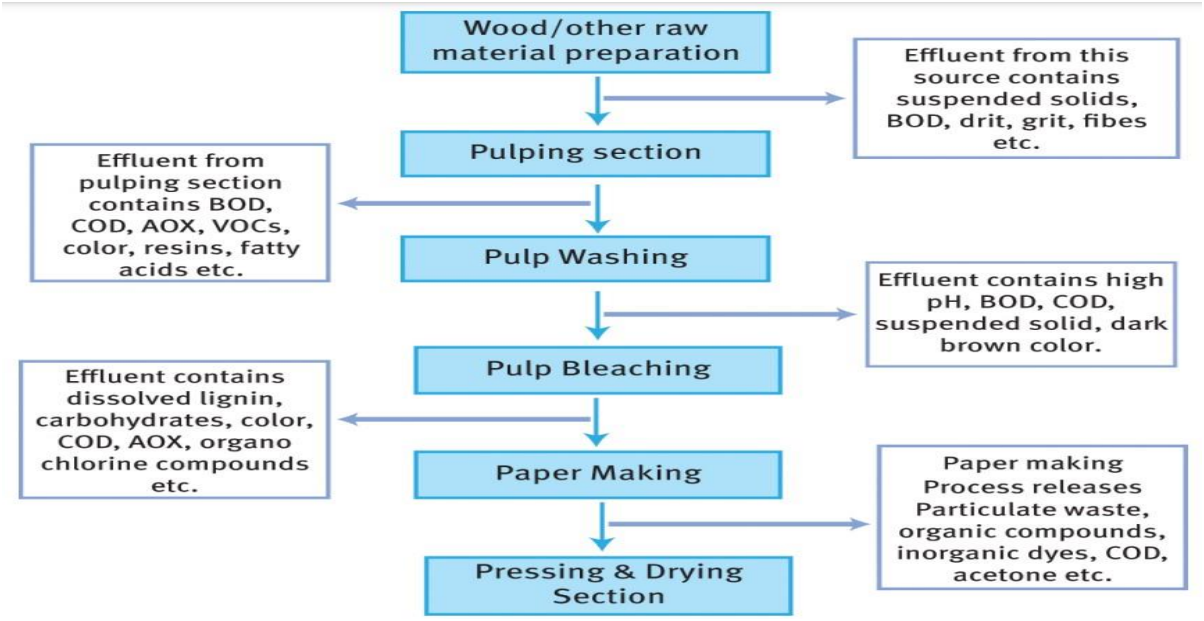

Fig. 1. 5 a Wastewater discharge from different sections in paper making process (Ram et al. 2020)

Table 1. 1 a Discharge norms/standards acc. to CPCB for large-scale P&P industry

Parameters	Concentration (mg/L, except pH)
pH	7.0-8.5
BOD [3 days at 27 ºC]	<30
COD	<300
Suspended Solids	<500

Source: CPCB, New Delhi

1.8 a Wastewater treatment system

A wide range of biological and chemical treatment strategies have been developed globally for the management of P & P mill wastewater. These approaches encompass aerobic processes like the activated sludge method, anaerobic treatments, coagulation-flocculation processes, ozonation, electrochemical treatments, and photocatalysis, as stated by (Assalin et al. 2009). Nonetheless, it is critical to recognize that aerobic biological activities are highlighted by high energy consumption and the production of significant biomass. Although successful, anaerobic biological processes may be sensitive to shock loading, necessitating further treatment before discharge. Notably, the activated sludge process is ill-suited for treating P&P industry wastewater due to the elevated temperature and complex organic compounds, which provoke significant settling issues such as bulking, as reported by(Hubbe

et al. 2016b). Although biological methods are effective and inexpensive, they require a lengthy hydraulic retention period, a big area, a high energy demand (for aeration), and a large amount of generated sludge as stated by (Davarnejad and Nasiri 2017). Physical/chemical approaches, on the other hand, have the disadvantage of high reagent costs and low COD elimination. Chemical precipitation of dissolved materials (alum, ferric chloride, aluminium chloride, ferrous sulphate, and ammonium aluminium sulphate) has the disadvantage of causing dewatering and disposal issues with the precipitated sludge. Additionally, the application of chemical treatment has the potential to result in secondary contamination as a consequence of the presence of chemical additives. Hence, the introduction of AOPs has demonstrated considerable promise as a viable alternative owing to its significant capability for the complete degradation of numerous persistent pollutants (Rey et al. 2012; Verma et al. 2023). The efficacy of advanced oxidation methods (Neha et al. 2020)is heavily dependent upon the initial potency and composition of the wastewater. In P&P the color persistence in secondary treated effluent is the key issue as that effluent cannot be reused in paper-making processes leading to wastage of so much water. Additionally, P & P industry wastewater poses a substantial and pressing threat to both human health and the integrity of receiving water bodies. The unregulated outflow of untreated wastewater raises significant environmental concerns, captivating the need for comprehensive treatment. In addition, it is necessary to establish recycling and reusing treated effluent systems to reduce the rising demand for freshwater resources (Okoro et al. 2023).

1.9 a The rationale of the study

The primary purpose of this study was to address the abatement of color from the wastewater generated by pulp and paper mills, intending to look for its feasibility that makes it suitable for reuse within the manufacturing process. Various studies have been conducted by the researchers where individual process was used for wastewater treatment in terms of color or organic compounds removal. Single AOPs such as photo-Fenton and photocatalysis have various success stories regardless of that these processes possess inherent encounters and shortcomings related to efficiency and process economics. The solar photo-Fenton process is pH-dependent and has a reduced quantum yield, whereas the solar photocatalytic process also has efficiency limitations. Given the aforementioned shortcomings, there is a compelling rationale for integrating these two processes rather than relying on them individually. By optimizing the combined treatment system, it becomes possible to achieve the desired treatment objectives within a shorter reaction time. Considering all the drawbacks, the present study has

a unique quality in that both photocatalysis and photo-Fenton work simultaneously as a single system, are inexpensive, offer no drawbacks, and treat the color from wastewater in a very short time. However, AOPs are often expensive, and one of the barriers to the widespread adoption of this treatment procedure in developing nations is its high operational costs, such as high energy consumption and chemical reagents. This study adopted the use of solar light for treatment and industrial waste materials to fabricate the composite to make the process economical. Different reactors were used to check the feasibility of the study in batch, recirculation(Thakur et al. 2021), and once-through mode. Additionally, the concept of circular economy was also followed as our study incorporated the waste industrial materials as an alternate source of iron required to drive the photo-Fenton process. A combination of conventional and modern techniques is used in the study i.e., coagulation/flocculation as a pretreatment to remove the stout color from some highly colored streams followed by AOP.

1.10 a Glimpse of Chapter 1b

The next chapter explores the treatment processes employed in the selected pulp and paper industry to tackle the issue of color in wastewater. The study thoroughly analyses different techniques used, such as physical, chemical, and biological methods, and emphasizes their efficacy in eliminating color-causing compounds. The chapter provides an in-depth analysis of various wastewater streams that are notorious for their color-related problems. offering a comprehensive overview of each stream's specific characteristics and challenges. Furthermore, it discusses the innovative approaches and technologies implemented to tackle color-related problems.

Chapter 1 b

1.1 b General background of treatment technologies for P&P industry wastewater

The wastewater treatment of the P&P industry encompasses a range of approaches, each exhibiting distinct levels of efficacy and limitations. Implementing biological treatment methods, while exhibiting positive environmental attributes, encounters obstacles related to microbial susceptibility and prolonged retention periods (Ashrafi et al. 2015; Haq et al. 2020). Chemical treatments work, but prices and how to handle the leftover chemicals are a worry (Toczyłowska-Mamińska 2017). Even though adsorption methods work well, they have problems like media saturation and complex regeneration (Chkirida et al. 2021). Membrane filtration works, but it has problems with fouling and costs a lot to run. Physical treatments like coagulation-flocculation have potential, but they need to be carefully optimized and are hard to handle because they create sludge (Saraswathi and Saseetharan 2012). Biological oxidation encounters limitations in cases where the incoming water contains substances resistant to biodegradation or proves inhibitory or toxic to microbial systems (Ram et al. 2020). In the broader context of wastewater treatment in the P&P industry, integrated approaches require intricate system design and advanced monitoring. Balancing effectiveness, cost considerations, and environmental impact underscores the need for a tailored approach to address the issue of P&P industry wastewater (Boguniewicz-Zablocka et al. 2020; Mainardis et al. 2024).

1.2 b Advanced treatment processes

Given the heightened environmental consciousness and adherence to international rules, there is more and more research going on to come up with new, cleaner technologies that work better and faster for wastewater treatment. In addition to biological processes, several advanced treatment methods encompass supercritical water oxidation (SWO) (Yabalak and Gizir 2020), electrochemical oxidation (Wang et al. 2007), wet oxidation (Zhang et al. 2020a), adsorption utilizing activated carbon (Temmink and Grolle 2005), and chemical oxidation. In the domain of P&P industry wastewater treatment, Advanced Oxidation Processes (AOPs) emerge as a promising option (Merayo et al. 2013; Gholami et al. 2017). Their efficacy in degrading complex organic compounds makes them a viable option for comprehensive wastewater treatment. AOPs excel in addressing the diverse range of contaminants present in P&P industry effluents. The oxidation process in AOPs is known for its efficiency in reducing organic pollutants and improving overall water quality. While challenges such as energy requirements

and by-product generation may exist, the inherent potency of AOPs in treating P&P industry wastewater positions them as a noteworthy choice, especially when considering their ability to achieve high levels of contaminant removal and enhance the environmental sustainability of the treatment process (Deng and Zhao 2015). The following is a summary of various advanced treatment technologies that are currently available for the treatment of effluents from the P&P industry.

1.3 b Overview of Advanced Oxidation Processes

AOPs have emerged as strong contenders in the field of wastewater treatment, with a specific focus on tackling bio-recalcitrant contaminants. AOPs are oxidation methods that hinge on the generation of reactive species, notably $OH^{\bullet}$, to effectively break down organic pollutants (Esplugas et al. 2002; Comninellis et al. 2008). Almost all AOPs rely on the powerful oxidation potential of hydroxyl radicals, ultimately resulting in the oxidation and mineralization of refractory pollutants. An exceptionally promising avenue for achieving nearly complete degradation of hazardous organic compounds involves the utilization of AOPs. These processes, as defined by (Glaze et al. 1987), encompass water treatment methods conducted at near-ambient temperature and pressure. Additionally, AOPs stand out as particularly promising for addressing color removal in wastewater, showcasing their efficacy in degrading bio-recalcitrant organic compounds. The efficacy of AOPs is substantiated by an extensive body of literature that primarily examines their utilization in the elimination of various contaminants, including dyes, phenols, pesticides, pharmaceuticals, polymers, and chlorophenols(Stasinakis et al. 2008; Oller et al. 2011). AOPs have demonstrated significant potential in treating real wastewater from a variety of industries, including pharmaceuticals, textiles, P&P mills, and others (Agulló-Barceló et al. 2013). In these applications, however, the question of whether to use AOPs as stand-alone procedures or in conjunction with conventional methods persists. In practical situations, it is frequently recommended to use AOPs as a pre-treatment before biological processes or as a tertiary treatment for optimal results (Oller et al. 2014).

AOPs can be classified into different categories based on their underlying mechanisms. These categories include photochemical oxidation processes, which involve photo-ozonation (UV/O_3), semiconductor-based photocatalysis (metal-oxide/UV), and photo-Fenton ($UV/H_2O_2/Fe^{2+}$) and chemical oxidation processes, including ozonation (O_3, O_3/H_2O_2) and Fenton (H_2O_2/Fe^{2+}), as illustrated in Fig.1.1 b Among these methods, semiconductor

photocatalysis using metal oxide has garnered significant attention over the past two decades due to its (a) cost-effectiveness, (b) low toxicity, (c) environmental friendliness, (d) ease of modification through doping, and (e) ability to sustain prolonged use without a substantial decrease in photocatalytic activity(Chatterjee and Dasgupta 2005; Chan et al. 2011). TiO_2(Saroj et al. 2020), WO_3, ZnO, MoO_4, and VO_4 are only a few examples of metal oxides that exhibit impressive photocatalytic capabilities (Chakrabarti and Dutta 2004; Guo et al. 2020). Because of its high catalytic activity, low cost, chemical stability, and non-toxic nature, TiO_2 has been examined more than any other photocatalyst (Saien et al. 2009).

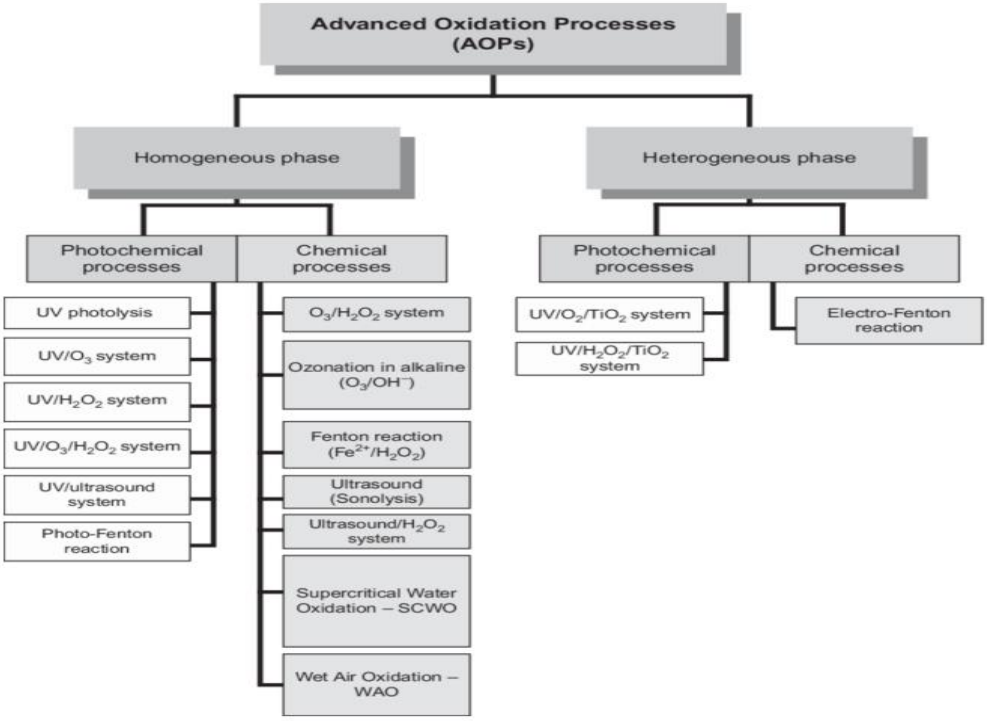

Fig. 1. 1 b Classification of AOPs (Biń and Sobera-Madej 2012)

1.3.1 b Homogeneous Advanced Oxidation Processes

When using homogeneous AOPs (single-phase systems) to remediate wastewater, an oxidant is used to generate radicals in the presence of ultraviolet light, which then attack organic pollutants to initiate oxidation. The effectiveness of the system depends on the production of powerful oxidant species, specifically hydroxyl radicals capable of oxidizing almost all organic pollutants. Key processes employed for homogeneous degradation include Hydrogen peroxide (UV/H_2O_2), Ozone (UV/O_3), Hydrogen peroxide and Ozone ($UV/H_2O_2/O_3$), and the Photo-Fenton system (Fe^{3+}/H_2O_2). UV radiation can be used in a variety of ways, but direct photolysis happens only when the targeted pollutant absorbs incident light

efficiently. However, in the case of UV/ozone and UV/hydrogen peroxide, this level of action is not replicated (Saien et al. 2009; Maniakova et al. 2020).

1.3.2 b Heterogeneous Photocatalysis

Heterogeneous photocatalysis gets its name from the fact that several phases or states of matter are involved in the catalytic process. In contrast to homogeneous catalysis, which uses a catalyst in the same phase as the reactants, heterogeneous photocatalysis uses a solid-phase catalyst, such as TiO_2, in conjunction with liquid-phase contaminants in wastewater (Gaya and Abdullah 2008; Dong et al. 2010). In the domain of actual wastewater treatment, heterogeneous photocatalysis is an innovative and promising approach. Under the influence of light, a solid-phase catalyst, typically comprised of semiconducting materials such as TiO_2, is used to facilitate the removal of color by the degradation of organic and inorganic pollutants in wastewater. The catalyst absorbs photons, thereby generating electron-hole pairs that promote redox reactions, which ultimately result in the removal of contaminants. This method has several advantages for wastewater treatment, including its ability to target a broad spectrum of pollutants and its relative simplicity of implementation (Cleveland et al. 2014; Luo et al. 2021).

In the context of environmental applications, TiO_2 photocatalysis is widely used for the degradation of airborne and waterborne organic and inorganic pollutants. TiO_2 catalyzes the formation of extremely reactive oxygen species, such as hydroxyl radicals ($OH^{\bullet}$) and superoxide ions ($O^{2\bullet-}$), when exposed to UV light(Ochiai and Fujishima 2012). These organisms possess potent oxidative properties, facilitating the transformation of contaminants into less hazardous metabolites. The key advantage of TiO_2 photocatalysis lies in its effectiveness against a broad spectrum of pollutants, including organic dyes, pesticides, and microbial pathogens. Additionally, TiO_2 is known for its stability, non-toxicity, and abundance, making it an environmentally friendly choice (Lee and Park 2013). The mechanism of TiO_2 photocatalysis is shown in 1.2 b.

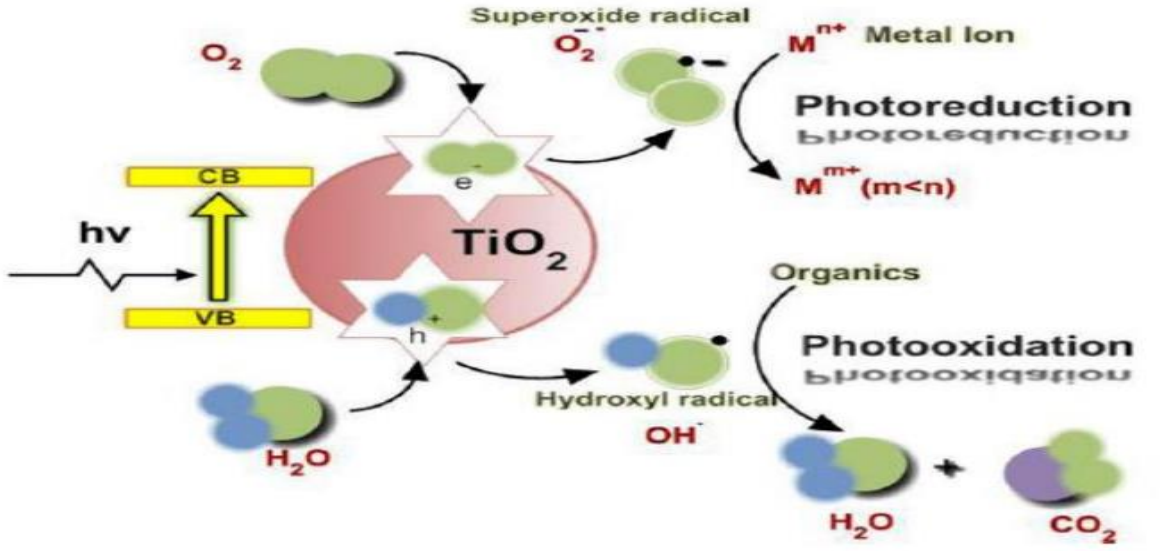

Fig. 1. 2 b Mechanism of TiO_2 photocatalysis [And et., al., 2010]

1.4 b Application of fixed bed pilot-scale photocatalytic reactors

The effective implementation of AOPs is critical for the commercialization of wastewater treatment. Scaling up conventional reactors is relatively simple compared to the challenges involved in scaling up solar reactors(Bansal et al. 2007). However, difficulties such as catalyst contact, mixing, flow patterns, temperature management, and mass transfer may hinder potential wastewater treatment process scale-up. Optimizing the exposed surface area becomes crucial in addressing these problems and ensuring the stable dispersion of sunlight within the reactor. Both axial and radial scale-up are regarded as critical in reaching this goal. Numerous research on the scale-up process employing TiO_2, notably in suspension form, have been undertaken. Annular photoreactors, photocatalytic Taylor vortex reactors, parabolic trough collectors (PTCs), and compound parabolic collectors (CPCs) are all being studied (Feitz et al.; Zayani et al. 2009).

A variety of experimental configurations at the pilot scale have been extensively recorded to investigate the photocatalytic removal of pollutants. The aforementioned technologies include a concentrating falling film reactor (Mehrjouei et al. 2013), PTCs (Ahmad et al. 2016), shallow pond reactors (Mozia et al. 2012), CPCs (Sordo et al. 2010; Alrousan et al. 2012), tubular reactors (Saran et al. 2018), falling film photoreactor, slurry bubble column reactor (Akach et al. 2020), thin-film reactor (Khan et al. 2012), and flat packed-bed reactors (Borges et al. 2021). However, the application of fixed bed catalysis at the field scale has not gained much traction. This lack of appeal may be attributed to concerns regarding the stability

and durability of the supports and catalysts. Additionally, mass transfer limitations and extended treatment times act as barriers to the scalable implementation of the process. The prolongation of treatment time and heightened energy consumption contribute to an increased treatment cost (Neoh et al. 2016).

In the context of the widespread execution of these systems, various factors, including the cost-effectiveness of the overall process, are considered. Fixed bed reactors with immobilized catalysts on the support are often regarded as the most favored choice for practical applications. The utilization of TiO_2 photocatalysis in its immobilized form is consistently favored, as evidenced by studies conducted by (Rimoldi et al. 2017; Blanco-Vega et al. 2017). To explore the economic potential of heterogeneous photocatalysis (Kumar et al. 2021), it is imperative to establish a reliable and cost-effective method for immobilizing TiO_2 on inert supports that possess a substantial exposed surface area. Over an extended period, the TiO_2 immobilized supports should maintain their structural and functional integrity, preventing both catalyst attrition and the detachment of catalyst particles from the surface.

Several studies have documented different types of supports used for immobilizing TiO_2. These include polystyrene beads (Fabiyi and Skelton 2000), concrete surfaces (Delnavaz and Ramezanianpour 2012), pebbles (Rao et al. 2012), silica gel beads (Li et al. 2015a), glass spheres (Borges et al. 2021), glass plates, and zeolite (Behravesh et al. 2020), etc. Despite the abundance of published research on supported catalysts, effective field-scale implementation remains elusive. The stability and durability of supported catalysts have not been thoroughly addressed in prior studies. Although the technique proves efficient and viable commercially, selecting inert, efficient, and robust materials for catalyst immobilization remains a persistent challenge for AOP scientists. In addition, mass transfer considerations and treatment times hinder the commercial applications of fixed-mode catalysis, as longer treatment times result in greater energy consumption (Cai et al. 2021).

1.5 b Concept of hybrid AOPs

The continuous development of combined hybrid systems demonstrates the efficacy of combining technologies such as photocatalysis-biodegradation (Collivignarelli et al. 2020), photo-Fenton-biological oxidation (Pariente et al. 2008; Changotra et al. 2019), photo-Fenton-coagulation, and flocculation (GilPavas et al. 2017), electro-oxidation (Pan et al. 2019), photocatalytic-ozonation (Mecha et al. 2017; Yu et al. 2019), and ultrasonic-photocatalysis. The integrated approach proved to be highly efficient than isolated processes for wastewater

treatment. Unlike conventional isolated AOPs, hybrid systems demonstrate heightened oxidation velocities, swifter kinetics, reduced durations for mass transfer operations, and more rationalized operational methodologies.

However, using iron as a catalyst in the photo-Fenton process has been linked to sludge development, which raises serious safety concerns (Silva and Baltrusaitis 2021). Simultaneously, the ozone disintegrates rapidly into oxygen during photocatalytic ozonation, making residue removal procedures more difficult. Furthermore, the relatively high expenses related to system maintenance and substantial energy consumption during the operational process impede the advancement of large-scale applications (Luo et al. 2015).

Taking into account the restrictions of other hybrid processes, the integration of two methods photocatalysis and photo-Fenton presents a reasonable solution to the encounters posed when these processes are applied independently (Bansal and Verma 2017). Integrated solar-powered AOPs demonstrate the ability to treat actual effluent at a low cost, which is a substantial benefit for wastewater treatment. The primary challenge of this hybrid process is to ensure that both mechanisms (photocatalysis and photo-Fenton) occur simultaneously without interfering with one another. The hybrid process is very useful in treating real industrial wastewater but the technique has not been explored well so far. Combining both photocatalysis and photo-Fenton in a single system has the potential to overcome the inherent disadvantages of each method and increase the process efficiency. To improve the efficiency of wastewater treatment, several studies have suggested harnessing the hybrid/dual effect of photo-Fenton and photocatalysis (Bansal et al. 2018). This method improves treatment efficacy by producing a large amount of $OH^{\bullet}$. The fundamental mechanism of this hybrid process involves the simultaneous reaction of TiO_2 particles and iron oxides. When exposed to light, TiO_2 particles undergo photoexcitation, resulting in the formation of electron (e^-) and hole pairs in the conduction band (Liu et al. 2017).

For the photo-Fenton reactions to initiate, Fe^{2+} reacts with H_2O_2 and converts into Fe^{3+} (Ruales-Lonfat et al. 2015). The e^- from photocatalysis i.e., conduction band electron (e^-_{CB}) combines with the Fe^{3+} and transforms it to Fe^{2+}, posing the recombination problem. When Fe^{3+} is present, it can react with the excited electrons from the photocatalyst, converting Fe^{3+} to Fe^{2+}. This reaction can help in separating the electron-hole pairs, reducing the recombination and thus increasing the photocatalytic efficiency(Romay et al. 2020).

When Fe^{3+} ions come into contact with TiO_2, the metal-oxygen link weakens and the charge imbalance causes some Ti^{4+} species to be replaced. This results in the creation of Ti^{3+} species and oxygen vacancies, which act as reactive species for wastewater treatment. This results in the separation of the electron-hole pair, which aids in the oxidation of contaminants (Kim 2016). This will result in higher $OH^{\bullet}$ production and so benefit the whole process. The presence of Fe^{2+} and Ti^{3+} has a synergistic effect on oxidation and reduction, resulting in improved wastewater treatment (Rincón and Pulgarin 2007).

In this context, the proposed study attempts to incorporate the in-situ dual processes (Photocatalysis and photo-Fenton) in fixed mode to visualize the feasibility of treating different streams of the P&P industry. The study also incorporates the idea of the circular economy by using waste materials in the fabrication of composite to make it more cost-effective.

The composite will be made from industrial waste materials like foundry sand (FS) and furnace blast sand (FBS). In previous studies by (Bansal et al. 2018), the materials FS and FBS were found to have distinct yet complementary roles when used in a photocatalytic composite. FS helps in providing structural strength to the catalyst, ensuring it is stable and durable. On the other hand, FBS, which contains iron, plays a critical role in enhancing the photocatalytic activity of the composite. When FBS is combined with a semiconductor photocatalyst, the iron within the FBS makes the composite visibly more active, meaning it is better at absorbing light and generating the necessary reactive species for the photocatalytic process. This is particularly important in photo-Fenton reactions, where iron leaching a process where iron ions are released into the solution is essential. Iron leaching is crucial because it helps generate hydroxyl radicals, powerful oxidizing agents that drive the degradation of pollutants in the photo-Fenton reaction. In summary, while FS provides structural support, FBS enhances the composite's effectiveness through iron leaching, making the combination of these materials highly effective for photocatalytic applications.

As discussed, these composite beads were susceptible to leaching out iron species under acidic conditions thus contributing to the photo-Fenton reaction along with on-going surface active photocatalysis. Besides photo-Fenton and photocatalysis, these composite beads were contributing to iron-oxide catalysis as well owing to the presence of few forms of iron-oxides on their surface. These iron-oxides could capture photon-excited electrons from the conduction band of TiO_2 thus promoting electron-hole separation thereby enhancing the overall catalytic activity. At the same time, this captured e^- tended to regenerate ferrous ions from ferric ions

hence stimulating the photo-Fenton reaction. Consequently, an abundance of hydroxyl radicals generated through different processes augmented the oxidative destruction of toxic pollutants present in the effluent. The detailed mechanism of the dual process is explained in Fig. 1.3 b**.** The whole mechanism is explained in Eqs. 1.1b-1.11b with a detailed step-wise explanation:

1.5.1 b Photocatalysis Reactions

✓ **Photon Absorption by TiO_2:**

$$TiO_2 + Sunlight \rightarrow e^-_{TiO_2(CB)} + h^+_{TiO_2(VB)} \qquad \textbf{1. 1 b}$$

- **Explanation:** TiO_2 absorbs sunlight, exciting an e^- from the valence band (VB) to the conduction band (CB), creating an electron-hole pair.
- **Significance for Color Removal:** The generation of electron-hole pairs initiates the photocatalytic process, enabling the breakdown of chromophores, which are the color-causing compounds in wastewater.

✓ **Reduction of Oxygen:**

$$e^-_{TiO_2(CB)} + O_2 \rightarrow O_2^- \qquad \textbf{1. 2 b}$$

- **Explanation:** The e^- in the conduction band reduces molecular oxygen (O_2) to form a superoxide anion (O_2^-).
- **Significance:** Superoxide anions are reactive oxygen species (ROS) that attack and degrade chromophores, contributing to the removal of color from the wastewater.

✓ **Oxidation of water:**

$$h^+_{TiO_2(VB)} + H_2O \rightarrow OH^- + H^+ \qquad \textbf{1. 3 b}$$

- **Explanation:** The hole in the valence band oxidizes water (H_2O) to generate hydroxyl radicals ($\cdot OH$) and protons (H^+).
- **Significance:** Hydroxyl radicals are highly reactive and effective in breaking down a wide range of organic pollutants, including chromophores, leading to significant color reduction.

✓ **Photo-Fenton Reactions**

- **Fenton reaction**

$$Fe^{2+}_{(leached)} + H_2O_2 \rightarrow Fe^{3+}_{(leached)} + OH^{\cdot} + OH^{-} \quad \textbf{1. 4 b}$$

- **Explanation:** Iron (II) (Fe^{2+}) reacts with hydrogen peroxide (H_2O_2) to produce iron (III) (Fe^{3+}), hydroxyl radicals (·OH), and hydroxide ions (OH^-).
- **Significance:** This reaction generates hydroxyl radicals, which are powerful oxidizing agents that break down chromophores, thus reducing the color of the wastewater.
- **Regeneration of Fe^{2+}:**

$$Fe^{3+}_{(leached)} + H_2O_2 \rightarrow Fe^{2+}_{(leached)} + H_3O^{+} + HO_2^{-} \quad \textbf{1. 5 b}$$

- **Explanation:** Iron (III) (Fe^{3+}) reacts with hydrogen peroxide to regenerate Fe^{2+}, producing hydroperoxyl radicals ($HO_2\cdot$) and hydronium ions (H_3O^+).
- **Significance:** Regeneration of Fe^{2+} is essential for the continuity of the Fenton cycle, ensuring sustained production of hydroxyl radicals that continue to degrade color-causing compounds.
- **Photo-Reduction of Fe^{3+} Using Sunlight:**

$$Fe^{3+}_{(leached)} + H_2O \xrightarrow{Sunlight} Fe^{2+}_{(leached)} + OH^{\cdot} + H^{+} \quad \textbf{1. 6 b}$$

- **Explanation:** Sunlight reduces Fe^{3+} back to Fe^{2+}, generating hydroxyl radicals (·OH) and protons (H^+).
- **Significance for Color Removal:** Sunlight enhances the regeneration of Fe^{2+}, boosting the efficiency of the Fenton process and increasing the degradation of chromophores.
- **Dual process (Photocatalysis + photo-Fenton):**
- **Electron transfer to Fe^{3+}:**

$$Fe^{3+}_{(leached)} + e^{-}_{(TiO_2)} + H_2O \rightarrow Fe^{2+}_{(leached)} + OH^{\cdot} + H^{+} \quad \textbf{1. 7 b}$$

- **Explanation:** The e^- from the TiO_2 conduction band reduces Fe^{3+} to Fe^{2+} in the presence of water, producing hydroxyl radicals (·OH) and protons (H^+).

- **Significance:** This reaction not only enhances the production of hydroxyl radicals but also addresses the issue of electron-hole recombination. By utilizing the conduction band electrons to reduce Fe^{3+}, the likelihood of electrons recombining with holes is reduced. This efficient separation of charges results in a more sustained production of reactive

species, which are essential for breaking down chromophores and removing color from wastewater.

- **Reduction of H_2O_2 by TiO_2 Electrons:**

$$e^-_{(TiO_2)} + H_2O_2 \rightarrow OH^{\cdot} + OH^- \quad \textbf{1. 8 b}$$

- **Explanation:** The e^- from TiO_2 reduces hydrogen peroxide (H_2O_2), generating hydroxyl radicals ($\cdot OH$) and hydroxide ions (OH^-).
- **Significance:** This reaction further contributes to the efficient use of conduction band electrons, reducing electron-hole recombination and increasing the concentration of hydroxyl radicals. These radicals are highly reactive and effective in degrading chromophores, leading to significant color removal.
- **Continuous Cycling of Fe^{2+} and Fe^{3+}:**

$$Fe^{2+}_{(leached)} + H_2O_2 \rightarrow Fe^{3+}_{(leached)} + OH^{\cdot} + OH^- \quad \textbf{1. 9 b}$$

$$Fe^{3+}_{(leached)} + H_2O_2 \rightarrow Fe^{2+}_{(leached)} + H_3O^+ + HO_2^- \quad \textbf{1. 10 b}$$

$$Fe^{3+}_{(leached)} + H_2O \xrightarrow{Sunlight} Fe^{2+}_{(leached)} + OH^{\cdot} + H^+ \quad \textbf{1. 11 b}$$

- **Explanation:** These reactions describe the continuous cycling of Fe^{2+} and Fe^{3+} facilitated by the photo-Fenton process. The regeneration of Fe^{2+} from Fe^{3+} through reactions with hydrogen peroxide and sunlight ensures a constant supply of Fe^{2+} for the Fenton reactions.
- **Significance:** The continuous cycling of iron between its Fe^{2+} and Fe^{3+} states minimizes the accumulation of iron in the system. This reduces the formation of iron sludge, a common issue in conventional Fenton processes. By maintaining iron in a soluble state and constantly regenerating it, the combined mechanism mitigates sludge generation, making the process more efficient and sustainable.

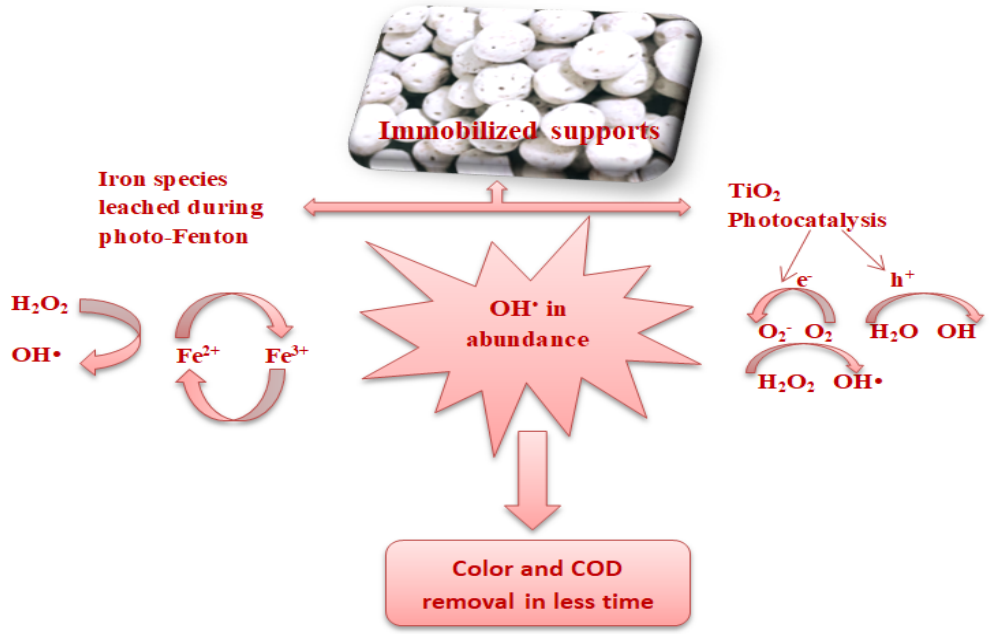

Fig. 1. 3 b Mechanism for in-situ dual process for treatment of P&P industry wastewater

This technology operates in a symbiotic manner, with one process complementing the other to address individual limitations effectively. The hybridization elevates reaction rates, thereby enhancing the performance of the treatment system. Furthermore, the controlled leaching of iron from inert beads for the photo-Fenton process avoids the formation of problematic iron sludge. The incorporation of both FBS and FS not only strengthens support structures but also increases binding capacity and iron concentration, contributing to both economic and operational efficiency (Bayraktar 2019).

The utilization of waste materials underscores the cost-effectiveness of the process. The hybrid system, detailed in Chapter 4 (Results and Discussion), demonstrates promising results, affirming its efficacy and synergistic advantages. Notably, the absence of sludge formation and the consistent availability of $OH^{\bullet}$ contribute to the overall success of the in-situ hybrid process, as expounded upon in the dissertation. The assessment of the proposed in-situ hybrid/dual process extends to its impact on efficiency through the reduction of treatment time, a crucial aspect in optimizing wastewater treatment protocols.

1.6 b Selection of various streams for the present study

For the selection of a particular stream for the present study, preliminary visits were made to the industry to understand the whole process of water and wastewater streams in general.

The preliminary visits were paid to the selected P&P industry in Punjab, India. The wastewater treatment was studied to understand the basic problem.

Based on our visits and discussions with our team & industry, three different streams were shortlisted which were targeted for our present study:

- Up-flow anaerobic sludge bioreactor (UASB)
- Alkali stream (I/L)
- Outlet Stream (O/L)

These three streams were selected based on the problem identified i.e. color persistence, but UASB and I/L were putting a major load which affected the final outlet stream i.e., O/L. Fig**.** 1.4 b shows the different targeted streams i.e., UASB stream, I/L stream, and O/L stream. UASB is a highly colored but low-volume stream whereas I/L has less color than UASB but more in volume. Out of these streams, UASB and I/L mostly contribute to the problem of color in the final treated effluent stream and O/L is the final treated stream with the highest volume which has color even after the treatment but has lesser color than the other two streams.

1.6.1 b Reason for selecting the following streams:

- **UASB stream:** This stream mainly originates from the initial stage i.e., the washing + chemical recovery stage. This stream comes after UASB treatment i.e. The UASB process is a highly efficient technique for treating colored wastewater generated by the P&P industry. In the course of this procedure, wastewater comprising colors and various contaminants is introduced into a reactor, wherein anaerobic microorganisms facilitate the decomposition of the organic substances. The UASB reactor possesses a distinctive configuration that facilitates the creation of a compact sludge layer, thereby retaining the bacteria and enhancing the efficacy of the treatment process(Mau et al. 2016; Gerber Van Doren et al. 2017; Gaur et al. 2020). During the upward flow of wastewater over the blanket, the bacteria enzymatically degrade the organic components, such as dyes, resulting in their conversion into less complex and less detrimental molecules. The aforementioned procedure is especially well-suited for the treatment of colored wastewater due to its ability to efficiently eliminate dyes and diminish the total pollution burden, hence enhancing the safety of the water for either release or reuse. The UASB treatment was not very successful in removing color from the wastewater as this stream has a low volume and can be targeted easily for further treatment to avoid the color load in the final stream.

- **I/L stream:** In the P&P industry, the alkali stream is referred to as such due to its predominant composition of alkaline substances, namely sodium hydroxide (NaOH) and sodium sulphide (Na_2S). These compounds possess a high alkalinity, indicating a significant pH level, which is crucial for multiple phases of the paper production process. The alkalinity of the stream helps to break down lignin, a complex organic polymer in wood fibers, during pulping and bleaching. This alkaline environment also helps to control pH levels in the pulp, which is critical for maintaining the effectiveness of various chemicals used in the papermaking process. Due to its alkaline nature and its essential role in the manufacturing process, this stream is commonly referred to as the alkali stream. The alkali stream in the P&P industry, in addition to being alkaline, often contains a significant amount of color due to the presence of lignin and other organic compounds. This color is a result of the breakdown of wood fibers and other materials during the pulping and bleaching processes. Because of its high color content, the alkali stream needs to be treated before it can be discharged into the environment or reused in the manufacturing process.
- **O/L stream:** This stream arises after biological treatment in the P&P industry and contains less color compared to streams from earlier stages but poses a unique challenge due to its significantly greater volume. This final effluent stream is the result of the combined treatment processes, including biological treatment, which have effectively reduced the color and organic load. However, despite the lower color content, the large volume of the O/L stream necessitates careful management and treatment. Efficient treatment of the O/L stream is crucial to ensure compliance with environmental regulations and to minimize the environmental impact of the P&P industry. Typical treatment techniques employed for this particular stream encompass sophisticated oxidation procedures, such as ozonation or UV irradiation, alongside filtration and sedimentation techniques to eliminate residual color and suspended particulates. Moreover, implementing tactics such as water reuse and process optimization can effectively mitigate the magnitude of this stream, making a significant contribution to the industry's overall sustainability. Innovations in wastewater treatment technologies continue to improve the management of the O/L stream, making it possible to achieve high levels of treatment and reduce environmental impact. By addressing the challenges posed by the volume of this stream and implementing effective treatment strategies, the P&P industry can further enhance its environmental performance and sustainability.

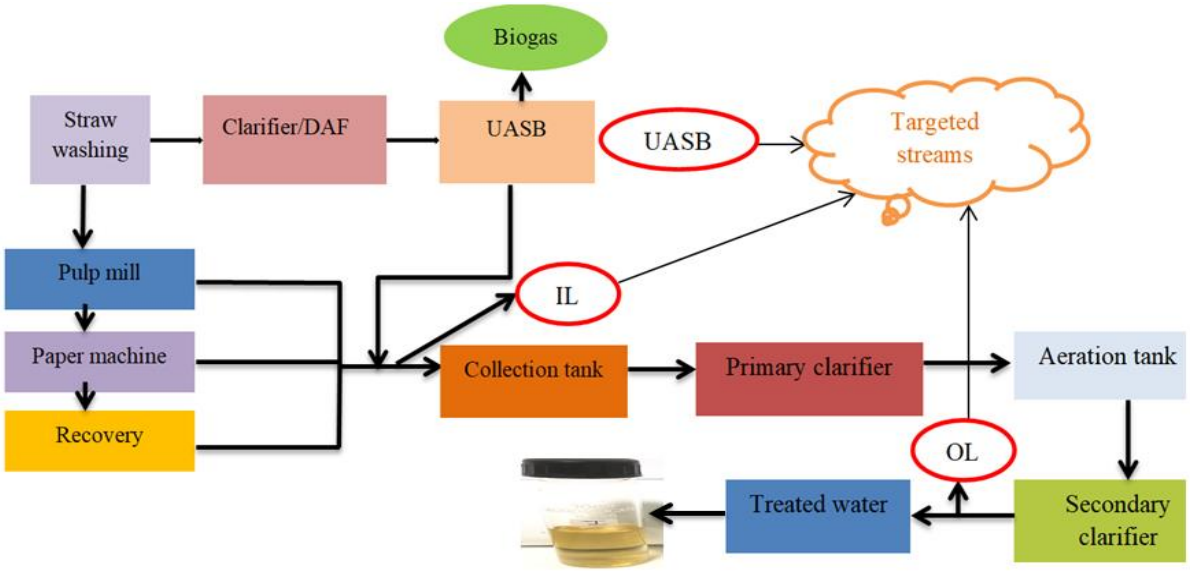

Fig. 1. 4 b Different targeted streams coming from several areas of the P&P industry

1.7 b The approach followed for the different selected streams

There are three different streams as aforementioned out of which UASB and I/L are highly colored streams that required pretreatment i.e., Coagulation/flocculation followed by dual process, whereas the final stream i.e., O/L stream had much lesser color so the dual technique could be applied directly as shown in Fig. 1.5 b. A combined approach was adopted for the treatment of UASB and I/L streams, which involved coagulation-flocculation followed by the dual technique of simultaneous photocatalysis and photo-Fenton process. Coagulation/flocculation was deemed necessary before the application of the dual technique, as both effluents exhibited a high level of color that impeded light penetration in the reaction system. By removing a portion of the color through coagulation/flocculation, the dual technique was successfully applied, resulting in excellent color removal efficacy.

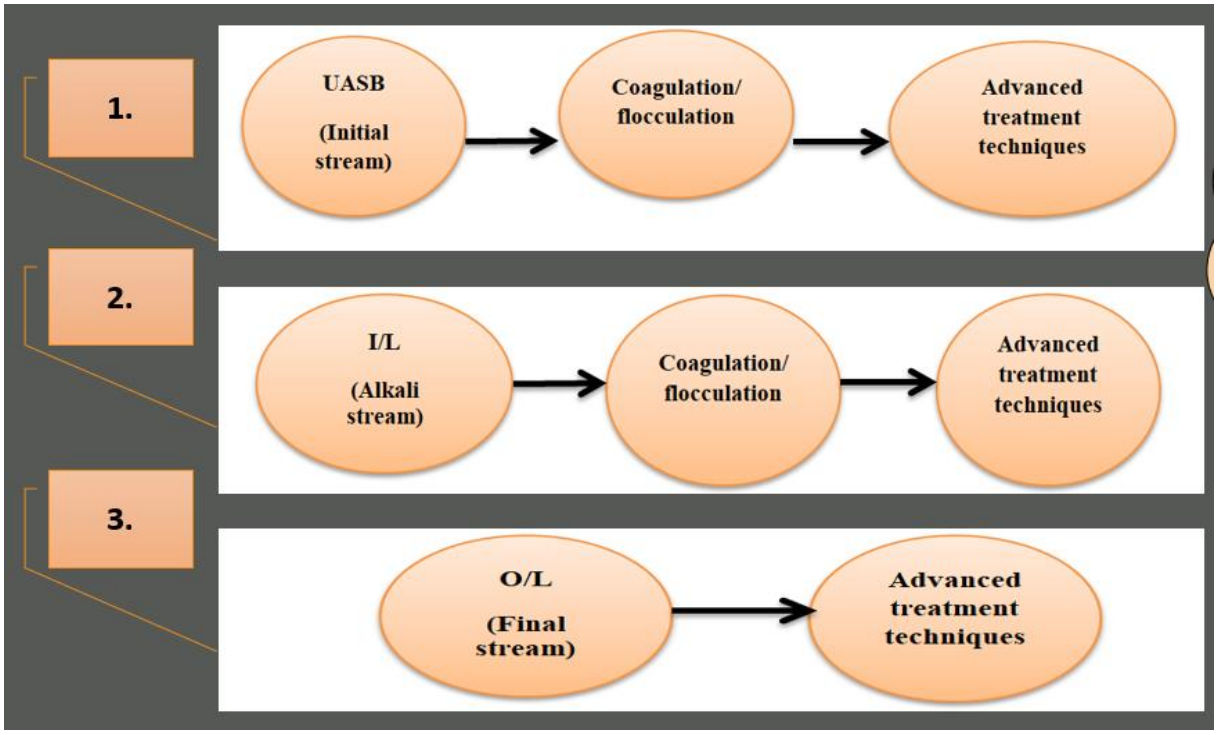

Fig. 1. 5 b Approach followed by different streams

1.8 b Objectives of the proposed study

The main aim of the study was to develop a novel composite and check the feasibility of its application to different targeted streams of real P&P industry wastewater.

- Fabrication of composite materials using TiO_2 as a photocatalyst incorporating industrial waste materials for natural doping.
- Feasibility of application of prepared composite for the treatment of agro-based industrial effluents as pre or post-treatment option and process optimization.
- Durability studies in terms of stability and catalyst intactness along with pilot-scale trials using a once-through reactor.

Chapter 2

Literature review

2.1 Overview

In recent years, government regulations for managing industrial wastewater have become more rigorous, particularly emphasizing a zero-liquid discharge (ZLD) approach (Tong and Elimelech 2016). This approach seeks to eliminate wastewater discharge into the environment and instead focuses on reusing treated effluent within industrial processes. In the textile industry, for example, efforts are being made to remove dyes and other contaminants from wastewater to allow for reuse (Ahmad et al. 2016). Similarly, the chemical and pharmaceutical industries are working to purify their effluent to recover valuable by-products and ensure environmental safety. In the P&P industry, a significant challenge remains in achieving complete color removal from the final treated effluent, which is crucial for reusing the water in the manufacturing process (Kamali et al. 2019). Nevertheless, the challenge of removing color from the final treated effluent remains. The presence of color in wastewater can be attributed to various compounds and contaminants, and its persistence in the treated effluent can have aesthetic and environmental consequences. To overcome this obstacle, paper industries are actively looking for advanced treatment technologies, process improvements, and strict quality control measures to consistently achieve color-free effluents (Hermosilla et al. 2015).

The evolving landscape of wastewater management regulations is prompting P&P industries to adopt a zero-liquid discharge approach, redirecting wastewater from agricultural use to production processes. While this transition aligns with sustainability goals, the quest for completely treated effluents underscores the ongoing commitment to environmental concerns and resource optimization within the P&P industry. In addition to these advanced treatment methods, biological treatment processes also play a crucial role in achieving comprehensive wastewater treatment. These methods leverage microbial activity to degrade organic pollutants, providing an effective and environmentally friendly solution (Ganzenko et al. 2014).

2.2 Biological treatment

Biological treatment technologies, which have capital and operating costs of 5-20 and 3-10 times more affordable than their chemical counterparts, are a cost-effective ally for biodegradable waste streams. (Mehta et al. 2015) Maximizing residence duration and pollutant

removal rates within biological processes is wise to maximize residence duration and pollutant removal rates within biological processes because of the financial benefit of lower capital investment and operational costs. Biological treatments grapple with issues such as low reaction rates, the intricate disposal of activated sludge, and the demanding parameters of pH and temperature for efficient execution (Scott and Ollis; Ogundele et al. 2023) Unlocking the full potential of biological therapies for biodegradable waste requires striking a balance with these complexities. A variety of biological methods, including aerobic and anaerobic processes, have been used to treat effluents from the P&P industry (Hubbe et al. 2016b; Toczyłowska-Mamińska 2017). Aerobic procedures are preferred due to their effectiveness and ease of usage (Saghafi et al. 2019). In suitable settings biological treatment, typically via activated sludge (ul Pala and Tokat 2002), has undeniable benefits for the elimination of organic molecules. Because of the dark color, and high toxicity of phenols, aliphatic chemicals, and industrial wastes, its usage in treating these effluents is limited. Furthermore, since the success of the process is fundamentally dependent on the viability and activity of the microorganisms (Aragaw 2021), it becomes necessary to adjust pH to an adequate value and to make carbon and oxygen available in adequate quantities (Kumar and Puri 2012).

Recent research endeavors have focused on the significant attention garnered by the application of anaerobic biological processes in treating wastewater from the P&P industry. Addressing the environmental concerns associated with this industrial effluent, researchers have delved into exploring the efficacy of anaerobic treatments. Notably, studies by (Chan et al. 2009; Zhang 2020) showcase the promising outcomes of employing anaerobic processes, underscoring their capacity to efficiently degrade complex organic compounds inherent in the industry's effluent streams. Utilization of anaerobic reactors, such as up-flow anaerobic sludge blanket (UASB) reactors, has emerged as a viable method, exhibiting robust performance in reducing chemical oxygen demand (COD) and mitigating the environmental impact of discharged effluents. Despite these advancements, there are still obstacles that remain, as emphasized by (Gomec 2010). Therefore, it is imperative to conduct further investigation and refinement of anaerobic treatment parameters to improve its effectiveness.

Despite the promise of anaerobic biological processes for P&P industry wastewater treatment, challenges persist. Notably, issues such as the incomplete degradation of recalcitrant compounds and the unintended production of methane underscore the ongoing need for optimization. Recognizing these drawbacks, this research advocates a comprehensive approach that integrates advanced treatment methods. In particular, Advanced Oxidation Processes

(AOPs) emerge as crucial protagonists in addressing the limitations of anaerobic processes (Paździor et al. 2019). AOPs, encompassing techniques like ozonation and advanced oxidation with hydrogen peroxide, offer a robust means to target persistent organic pollutants, ensuring a more thorough and environmentally compliant treatment. This review will delve into the pivotal role of AOPs in the context of P&P industry wastewater treatment, shedding light on their importance in overcoming the drawbacks associated with conventional treatments.

2.3 Assets and liabilities of the Advanced Oxidation Processes

AOPs employ oxidative technologies that generate highly reactive hydroxyl radicals ($OH^{\bullet}$), which have a higher oxidation potential than other oxidants (Bautitz and Nogueira 2010; Prieto-Rodríguez et al. 2013). AOPs offer an innovative and efficient solution to conventional challenges in wastewater treatment. These solutions are imperative for enhancing the competitiveness of various industrial sectors within the global water technology domain (Comninellis et al. 2008).

AOPs are gaining popularity in both industrial and academic communities, as evidenced by the expanding number of publications in scientific journals related to environmental applications (Comninellis et al. 2008). The majority of published articles focus on either TiO_2 photocatalysis or photo-Fenton processes, as highlighted by (Hashimoto et al. 2005; Rahim Pouran et al. 2015). These methodologies have shown promising outcomes in degrading various persistent pollutants in water, as demonstrated by studies such as (Nakata and Fujishima 2012; Sophia A. and Lima 2018). Nonetheless, it is vital to highlight that both strategies have inherent limitations that limit their practical application in the field.

2.3.1 Application of TiO_2 photocatalysis

TiO_2 photocatalysis has emerged as a tough contender in the realm of real wastewater treatment, offering a versatile and sustainable approach to address complex pollutant matrices. The process hinges on the activation of TiO_2 catalysts by ultraviolet (UV) light, generating electron-hole pairs that, in turn, activate redox reactions leading to the formation of highly reactive oxygen species (ROS), notably hydroxyl radicals ($OH^{\bullet}$) and superoxide ions ($O2^{\bullet-}$) (Liu et al. 2012; Nakata and Fujishima 2012). In the context of real industrial wastewater treatment, particularly in sectors such as pulp and paper, TiO_2 photocatalysis showcases remarkable efficacy in the degradation of organic pollutants and the removal of color-causing compounds. Its applicability spans a broad spectrum of contaminants, making it a compelling

choice for the diverse and intricate composition of real wastewater streams (Zhang et al. 2014; Rajput et al. 2021).

Countless publications explore the elimination of micro-pollutants from water through photocatalysis, employing TiO_2 as a standalone particulate (Doll and Frimmel 2005; Pérez-Estrada et al. 2005). Studies suggest that the effectiveness of photocatalytic systems depends on particular operational aspects, such as the amount and properties of the catalyst, particularly its crystalline phase, porosity, and specific surface area. Additional significant factors include the initial concentration of the substrate, light intensity, amount of oxygen present, pH of the solution, and presence of organic and inorganic substances in the solution. Typically, the photocatalytic rate displays a linear correlation with the catalyst concentration till a specific dosage is reached. Above this threshold, light cannot be effectively absorbed by the solution, which affects the photocatalytic efficiency.

The rate of degradation via photocatalysis typically shows a linear relationship with catalyst concentration until it reaches a certain point where beyond this threshold, the effective light penetration into the solution is hindered and has an impact on degradation efficiency (Gaya and Abdullah 2008). This linear relationship between photocatalytic rate and light intensity has been proven by numerous studies (Qamar et al. 2008; Pareek et al. 2008). Furthermore, the pH of the solution that modifies ionization states of organic compounds, surface charge properties as well as altering the rate of hydroxyl radical formation during reactions plays an important role in this matter (Schwegmann et al. 2013; Haroune et al. 2014). The point of zero charge (PZC) of TiO_2 lies between pH 4.5 and 7.0 (Chong et al. 2010). Acidic organic compounds degrade more efficiently at low pH due to enhanced adsorption on the TiO_2 surface (Gao et al. 2011). Conversely, alkaline organic substances show improved degradation rates at higher pH levels (Ji et al. 2013; Haroune et al. 2014). Dissolved oxygen acts as an electron scavenger, forming superoxide radicals that react with H_2O_2 to produce additional hydroxyl radicals, further enhancing degradation (Wang et al. 2011; Guo et al. 2013). TiO_2 photocatalysis offers advantages such as minimized formation of harmful byproducts, contributing to its environmental sustainability. Despite its notable advantages, challenges persist, including the reliance on UV light for catalyst activation and the need for efficient catalyst recovery methods. Additionally, TiO_2 catalysts face challenges in wastewater treatment due to their high production costs, difficulties in separating the nanoparticles after treatment, and complexities in scaling up for large applications. Separation is especially problematic, as nanoparticles are hard to recover without advanced filtration, which adds cost and risks catalyst loss. Scaling up

requires efficient reactor designs for uniform light distribution and mixing, which becomes energy-intensive, particularly when UV light is required. Nevertheless, ongoing research and innovation in TiO_2 photocatalysis continue to push the boundaries, optimizing the technology for real-world wastewater treatment scenarios and positioning it as a promising solution for addressing the environmental impact of industrial effluents.

2.3.2 Application of photo-Fenton process

The efficacy of the photo-Fenton process in substantially reducing pollutant loads has been demonstrated in numerous studies that have investigated its application in the treatment of wastewater from the P&P industry. For example, (Ribeiro et al. 2020) investigated kraft pulp mill effluents and achieved significant reductions in AOX (up to 90%) with optimal conditions (pH 2.2, 169 mM hydrogen peroxide). Similarly, (Bajpai and Bajpai 1994) successfully treated wastewater from a paper recycling facility, achieving up to 85% COD removal and 90% color reduction, particularly when combined with biological pre-treatment. This combination improved the efficacy of the photo-Fenton process by reducing the initial pollutant load. (Ginni et al. 2014a) explored treating paper mill wastewater using UV light in the photo-Fenton process, achieving up to 95% color removal and 80% COD reduction. They emphasized the importance of optimizing pH (3.0), hydrogen peroxide (150 mg/L), and iron (15 mg/L) concentrations for maximum efficiency. (Amat et al. 2009)focused on bleaching process effluents, which contain high levels of chlorinated organic compounds and color, achieving up to 90% reduction in chlorinated compounds and significant color removal under similar conditions. The photo-Fenton process was employed by (Navalon et al. 2011) to treat black liquor from the kraft process, a highly polluted effluent. The process was able to achieve up to 70% COD removal and 85% color reduction. This investigation underscored the necessity of pretreatment to mitigate the initial pollutant burden to enhance the efficiency of the process. Under optimal conditions of pH 3.0, 100 mg/L hydrogen peroxide, and 10 mg/L iron, (Beltran De Heredia et al. 2001) achieved up to 80% lignin degradation and 90% color reduction in their investigation of lignin and its derivatives. (Ramírez et al. 2010) demonstrated the feasibility of using solar irradiation in the photo-Fenton process to treat paper mill wastewater, achieving up to 85% COD reduction and 90% color removal. This approach proved to be cost-effective compared to using artificial UV light. Durán 2011 treated effluents from a cardboard manufacturing plant, achieving up to 80% COD removal and 85% color reduction, with optimal conditions of pH 3.0, 120 mg/L hydrogen peroxide, and 12 mg/L iron. Although the

homogeneous photo-Fenton process has shown promise as an effective solution for treating bio-recalcitrant pollutants, it comes with certain drawbacks, including:

- Elevated process costs (De Torres-Socías et al. 2015)

- Limited catalyst regeneration (Rahim Pouran et al. 2015)

- Requirement for high doses of H_2O_2 (Yu et al. 2020)

- Production of substantial amounts of iron sludge(Hermosilla et al. 2012)

2.3.3 Fixed bed AOPs for treating actual industry wastewater

Advanced oxidation processes (AOPs) have gained significant attention for their ability to degrade a wide range of pollutants in wastewater. The fixed bed configuration of AOPs has emerged as a viable option for enhancing treatment efficiency and scalability. This review examines the application of fixed bed AOPs in treating wastewater, with a focus on the P&P industry and other industrial sectors. Fixed bed AOPs involve immobilizing catalysts or reactive media on a fixed support within a reactor. This configuration allows for continuous flow treatment, improved contact between pollutants and reactive species, and easier separation of catalysts from the treated water. Commonly used AOPs in fixed bed configurations include photocatalysis, ozonation, and the photo-Fenton process. P&P wastewater contains high levels of organic pollutants, color, and recalcitrant compounds such as lignin, chlorinated phenols, and resin acids. Traditional treatment methods often fall short of effectively reducing these pollutants, making AOPs a suitable alternative. (Kansal et al. 2007) investigated the degradation of P&P mill effluent using a fixed bed reactor with TiO_2 as the photocatalyst. The study achieved significant reductions in COD (75%) and color (85%). Optimal conditions included UV light exposure, a pH of 6, and a hydraulic retention time (HRT) of 3 h. (Lee and Shoda 2008) explored the use of a fixed bed ozonation reactor for treating paper mill wastewater. The study showed high removal efficiencies for COD (80%) and color (90%). Optimal conditions were a pH of 7, an ozone dose of 50 mg/L, and an HRT of 2 h. (Gonçalves et al. 2021) applied the photo-Fenton process in a fixed bed reactor for treating kraft pulp mill effluents. The study achieved COD removal of 85% and color reduction of 90%. Optimal conditions were a pH of 3, a hydrogen peroxide concentration of 100 mg/L, and an iron concentration of 10 mg/L. (Chong et al. 2015) conducted a study on the use of UV-LEDs with a fixed bed TiO_2 photocatalytic reactor for treating paper mill wastewater. The research highlighted COD removal of 70% and color removal of 80%. Optimal conditions included UV-LED light

exposure, a pH of 5, and an HRT of 4 h. (Kabra et al. 2004) studied the treatment of textile dye wastewater using a fixed bed photocatalytic reactor with TiO_2. The reactor achieved dye degradation of 80% and COD reduction of 75%. Optimal conditions included a pH of 5.5, UV light exposure, and an HRT of 2 h. (Mohammed et al. 2021) explored the treatment of textile wastewater using a fixed bed reactor with immobilized TiO_2 and ZnO nanoparticles. The study demonstrated dye degradation of 85% and COD reduction of 80%. Optimal conditions were a pH of 6, UV light exposure, and an HRT of 3 h. (Baresel et al. 2016) investigated the removal of pharmaceutical compounds from wastewater using a fixed bed ozonation reactor. The study demonstrated removal efficiencies for various pharmaceuticals up to 90%. Optimal conditions included a pH of 7.5, an ozone dose of 60 mg/L, and an HRT of 1.5 h. (Alvarado-Camacho et al. 2022) investigated the use of a fixed bed TiO_2 photocatalytic reactor for treating petrochemical wastewater. The study highlighted COD removal of 78% and removal of phenolic compounds of 80%. Optimal conditions included UV light exposure, a pH of 4.5, and an HRT of 2.5 h.

2.3.3.1 Several factors influence the efficiency of fixed bed AOPs in treating industrial wastewater:

- **Catalyst Immobilization**: The method and stability of catalyst immobilization on the fixed bed support significantly impact the treatment efficiency and longevity of the catalyst.
- **Reactor Design**: The design and configuration of the fixed bed reactor, including flow rates, bed depth, and light penetration (for photocatalytic processes), are critical for optimizing pollutant degradation. In fixed-bed AOP photocatalytic systems, shallow reactor depths with greater surface area are essential for optimizing pollutant degradation. A shallow bed enhances light penetration and allows pollutants to contact the catalyst surface more effectively, maximizing the reaction rate. Adequate bed depth balances light distribution and flow to ensure pollutants are thoroughly exposed to active sites.
- **Operational Parameters**: Parameters such as pH, concentration of oxidants (e.g., hydrogen peroxide in the photo-Fenton process), and the presence of competing substances can affect the overall efficiency of fixed bed AOPs.

2.3.3.2 While fixed-bed AOPs offer several advantages, they also face challenges:

1. **Catalyst Deactivation**: Over time, the immobilized catalysts may become deactivated due to fouling or poisoning by contaminants in the wastewater.

2. **Scaling Up**: Transitioning from laboratory-scale to industrial-scale fixed bed reactors requires addressing issues related to reactor design, operational stability, and maintenance. Scaling up fixed-bed AOPs poses several challenges, such as uneven light distribution, inefficient mass transfer, and scaling limitations in large reactors. Recent studies have proposed solutions to address these issues, including using multi-layered beds (Claes et al. 2021), which allow better light penetration and more efficient pollutant contact. Hybrid reactor designs that combine fixed-bed and fluidized-bed systems have also been explored to enhance mass transfer and reduce energy consumption (Mohapatra et al. 2021). Furthermore, advanced reactor configurations such as transparent reactors (Sacco et al. 2020) and modular systems offer scalability by facilitating better control over flow and light exposure, improving overall efficiency (Zhu et al. 2021).
3. **Cost**: The initial setup and operational costs of fixed bed AOPs can be high, particularly for processes requiring specialized catalysts or light sources.

Fixed bed AOPs represent a promising technology for the treatment of industrial wastewater, including effluents from the P&P industry. Their ability to degrade complex and recalcitrant pollutants, coupled with the advantages of continuous operation and easier catalyst recovery, makes them an attractive option. The downsides can be repressed by developing more robust and cost-effective catalysts, optimizing reactor designs, and integrating fixed bed AOPs with other treatment methods to enhance overall wastewater treatment efficiency (Pareek et al. 2008; Oliveira 2014; Miyawaki et al. 2016).

2.3.4 Enhanced photo-response efficiency of TiO_2

Research in field-scale applications of Advanced Oxidation Processes (AOPs) is increasingly focusing on harnessing natural solar radiation. Utilizing natural sunlight instead of artificial UV lamps offers an environmentally friendly and cost-effective solution for photocatalysis and photo-Fenton-like processes (Chan et al. 2003). Solar-driven photocatalytic methods are particularly well-suited for countries such as India, which benefits from abundant sunlight throughout the year. When considering solar-driven photocatalytic processes, one of the main challenges is identifying a suitable material or catalyst that can effectively harvest solar radiation. Additionally, the catalyst must be capable of resisting electron-hole recombination (Park et al. 2017). Although TiO_2 has been widely studied for its photocatalytic degradation of various pollutants due to its affordability and photostability (Schneider et al. 2019), it has limitations such as high electron-hole recombination and limited absorption only

in the UV spectrum. To enhance the photocatalytic efficiency of TiO_2, research has been focused on reducing electron-hole recombination and improving light absorption properties. Key strategies include optimizing the physical characteristics of the photocatalyst, such as particle size (Li et al. 2015b), crystallinity (Tanaka et al. 1991), morphology (Lakshminarasimhan and Varadaraju 2008), and crystal facets, which can increase photocurrent and photoluminescence. Additionally, various structural modifications, such as doping with metals or non-metals and forming nanocomposites, have been explored to develop highly efficient photocatalysts (Huang et al. 2015; Lin et al. 2016; Aba-Guevara et al. 2017). Modifying TiO_2 with metals and non-metals not only reduces its band gap but also mitigates electron-hole recombination. Research has shown that doping TiO_2 with various noble metals such as Ag (Suwanchawalit et al. 2012), Pt (Kim et al. 2005), Au (Primo et al. 2011), and Pd (Ismail 2012), as well as transition metals like Fe (Yang et al. 2009), Cr (Deng et al. 2009), and Ni (Haq et al. 2016), and non-metals such as N (Cheng et al. 2016), C (Ananpattarachai et al. 2016), S (Ksibi et al. 2008), and B (Li et al. 2013), enhances its properties(Kumar et al. 2019). Compared to undoped TiO_2, these modified versions exhibit superior light absorption capacity, which significantly improves photocatalytic processes by enhancing oxidation-reduction reactions, preventing electron-hole recombination, and increasing organic adsorption, thereby boosting overall photocatalytic efficiency. Numerous studies have confirmed that modifying TiO_2 with non-metals can significantly extend its photo-response efficiency, enabling it to become active even under visible light. In contrast, doping TiO_2 with noble metals helps to inhibit the recombination of charge carriers on the TiO_2 surface by transferring photon-excited electrons to these metals. (Morikawa et al. 2001) was among the first to demonstrate that nitrogen doping could effectively narrow the band gap of TiO_2, thereby enabling visible light absorption. Their research showed that nitrogen atoms substituted for oxygen in the TiO_2 lattice, resulting in enhanced photocatalytic activity under visible light irradiation. (Liu et al. 2010) demonstrated that doping TiO_2 with gold nanoparticles significantly suppressed the recombination of photogenerated electron-hole pairs. The gold nanoparticles acted as electron traps, facilitating the transfer of photo-excited electrons from TiO_2 to the metal, thereby prolonging the lifetime of charge carriers and enhancing photocatalytic activity. (Zhang et al. 2015) explored the effects of silver doping on the photocatalytic properties of TiO_2 and observed that silver nanoparticles effectively improved the separation of charge carriers. The plasmonic properties of silver also contributed to the absorption of visible light, further enhancing the photocatalytic performance. (Mahboob et al. 2021) found that platinum-doped TiO_2 exhibited increased photocatalytic efficiency due to the effective inhibition of electron-

hole recombination. Platinum particles on the TiO_2 surface provided active sites for the transfer of photo-excited electrons, thereby extending the photo-response efficiency of TiO_2. (Sood et al. 2015) studied the photocatalytic degradation of organic pollutants using iron-doped TiO_2. They reported enhanced degradation rates for phenol and other organic compounds under visible light, attributing the improvement to the efficient separation of charge carriers facilitated by iron doping. (Moradi et al. 2019) synthesized iron-doped TiO_2 nanotubes and evaluated their photocatalytic performance. The study found that the iron-doped nanotubes exhibited superior photocatalytic activity under both UV and visible light, highlighting the role of iron in extending the photo-response of TiO_2.

Despite the numerous studies on doped or co-doped photocatalysts discussed above, none have demonstrated field-scale applications of these modified catalysts. These studies face several limitations that hinder their large-scale application, including the following:

- Preparation of modified TiO_2 in almost all studies involves tedious methods and costly raw materials.
- The use of modified TiO_2 in suspension mode in most studies requires an expensive catalyst separation step post-treatment.
- To harness the advantages of doping or co-doping, the process must be economically scaled up.

2.3.5 Application of AOPs in the P & P industry

The P&P industry produces wastewater that is rich in lignin, chlorinated organic compounds, and dyes, posing significant challenges for traditional treatment methods. TiO_2 photocatalysis has emerged as a promising technique to address these pollutants effectively. Various studies have demonstrated the potential of TiO_2 photocatalysis in treating P&P industry wastewater. (Dahm and Lucia 2004) investigated the degradation of lignin and phenolic compounds in paper mill effluents using TiO_2 photocatalysis. The study found that TiO_2 photocatalysis significantly reduced chemical oxygen demand (COD) and color, demonstrating effective degradation of organic pollutants. The authors reported that more than 80% of lignin and phenolic content was removed after 4 h of UV irradiation with TiO_2. (Kansal et al. 2008) studied the photocatalytic degradation of kraft pulp bleaching effluent using TiO_2. The research highlighted that TiO_2 photocatalysis not only reduced the COD but also led to a substantial decrease in absorbable organic halides (AOX), indicating the breakdown of chlorinated organic

compounds. The study achieved up to 75% COD removal and 85% AOX reduction after 6 h of treatment. (Alhaji et al. 2017) explored the use of immobilized TiO_2 on various supports to treat paper mill wastewater. The study found that immobilized TiO_2 provided stable and reusable photocatalytic activity. The researchers reported high removal efficiencies for both color and COD, achieving up to 80% COD reduction and near-complete color removal in repeated cycles, showcasing the catalyst's durability. (Ksibi et al. 2003) conducted a study on the photocatalytic degradation of black liquor, a highly polluting by-product of the P&P industry, using TiO_2. The results showed that TiO_2 photocatalysis effectively reduced the toxicity and organic content of black liquor. The study achieved around 81% COD reduction and significant detoxification of the effluent, making it safer for discharge or further treatment. (Rahimi et al. 2016) investigated the photocatalytic degradation of methylene blue dye in simulated textile mill effluent using TiO_2. The study demonstrated that TiO_2 photocatalysis could achieve complete decolorization and significant COD reduction within a short period. The authors emphasized the importance of optimizing operational parameters such as pH, catalyst dosage, and light intensity to maximize treatment efficiency. The Fenton process, which involves the reaction of hydrogen peroxide (H_2O_2) with ferrous iron (Fe^{2+}) to produce hydroxyl radicals, is widely studied for treating P&P mill effluents. The photo-Fenton process, an enhancement of the Fenton reaction using UV light, further increases the generation of hydroxyl radicals. (Amaral-Silva et al. 2016) examined the treatment of bleached eucalyptus kraft pulp mill effluent using the Fenton process. The study reported significant reductions in COD and color, achieving up to 70% COD removal and 80% color removal under optimal conditions. The authors highlighted the process's effectiveness in degrading complex organic molecules and reducing toxicity. (Chamorro et al. 2013) investigated the photo-Fenton treatment of paper mill wastewater. The results showed that the addition of UV light significantly enhanced the degradation efficiency, achieving over 90% color removal and substantial reductions in COD and aromatic compounds. The study emphasized the synergistic effect of UV light and Fenton reagents in breaking down recalcitrant pollutants. Ozonation, which uses ozone (O_3) as a powerful oxidizing agent, is effective in degrading a wide range of organic pollutants in P&P industry wastewater. (Pokhrel and Viraraghavan 2004) conducted a comprehensive review of ozonation applications in P&P industry wastewater treatment. The review highlighted several studies demonstrating the effectiveness of ozonation in degrading lignin, phenolic compounds, and chlorinated organic pollutants. The authors concluded that ozonation is a promising AOP for improving biodegradability and reducing the toxicity of P&P effluents. Electrochemical oxidation involves the generation of reactive species through electrolysis, offering a clean and

efficient method for treating industrial wastewater. (Martínez-Huitle and Brillas 2009) reviewed electrochemical processes for the treatment of industrial wastewater, including applications in the P&P industry. The review emphasized the advantages of electrochemical oxidation, such as high efficiency, environmental compatibility, and the ability to treat concentrated effluents. The authors noted that electrochemical methods could complement biological treatments by degrading recalcitrant pollutants.

2.4 AOPs at pilot scale

To ensure that AOPs can be effectively applied at a field scale shortly, it is essential to conduct scale-up trials of lab-scale results. Successfully implementing a large-scale photocatalytic treatment process requires a multidisciplinary approach to address all operational parameters that influence the capture and subsequent utilization of photons within a reactor (Motegh et al. 2014). Photocatalytic reactors can be classified into concentrating and non-concentrating types. Concentrating reactors utilize parabolic trough concentrators (PTC) and rely on direct solar radiation. These reactors, which necessitate solar tracking devices, are costly and challenging to maintain. They are capable of capturing a large number of photons across nearly all wavelengths, and the thermal energy from the concentrated radiation can be used for other applications simultaneously (Parra et al. 2001). On the other hand, non-concentrating reactors are simpler and more cost-effective, using both direct and diffused solar radiation, which makes them more efficient(Nogueira and Jardim 1996).

Photocatalytic reactors have considerably increased the possibility for field-scale applications, assuming certain design changes are made. Several notable scientists have undertaken extensive kinetic studies of reactors using the fundamental concepts of AOPs (Ola and Maroto-Valer 2015). However, these investigations have not determined whether to use the heterogeneous/homogeneous photo-Fenton or heterogeneous photocatalytic method. Compound parabolic collectors (CPCs) are widely used in the literature to treat wastewater, either by photo-Fenton process (Fallmann et al. 1999; García-Montaño et al. 2008) or photocatalysis ((Fernández-Ibáñez et al. 2015; Haranaka-Funai et al. 2017). The reflector design of CPC, capable of capturing both direct and diffuse solar radiation, has demonstrated excellent performance efficiency in solar photochemical and photocatalytic applications (Malato et al. 1997; Sattler et al. 2004). However, the use of expensive reflectors and associated maintenance issues are significant drawbacks of these types of collectors. (Gernjak et al. 2004) conducted a comparative evaluation of the homogeneous photo-Fenton process and the

heterogeneous photocatalytic process for treating olive mill wastewater at a pilot scale, utilizing both compound parabolic collectors (CPC) and a falling-film reactor. The photo-Fenton process demonstrated superior effectiveness compared to photocatalysis in terms of pollutant removal and mineralization efficiency. The outcomes were nearly comparable for both types of pilot-scale reactors, i.e., compound parabolic collectors (CPC) and falling-film reactors (FFR). Despite these promising results, the industrial-scale application of either the homogeneous photo-Fenton process or heterogeneous photocatalysis remains unachieved due to certain inherent limitations of these techniques. The photo-Fenton process encounters several difficulties in actual wastewater treatment scenarios, such as producing iron sludge, problems with catalyst regeneration, and the need for large oxidant dosages. Similar challenges with catalyst separation and recyclability impede slurry photocatalysis. The combined effects of these problems limit the widespread use of these otherwise efficacious therapeutic modalities.

TiO_2 photocatalysis application is often favored in its fixed form. Various research have looked into the use of fixed-bed photocatalysis for pilot-scale wastewater treatment. When building such reactors, it is critical to have a high ratio of immobilized catalyst to lighted surface area. Furthermore, maintaining a suitable contact density between the catalyst and the aqueous solution improves the reactor's degrading efficiency. In one study, the efficacy of five continuous stirred tank reactors (CSTRs) linked in series was tested for the photocatalytic degradation of 10 ppm of 2,4-dinitrophenol (DNP) in an aqueous solution (Miyawaki et al. 2016). Each reactor, formed like a square container, had TiO_2 immobilized on a glass plate and was lit by two 4 W blacklight blue fluorescent lights. This setup successfully increased the degradation rate by mitigating the issue of film diffusion resistance associated with immobilized catalysts. The non-concentrating pebble bed photocatalytic reactor (PBPR) has been studied for its effectiveness in degrading and decolorizing reactive dye solutions. This reactor consists of a horizontal or inclined trough, designed to facilitate the photocatalytic process. (Rao et al. 2012) demonstrated that the PBPR could achieve simultaneous decolorization and mineralization of dyes, with a total mineralization efficiency of 28%. (Stephan et al. 2011) designed and modeled a falling film closed loop fixed bed step reactor for the photocatalytic degradation of pesticides such as metolachlor and chlortoluron. In this reactor, TiO_2 was immobilized on cellulose fiber cloth, which was then fixed on the steps of the reactor. This innovative design facilitated effective contact between the pollutants and the photocatalyst, enhancing the degradation process. (Zayani et al. 2009) explored the

photocatalytic degradation of a commercial azo dye, Yellow Cibacron FN-2R (YC), using a pilot-scale solar thin-film fixed-bed reactor (TFFBR). This reactor design leverages solar energy to drive the photocatalytic process, providing an efficient means for the treatment of dye-contaminated wastewater on a larger scale. Further research by (Ali et al. 2020) focused on a pilot-scale photocatalytic reactor using immobilized TiO_2 for the treatment of paper mill effluents. The study demonstrated that the reactor could achieve reductions of 75% in COD, 85% in color, and 65% in turbidity over a treatment period of 8 h. These results proved the reactor's viability for large-scale applications, showcasing its efficiency in significantly reducing key pollutants. Similarly, (Asgari et al. 2022) investigated a pilot-scale solar photocatalytic reactor for treating wastewater from a P&P mill. This reactor utilized a compound parabolic collector (CPC) system to maximize sunlight capture, achieving 80% degradation of organic pollutants and 90% color removal within 6 h of operation. The study varied factors such as the initial concentration of pollutants, the intensity of sunlight, and the flow rate of the wastewater to optimize the reactor's performance, demonstrating its effectiveness in industrial wastewater treatment applications.

Although extensive literature exists on fixed-bed photocatalytic reactors, scaling them up for commercial applications presents significant challenges. The primary limitations of pilot-scale fixed-bed studies include (Bansal et al. 2018; Thakur et al. 2020a; Puri and Verma 2023):

- Extended treatment duration

- Elevated energy expenses

- Inefficient recyclability of the immobilized catalyst

- Resistance due to film diffusion

- Recurrent electron-hole recombination

Addressing these issues is crucial for commercial viability.

2.5 Combination of simultaneous Photocatalysis and photo-Fenton process

The integration of photocatalysis and the photo-Fenton process has been explored as an AOP for enhancing the treatment of wastewater, including effluents from the P&P industry. This combination leverages the strengths of both processes to achieve higher degradation efficiencies and overcome some limitations inherent in each method. The increased emphasis on developing environmentally acceptable and effective treatment methods to entirely

eradicate persistent organic contaminants from wastewater has prompted scientists to investigate novel changes to current advanced wastewater treatment technology. This field's research is continually focused on reducing treatment time and optimizing process costs. To boost treatment efficiency and decrease the duration of the photocatalytic reaction, several efforts have been made and reported in the literature to increase the concentration of hydroxyl radicals in the photocatalysis process. The addition of oxidants such as H_2O_2, $S_2O_8^{2-}$, IO_4^-, and ClO_4^- has been demonstrated to effectively enhance the reaction rate (Aljuboury et al. 2015). Several studies have also explored the coupling of photocatalysis with the photo-Fenton process to achieve higher degradation efficiency in treatment systems (Bansal and Verma 2017; Gutierrez-Mata et al. 2017; Su et al. 2021). (Ginni et al., 2014) reported a synergistic effect when combining photo-Fenton and photocatalysis processes, resulting in improved treatment efficacy for hospital wastewater compared to using each process individually. The process efficiency saw substantial improvement, achieving a decent removal of COD and significantly reducing treatment time. The enhancement in degradation efficiency with the addition of Fenton reagent to the TiO_2 photocatalytic system is due to the simultaneous generation of hydroxyl radicals by both photocatalysis and photo-Fenton processes. Furthermore, the presence of iron prevents the recombination of electrons and holes in TiO_2, thereby boosting its photocatalytic activity (Zhu et al. 2004). Several studies have explored the simultaneous application of photocatalysis and photo-Fenton processes in treating P&P industry effluents, yielding promising results. (Wang and Chen 2020) explored a pilot-scale reactor for treating textile and P&P industry effluents, using 15 mg/L Fe^{2+}, 300 mg/L H_2O_2, and 0.5 g/L TiO_2, resulting in 88% COD reduction and 92% color removal in 4 h. (Arslan-Alaton and Caglayan 2006) investigated pulp mills effluent degradation with 10 mg/L Fe^{3+}, 250 mg/L H_2O_2, and 0.8 g/L TiO_2, achieving 80% COD reduction, 75% decolorization, and enhanced biodegradability over 5 h.

According to the studies discussed, the combined process of photocatalysis and photo-Fenton has demonstrated exceptional treatment efficiency by addressing many of the issues associated with the individual processes, such as electron-hole recombination, long treatment times, and mass transfer challenges. However, the viability of this integrated process for commercial or large-scale applications remains uncertain for the following reasons:

- Most of the reported studies involve scenarios where both catalysts are in suspension form, limiting the practical applicability of the technique due to the high costs associated with separating the catalyst after treatment.

- Additionally, no studies have yet demonstrated the complete immobilization of both catalysts (iron source and TiO_2) for pollutant degradation.

Fixed-bed studies utilizing cost-effective and durable catalyst-immobilized inert supports that combine both photocatalysis and photo-Fenton processes simultaneously could revolutionize wastewater treatment. Additionally, these supports, when used with doped catalysts to incorporate modified photocatalysis alongside photo-Fenton, could represent a groundbreaking advancement in the field of AOPs for water treatment.

2.6 Summary

AOPs have proven to be more effective than traditional water treatment methods in treating and removing different types of persistent organic pollutants from industrial wastewater. Their practical use in the field hasn't been fully studied yet, though. Despite heterogeneous photocatalysis with suspended TiO_2 achieving fairly good pollutant removal efficiency, several operational issues limit its industrial-scale application. These include the costly post-treatment separation of the catalyst, poor solar spectrum utilization, charge carrier recombination, and inefficient catalyst recovery. The homogeneous photo-Fenton process, while demonstrating superior pollutant removal and mineralization efficiency compared to photocatalysis, faces challenges such as iron sludge generation, catalyst regeneration difficulties, and the need for high doses of H_2O_2, restricting its large-scale use. Although the heterogeneous photo-Fenton process addresses iron sludge generation, it suffers from significantly reduced efficiency, posing challenges for effective industrial wastewater treatment.

Some challenges associated with heterogeneous photocatalysis, such as the costly separation of the catalyst after treatment, have been addressed by immobilizing the catalyst on inert supports. However, this approach introduces new limitations, including longer treatment times, mass-transfer issues, and poor recyclability of the immobilized catalyst, which remain unresolved. While doping the catalyst with metals or non-metals has mitigated issues like inefficient solar light usage and charge carrier recombination, the complex and costly synthesis procedures using expensive precursors continue to be a significant drawback. Additionally, there is a lack of studies on the immobilization of doped catalysts, further hindering progress in this area.

Numerous pilot-scale reactors, including those using homogeneous photo-Fenton, heterogeneous slurry, and fixed-bed photocatalysis, have been explored in the literature (Sordo

et al. 2010; Mozia et al. 2012). Compound parabolic collectors (CPCs) have shown significant potential for eliminating a variety of pollutants; however, their high capital costs pose economic challenges for AOPs(Malato et al. 1997). Consequently, non-concentrating solar fixed-bed reactors have emerged as a more economical and viable option for wastewater treatment(Parra et al. 2001). Despite this, no studies have conclusively demonstrated the long-term use or sustained activity of immobilized catalysts under continuous flow conditions. Therefore, further research is necessary to optimize the design and parameters of fixed-bed photocatalytic reactors for enhanced performance and feasibility. The dual process idea, which combines photocatalysis and photo-Fenton, has not received much attention in the literature. The existing studies have shown notable improvements in process efficiency, effectively addressing many of the issues encountered in standalone processes. However, fixed-bed studies utilizing this combined approach have yet to be explored, preventing the commercial realization of this promising technique.

2.7 Lacunae

- A lot of studies have shown the efficacy of AOPs for the treatment of actual wastewater, yet their field-scale applications are scarcely reported.
- Moreover, applications of dual-processes (Photocatalysis & photo-Fenton) have not been extensively studied on the color reduction of the actual waste.
- There is a need to understand the feasibility of the application of dual-process in actual industrial streams.
- Durability and stability issues of the supported catalyst for its prolonged use are not covered effectively in the literature.
- There is still a need to identify and plug the gap for execution of lab scale studies to pilot scale for facilitating the industrial applications.
- The scale-up trials once through practice have not been evaluated much for in-situ dual effect.

2.8 Objectives

- Fabrication of composite materials using TiO_2 as a photocatalyst incorporating industrial waste materials for natural doping.

- Feasibility of application of prepared composite for the treatment of agro-based industrial effluents as pre or post treatment option and process optimization.
- Durability studies in terms of stability and catalyst intactness along with pilot-scale trials using once through reactor

Chapter 3

Materials and Methods

3.1 Overview

This chapter represents the methods followed, the standard procedure adopted, and materials used to carry out the proposed research. This section also includes the characterization of the prepared composite beads. Detailed experimental setup for batch and continuous study was also addressed.

3.2 Chemicals and reagents

A TiO_2 catalyst, comprising 70% anatase and 30% rutile phases, possessing a BET surface area of 50 m^2 g^{-1} and particle size measuring 30 nm, was procured from Evonik Industries, India, and employed as the photocatalyst. Local industrial sources in Patiala, Punjab, India, provide clay, FS, and FBS, which were used to fabricate spherical beads functioning as an iron source in this study. An oxidant, hydrogen peroxide (H_2O_2), at a concentration of 30% w/v, was sourced from Ranbaxy, India. To maintain the requisite acidic pH conditions during the treatment process, an acetate buffer, formulated from >99.5% acetic acid and 98.5% sodium acetate, was acquired from Loba Chemie Pvt Ltd, Maharashtra, India.

Several compounds, including hydroxylamine hydrochloride, ammonium acetate, 1, 0-phenonthralein monohydrate, concentrated hydrochloric acid (HCl), ferrous ammonium sulphate, and potassium permanganate, were used to estimate iron concentration (Total, ferric and ferrous). For the evaluation of $OH^{\bullet}$ in the context of photocatalytic color removal, we purchased Terephthalic acid (TPA) from Merck (U.S.) with a purity greater than 98%. In our endeavours to ascertain chemical oxygen demand (COD), our choice of reagents encompassed potassium dichromate ($K_2Cr_2O_7$) and concentrated sulfuric acid (H_2SO_4), both of analytical grade (AR) and sourced from SD Fine Chemicals Ltd. (India). Analytical-grade silver sulphate ($AgSO_4$) and concentrated sulfuric acid (H_2SO_4) were acquired from SD Fine Chemicals Ltd. (India) for use in COD estimation. Additionally, reagents including phosphate buffer, calcium chloride ($CaCl_2$), ferric chloride ($FeCl_3$), magnesium sulphate ($MgSO_4$), and sodium hydroxide (NaOH), all meeting the analytical-grade standards, were also purchased from SD Fine Chemicals Ltd. (India) for COD determination.

Furthermore, in the realm of biochemical oxygen demand (BOD) determination, we relied on a selection of reagents including calcium chloride ($CaCl_2$), phosphate buffer, ferric chloride ($FeCl_3$), sodium hydroxide (NaOH), and magnesium sulphate ($MgSO_4$), all meeting the standards of analytical grade (AR) and procured from SD Fine Chemicals Ltd. (India). Phosphoric acid, sulfanilamide, N-(1 Napthyl)-ethylene diamine dihydrochloride, Barium chloride, sodium tetra borate, boric acid, sodium thiosulfate, methylene blue, and isopropyl alcohol are all additional reagents used to analyze (sulphate, and ammoniacal nitrogen). All of these chemicals were purchased from Loba Chemie Pvt. Ltd. (India) and were of analytical quality. All aqueous solutions were created using double-distilled water. Different scavengers like p-benzoquinone (BQ) for neutralizing $O^{2\bullet-}$, disodium ethylene diamine tetra acetic acid (EDTA) for neutralizing h^+, and tert-butyl alcohol (TBA) was chosen as the quencher for $OH^\bullet$.

3.3 Analytical methods

Using standard APHA (2017) procedures, the physio-chemical examination of wastewater was carried out. Biochemical oxygen demand (BOD) (APHA, 2017), Chemical oxygen demand (COD) ((APHA, 2017: Sec. 5220 (B)), and for iron estimation ((APHA, 2017: Sec. 3111(B)). By measuring the synthesis of a fluorescent chemical (2-hydroxy terephthalic acid), photo-luminance spectrophotometry (LS-45, Perkin Elmer) was used to validate the generation of $OH^\bullet$.

3.4 Industrial Effluent Samples

As discussed, three different effluent streams were selected for the targeted study i.e.,

1. UASB stream i.e., highly colored stream coming from pulp washing and cooking.
2. I/L stream i.e., coming from paper making and bleaching process, this stream also contains a reasonably good amount of color.
3. O/L stream also known as outlet stream i.e., high volume stream but has comparatively less color this stream comes after the final treatment yet contains color. These streams were collected from three different stages i.e., stage 1, stage 2, and, stage 3 as shown in Fig. 1.4 b. Before collection of the samples, the containers were thoroughly washed with water and then rinsed with the respective effluent to be stored. The samples were taken and kept in cold storage (4^oC).

3.5 Fabrication and Immobilization of Composite Beads with Titanium Dioxide (TiO_2)

3.5.1 Analysis of sands used as iron source for the composite

To attain successful dual-process outcomes in this study, it was imperative to have two key components: adequate iron levels in the industrial waste, along with the catalyst's intactness and the presence of TiO_2 complexes. To confirm these factors, various techniques were employed to check various factors:

- Presence of Iron
- TiO_2 intactness/thickness
- Confirmation of Fe and TiO_2 complexes
- The durability of the composite

SEM analysis of the sands used in catalyst preparation revealed that FS had a coarser structure compared to the finer structure of FBS, as expected. Fig. 3.1 shows SEM images of both FS and FBS samples, which display uniformly sized, compact particles with smooth, rounded edges, lacking sharp corners. While the majority of particles are homogeneous, a few exhibit distinct grains with molten-like textures. EDS analysis of these phases identified elements such as Fe, O, Ca, Al, Mn, Cl, Na, and Mg. The presence of iron in these sands suggests their suitability as an alternative iron source for the photo-Fenton process. (Colmenares et al. 2013)

.

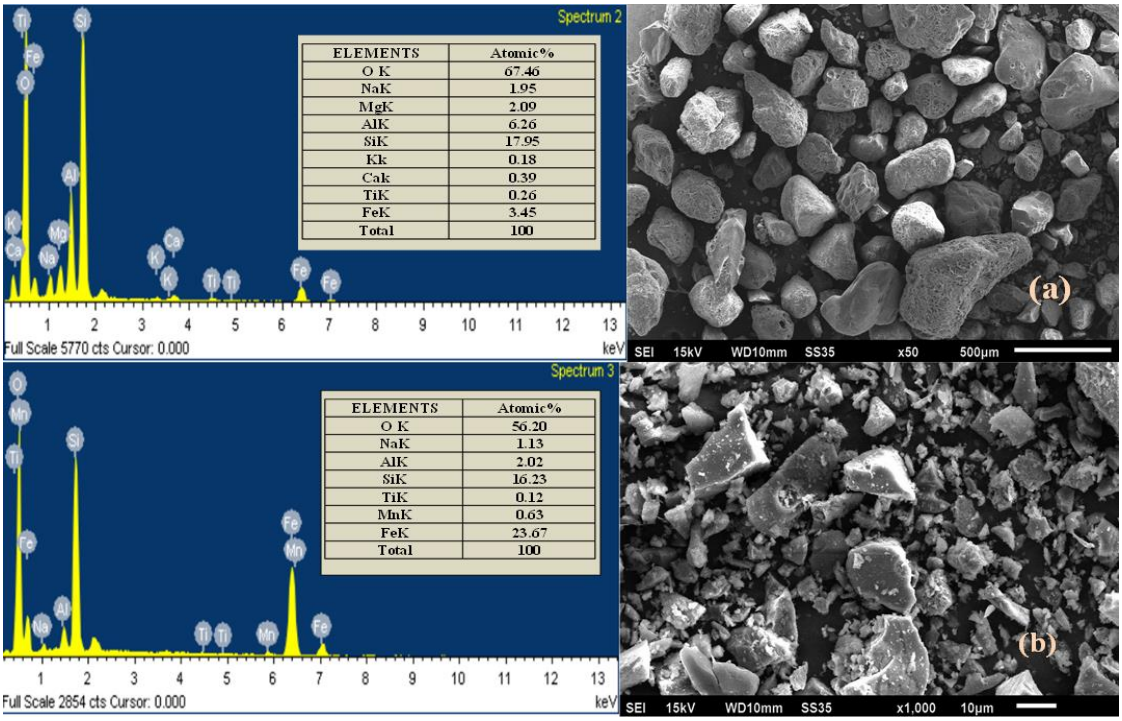

Fig. 3. 1 (a) Compositional characterization through SEM/EDAX analysis of Furnace blast sand (FBS) (b) Compositional characterization through SEM/EDAX analysis of Foundry sand (FBS)

3.5.2 Fabrication of the support/uncoated beads

Throughout we used the nomenclature of beads i.e., clay beads and $FeTiO_2$-coated beads made up of:

- Foundry Sand (FS)
- Furnace Blast Sand (FBS)
- Clay

To make the spherical beads, FS and FBS were mixed with clay in a specific 2:1:1 ratio and subsequently air-dried at room temperature. This particular mixture ratio was chosen based on its demonstrated efficacy in enhancing the composite's structural integrity, as outlined in our previous research findings (Bansal and Verma 2017). The clay component in this process served as a vital binding agent for the bead formation. The beads were meticulously measured to possess a diameter of 12 mm, assessed from four distinct orientations using a vernier calliper. Following this measurement, the beads were subjected to a thermal treatment at 800 °C for a duration of approximately 1.5–2.0 h, and later, they underwent a curing process lasting 48 h in water. This curing procedure has been recognized to significantly bolster the support material's

durability and strength, a fact supported by the work of (Amadi and Osu 2018). The fabrication process is shown in Fig. 3.2. Before the intended use, the pH of the effluent was made acidic, which serves the purpose of facilitating the leaching of iron from the beads, which shows the presence of Fe^{2+} and Fe^{3+} ions within the solution. Subsequently, these beads were employed to investigate the impact of the Fenton and photo-Fenton processes on the removal of color from actual wastewater sourced from the P&P industry.

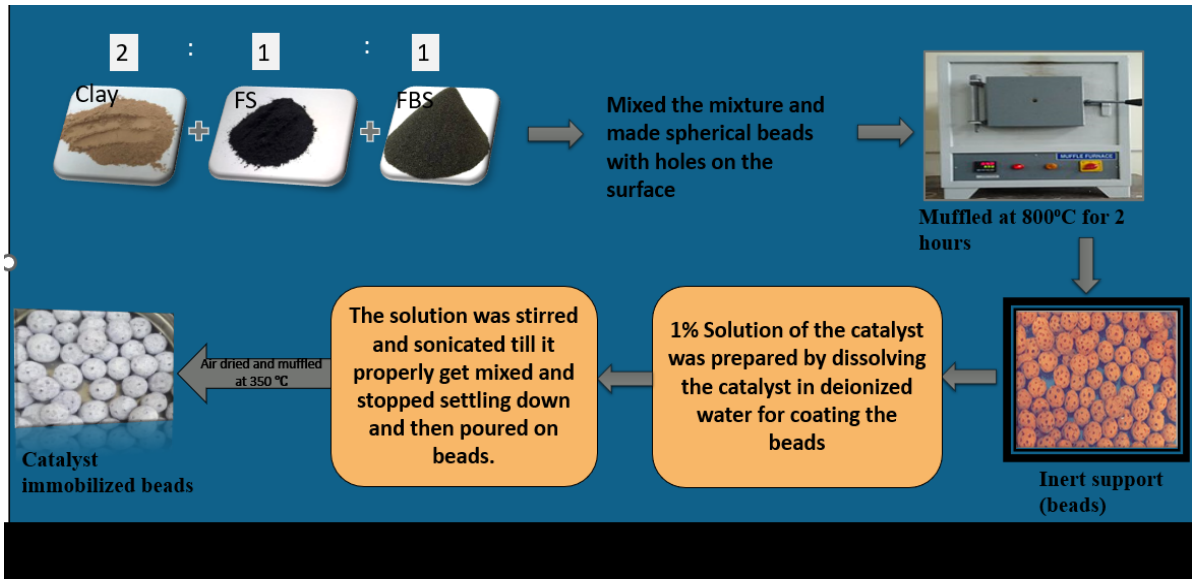

Fig. 3. 2 Fabrication of the composite beads

3.5.3 Clay Beads fabrication for Photocatalytic Applications

In the absence of FS and FBS (i.e. iron source), simple clay beads were prepared and subjected to 800 °C heating for 1.5-2.0 h. Subsequently, a 1% (w/v) TiO_2 catalyst coating was applied to these beads through the dip-coating method, as detailed in the work by (Bansal and Verma 2017). Before the coating process, the TiO_2 mixture underwent sonication to ensure homogenous particle dispersion. To achieve comprehensive coverage of the beads, they were coated twice with the TiO_2 solution. After allowing the beads to air dry at room temperature, they were treated in a muffle furnace at 350 °C for 1.5 h to ensure optimal adhesion of the TiO_2 to the composite beads' surface. After this, a thorough washing with distilled water was carried out to remove any loosely bound TiO_2, followed by oven drying at 100 °C for further processing.

3.5.4 Fabrication of Fe-TiO_2 composite beads

The beads were handcrafted with precise control over their size, composition, and structure. The initial blank beads mentioned in **subsection 3.5.3** were coated with a 1% (w/v) sonicated TiO_2 solution to make composite beads. The beads were double-coated with catalyst to assure adequate coverage. The coated beads were then desiccated at room temperature and heated for 1.5 h at 350 °C. Fig. 3.3 depicts images of uncoated beads and beads coated with TiO_2, while Fig. 3.4 depicts elemental mapping confirming the presence of iron and TiO_2 in composite beads. As depicted in Fig. 3.5 scanning electron microscopy (SEM) analysis revealed that the TiO_2 coating on the support had a thickness of 71µm. Following the immobilisation of TiO_2, the supports were referred to as 'composite' to signify that they contained both catalysts (iron from FS & FBS) and TiO_2). Then, these Fe-TiO_2 composite nanoparticles were used to study the fixed mode hybrid effect.

Fig. 3. 3 Image of Uncoated and TiO_2-coated beads

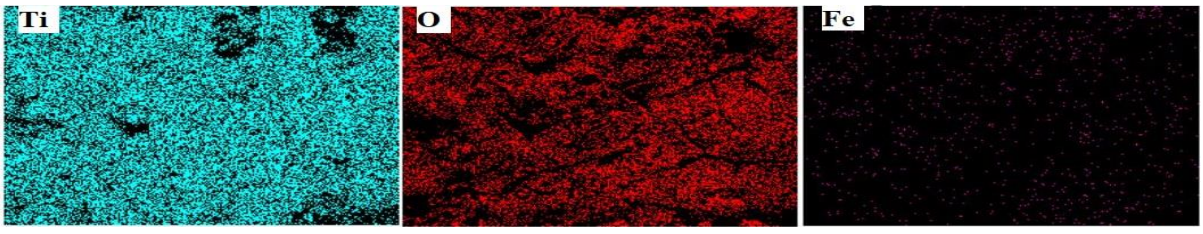

Fig. 3. 4 Elemental mapping of the fabricated catalyst

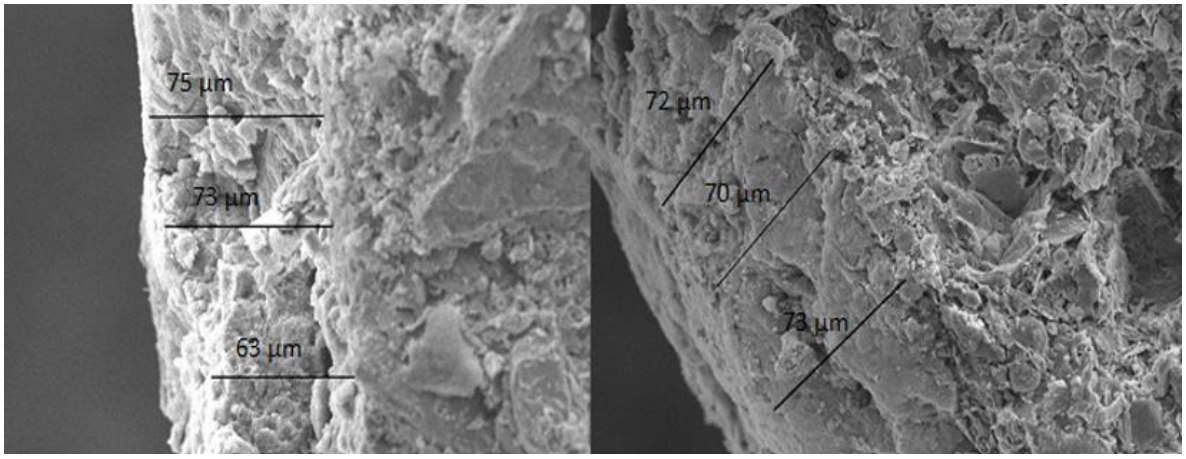

Fig. 3. 5 SEM analysis of TiO_2 coating thickness

3.5.4.1 Leaching of Iron from the Composite beads

The present investigation can be ascribed to the concurrent in-situ impact of the active TiO_2 layer, as elucidated in the preceding section, which induces photocatalysis. Additionally, it explores the release of iron from the beads in acidic conditions, subsequently triggering a photo-Fenton process. To assess the extent of iron leaching from the beads into the solution, the concentrations of ferric and ferrous ions were monitored at specified time intervals (refer to Table 3.1), following the methodology outlined in APHA (2017).

Table 3. 1 Iron leaching in the form of Total, ferrous, and ferric iron

Time (min)	Ferric (µg L^{-1})	Ferrous ion (µg L^{-1})	Total iron (µg L^{-1})
20	40	41.15	81.15
40	41.92	46.92	88.84
60	44.23	51.53	95.76
90	36.53	56.53	93.06
120	37.69	61.92	99.61

3.5.4.2 Characteristic analysis of the composite beads

Before going into process detail, let's first discuss the need to perform these characterization techniques:

- **UV-DRS**: The UV-Visible Diffuse Reflectance Spectroscopy (UV-DRS) analysis of the beads was conducted to verify the reduction in the bandgap of TiO_2 after incorporating FS and FBS as iron sources. This analysis is crucial for understanding the impact of these iron sources on the photocatalytic properties of TiO_2, as a reduced bandgap can enhance the material's ability to absorb visible light, thereby improving its photocatalytic efficiency.
- **XRD**: The X-ray Diffraction (XRD) technique was employed to confirm the formation of complexes between iron and TiO_2, validating the successful synthesis of the composite material. XRD gives insights into the crystalline structure and phase composition. The presence of these complexes indicates a successful doping process. By incorporating iron, the bandgap of TiO_2 can potentially be reduced. This has been confirmed through the use of additional techniques such as UV-DRS, which directly measures changes in the bandgap as explained earlier. he reduced bandgap enhances the material's photocatalytic activity by making it more responsive to visible light, thereby improving its efficiency in applications like wastewater treatment.
- **SEM/EDS**: It is capable of evaluating the consistency of the elemental distribution in the composite material. Ensuring even dispersion of elements is crucial for maintaining the material's overall properties and performance. SEM can provide highly detailed images of the surface morphology of the composite material. It confirms the intactness of TiO_2 on the surface of beads. Whereas EDS can easily determine the elemental composition of the material. It can identify and quantify the presence of different elements within the composite, verifying the incorporation of specific elements like Fe, Ti, O, etc.
- **FTIR:** FTIR (Fourier Transform Infrared Spectroscopy) analysis reveals valuable insights into the chemical bonds and functional groups found within the composite material. Through the identification of characteristic absorption bands, FTIR can determine the various types of chemical bonds and functional groups present in the material. This includes bonds like Ti-O, Fe-O, or any other relevant bonds found in a TiO_2-iron composite. FTIR is capable of detecting structural changes that arise from the inclusion of various elements or compounds. For instance, it can detect alterations in the TiO_2 lattice when iron is added, which could be seen through shifts or variations in the intensity of certain absorption bands.

- **XPS**: X-ray Photoelectron Spectroscopy (XPS) is crucial for analysing composite materials like a TiO_2-iron composite due to its ability to provide detailed information on elemental composition and chemical states. With XPS, one can easily differentiate between various oxidation states of elements, like Fe^{2+} and Fe^{3+}, and gain insights into surface interactions. This technique allows the analysis of chemical bonding and interactions occurring at the surface. This technique is invaluable for understanding the material's electronic structure and optimizing its properties for applications like photocatalysis in wastewater treatment.

In this comprehensive investigation of the hybrid process, we conducted a thorough analysis of spherical Fe-TiO_2 beads to confirm the coexistence of iron and TiO_2 within a single system. Various analytical techniques, including UV-DRS (Ultraviolet-Visible Diffuse Reflectance Spectroscopy), XRD, FT-IR, and SEM-EDS (Scanning Electron Microscopy with Energy-dispersive Spectroscopy), were employed. The chemical composition, morphology, and uniformity of the catalyst were assessed using a Scanning Electron Microscope (SEM) (JSM-6510LV, JEOL (Japan)) equipped with EDS. To enhance sample conductivity, a platinum layer was uniformly deposited on the specimens using an auto fine coater (Model: JEC-3000FC). For crystallographic analysis, XRD was conducted over a scanning range of 20–80 degrees using an X'Pert high score instrument, with Copper-Kα radiation at λ=1.5418 Å. The bandgap energy of the catalyst was determined through UV-vis diffuse reflectance spectroscopy (DRS) using a UV-2600 spectrometer by Shimadzu (Asia Pacific). $BaSO_4$ was employed as a standard reflectance, and measurements were taken within the wavelength range of 200-800 nm. Furthermore, the evaluation of compound bonding, linkages, and functionalized groups was performed using a Fourier Transform Infrared Spectrophotometer, model RZX (Perkin Elmer), with KBr pellets, scanning across the range of 4000 to 200 cm^{-1}. FTIR spectra were generated by mixing 0.5 mg of the synthesized material with 20 mg of potassium bromide.

3.5.4.3 Experimental Setup and Methodology for Investigating Hybrid Effects in Laboratory-Scale Reactors

The lab-scale photocatalytic reactions were performed in the sunlight at the Thapar Institute of Engineering and Technology, Patiala, between 11:30 am and 3 pm (30.3564° N, 76.3647° E). The average solar intensity during this period was measured to be 553 W m^{-2} using a lux meter. The reactions were conducted in batch-scale glass reactors (height 5 cm × diameter 17 cm) having a capacity of 1000 mL, and composite beads covered the reactor

surface as shown in Fig. 3.6. For every batch reaction, 200 mL of effluent was used as a working solution for treatment, and the desired pH was maintained using acetate buffer for both the effluents i.e., UASB, outlet stream and alkali stream. An acidic pH was maintained to initiate the photo-Fenton process, and H_2O_2 was used as an oxidant. The two air spargers were placed at an equal distance from the reactor's centre, and the flow rate was kept constant at 3.5 mL min^{-1} to maintain reaction consistency. The process optimization involved the systematic variation of several parameters, including H_2O_2 dosage, pH level, bead size, and catalyst dose. All experiments were conducted in triplicate, with the results presented as the mean of the three samples, and error bars representing the standard deviation are depicted in the figures. The % color reduction was calculated using Eq. 3.1 and the % COD removal was determined using Eq. 3.2.

$$\%\ \boldsymbol{color\ removal} = \frac{\boldsymbol{i-f}}{\boldsymbol{i}} \times \mathbf{100} \qquad \mathbf{3.1}$$

Where i = initial concentration of color and f = final concentration of color after treatment.

$$\%\ \boldsymbol{COD\ removal} = \frac{\boldsymbol{C_i - C_f}}{\boldsymbol{C_i}} \times \mathbf{100} \qquad \mathbf{3.2}$$

Where C_i = initial COD (mg/l) and, C_f = final COD after treatment.

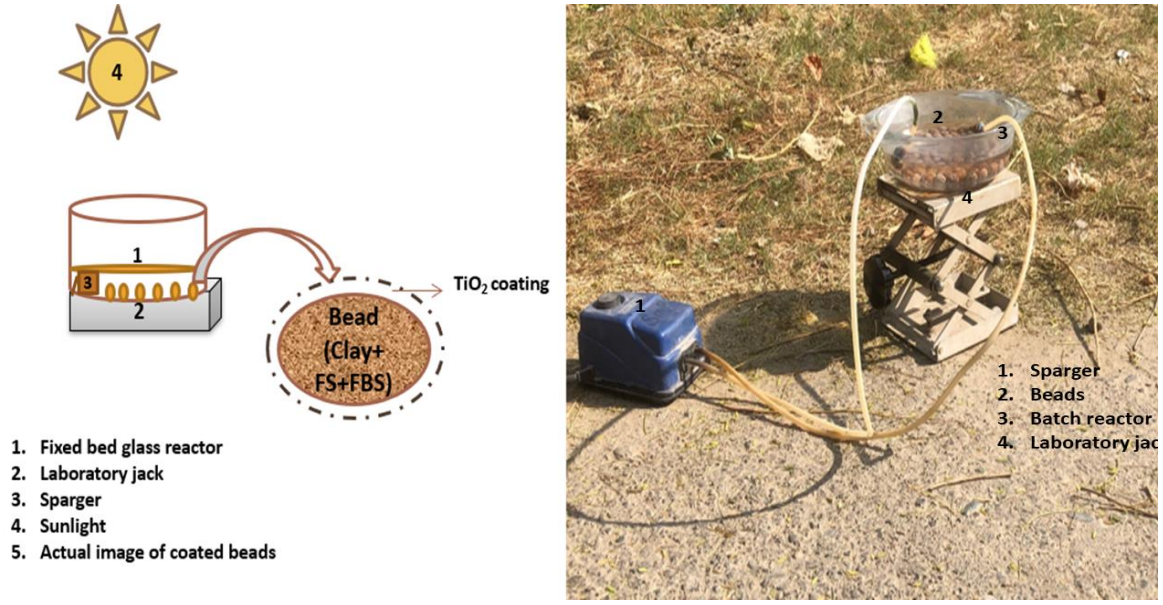

Fig. 3. 6 Line diagram and actual image of Batch scale glass reactor

3.5.4.4 Recirculating fixed bed reactor at a pilot scale

For the treatment of actual wastewater from the P and P industry, a solar flat-bed glass reactor (measuring 40 cm × 20 cm × 2.5 cm) was employed. The reactor featured a single inlet and outlet and was equipped with four removable baffles, as illustrated in Fig. 3.7. Designed to handle a maximum volume of 5L, the reactor operated in a recirculation mode. The respective stream, along with an appropriate quantity of oxidant, was conveyed from the storage tank to the reactor. Here, it traversed through composite beads at an optimal flow rate before returning to the storage tank. To maintain a stable acidic pH, acetate buffer was added to the solution after it had undergone pre-treatment through the coagulation/flocculation process. Regular sampling involved collecting approximately 4-5 ml samples at specified intervals for subsequent analysis.

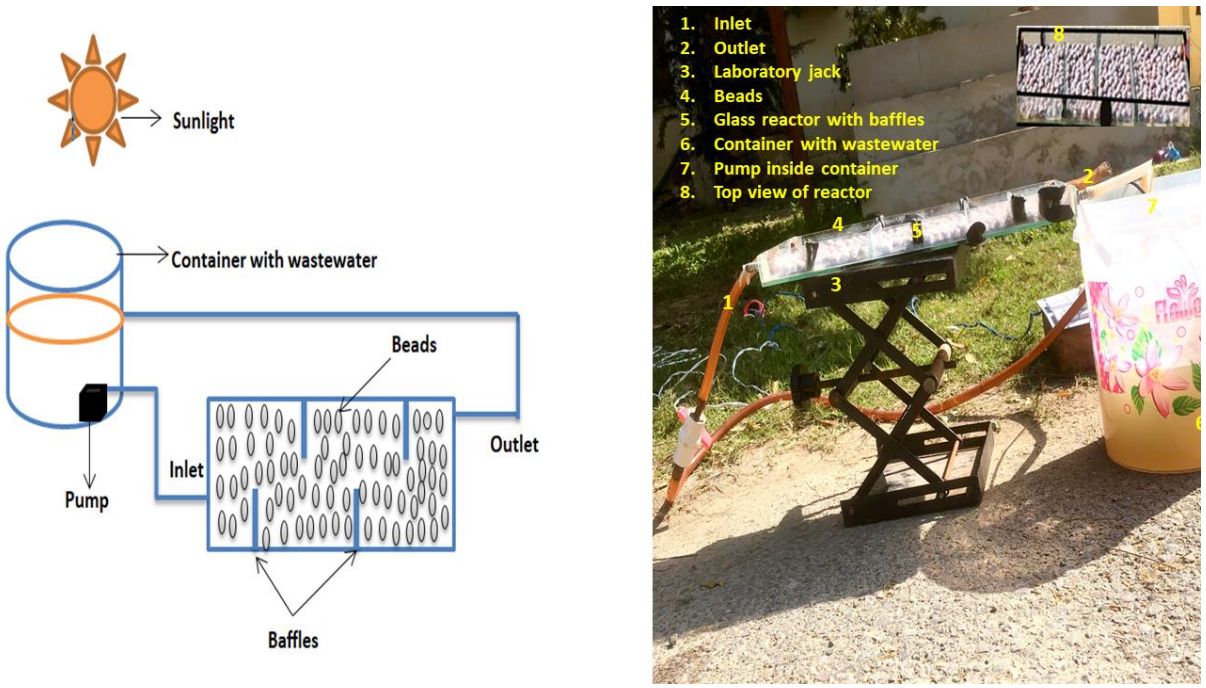

Fig. 3. 7 Line diagram and actual image of recirculating glass reactor

3.5.4.5 Solar fixed-bed reactor at the pilot scale with a once-through operation.

To achieve color removal, the existing system employs a configuration consisting of three interconnected glass reactors arranged sequentially. Each reactor has dimensions of 40 cm in length, 20 cm in width, and 2.5 cm in height. In this study, these reactors are filled with Fe-TiO_2 composite beads to enable a dual process when exposed to solar radiation. The entire system operates continuously, with a cylindrical tank used for pumping real wastewater streams

into the reactor. A peristaltic pump maintains a consistent flow, with the outlet of the first reactor connected to the inlet of the second reactor, and this connection continues for subsequent reactors in the system. Fig. 3.8 illustrates the schematic diagram of the once-through reactor. All experiments were conducted between September and October, from 11:00 AM to 2:30 PM, at the Thapar Institute of Engineering and Technology in Patiala, India, located at coordinates 30.3564° N latitude and 76.3647° E longitude. To initiate the reaction, a sequence of fixed bed solar reactors was exposed to direct sunlight, with the outlet of the first reactor serving as the inlet for the next. A lux meter was utilized to measure solar irradiation at regular intervals, typically ranging from 590 to 600 W/m^2.

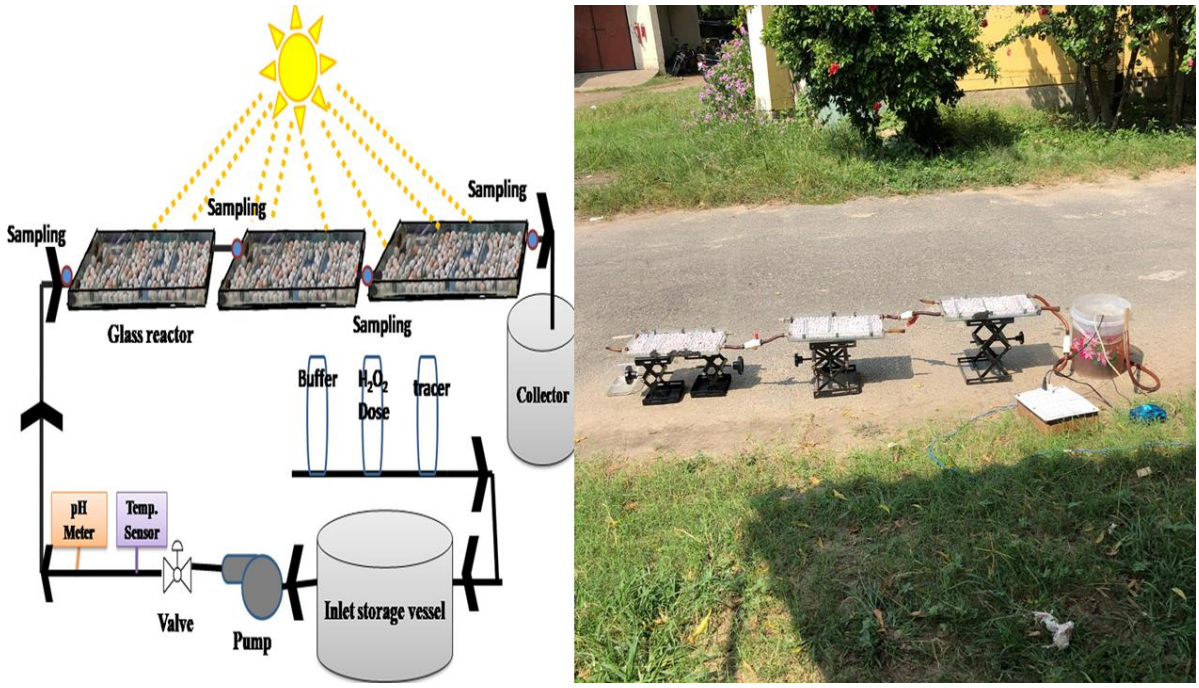

Fig. 3. 8 Line diagram and actual image of the once-through pilot-scale reactor

3.5.4.6 Mathematical modelling used in the present study:

3.5.4.6.1 Box-Behnken design

BBD is a statistical method used for the optimization of processes. Its application in wastewater treatment, particularly for color removal, offers several advantages:

- Optimization of Multiple Variables: It allows for the simultaneous optimization of multiple factors, which is crucial in complex processes like wastewater treatment where variables such as pH, coagulant dosage, and catalyst dose need to be optimized.

- Efficiency: The design requires fewer experimental runs compared to other response surface methodologies, making it more cost-effective and time-efficient.
- Interaction Effects: It can accurately simulate the interactions between variables, giving a thorough grasp of the dynamics of the process and aiding in the determination of the best conditions for optimal color removal.

3.5.4.6.2 Log-Linear Model

The Log-linear model is used to describe the relationship between variables through a logarithmic transformation. Its application in wastewater treatment can be explained by:

- Simplification of Non-Linear Relationships: Processes in wastewater treatment often display non-linear relationships. The Log-linear model simplifies these relationships, making them more accessible for analysis and interpretation.
- Handling Large Variability: The model is highly effective in handling data that covers a wide range of values, which is often encountered in wastewater treatment processes due to the significant variations in pollutant concentrations.
- Statistical Analysis: It enables the application of linear regression techniques to test hypotheses and make predictions, offering a strong framework to comprehend the impact of various treatment conditions on color removal.

3.5.4.6.3 Weibull Model

The Weibull model is a highly flexible statistical model commonly employed in survival analysis and reliability engineering. When it comes to wastewater treatment:

- Flexibility: Weibull models can match a wide range of data patterns observed in treatment procedures since they can take on multiple shapes based on their parameters.

3.5.4.6.4 Biphasic Model with Shoulder

This model is appropriate for understanding the intricate kinetics of color removal processes that do not adhere to simple first-order kinetics. Detailed Mechanistic Insights: The model provides a more detailed understanding of the treatment dynamics, allowing for better control and optimization of the process.

To design the experiment, we utilized Design Expert software, employing the principles of Response Surface Methodology (RSM). RSM comprehends a wide array of statistical and mathematical techniques tailored for modelling and interpreting results when the outcome of interest is influenced by various variables. This software helps to optimize the response by examining the impact of different parameters. RSM proves invaluable in this context due to its efficiency in saving time and facilitating the comprehension of relationships between controlled input parameters and response variables, collect data rapidly and reliably, and substantially reduce the number of required experimental trials, thereby saving money and time (Tan et al. 2017). Therefore, RSM is efficaciously executed in optimization of different parameters for removal of color from real P & P industry wastewater. Hence, the implementation of RSM has proven to be effective in optimizing several parameters pertaining to colour removal. The Response Surface Methodology (RSM) is a commonly employed numerical and statistical approach for modelling and analysing processes in which the outcome of interest is influenced by various parameters. This approach seeks to optimise the response (El-Naas et al. 2016; Yousefi et al. 2021). The variables that influence the process are known as independent variables, while the outcomes are known as dependent variables (Khuri and Mukhopadhyay 2010). The response variables were modelled using a second-order nonlinear regression model in the form of a quadratic polynomial equation, as represented by Eq. 3.3.

$$\boldsymbol{R = \beta_0 + \sum_{i=1}^{K} \beta_i x_i + \sum_{i=1}^{K} \beta_{ii} x_{i^2} + \sum_{i,j=1} \sum_{i<j} \beta_i x_i x_j} \qquad \textbf{3. 3}$$

In this context, we designate constant regression coefficients as β0, βi, βii, and βij. The coded input factors are represented as xi and xj, while e stands for the error function, and R represents the response variable.

First-order, 2k factorial, Plackett–Burman, and simplex designs are among the most frequently used design strategies. First-order polynomials, while useful, have limitations in terms of stability, variance prediction, and addressing lack of fit issues arising from surface curvature and factors. Therefore, second-order polynomial studies are required to develop a quadratic response surface model, mitigating the drawbacks of first-order designs and enhancing the optimization procedure. Second-order symmetrical designs like the Box–Behnken design, Do Ehlert design, central composite design, and three-level factorial design are all viable options. For our current investigation, we opted for the Box–Behnken design.

3.5.5 Box-Behnken design

The Box-Behnken design was introduced by George Box and Donald Behnken in 1960. As depicted in Fig. 3.9 this design offers a three-factor layout that facilitates the accurate evaluation of both first- and second-order coefficients within the mathematical model (Özgen and Yildiz 2010). It represents a subset of 3 k factorial combinations, making it exceptionally advantageous and cost-effective in situations involving a large number of variables, such as industrial research (Khuri and Mukhopadhyay 2010).

Box–Behnken designs (BBD) are classified as rotatable or nearly rotatable. They are constructed using a three-level approach per factor (-1, 0, +1), avoiding the design space's extremities by combining the cube's center and extreme levels. Therefore, BBD is a combination of fractional factorial and incomplete block designs, purposefully excluding the extreme vertices to maintain the design's rotatability (Hanrahan and Lu 2006). To determine the number of experimental trials (N) required for optimizing process parameters, you can utilize the formula provided in Eq. 3.4, as detailed by (Bezerra et al. 2008).

$$\boldsymbol{N = 2k(k-1) + C_0} \qquad \textbf{3. 4}$$

where k represents the number of factors and C_0 represents the number of replicates for the central coordinates. So, Box-Behnken is a good and efficient design under response surface methodology because it can be used to do things like (i) find models that fit (or don't fit), (ii) build sequential designs, (iii) use blocks, and (iv) estimate quadratic model parameters (Ferreira et al. 2007). The experiments were designed using RSM by BBD through design expert software. The experimental design utilized the statistics software Design-Expert 6.0.8, developed by Stat-Ease Incorporated and headquartered on East Hennepin Ave, Minneapolis, United States. The RSM aids in the analysis of experimental data along with the optimization of selected input operational parameters such as H_2O_2 dose (A), pH (B), and surface area covered by beads (C). An analysis of variance (ANOVA) was used to figure out how the operational process factors affected the responses.

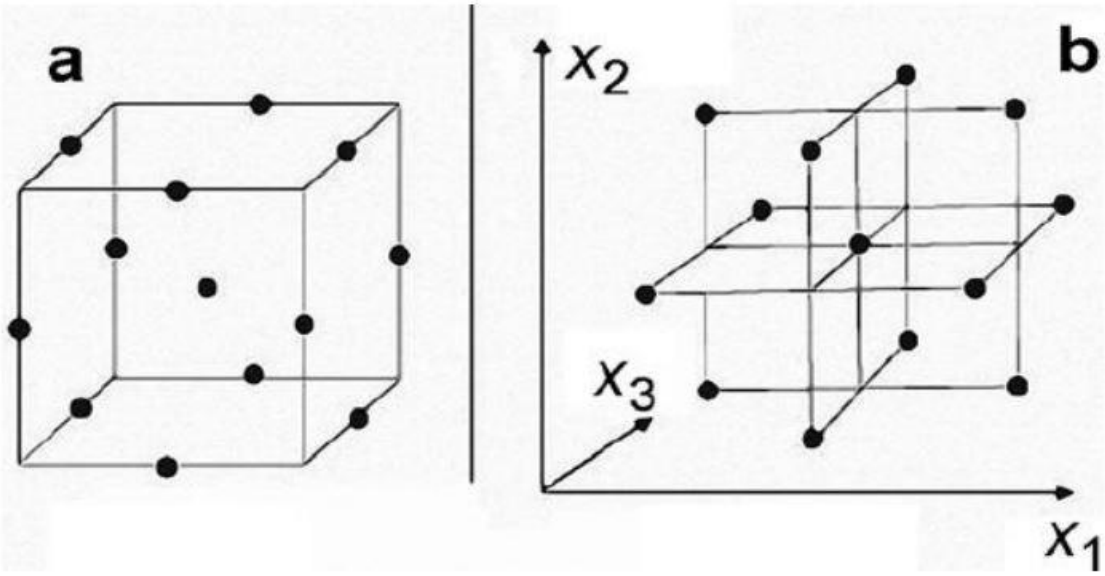

Fig. 3. 9 Box–Behnken design for a three-factor experiment (Kandananond 2010)

3.5.5.1 Kinetic models in wastewater color removal

To analyse color removal, three distinct kinetic models were employed: log-linear, Weibull, and biphasic shoulder, which are described below. The experimental data was subjected to non-linear regression analysis to determine the kinetic coefficients. For fitting the experimental values, Microsoft Excel's Solver tool and the software GinaFiT (developed by (Geeraerd et al. 2005) were utilized. The accuracy of the discoloration results fitting was assessed using RMSD and R^2 values. Additionally, mathematical and experimental results were graphically compared to ensure the adequacy of the selected models.

3.5.5.1.1 Log-linear model

It is an evolved version of Chick's equation, which shows the relationship between the amount of color removal and the amount of catalyst used for color removal as given in Eq. 3.5.

$$logC = \log C_0 - \frac{K_{MAX}.t}{\ln 10} \qquad \textbf{3. 5}$$

Where K_{MAX} = Rate of color removal and t = Time (min.)

3.5.5.1.2 Weibull model

The Weibull model is a probabilistic model that provides a comprehensive description of the variability in system behaviour. This model accounts for the heterogeneous nature of pollutant distribution. Moreover, the efficiency of pollutant removal is influenced by the

duration of exposure to stress conditions and the required contact time for each pollutant molecule to undergo mineralization. The mathematical representation of the Weibull model is given by Eq. 3.6.

$$\boldsymbol{logC = logC_0 - \left(\frac{t}{\delta}\right)^m} \qquad \textbf{3. 6}$$

In the equation, the variables are defined as follows: C represents the change in concentration over time, C_0 is the initial concentration of the pollutant, δ stands for the initial decimal reduction time in minutes, and m represents the curve shape factor.

3.5.5.1.3 Biphasic model with the shoulder

The equation provided represents a modified version of the biphasic model, which accounts for curves exhibiting a preceding shoulder phenomenon. This model captures the characteristics of the biphasic behaviour while incorporating the presence of a shoulder. The mathematical expression for the biphasic shoulder model is given by Eq. 3.7.

$$\boldsymbol{log\frac{N_t}{N_0} = log\left\{fe^{-K_1 t}\frac{e^{Ks_1}}{\left(e^{Ks_1-1}\right)e^{-K_1 t}} + (1-f)e^{-K_2 t}\left\{\frac{e^{Ks_1}}{1+e\,K_{s_1}{}^{-1}e^{-K_1 t}}\right\}^{\frac{K_1}{K_1}}\right.} \qquad \textbf{3. 7}$$

Where N represents the total quantity of pollutants and N_1 and N_2 represent the number of non-mineralized pollutants. F is defined as $N_1(0)/N_2(0)$ and K_1 = First kinetic rate constant.

Chapter 4

Results and Discussion

4.1 Overview

This chapter deeply discusses the different real agro-based P&P industry streams and their treatment. Various parameters helped in determining the efficacy of the process. Efforts have been made to explore how the coexisting operation of two different processes in a fixed manner within the same system when exposed to natural solar radiation, can enhance process efficiency and shorten the treatment duration. The hybrid effect was also studied using a dual process along with coagulation/flocculation. Coagulation/Flocculation here served as a pretreatment for two of the streams which were highly colored so, the dual process being an AOP cannot be applied directly as discussed in the chapter 3. In this current study, we've endeavoured to incorporate both photocatalysis and photo-Fenton simultaneously within the same system. This in-situ dual process effectively addresses the individual shortcomings of photocatalysis and photo-Fenton, such as electron-hole recombination, iron sludge generation, and extended treatment time. The dual in-situ process produced an abundance of hydroxyl radicals. The findings substantiate a significant decrease in treatment time with the in-situ dual process compared to individual processes (photo-Fenton or photocatalysis). Incorporating waste materials like FBS and FS underscores the economic viability of the process.

The study has been carried out In fixed form for all three different reactors I.e., Batch, recirculation, and, once through reactors. Extensive research was conducted to determine the effect of various operational factors, including the size of the support material, the amount of catalyst in terms of % surface area covered by the beads, pH, and the oxidant dose. The selected support material adds new dimension to the process by generating in-situ photo-Fenton (modified in-situ dual process) for the color removal of particular streams. Durability analyses were conducted on the immobilized catalyst structure to assess the economic viability of the technology as presented.

Color removal studies were carried out systematically for all the selected streams. The process optimization was performed for all the streams mostly manually and some streams we used the design expert software.

Different glass reactors of different capacities for batch, recirculation study and scale-up once through glass reactor in series were used.

Section-A

- Selection of different streams from agro-based P & P industry.
- Selection of different novel support material and fabrication of the composite.
- Flow chart of work flow of different selected streams.

Section-B

- Study of UASB stream in Batch, recirculation, as well as once through mode along with the parametric optimization.
- Coagulation/Flocculation was studied as a pre-treatment followed by advanced treatment technique.
- Durability studies were conducted in terms of a number of recycles along with the leaching of iron content and further reconfirmed using various characterizations including SEM/EDX, XRD, FT-IR, and UV-DRS.
- Cost of the stream was also calculated for the scale-up study using once through process.

Section-C

- Study of I/L stream in Batch, recirculation, as well as once through mode along with the parametric optimization.
- Coagulation/Flocculation was studied as a pre-treatment followed by advanced treatment technique.
- Durability studies were again conducted for I/L stream to confirm the behaviour of composite as this stream is different than the first one.
- Cost analysis was performed for Once through process in scale-up study.

Section-D

- Study of O/L stream in Batch, recirculation, as well as once through mode along with the parametric optimization.
- Direct advanced treatment technique was studied for O/L stream.
- Durability studies were again conducted for O/L stream to confirm the behaviour of composite, as this stream is different than the other two streams.
- Cost analysis was performed for Once through process in scale-up study.

Section A

4.2 Industrial streams selection

The targeted streams were chosen based on preliminary visits to the P&P industry for the treatment of a major industrial problem, i.e., residual color in treated wastewater. After visiting the whole paper manufacturing plant including the effluent treatment plant (ETP), three different areas/streams were targeted to check the feasibility of the treatment technology as shown in Fig. 4.1.

- The first stream that was selected is known as the UASB stream as it comes just after UASB treatment and comprises the highest amount of the color. The UASB stream in the paper industry is an effluent stream that emerges after Up-flow Anaerobic Sludge Blanket (UASB) treatment, typically rich in color due to high lignin content. This stream originates from the straw washing and pulping processes, where lignin and other organic materials are released during the breakdown of plant fibers, contributing to its dark appearance.
- The I/L stream in the paper industry refers to an alkali waste stream, primarily originating from the chemical recovery process during pulp production. This stream typically contains residual chemicals like sodium hydroxide and other byproducts from the pulping and bleaching stages. The I/L stream has high color but relatively lesser than the UASB stream.
- The O/L stream in the paper industry is the final effluent stream, emerging after secondary treatment processes. While it still contains some residual color, mainly from remaining organic compounds like lignin, its color intensity is lower compared to the UASB and I/L streams. Despite the reduced color, the O/L stream typically has a higher volume, as it collects and processes the combined wastewater from various stages of the pulp and paper production.

The present study focused on checking the feasibility of the advanced techniques on all the streams either isolated or in combination with other processes. Fig. 4.1 shows processes in the P&P industry plant and the different targeted streams. After the effluents were collected, they were characterized to check various initial parameters which are shown in Table 4.1.

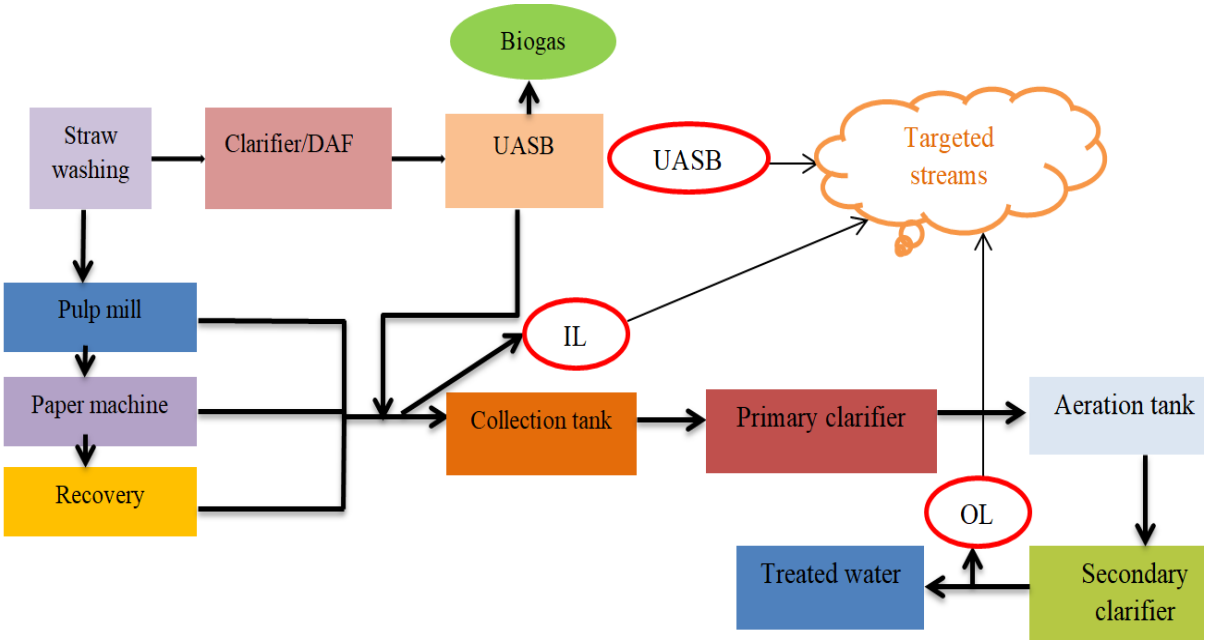

Fig. 4. 1 Targeted wastewater streams from the P&P industry

Table 4. 1 Characterization of different targeted streams

Type of effluent	TDS (ppm)	TSS (mg/L)	pH	COD (mg/L)	Color (a.u.)
UASB	2250-2300	1170	7.5	2200-2500	0.8
I/L	2600-2700	1140	8.2	1600-1800	0.69
O/L	1600-1700	570	7.8	200-250	0.14

4.2.1 Selection of the support material

Throughout we used nomenclature of beads i.e., clay beads and $FeTiO_2$ coated beads made up of:

- Foundry Sand (FS)
- Furnace Blast Sand (FBS)
- Clay

After conducting a literature review and a series of preliminary experiments, clay was chosen as the support material due to its inert nature, cost-effectiveness, and durability. FS and FBS were used as substitute materials for iron as they are good source of iron, provides better strength to the support material, and are readily available. Additionally, using these waste materials aligns with sustainable practices by repurposing industrial by-products, thus contributing to cost reduction and environmental conservation.

To create the spherical beads, FS and FBS were mixed with clay in a 2:1:1 ratio, chosen for its effectiveness in enhancing the composite's structural integrity, as reported by(Bansal and Verma 2017) . The beads, each 12 mm in diameter, were measured using a vernier caliper and then thermally treated at 800 °C for 1.5–2 hours, followed by a 48-hour water curing to improve durability (Amadi and Osu 2018). The fabrication process is shown in Fig. 4.2. Prior to the intended use, the pH of the effluent was made acidic in nature, which serves the purpose of facilitating the leaching of iron from the beads, which shows presence of Fe^{2+} and Fe^{3+} ions within the solution. Subsequently, these beads were employed to investigate the impact of the Fenton and photo-Fenton processes on the removal of color from actual wastewater sourced from the P&P industry.

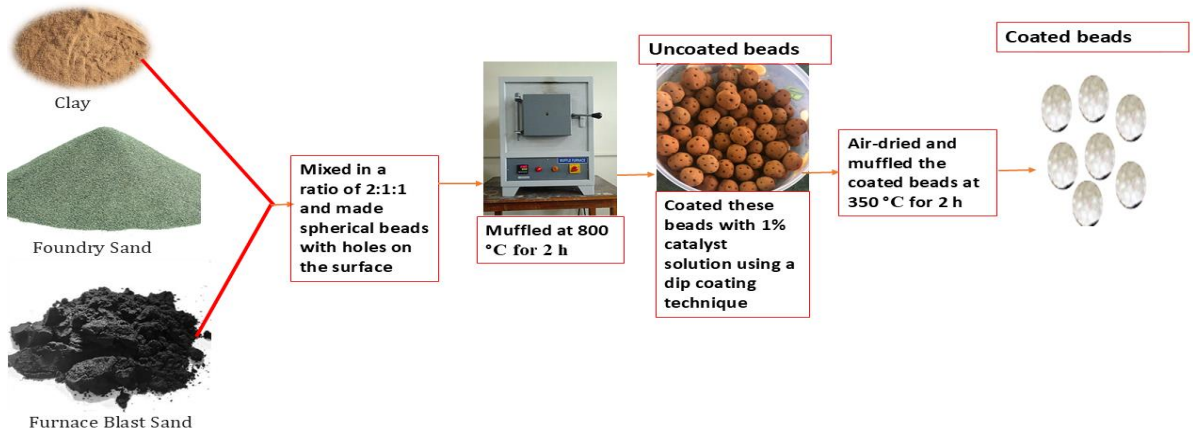

Fig. 4. 2 Fabrication of the composite beads

4.2.2 Fabrication of Fe-TiO_2 composite beads

The beads were carefully handcrafted to ensure consistent size, composition, and structural integrity. Initially, blank beads, as described in subsection 4.2.1, were coated with a 1% (w/v) TiO_2 solution that had undergone sonication to form composite beads. To achieve sufficient

catalyst coverage, a double coating was applied. The coated beads were then air-dried at ambient temperature and subsequently heated at 350 °C for 1.5 hours. Figure 4.3 illustrates the appearance of both uncoated and TiO_2-coated beads.

Fig. 4. 3 Image of Uncoated and TiO_2 coated beads

4.2.3 Roadmap followed for all the selected streams

For the UASB and I/L streams, a slightly modified approach was employed by integrating coagulation/flocculation as a pretreatment step. This pretreatment was crucial due to the intense coloration of these streams, which hindered light penetration during the dual process. By initially reducing the color intensity, the effectiveness of the AOP, specifically the dual technique, was significantly enhanced for both streams. This strategic modification ensured optimal treatment performance and improved overall efficiency.

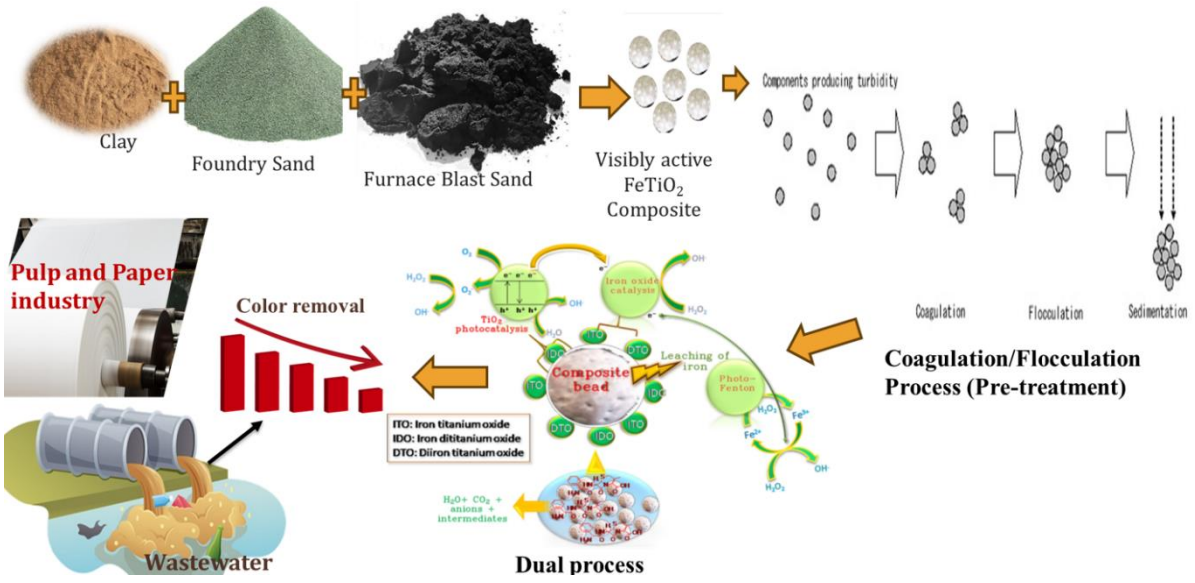

Fig. 4. 4 Approach followed for UASB and I/L stream

❖ For O/L stream direct AOP was applied as it does not contain as much color as the other two streams, so light penetration was not an issue in this case.

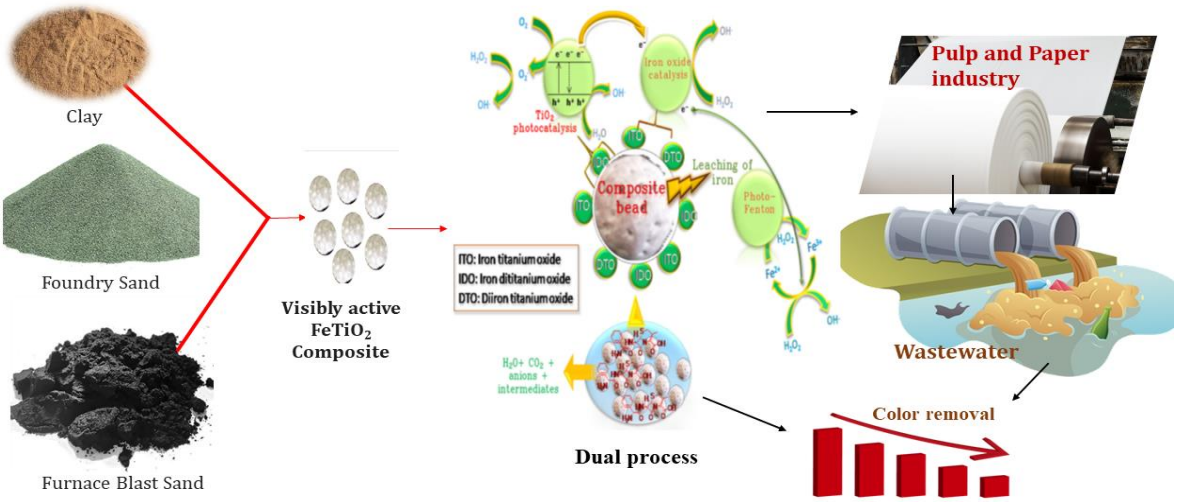

Fig. 4. 5 Approach followed for O/L stream

Section B

4.3 Preliminary study of UASB stream

As stated earlier, this stream had a greater amount of color in comparison to other streams. Nevertheless, a notable benefit of this stream is its minimal volume, which facilitates its targeting and management compared to streams with significantly larger amounts of wastewater.

Preliminary reactions in a batch reactor were carried out to establish the boundary conditions. First, the adsorption experiment was carried out in a dark environment with only blank beads, yielding negligible reduction in effluent color. This could be owing to the creation of an effluent monolayer over the beads, resulting in negligible color reduction. Photolysis was also performed under sun irradiation with blank beads covering the reactor's surface. After adding the waste effluent to the reactor, a change in the color of the effluent was detected while it was being exposed to solar light. It was discovered that there was no discernible shift in the color of the effluent. This demonstrated that the solar light by itself was unable to change the concentration of the color of the effluent. Both the absence of light and the presence of sunlight were used to investigate the impact of oxidant dosage on color removal. The findings revealed no discernible change in % color removal. Fig. 4.6 shows all the preliminary reactions performed in dark and sunlight for color removal.

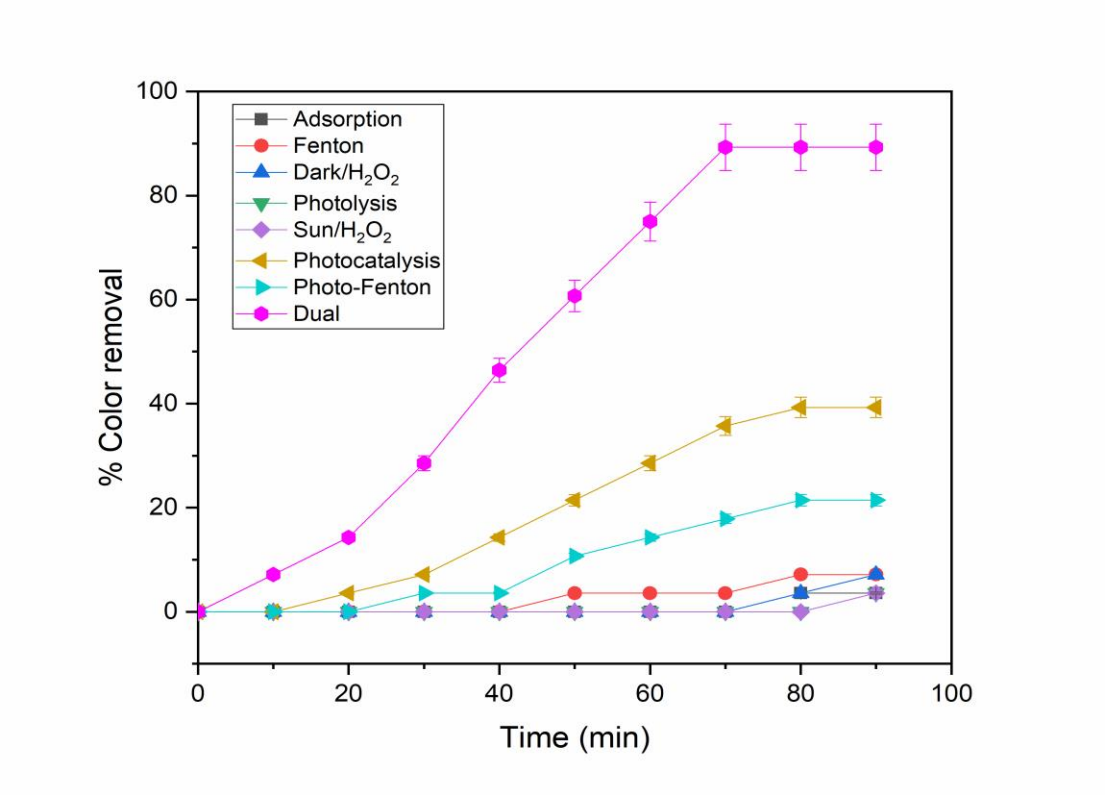

Fig. 4. 6 Preliminary study of UASB stream in dark and sunlight

4.3.1 Combined approach (Coagulation/Flocculation followed by the dual process) for treatment of UASB stream at Batch scale

This technology was developed specifically for the treatment of industrial wastewater one of which is agro-based P&P industry. The treatment method consisted of a two-step process, starting with coagulation-flocculation and progressing to the simultaneous use of photocatalysis and the photo-Fenton process. The implementation of the coagulation-flocculation process was considered necessary because of the high concentration of dark-colored substances in the effluent, which obstructed the penetration of light in the reaction system. The dual-process treatment method, developed for industrial wastewater such as that from agro-based P&P industries, begins with coagulation-flocculation to reduce the high concentrations of dark-colored substances that obstruct light penetration. However, while this process removes a significant portion of color, it also generates large volumes of sludge, which pose disposal and handling challenges. Additionally, coagulation-flocculation is ineffective against certain persistent organic compounds, such as phenols, polyaromatic hydrocarbons (PAHs), and lignin derivatives. This is why in-situ dual process is necessary to remove these resistant compounds and achieve a good amount of color removal.

The coagulation/flocculation procedure was conducted within a temperature range of 25-27 ℃ in a jar testing apparatus. Beakers with a capacity of 1L were employed for treating replicate samples, and the results were obtained by averaging the collected data. Each 1000 mL sample in the beakers received a 12% PAC solution. pH adjustment to the desired level was achieved using either 1M NaOH or 1M H_2SO_4. The sample mixture underwent an initial stirring at 120 rpm for one min., followed by a slow agitation for the subsequent 20 min. Following 60 min. of settling, the supernatant was subjected to separation. The % color and % COD removal were subsequently calculated using the procedures detailed in the material and method section. This procedure guaranteed the acquisition of dependable and consistent data for subsequent analysis.

The dual technique was successfully applied after the initial color reduction was accomplished through coagulation-flocculation, leading to a substantial enhancement in the effectiveness of color removal. The dual technique integrated photocatalysis, where a light-activated catalyst facilitated the breakdown of contaminants, and the photo-Fenton process, which involved the use of hydrogen peroxide and iron under light conditions to generate hydroxyl radicals for efficient pollutant degradation. This sophisticated approach was successfully employed to address the complexities of industrial wastewater treatment, demonstrating a promising avenue for enhanced efficacy in pollutant removal. The comprehensive strategy adopted here not only tackled color issues but also showcased a multifaceted treatment protocol suitable for addressing the challenges posed by agro-based P & P industry effluents.

4.3.1.1 pH optimization for coagulation/flocculation at Batch scale

In the P & P sector, different manufacturing processes generate wastewater that contains suspended particles, including colorants and other pollutants. In this kind of effluent, one would use coagulation/flocculation process frequently as a treatment method. The process efficiency is highly influenced by pH in terms of particle charge and coagulant behaviour. In this study, we aimed to investigate the effect of pH on the efficiency of coagulation/flocculation for removal of colour from the effluent generated by P&P industry. Among these experiments the most favourable results were obtained at pH 5 with pH varied from 4 to 7. P&P industry has a critical economic element in wastewater treatment influencing overall viability and sustainability of such a process. Therefore, it is important in the P&P industry that optimization considers both technical and economic factors. Best % color removal (62.2%) for UASB was

observed at optimized pH 5 as shown in Fig. 4.7 a emphasizing the importance of pH as an important parameter during operations.

4.3.1.2 Optimization of coagulant dose for coagulation/flocculation at Batch scale

Precisely optimizing the dosage of coagulant in water treatment operations is a crucial technique to improve operational efficiency, save money on chemicals, and comply with strict water quality laws. The research involved methodically altering the dosages of PAC from 1.0 to 8.0 g/L, while keeping the pH constant at 5. There was a marginal difference between 4.84 g/l and 5.5 g/l PAC dose results, due to economic reasons we chose 4.84 g/l as an optimized coagulant dose. The results of this experiment showed that the highest level of effectiveness in removing color, reaching 64.1%, was attained when a specific dose of 4.84 g/L of PAC was used. The observed trend revealed a precise equilibrium in the dosage of coagulant, where insufficient doses resulted in diminished color removal, while excessive doses failed to impart substantial improvements. Beyond the optimal point, an inherent risk of colloidal re-dispersion was identified, emphasizing the importance of precision in coagulant application. The intricate interplay of PAC's mechanism was elucidated, wherein multivalent aluminum ions were instrumental in neutralizing charged colloidal particles. The subsequent creation of aluminum flocs efficiently captured colloidal particles, aiding in their settling (Taylor et al. 2013). Fig. 4.7 b depicts the optimum coagulant dose graph concerning % color removal for the UASB stream, graphically encapsulating the subtle relationship discovered in this investigation. This study not only provides practical insights for water treatment practitioners but also emphasizes the need for coagulant dose optimization in creating cost-effective and environmentally sustainable water treatment solutions.

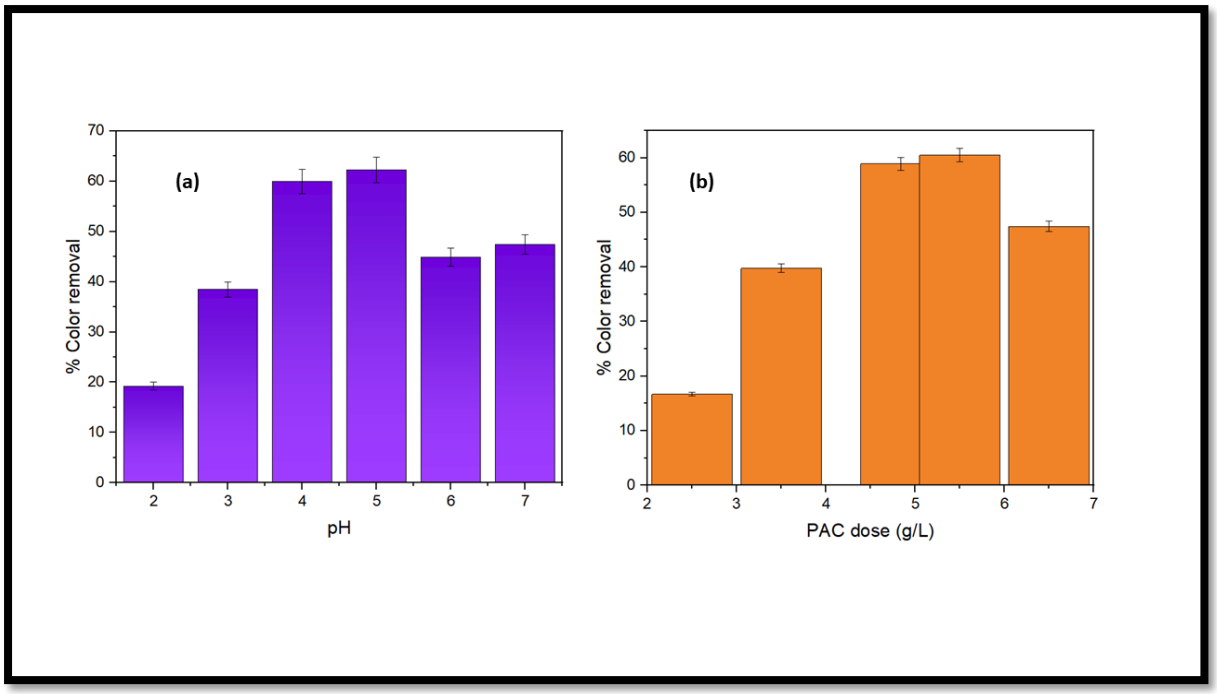

Fig. 4. 7 (a) Effect of pH on % color removal (t=20 min., PAC dose = 5 g/l) (b) Effect of PAC dose on % color removal (t=20 min., pH = 5)

4.3.2 Dual study for UASB stream at batch scale

4.3.2.1 Oxidant dose optimization for dual process

The importance of H_2O_2 has been established in the literature where it contributes to more $OH^{\bullet}$. In our study it contributes to both processes simultaneously, the contribution of H_2O_2 is significant as H_2O_2can directly participate by either accepting e^- from the conduction band of the photocatalyst, leading to the formation of more hydroxyl radicals, or decomposing under light exposure to generate $OH^{\bullet}$ radicals itself. This enhances the degradation of complex organic pollutants in the effluent. In the photo-Fenton process, H_2O_2 interacts with ferrous ions (Fe^{2+}) in the presence of UV or visible light to produce $OH^{\bullet}$ through the Fenton reaction. The light accelerates the regeneration of Fe^{2+} from Fe^{3+}, maintaining a continuous cycle of radical generation. This process is particularly effective in breaking down resistant organic compounds like phenols, lignin derivatives, and other chromophoric substances contributing to color. In this study, we explored the innovative field of Fe-TiO_2 composites with an in-situ dual effect, placing special emphasis on the influence of varying H_2O_2 concentrations. This study is extremely important as incorporating H_2O_2 leads to a considerable increase in the dual effect. Deciding what quantity of H_2O_2 is suitable for hydroxyl radicals' generation is very critical, as it has a direct effect on how much color that would be disintegrated. It must be noted that TiO_2

photocatalysis only partly generates hydroxyl radicals; they are also formed by parallel processes such as photo-Fenton and iron oxide catalysis. However, excessive H_2O_2 addition can cause scavenging effects thereby reducing the rate of color removal (Zhao et al. 2004). This study strategically incorporated H_2O_2 for its dual functionality, participating in both the photo-Fenton and photocatalytic reactions. During the photocatalytic process, the addition of oxidizing agents, such as H_2O_2, interacts with the electrons in the conduction band, thereby hindering the recombination of electrons and holes. This synergistic mechanism significantly enhances the generation of ROS and $OH^{\bullet}$ which in turn, enhances the removal of color from wastewater. The experiments varied the amount of H_2O_2 added, from 0.2 to 0.6 g/L and measured the impact on color removal efficiency. A notable improvement was seen in the efficiency of color removal when the H_2O_2 concentration reached 0.4 g/L for the UASB stream as shown in Fig. 4.8 a. However, further increasing the H_2O_2 dosage led to a decrease in color removal efficiency. This reduction is likely due to the scavenging action of H_2O_2, where it consumes hydroxyl radicals ($OH^{\bullet}$), as shown in Eqs. (4.1-4.3). Interestingly, our study identifies an optimal concentration of H_2O_2 that is lower than those reported in prior studies for similar experiments (Ginni et al. 2014a; Grötzner et al. 2018a; Yuliani et al. 2018) which removed 89.9% color from the stream. Overall, our findings highlight the importance of optimizing H_2O_2 dosage in dual processes for wastewater treatment. The knowledge gained from this study could aid in the design and optimization of wastewater treatment processes, ultimately leading to improved water quality and environmental sustainability.

$$e^{-}_{(CB)} + H_2O_2 \rightarrow OH^{\bullet} + OH^{-} \quad \textbf{4. 1}$$

$$H_2O_2 + OH^{\bullet} \rightarrow OH^{\bullet}_2 + H_2O \quad \textbf{4. 2}$$

$$OH^{\bullet}_2 + OH^{\bullet} \rightarrow H_2O + O_2 \quad \textbf{4. 3}$$

4.3.2.2 pH optimization for dual process

In dual-process studies, the photo-Fenton technique relies on iron leaching from beads in acidic conditions, making pH very important (Bansal et al., 2018; Puri et al., 2021; Thakur et al., 2020). To find the best pH level, experiments were done between pH 3.5 and 6.5 with an optimized amount of H_2O_2, as shown in Fig. 4.8 b. It was found that when the pH was below 4.5, the % color removal decreased because of the $OH^{\bullet}$ scavenging effect. On the other hand,

increasing the pH from 4.5 to 6.5 also decreased color removal. This decrease is due to the hydrolysis of Fe^{3+} and the formation of FeO (OH) precipitates, which results in fewer $OH^{\bullet}$ radicals.

Fig. 4.8 b shows that the maximum color removal of 90% which was achieved at pH 4.5 within 90 min., and this pH was used for the rest of the study. At higher pH levels, HO_2^- forms, which is less reactive, leading to the creation of O_2 and H_2O when reacting with H_2O_2. However, the formation of $OH^{\bullet}$ is essential for this study, emphasizing the need to optimize pH for the best results. This highlights the importance of maintaining the right pH level to maximize color removal.

4.3.2.3 Catalyst dose optimization

In this study, the catalyst dose was expressed as the % surface area covered by catalyst-coated beads for wastewater treatment using a dual process. We varied the number of beads to find the optimal catalyst dosage, considering the reactor area while maintaining a constant H_2O_2 dose as described earlier. The findings indicated that a low catalyst dosage, represented by 50% surface area coverage, resulted in less effective color removal from the effluent. However, increasing the percentage of surface area covered by beads from 50% to 100% significantly improved removal efficiency, as indicated by the increasing trend in the % color removal graph. Beyond 100 % coverage the % color removal was declined, this can be attributed to the beads overlapping. This overlap restricted the availability of active sites, lowered the amount of light that could penetrate, and hampered the binding of pollutants to the composite. A good color removal of 90.62% achieved at 100% surface area coverage for UASB stream, as depicted in Fig. 4.8 c in just 90 min. These findings align with previous studies highlighting the importance of having sufficient active sites for effective catalyst performance (Puri and Verma, 2023; Thakur et al., 2020).

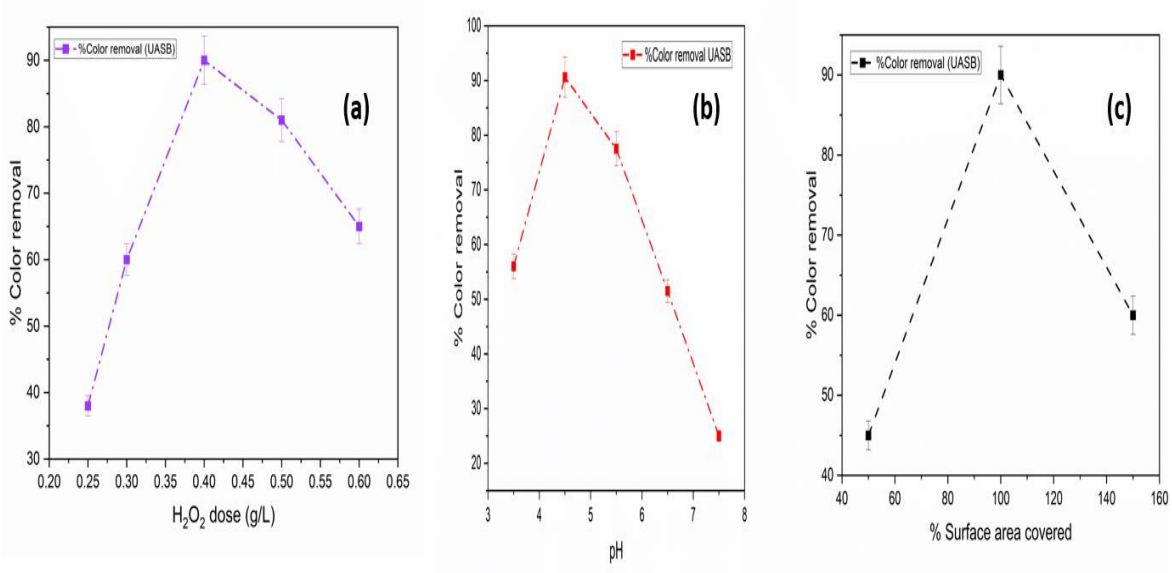

Fig. 4. 8 (a) Effect of H_2O_2 dosage on % color removal (t= 90 min., pH= 5, % S.A covered= 100) (b) Effect of different pH on % color removal (t= 90 min., H_2O_2 dose = 0.45 g/L), % S.A covered= 100) (c) Effect of change in % Surface area covered by the beads on % color removal (t= 90 min., pH= 4.5, H_2O_2 dose = 0.45 g/L)

4.3.2.4 Mineralization

To validate the oxidation process, a mineralization study was conducted to measure COD reduction. The study found that the dual effect approach, which combined photocatalysis and photo-Fenton processes, was more effective at reducing COD than either photocatalysis or photo-Fenton alone. The dual effect approach's higher effectiveness was related to its capacity to generate much more $OH^{\bullet}$, which aids in the breakdown of organic contaminants in wastewater. This was substantiated by a graph illustrating the $OH^{\bullet}$ radical generation of each process, which revealed that the dual effect process generated the most $OH^{\bullet}$ is shown in Fig 4.9. Fig. 4.9 depicts the $OH^{\bullet}$ generation of each process, clearly demonstrating that the dual effect process produced a considerably larger number of $OH^{\bullet}$. The dual effect process achieved a COD removal of 66.66 % for the UASB stream, while the isolated photocatalysis and photo-Fenton processes achieved 20 % and 8 % COD removal respectively as shown in Fig 4.10.

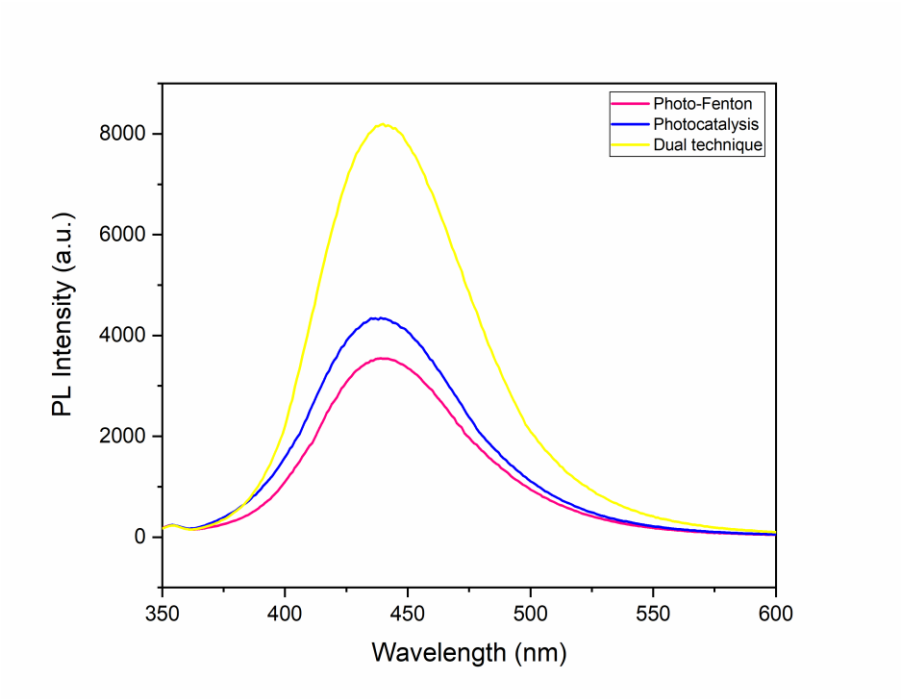

Fig. 4.9 Illustrated enhanced prominence of OH• in Dual Photoluminescence Spectroscopy compared to isolated processes

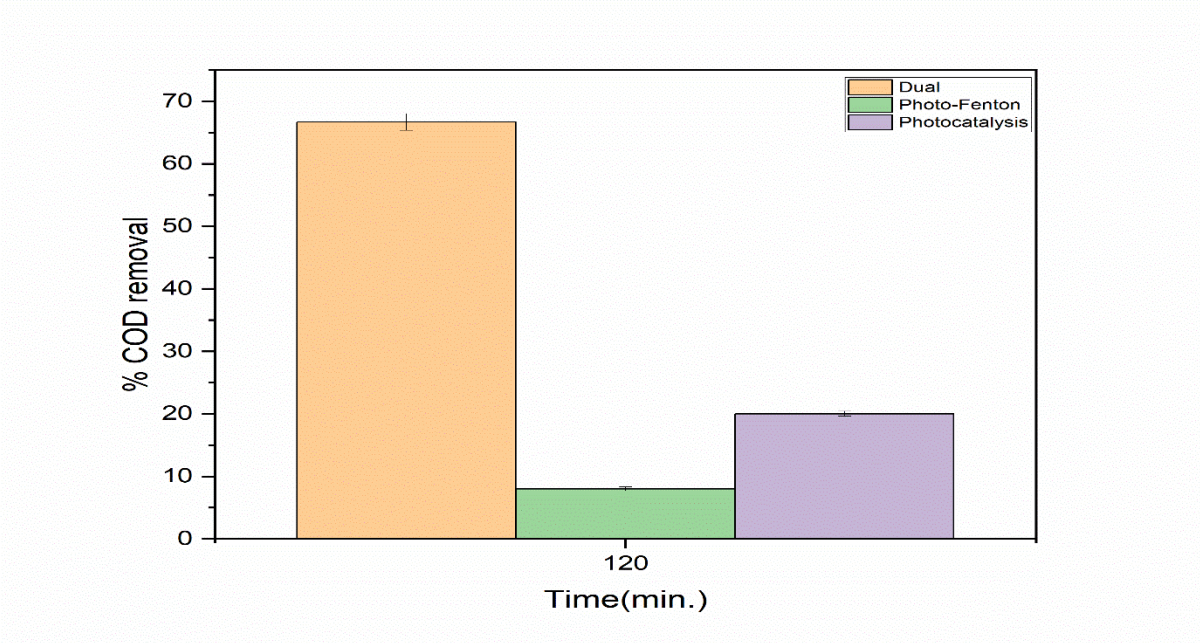

Fig. 4. 10 % COD removal by different processes for UASB stream

4.3.3 Study of UASB stream in recirculation mode

To enhance the applicability of AOPs at the field scale, it is important to validate their effectiveness through scale-up trials based on laboratory-scale results. In this context, the present study focuses on scaling up the in-situ hybrid effect using composite beads for the color removal from different P&P streams, culminating in the development of pilot-scale solar reactors. The selection of Fe-TiO_2 composite beads for the scale-up studies was motivated by their exceptional recyclability (>100 recycles), a level of performance not reported with any other support material in the existing literature. Moreover, the cost-effectiveness of this process is expected to be significantly improved owing to the economical nature of Fe-TiO_2 composite beads. The pilot-scale reactor considered for this study was a sunlight-assisted re-circulation type fixed-bed glass reactor with a total working volume of 5 L. This choice was made to ensure the practical feasibility and scalability of the process. The before and after treatment characterization of the effluent is given in Table 4.2.

Table 4. 2 Characterization of the effluent before and after treatment

Parameter	**Before treatment**	**After Coagulation**	**After ATT (Dual)**
COD (mg/L)	2200	1280	600
BOD (mg/L)	1200	264	88
Color (a.u)	0.78	0.139	0.08
TDS (mg/L)	2250	Not measured	896
TSS (mg/L)	1170	Not measured	367
pH	7.5 (Raw effluent) and 5 (after setting pH)	5.5	4.8

4.3.3.1 Methodology adopted for the selected stream

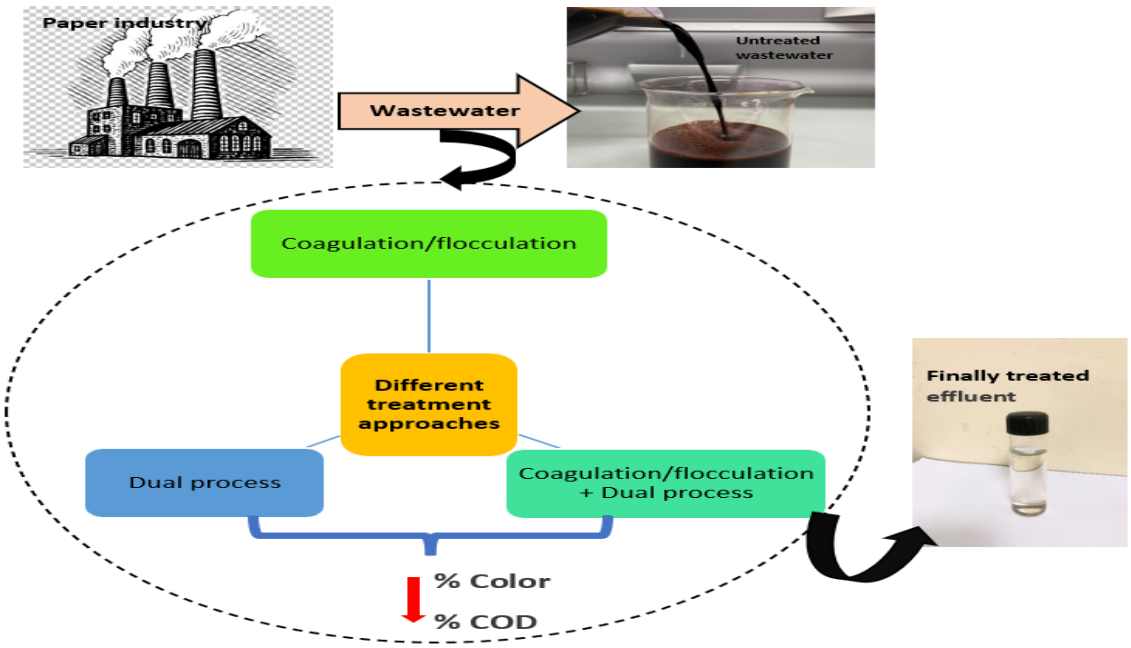

Fig. 4. 11 Methodology adopted for treating the UASB stream

4.3.3.2 Types of approaches

The whole study is divided into three different treatment approaches according to the need of the process, i.e. approach 1 (Only dual process), approach 2 (only coagulation/flocculation), and approach 3 (coagulation/flocculation + dual process) as shown in Fig. 4.12.

Firstly, dual process i.e., treatment approach 1, where the selected effluent stream was subjected to dual process using fabricated composite beads in a reactor, which gave a very insignificant color reduction of 18.6% and almost negligible COD reduction at optimized conditions as shown in Fig. 4.12. It might be due to the dense color of the effluent due to which there was a massive hindrance for light penetration. If light penetration would be hindered, then the photocatalyst cannot work efficiently hence less color reduction takes place. So before performing dual it becomes necessary to reduce a certain amount of color using some pre-treatment like coagulation/flocculation.

Subsequently, the second approach was followed i.e. coagulation/flocculation to reduce the dense color of the effluent so that the photocatalytic process can be carried out efficiently.

All the experiments were carried out at pH 5 which was in the vicinity of the optimized pH values stated in the literature (Kim 2016; Grötzner et al. 2018b). The coagulation was carried out at optimized conditions i.e. 5 pH and 4840 mg/L coagulant dose to check the effective color and COD reduction. These optimized conditions removed almost 60% of color and ~ 23% COD thus, were chosen as a pre-treatment option before carrying out the dual process.

Finally, the effluent was treated following approach 3 i.e. coagulation/flocculation followed by a dual process (photocatalysis + photo-Fenton) as only coagulation and the only dual process failed to remove a significant amount of color and COD from the effluent. Initially, the dense color of effluent was removed by coagulation to confiscate the light hindrance issue. Further, the remaining color and COD were treated by a dual process comprising a combination of simultaneous photocatalysis and photo-Fenton which gave a very good productivity for both % color and % COD removal i.e. 89.74 % and 53.12% respectively.

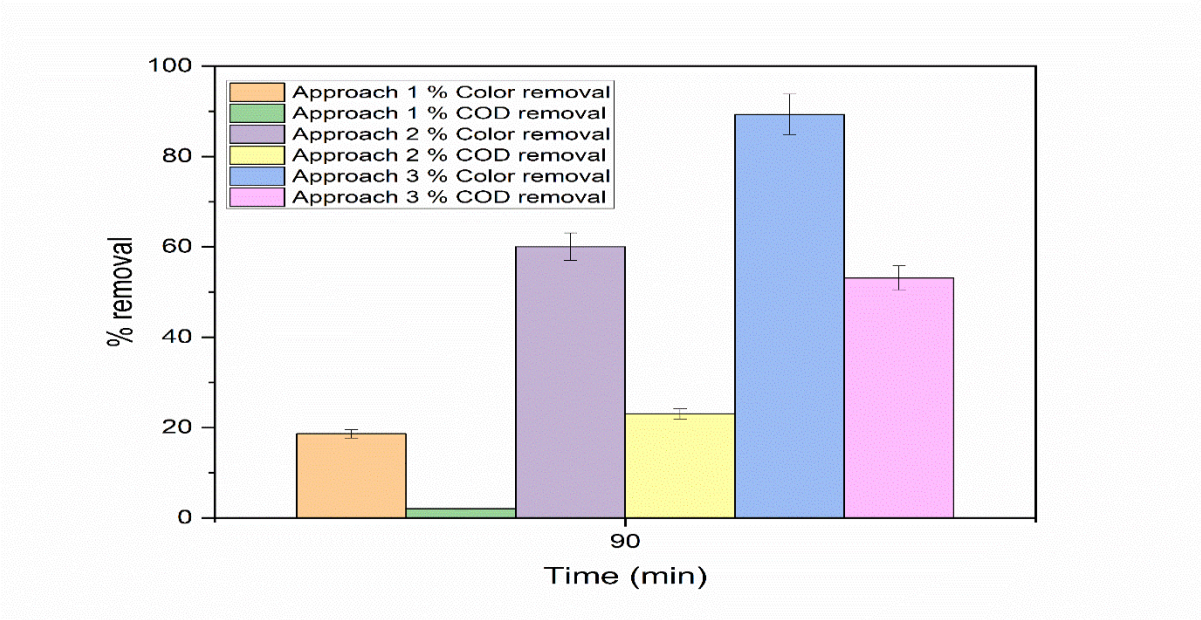

Fig. 4. 12 Effect of different approaches on % color and % COD removal Process optimization

Here also a similar approach was followed i.e., coagulation/flocculation was applied as a pretreatment followed by the AOP i.e., the dual technique for both % color and % COD removal as given in **section 4.3.1**.

The relationship between operating parameters for coagulation (pH and coagulant dose) and dual process (catalyst dose (% surface area covered by the beads), H_2O_2 dose, and size of beads) and output (% color and % COD removal).

During the coagulation/flocculation process, pH was varied between 4 and 7. The choice of pH 5 for the entire study was made because it offered optimal results while balancing process economics. This pH value is consistent with the findings of other researchers working on similar effluents for coagulation/flocculation (Irfan et al. 2013; Kim 2016). At the optimized pH of 5, the study achieved a color removal efficiency of 60% and a COD removal efficiency of 40.9%, as shown in Fig. 4.13 a.

The second parameter optimized for the coagulation study was the coagulant dose. After optimizing the pH (5.0), the effect of coagulant i.e. PAC was assessed by varying its dose from 1000-8000 mg/L. The best color (63.1%) and COD (41%) removal occurred at 4840 mg/L of PAC per litre of the effluent. Further increasing the PAC dose, no significant improvement in results was observed as an excessive amount of coagulant may cause re-dispersion of colloids. PAC neutralizes the charged colloidal particles by generating multivalent aluminium ions. The aluminium flocs formed after coagulation then enmesh the colloidal particles and let them settle (Taylor et al. 2013)**.** Fig. 4.13 b shows the optimized graph of coagulant dose for color and COD removal.

For the dual study, the first parameter studied was the effect of the H_2O_2 dose as shown in Fig. 4.13 c Various studies have reported the effect of H_2O_2 on photocatalysis and the photo-Fenton process, as it is an engrained method for improving the $OH^{\bullet}$ production in the reaction (Giri and Golder 2014; Yoon et al. 2017; Zhang et al. 2022). The oxidant plays a major role in photocatalysis by preventing electron-hole recombination by reacting with conduction band electrons as given in Eqs. 4.20-4.22. The present study involves the simultaneous consumption of H_2O_2 by both processes in a single reaction system. To evaluate the effect of H_2O_2 different sets of reactions were carried out by varying H_2O_2 within 200-800 mgL^{-1}. Keeping time and pH constant i.e. 90 min and 5 respectively, the oxidant effect was monitored for both color and COD removal. It was observed that the COD and color removal were constantly incrementing up to 600 mgL^{-1} but after that both started to decline when the dose was further increased from 600 mgL^{-1}. A good % color and % COD removal was observed at optimized oxidant dose i.e., 88.9 % and 48.5% respectively. The drop in % color and COD removal is owed to the scavenging effect of H_2O_2 i.e. H_2O_2 starts to consume $OH^{\bullet}$ by itself as shown in Eqs. 4.20-4.22.

This optimal dose is lower than what other researchers reported in the literature for similar kinds of studies (Ginni et al. 2014b; Grötzner et al. 2018b; Yuliani et al. 2018).

The impact of % surface area covered by the beads (catalyst dose) on the treatment of wastewater was examined as the second parameter for the dual process in this study. It was executed by varying the number of catalyst-coated beads to get an optimized value of catalyst required for the dual study. The H_2O_2 (600 mgL^{-1}) and time (90 min.) were kept constant and the beads varied in the range of 20%-120% of the area of the reactor covered by the beads as given in Fig. 4.13 d with only 20% of the surface area covered, the graph showed less removal of both color and COD. Subsequently increasing the catalyst surface area, the graph showed substantial increase till 100% area covered. Increasing the beads to >100% surface area showed a negative trend as shown in Fig. 4.13 d The explanation for this could be that with fewer beads, less active sites were present but with increasing catalyst surface area the graph started incrementing as sufficient active sites were provided (Yang et al. 2019; Puri et al. 2021). Increasing beads beyond >100% might offer large catalyst surface area, but overlapping of beads resulted in the capping of the active sites and caused problems in sufficient light penetration and hindered the binding of pollutant to the composite which is important for reaction, hence reduction of catalyst active sites caused decrement in the % color and % COD removal (Idris et al. 2012; Shet and Shetty 2016). A good % color and % COD removal of 89% and 53% respectively was observed at an optimized catalyst dose.

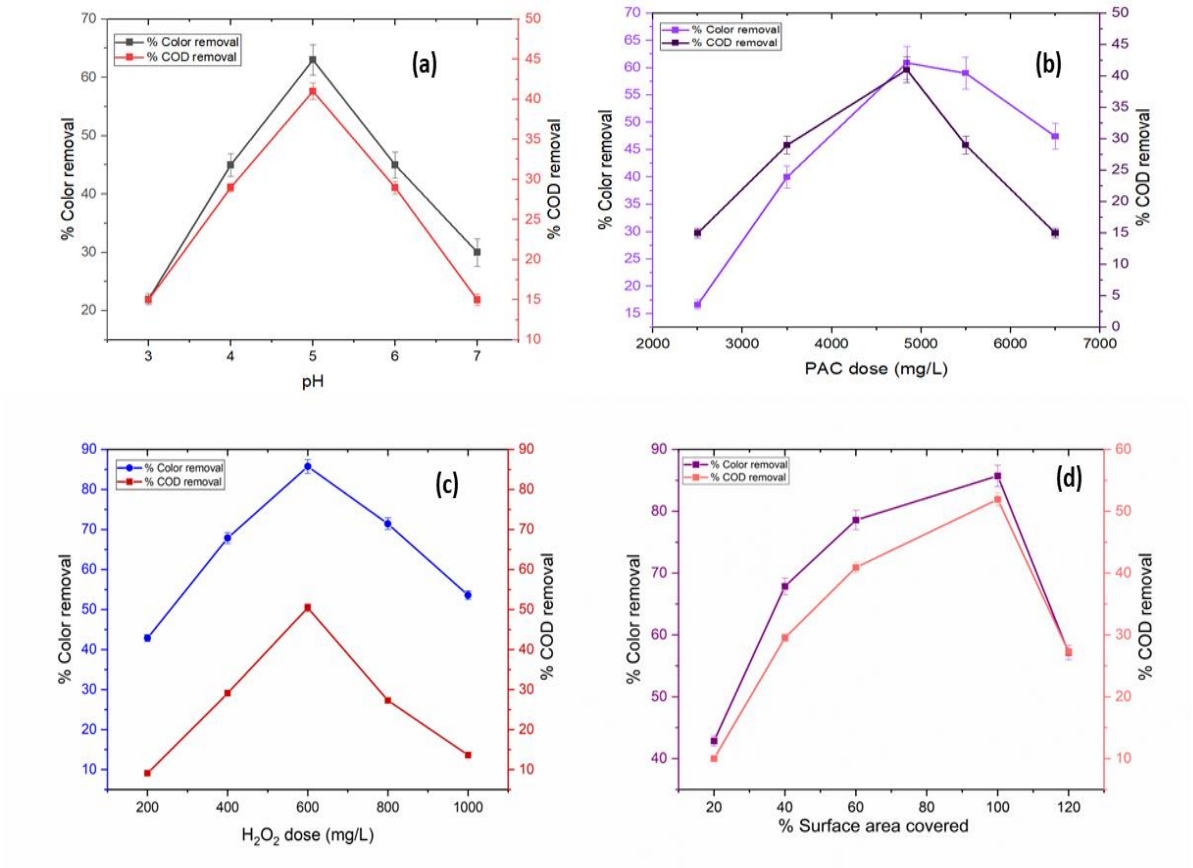

Fig. 4. 13 (a) Effect of pH on % color and % COD removal in coagulation/flocculation (V = 4.0 L, PAC = 4840 mg/L) (b) Effect of PAC dose on % color and % COD removal in coagulation/flocculation (pH = 5, V = 4.0 L) (c) Effect of oxidant dose % color and % COD removal in dual process (S.A covered = 100%, pH = 4.5, V = 4.0 L) (d) Effect of catalyst dose on % color and % COD removal in dual process (H_2O_2 = 600 mg/L pH = 4.5, V = 4.0 L)

Finally, bead size was varied to study its effect on color and COD removal using a dual process. Actually, bead size plays a very prominent role in offering exposed surface area for better decolorization and demineralization of the wastewater in fixed-bed studies. In this context, the beads were varied according to diameter in the range of 12-20 mm using a screw gauge. It can be seen in Fig.4.14 that 12 mm diameter bead provided the maximum surface area for the reaction and accordingly best decolorization and degradation was achieved. With further increase in bead size, effective exposed surface area was decreased, which eventually lead to decrease in reaction rate (Rincón and la Motta 2019; Zhang et al. 2020b). However, with bead size less than 12 mm, problems of catalyst intactness and effective iron leaching could

hinder the reaction rate for treating the target waste water. In this context, 12 mm size composite bead was chosen for the whole study due to its better efficiency.

The optimized parameters for dual study gave a very good output for both % color and % COD removal i.e. 89.74% and 53.12% respectively.

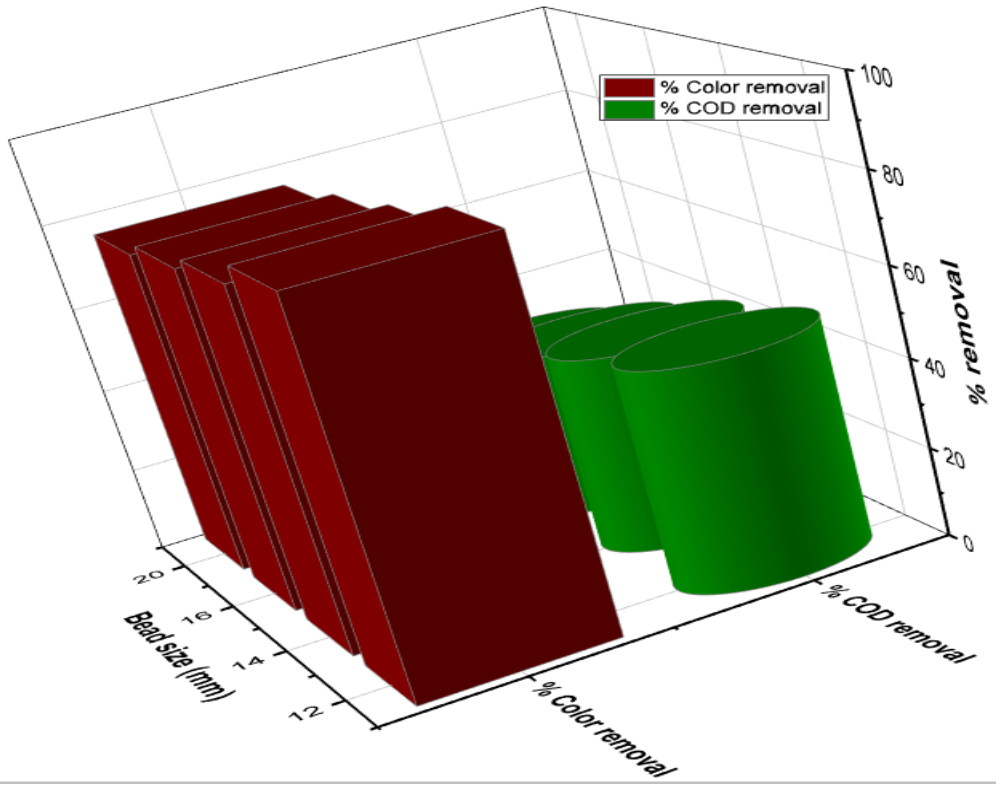

Fig. 4. 14 Effect of bead size on % color and % COD removal (pH = 4.5, V = 4 L, H_2O_2 = 600 mg/L, S.A covered = 100%, Time = 90 min.)

4.3.3.3 Durability studies

The chief advantage of this study is outstanding efficacy of composite beads even after 50 recycles. The beads were effectively recycled 50 times without experiencing any appreciable slowdown in activity. The recycling efficiency of beads were evaluated in terms of color and COD removal. There was only 8-10% reduction in color removal and almost 12-15% reduction in COD removal after 50 runs shown in Fig 4.15 a. Not only the % color and COD removal confirmed the efficiency of beads after several recycles but few other techniques confirmed the catalyst intactness along with presence of iron as given in section 3.1. Furthermore, iron leaching was also checked after 50 recycles which also gave very good results with only 0.6-1% reduction in activity as given in Fig. 4.15 b. To date a very limited

studies have been reported having such a high durability of the catalyst especially concerning real waste making this catalyst feasible for commercial scale applications.

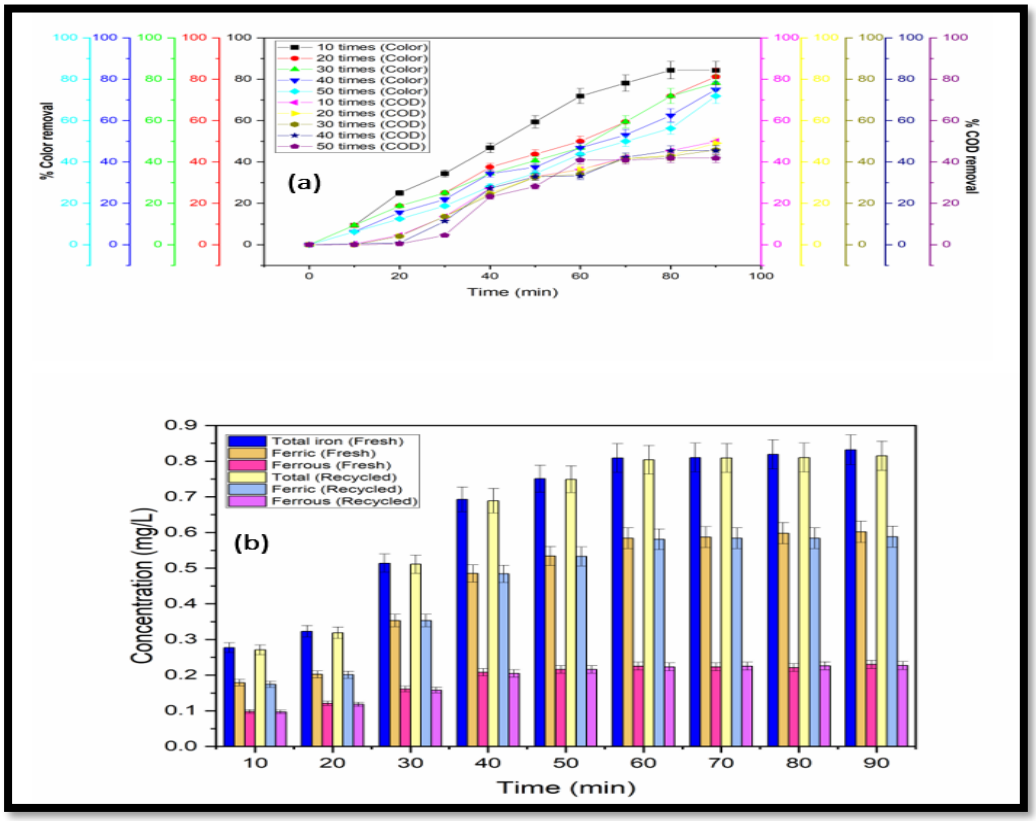

Fig. 4. 15 (a) Durability study in terms of % color and % COD removal in 50 times recycled composite beads (b) Durability study in terms of iron leaching in fresh and 50 times recycled composite beads

4.3.4 Once through plug-flow approach using fixed bed reactor

Recent emphasis has focused on the development of continuous photocatalytic systems, such as plug-flow reactors (PFR) and continuous stirred tank reactors (CSTR), due to their potential for large-scale wastewater treatment applications(Miyawaki et al. 2016). PFRs have become popular in continuous flow systems due to their ability to eradicate axial mixtures, resulting in higher productivity and selectivity (Prokop et al. 1997). Despite these advantages, the practical implementation and visualization of PFRs in photocatalytic processes have not been extensively studied. Despite this, the visualization and practical implementation of PFRs in photocatalytic processes were not extensively explored. This study breaks new ground by developing a pilot-scale, once-through cascade reactor system that incorporates an in-situ dual effect to simulate a PFR for color removal from real P&P industry wastewater.

To our knowledge, this is the first documented attempt to visualize and approach a PFR within a continuous photocatalytic system tailored for this purpose. Incorporating an in-situ hybrid effect into the PFR setup optimizes the degradation process by enhancing the interaction between the photocatalyst and pollutants. This approach can lower operational costs while increasing scalability, providing a long-term solution for industrial wastewater treatment. Furthermore, this innovative method sets a precedent for future research and applications in various industries, potentially leading to significant environmental and economic benefits. The reaction setup is shown in Fig. 4.16.

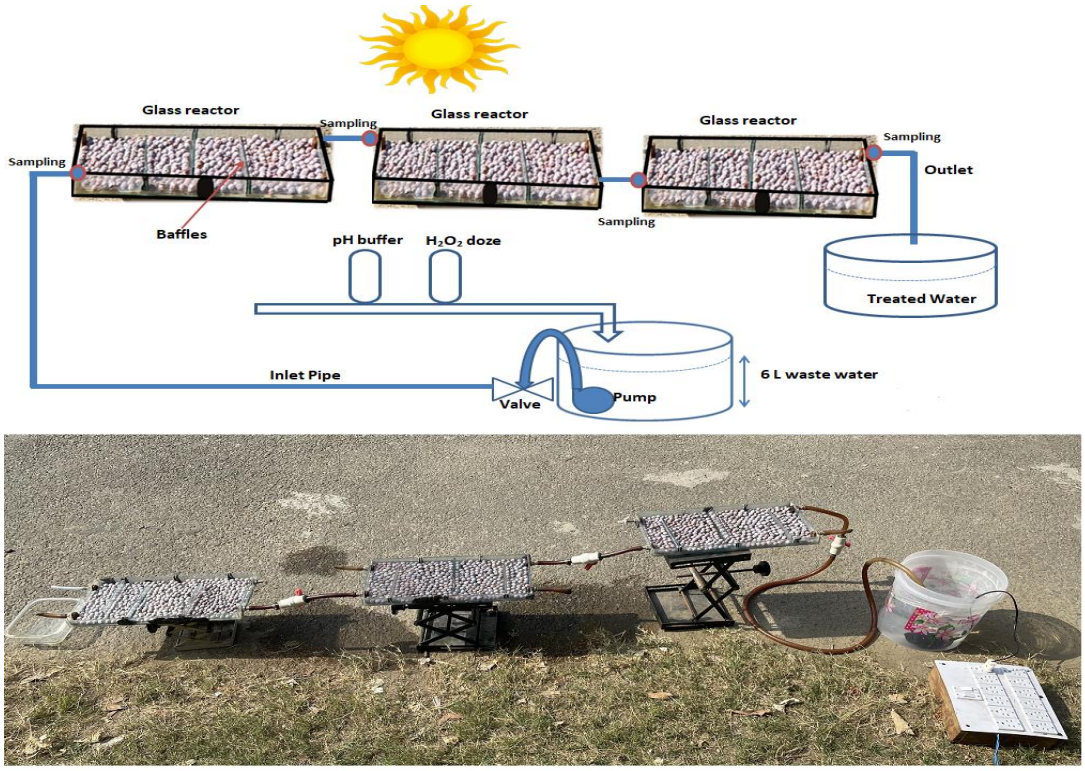

Fig. 4. 16 Line diagram and actual image of the once-through pilot-scale reactor used for study

4.3.4.1 Dual effect pre-eminence in cascade reactors for UASB stream

In this work, dual effect was successfully shown at the pilot scale with a cascade reactor. Three packed-bed glass reactors in sequence, running in a once-through mode and with a 10 L working capacity made up this system. The in-situ dual-process significantly reduced the treatment time for color removal compared to individual processes. Implementing the in-situ dual effect in a cascade reactor with three reactors in series allowed the system to approximate a plug flow reactor (PFR), achieving 84.4% color removal and 45% COD reduction within a retention time of 45 min. under optimized conditions. The primary reactive oxygen species

(ROS) responsible for color removal was identified as hydroxyl radicals ($OH^{\bullet}$), confirmed through trapping studies. Additionally, the Fe-TiO_2 composite used in the process demonstrated exceptional durability and recyclability, performing effectively for over 100 recycles under continuous flow conditions. This was verified through various characterizations, including SEM/EDS, XRD, DRS, and FTIR analyses. To assess the practical feasibility of this high-performance once-through reactor system, a comprehensive cost analysis of the treatment process is included in a later section.

4.3.5 Experimental study

4.3.5.1 Coagulation/Flocculation

Again, here coagulation/flocculation was adopted as a pretreatment because stream has a dark color. The brief discussion has been explained in section 4.3.1. During the experiments, the pH was varied between 4 and 7 to identify the optimal conditions. The most effective color reduction was observed at an optimized pH 5. The optimized reaction resulted in significant improvements, with color removal reaching 62% and COD reduction reaching 41%. At an optimized pH, the PAC dose was varied ranging from 1 to 6 ml/L. The most favourable outcomes for color elimination (64.1%) and COD reduction (41.81%) were attained while using a PAC concentration of 5 ml/L Fig.4.17 a-b depicts the optimized graph showcasing the optimized pH and an appropriate amount of coagulant dosage required for effective elimination of both % color and % COD.

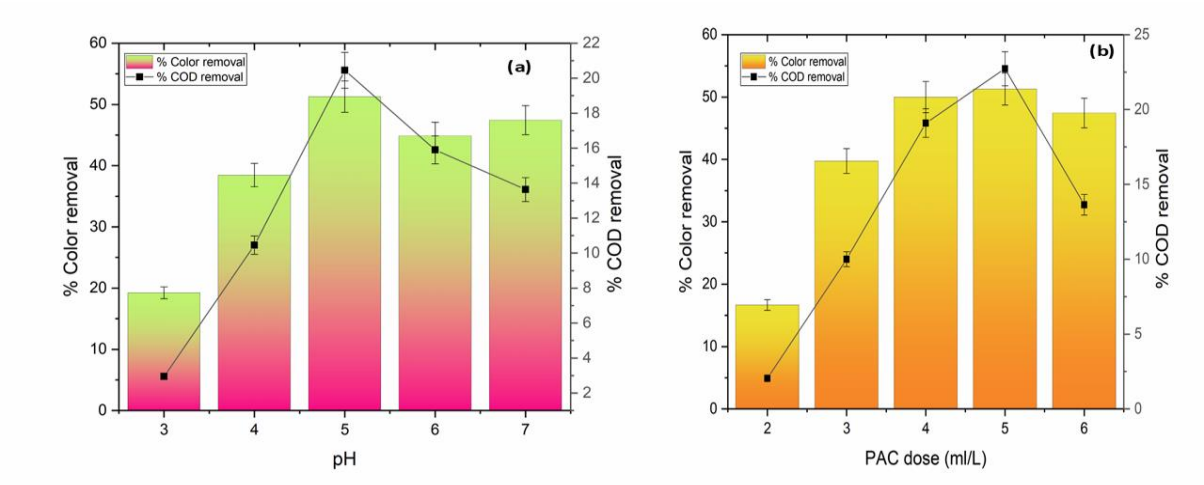

Fig. 4. 17 (a) Effect of pH on % color and % COD removal in coagulation/flocculation (t=20 min. PAC dose= 5 ml/L) (b) Effect of PAC dose on % color and % COD removal in coagulation/flocculation (t=20 min., pH= 5)

4.3.6 Process optimization for dual process

Different factors like number of reactors, number of baffles, flow rate, % surface area covered and role of different quenchers were varied to obtain the best-optimized results for the color removal of the given streams provided by the agro-based P & P industry using dual study.

4.3.6.1 Effect of % surface area covered by beads

In this investigation, we sought to establish the ideal number of composite beads required for effective color removal by modifying the number of beads in terms of % surface area (S.A) covered. We evaluated coverage percentages ranging from 50% to 100% and saw a significant improvement in color removal with greater surface area covered, as illustrated in the Fig. 4.18 a. Increasing the number of composite beads results in more exposed surface area and a greater amount of catalyst. This increased catalyst presence accelerated the rate of color removal across all streams. As the streams flowed through consecutive reactors, they encountered newly introduced fixed-bed composite catalysts in each reactor, extending the active sites and generating more active radicals. This process significantly enhanced color removal efficiency. However, when we increased the surface area coverage to 110%, there was neither an increase nor a decrease in the % color removal. Therefore, we determined that the optimal configuration was 100% exposed surface area, resulting in color removal efficiency of 84% for the UASB stream. This setup provided the best balance between the % S.A covered by the beads and the effectiveness of color removal, demonstrating that maximizing surface area exposure up to 100% is crucial for improving treatment efficiency.

4.3.6.2 Effect of the number of reactors

In this work, we used a series of three reactors to investigate the effects of various treatment configurations on the color removal efficiency of UASB effluent. Our experimental apparatus treated 10 L of UASB stream containing H_2O_2 under natural solar light, aiming to assess the system's practical application and sustainability. The results, illustrated in the accompanying Fig. 4.18 b, show that the color of the streams decreased as they passed through each successive reactor. The series of three reactors plays a significant role in determining the residence time of pollutants with the active sites of the composite material, which in turn affects the color removal rate. Specifically, after passing through the first reactor, with an approximate residence time of 15 min., there was a 31% reduction in color in the UASB stream. When the second reactor was added, the color removal increased to 53%. Upon introducing a third

reactor, the color removal efficiency reached 84.4%. Beyond this, further reactors were not taken into consideration because the ideal number of reactors depends on a variety of criteria, not just the percentage of color removal, but also operational efficiency and economic viability. The entire procedure was conducted in a once-through mode at a consistent flow rate, ensuring uniform treatment conditions. This study found that increasing the number of reactors in series can greatly improve color removal efficiency. However, the choice of reactors must balance economic and operational aspects to ensure viability. Achieving this balance is crucial for the practical implementation of wastewater treatment technologies.

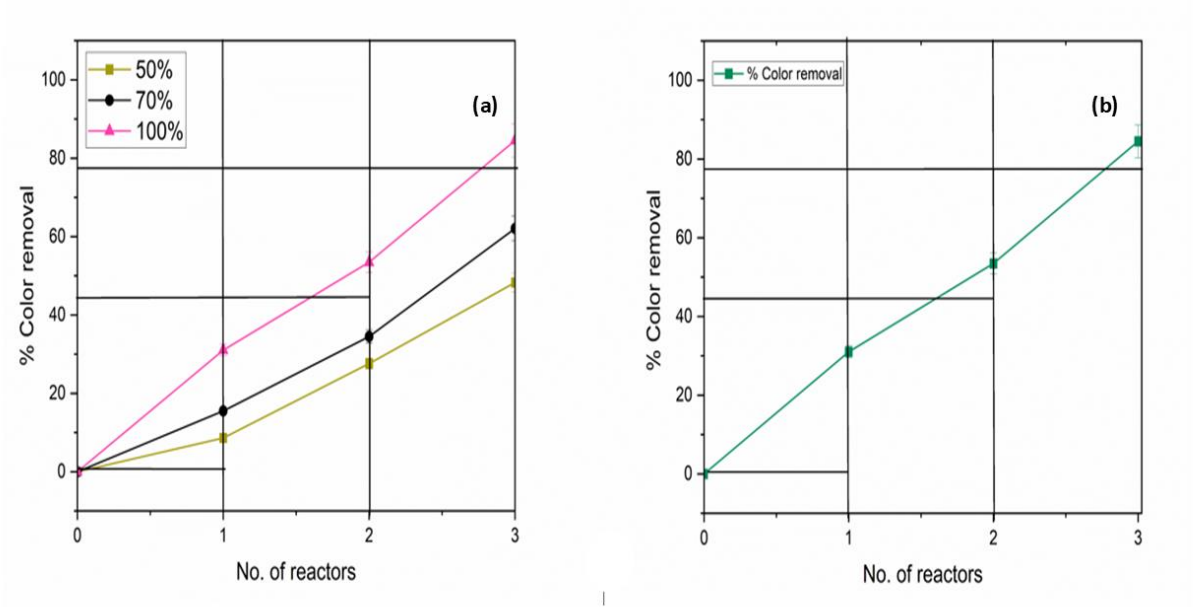

Fig. 4. 18 Change in the % color removal with (a) variation in the % surface area covered by the beads (t=45 min., No. of reactors= 3, Flow rate= 7.0 Lh^{-1}) (b) variation in the number of reactors (t=45 min., % S.A covered= 100, Flow rate= 7.0 Lh^{-1})

4.3.6.3 Effect of flow rate

For this study, we examined how the flow rate affects the efficiency of color removal in UASB effluent. We experimented with different flow rates, ranging from 4.0 ± 1.0 L h^{-1} to 12.0 ± 1.0 L h^{-1}. According to the Fig. 4.19 a, it is evident that the most effective color removal was observed at the lowest flow rate of 4.0 ± 1.0 L h^{-1} yet we chose 6.0 ± 1.0 L h^{-1} as due to marginal difference between results of both flow rates i.e., 4.0 L h^{-1} and 6.0 L h^{-1}. As the flow rate increased towards 12.0 ± 1.0 L h^{-1}, there was a noticeable decline in the color removal efficiency. This decrease is probably caused by the shorter duration of contact between the

pollutants and the active sites of the composite material when the flow rates are higher. While reducing the flow rate below 6.0 ± 1.0 L h^{-1} might further improve color removal, it would not be commercially viable due to increased processing time and higher electricity consumption, which would raise the overall process cost. Therefore, considering the economic aspect, we observed that the color removal efficiency showed only a marginal difference between the flow rates of 4.0 ± 1.0 L h^{-1} and 6.0 ± 1.0 L h^{-1}. Notably, a color removal efficiency of 84% was observed in the UASB stream. To balance efficiency and practicality, we selected a flow rate of 6.0 ± 1.0 L h^{-1} for the entire study, as it provides a more economically viable option while maintaining high color removal efficiency.

4.3.6.4 Effect of different scavengers

To determine the primary oxidative species or radicals (such as $OH^{\bullet}$, $O^{2\bullet-}$, and h^{+}) responsible for the color removal from UASB stream using the Fe-TiO_2 composite, a series of experiments were conducted under optimal conditions. As depicted in Fig. 4.19 b various quenching agents were utilized, including tert-butyl alcohol (TBA) for $OH^{\bullet}$, disodium ethylenediaminetetraacetic acid (EDTA) for h^{+}, and p-benzoquinone (BQ) for $O^{2\bullet-}$. The results indicated that the % color removal was diminished in the presence of each quenching agent. This suggests that each of the previously mentioned oxidative species plays a role in the color removal process. A significant reduction of approximately 40-50% in color removal was observed for the UASB stream when TBA quencher was used, highlighting the crucial role of $OH^{\bullet}$ radicals in the color removal process. This indicates that $OH^{\bullet}$ radicals are the primary active species in the dual process of color removal.

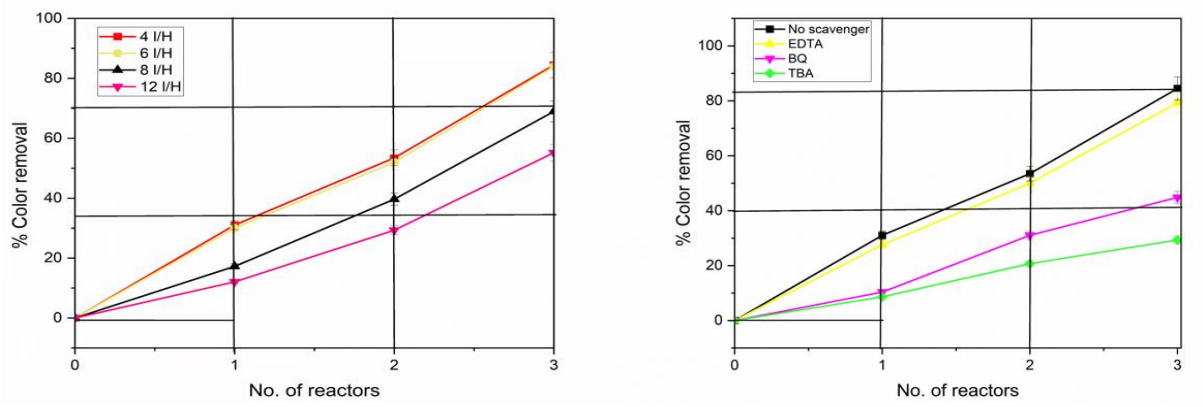

Fig. 4. 19 Change in the % color removal with (a) variation in flow rate (t=45 min., No. of reactors= 3, % S.A covered= 100) (b) variation in different scavengers used a) variation in flow rate (t=45 min., No. of reactors= 3, % S.A covered= 100, flow rate= 6.0 Lh^{-1})

4.3.7 Characterization analysis

4.3.7.1 SEM/EDS analysis of sands

To attain successful dual-process outcomes in this study, it was imperative to have two key components: adequate iron levels in the industrial waste, along with the catalyst's intactness and the presence of TiO_2 complexes. To confirm these factors, various techniques were employed.

The SEM examination of the sands used in the catalyst fabrication showed that FS had a coarse structure while BS had a fine structure, as anticipated. Fig. 4.20 displays the results of the SEM analysis conducted on samples of FS and BS. The particles in the samples have a homogeneous size distribution and appear as compact particles with smooth, rounded edges rather than sharp angles. While most particles appear uniform, a small percentage exhibit distinct grains with molten phases. Analysis of these molten phases using EDS revealed that they consist of Fe, O, Ca, Al, Mn, Cl, Na, and Mg. The presence of iron in the sands indicates that they can serve as a good alternative source of iron for the photo-Fenton process (Colmenares et al. 2013).

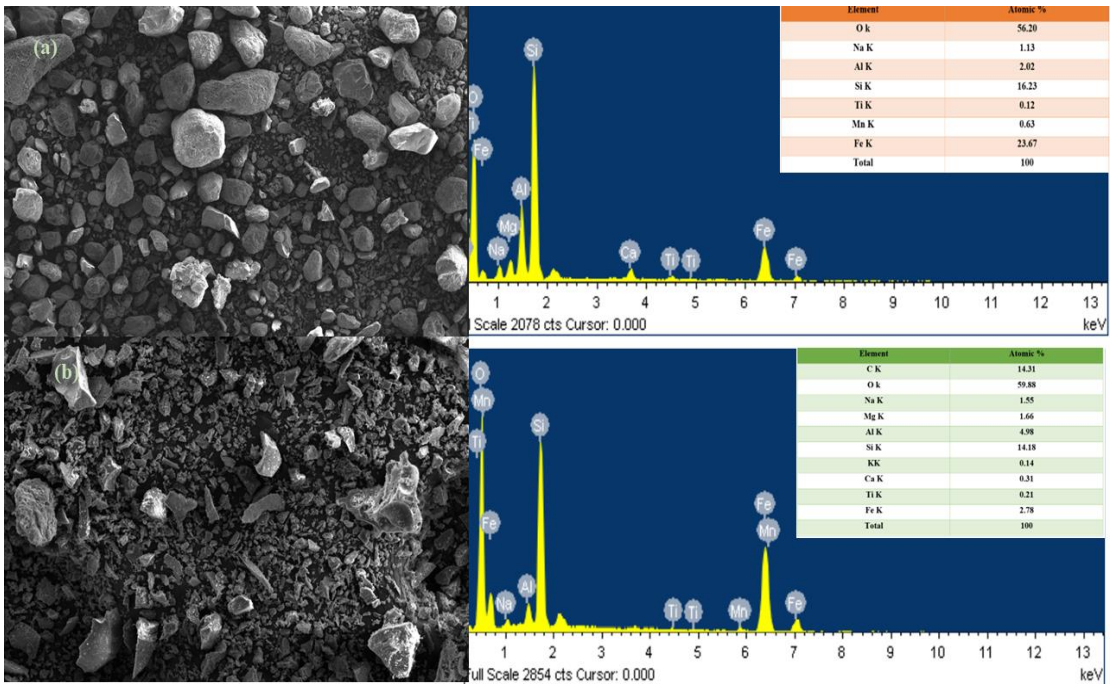

Fig. 4. 20 (a) Compositional characterization through SEM/EDS analysis of Furnace blast sand (FBS) (b) Compositional characterization through SEM/EDS analysis of Foundry sand (FBS)

4.3.7.2 FESEM/EDS analysis of composite

As expected, the results depict the uniform distribution of TiO_2 on the surface. Fig. 4.21 presents the findings of this study which used field emission scanning electron microscopy (FESEM) and energy-dispersive X-ray spectroscopy (EDS) to analyse the morphology and elemental composition of fresh and used beads coated with TiO_2. The FESEM imaging technique captured detailed, high-resolution images that provided valuable insights. The examination of these images revealed a visually striking white and glossy surface, serving as strong evidence of the catalyst's integrity. Subsequent EDS analysis confirmed the presence of titanium (Ti), iron (Fe), and oxygen (O) elements as shown in Fig. 4.21. Notably, when comparing the surface morphology of the freshly coated beads and those that had undergone 50 recycling cycles, they exhibited similar characteristics. These compelling findings from the FESEM/EDS analysis strongly indicate the remarkable efficacy and viability of the composite beads, positioning them as highly promising for widespread industrial applications. These results shed light on the tremendous potential of TiO_2-coated beads as catalysts across a range of industries.

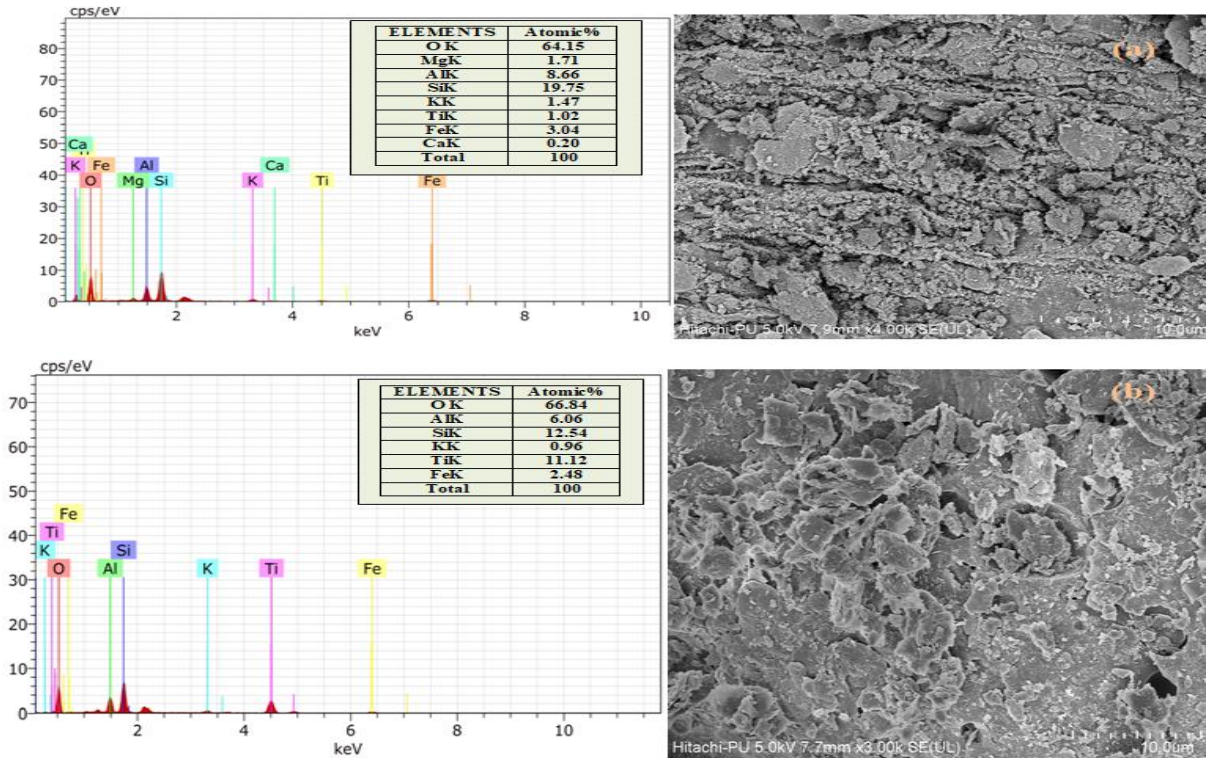

Fig. 4. 21 FESEM and EDS images of (a) freshly coated and (b) recycled composite bead

4.3.7.3 X-ray diffraction

X-ray diffraction (XRD) analysis was conducted to validate the hypothesis of the natural doping phenomenon for Fe-TiO_2 and to determine the crystalline phases of TiO_2. The results confirmed the presence of a highly crystalline composite with distinct and intense peaks. The peaks in the XRD pattern were characteristic of the anatase phase (25.4°, 37.8°, 48°, 55°, 62.6°) and rutile phase (26°, 36°, 55°) in all three i.e., raw TiO_2 sample, fresh beads as well as in recycled beads as shown in Fig. 4.22. Additionally, the characteristic peak of Fe was observed as iron titanium oxide (ITO), confirming the natural doping of Fe with TiO_2. Remarkably, the peaks remained prominent even after 100 recycles, indicating no distortions in the catalyst. Specifically, the ITO particles at 70.3° and 75.28° planes indicated that photoexcited electrons from the TiO_2 photocatalytic process were trapped by Fe^{3+} for the redevelopment of Fe^{2+} confirming the presence of photo-Fenton and photocatalysis in one unit. This observation was further corroborated by UV-DRS analysis, as discussed in the following section. In light of these discoveries, it appears that the presence of ITO particles can boost the effectiveness of the iron-titanium oxide catalyst under visible light.

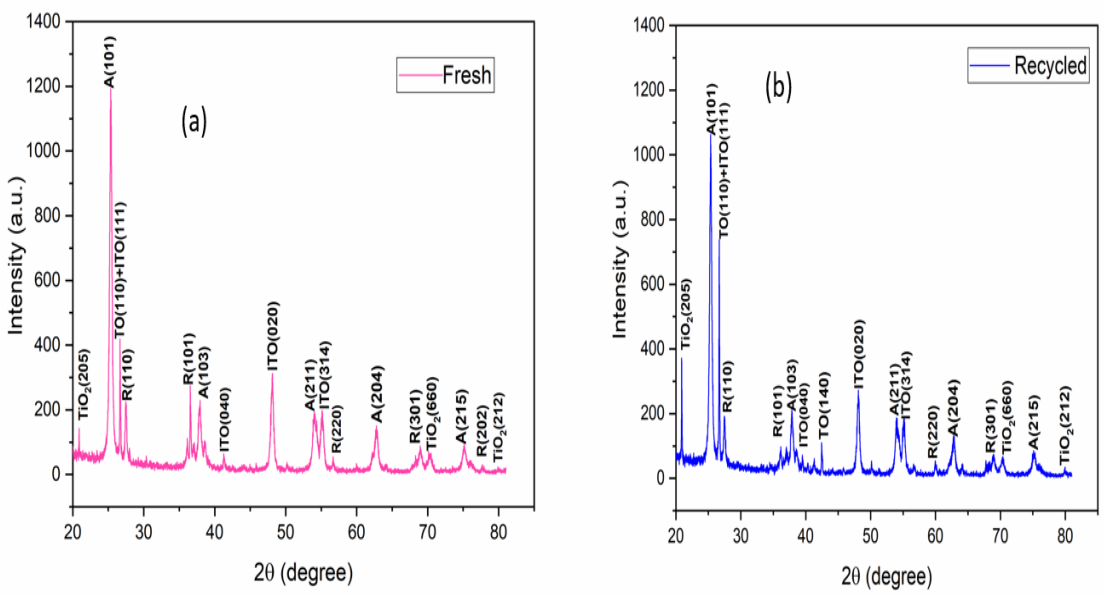

Fig. 4. 22 (a) XRD pattern of freshly coated and recycled composite bead

4.3.7.4 UVDRS analysis

Confirmation of the catalyst's visible activity primarily relied on UV-visible diffuse reflectance spectroscopy (DRS), highlighting the presence of Fe-TiO_2 complexes. A reference compound, barium sulphate ($BaSO_4$), was employed, and the analysis spanned a wavelength range of 200-800 nm. The tested samples encompassed raw TiO_2, the freshly prepared composite, and the composite after recycling. Fig. 4.23 depicted the spectral data, revealing that the bandgap of raw TiO_2 (3.2 eV) exceeded that of both the fresh composite (2.9 eV) and the recycled composite (2.8 eV). Furthermore, the absorbance values exhibited an increase from 415 nm for raw TiO_2 to 430 nm and 452 nm for the fresh and recycled composites, respectively. These findings strongly indicate the catalyst's visible activity, primarily attributed to the presence of Fe-TiO_2 complexes, which was corroborated by XRD analysis. The enhanced absorbance in the visible spectrum signifies improved light absorption by the catalyst, consequently enhancing its photocatalytic performance. These results offer valuable insights into the effective design of catalysts in various photocatalytic applications.

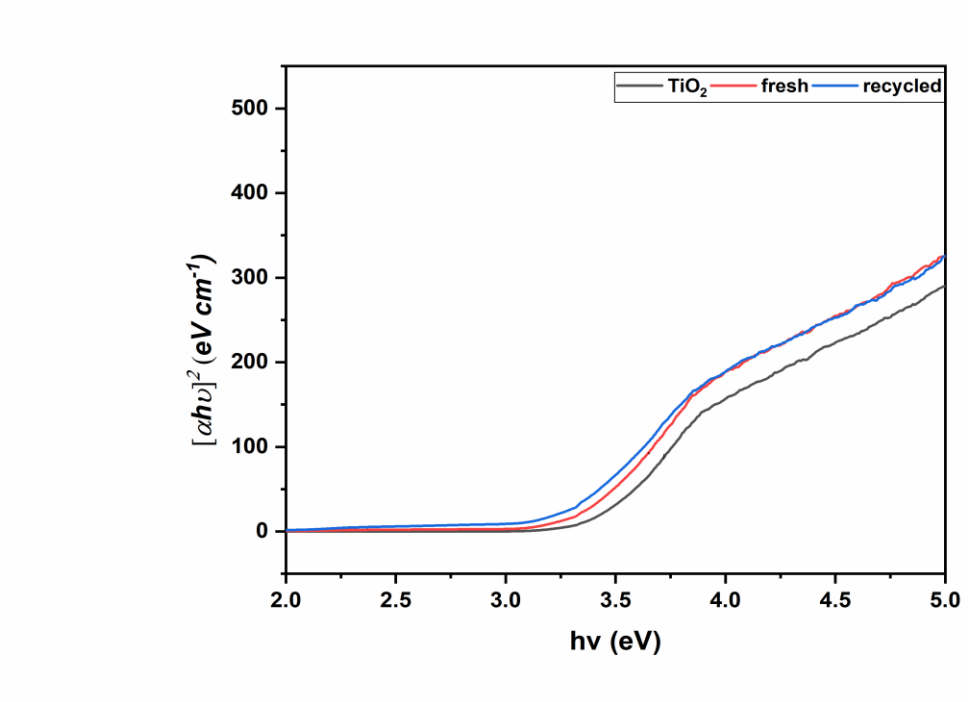

Fig. 4. 23 UVDRS analysis of the Raw TiO_2, Fresh and recycled composite beads

4.3.7.5 HRTEM analysis

The morphology and lattice spacing of both fresh and recycled Fe-TiO_2 composites were examined using high-resolution transmission electron microscopy (HRTEM), as illustrated in Fig. 4.24. The HRTEM images reveal lattice-like patterns of Fe-TiO_2 particles with lattice spacings between 0.35 nm and 0.36 nm. This specific range of lattice spacing is indicative of the TiO_2 anatase (101) crystal plane. The analysis highlights the integrity of the anatase phase in both fresh and recycled samples, suggesting that the recycling process does not significantly alter the crystalline structure of the Fe-TiO_2 composite. Furthermore, the consistent lattice spacing observed in recycled samples underscores the potential for multiple uses of the composite in photocatalytic applications without compromising its structural properties. This stability is crucial for the practical implementation of Fe-TiO_2 composites in continuous wastewater treatment systems, ensuring sustained efficiency over extended operational periods.

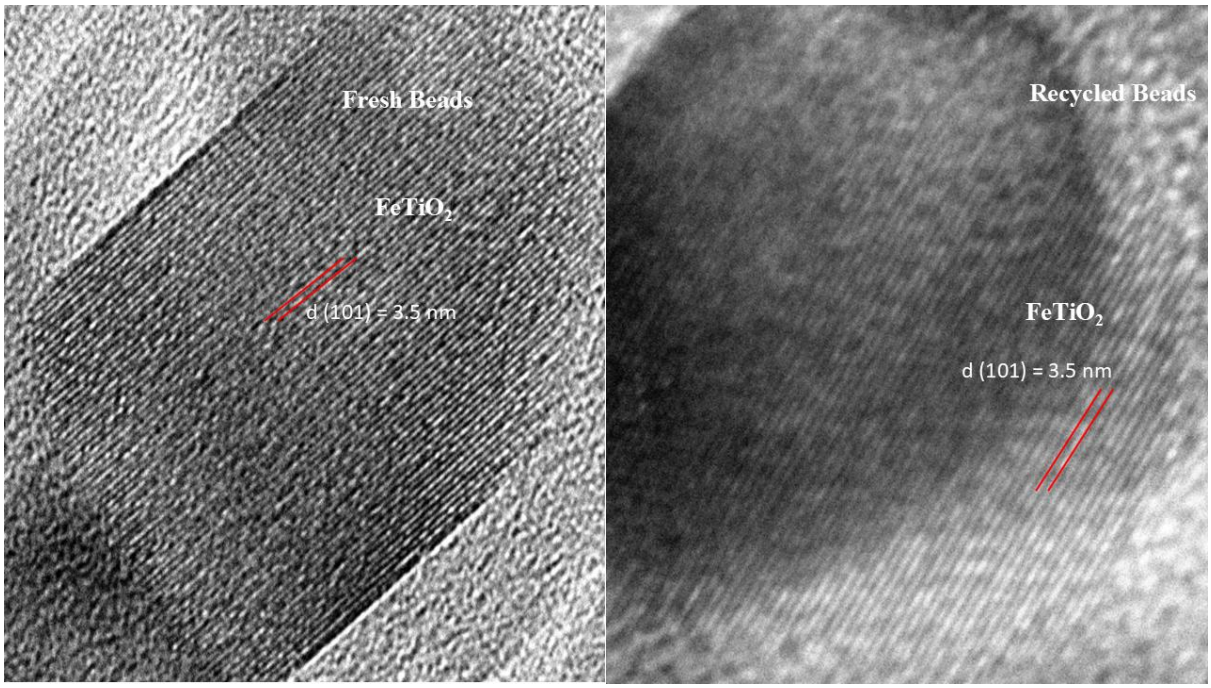

Fig. 4. 24 HRTEM analysis of freshly coated and recycled beads

4.3.7.6 Photoluminescence study

The importance of dual mechanism was validated by detecting the hydroxyl radicals ($OH^{\bullet}$) generated by three distinct photocatalytic methodologies: isolated photocatalysis, photo-Fenton reaction, and a dual process i.e., simultaneous photocatalysis and photo-Fenton process, as analysed via photoluminescence spectroscopy. The results showed that the combination

technique/dual process is more effective than solo photo-Fenton and solo photocatalysis in producing OH•. The photoluminescence spectra shed light on the electron-hole interactions within the photocatalysts, enhancing our understanding of their operational dynamics. This research advances the development of more effective and eco-friendly photocatalytic solutions for treating wastewater. Fig. 4.25. encapsulates the comparative analysis of OH• generation rates across the evaluated photocatalytic processes, underscoring its critical role in eliminating color from wastewater. Such insights are pivotal for refining the design and efficiency of photocatalytic systems dedicated to water purification efforts.

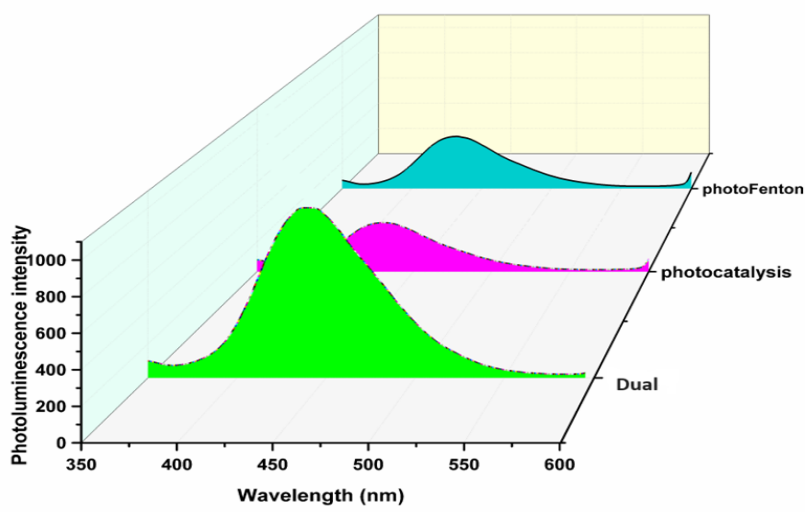

Fig. 4. 25 Photo luminance spectra of OH• for different processes

4.3.8 Cost analysis

Precise cost estimation is of paramount importance in dual scale-up studies. Insights into the financial implications and feasibility of implementing these processes are provided to stakeholders by this analysis. It facilitates decision-making, optimizes processes, and guarantees economically viable solutions to environmental challenges. Process economics would unquestionably be taken into account in any commercial-scale implementation of any technique. The present investigation concentrates on the estimation of process economics by integrating the estimated cost of primary materials and other process factors. The cost estimate associated with wastewater treatment is presented in Table 4.3. However, once the design elements of industrial-scale reactors are considered, the estimated cost may be further adjusted. Let's assume that the amount of wastewater is 10,000 L in order to estimate the cost of treatment

for a current-scale reactor. For this estimate, the 0.6 scaling-up rule was used, which can be seen in the Eq. 4.4.

$$\boldsymbol{COST_B = COST_A \left(\frac{SIZE_B}{SIZE_A}\right)^N} \qquad \textbf{4. 4}$$

Where N = Exponent size, $SIZE_A/SIZE_B$ = Dimensionless size factor and value of N were reported from (Tribe and Alpine 1986)

The key advantage of this study is the multiple times reusability of the beads which cut down a lot of burden of catalyst recovery/making cost for every cycle proving it to be a good option for its commercial application. The scaleup study estimation is given in Table 4.3.

Table 4. 3 Cost analysis for the complete Dual-process and scale-up study for UASB stream

Capital Cost	**Energy consumption**
Cost of Reactor fabrication= 35 US$ Buffering of tank =2 US$ The cost of fittings and piping= 10 US$ Any pre-treatment required = 2.4 US$ The total cost involved in fabrication = 49.4 US$	Cost of energy consumption = 0.81 $/kwh
Catalyst and raw material	**Other costs involved**
The cost involved in catalyst Raw material cost (FS, FA, and clay) = 0US$ Cost of TiO_2 catalyst (36 gm) = 1.152US$	Various controls involved = 1US$ Various other costs = 7US$ Contingency cost = 2US$

Electricity consumption using muffle=0.75 kwh×0.064 $/kwh= 0.048$ Total Price = 1.2 US$	
Cost of the oxidant involved H_2O_2 usage for 100 runs= 350 ×100=35000 mL The total cost of H_2O_2 used= 2.9 US$	**Total cost** Overall Total cost involved = 64.31 US$ for 100 recycles for 10 L Cost of 1 cycle for handling 10 L = 0.64 US$ Treatment cost/ L per cycle = 0.064 US$
Scale-up cost analysis (10,000L) Scale-up cost of raw material = 70.39 US$ Scale-up cost of energy consumption = 55.60 US$ Scale-up cost of oxidant = 119.52 US$ Scale-up cost of reactor fabrication = 532.64 US$ Other miscellaneous cost and contingency = 428.97 US$ Total cost = 1207.12 US$ (for 100 reactions handling 10,000L Volume) Cost for 1 reaction per cycle = 0.00120 US$	

The cost analysis for treating effluent through a once-through technique reveals an overall expenditure of 64.31 US$ for 100 recycles handling 10 L, translating to a treatment cost

of 0.064 US$ per litres per cycle. Scaling up to 10,000 L, the total cost rises to 1207.12 US$ for 100 reactions, with a cost per cycle of 0.0012 US$. Despite the initial expenses associated with reactor fabrication, energy consumption, and the use of oxidants like H_2O_2, there is potential for significant cost reduction. In the paper industry, where large volumes of effluent are treated, reusing the composite material and optimizing the oxidation processes can lead to further cost savings. By enhancing the recovery and reuse of catalysts and other materials, minimizing energy consumption through process optimization, and improving the efficiency of chemical usage, the overall treatment costs can be reduced. Additionally, reusing the treated effluent in other processes can help lower the demand for fresh water, thereby contributing to more sustainable and cost-effective operations.

4.4 Preliminary study of I/L stream

Fig. 4.26 illustrates the outcomes of various preliminary reactions conducted in a batch reactor to determine the effectiveness of different processes in removing color from an effluent. The experiments were aimed at establishing boundary conditions by examining the impact of different variables like light exposure, oxidant dosage, and the use of blank beads.

4.4.1 Adsorption Experiment:

- Conducted in a dark environment using blank beads.

- The results showed slight color reduction in the effluent.

- This lack of effectiveness is likely due to the formation of a monolayer of effluent on the beads, which hinders further adsorption and results in minimal color removal.

4.4.2 Photolysis under Solar Irradiation:

-In this experiment, blank beads were used to cover the reactor's surface while the effluent was exposed to sunlight.

- A change in the color of the effluent was initially observed, but ultimately, there was no significant reduction in color.

- This outcome suggests that solar light alone is insufficient to alter the color concentration of the effluent, indicating that photolysis by itself is not effective for color removal.

4.4.3 Impact of Oxidant Dosage in Dark and Sunlight:

- The effect of varying oxidant dosages on color removal was tested both in the absence of light and under sunlight exposure.

- The findings indicated no significant difference in the percentage of color removal between these two conditions.

- This suggests that neither the presence of light nor the oxidant dosage, within the tested range, has a meaningful impact on enhancing color removal.

The results highlight that a dual process combining methods such as photocatalysis and the photo-Fenton process could be more effective in achieving higher percentages of color removal. This synergy could be due to the complementary mechanisms of the processes involved.

The preliminary experiments indicate that simple adsorption or exposure to solar light alone is insufficient for effective color removal. The data underscores the potential need for more advanced or combined processes, such as a dual process involving photocatalysis and the photo-Fenton reaction, to achieve significant color reduction in the effluent. The graph thus serves as an important reference for optimizing conditions and selecting more effective treatment methods in subsequent studies.

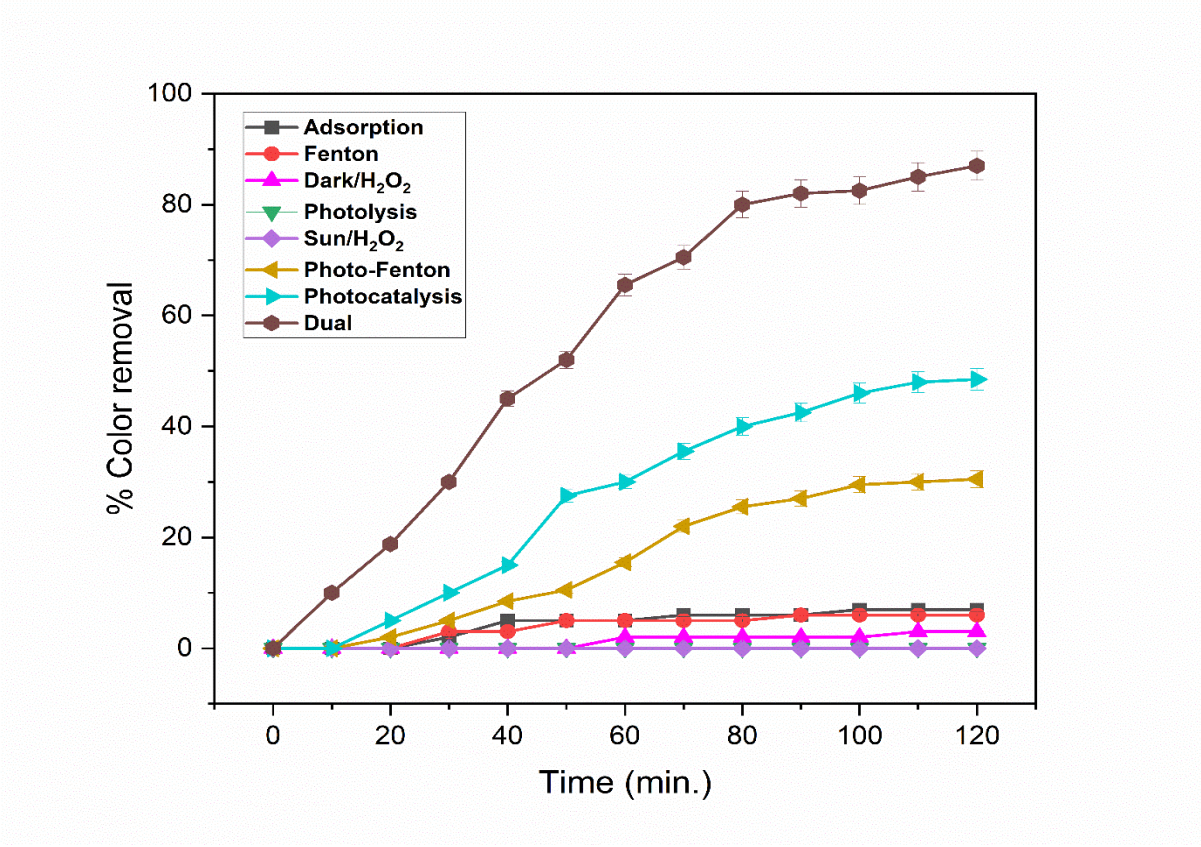

Fig. 4. 26 Preliminary study of I/L stream in dark and under solar light

4.4.4 Combined approach (Coagulation/flocculation followed by the dual process) for I/L effluent treatment at Batch scale

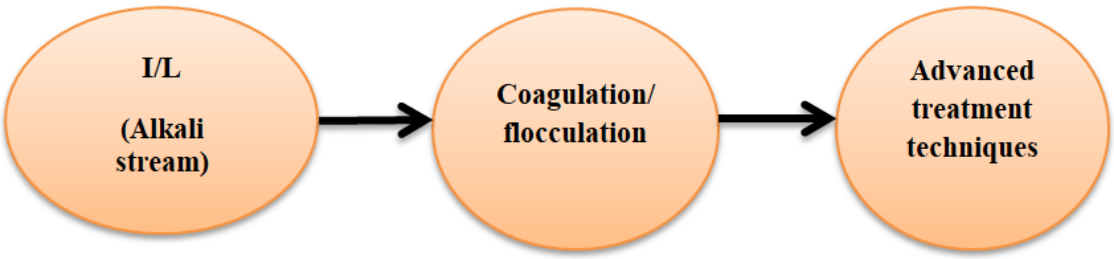

Fig. 4. 27 Approach followed by I/L stream

This study focused on treating the I/L stream from an agro-based P&P industry using a two-step process: coagulation-flocculation followed by simultaneous photocatalysis and the photo-Fenton process as shown in Fig. 4.27. The initial coagulation-flocculation step was essential to mitigate the dark color content of the effluent, which impeded light penetration in the subsequent reaction system. After color reduction through coagulation-flocculation, the dual technique significantly enhanced color removal efficiency. Photocatalysis, using a light-activated catalyst, facilitated contaminant breakdown, while the photo-Fenton process employed hydrogen peroxide and an iron catalyst under light conditions to generate hydroxyl radicals for effective pollutant degradation.

4.4.4.1 Effect of coagulant dose on coagulation/flocculation process

Following the precise adjustment, the pH levels to 6 specifically for the I/L stream, the study delved into assessing the impact of the coagulant, namely PAC. Various doses of PAC, ranging from 1.0 to 8.0 g/L, were thoroughly investigated. The most effective color removal in the I/L stream was identified at a PAC dosage of 3 g/L, leading to a significant color removal rate of approximately 45%. Despite obtaining superior results with a concentration of 3 g/L, a practical decision was made to designate 2.5 g/L as the optimized dosage. This choice was grounded in the negligible difference observed in outcomes between the two PAC volumes tested i.e., hardly 2% difference. Notably, the economic viability of selecting 2.5 g/L further solidified its status as the preferred dosage. Furthermore, it was shown that increasing the PAC dosage above the optimal level did not result in significant improvements. Excessive coagulant quantities were found to induce the re-dispersion of colloids. The mechanism of PAC involves the generation of multivalent aluminum ions, which neutralize charged colloidal particles. The resulting aluminum flocs effectively entrap the colloidal particles, facilitating their settlement,

as described by (Taylor et al. 2013). The optimized graph depicting coagulant dosage about % color removal for both streams is visually presented in Fig.4.28 a. This graph demonstrates the effectiveness of the selected PAC dosage in the I/L stream.

4.4.4.2 Effect of pH on coagulation/flocculation process

In the P&P industry, wastewater containing suspended particles, including colorants and other pollutants, is generated during various manufacturing processes. The coagulation/flocculation process is commonly used for the treatment of such wastewater. pH is a crucial parameter that affects the efficiency of the process, as it influences the charge of the particles and the performance of the coagulant.

This study examined the impact of pH on the coagulation/flocculation efficiency for color removal in P&P industry wastewater, varying the pH from 4 to 7. Optimal results were achieved at pH 6 for the I/L effluent, maintaining this level throughout the study (as shown in Fig. 4.28 b). The pH optimization at 6 resulted in a significant 43.47% color removal. This finding highlights the importance of pH as a critical operational parameter, emphasizing the need to balance technical efficiency and economic feasibility in the P&P industry wastewater treatment processes.

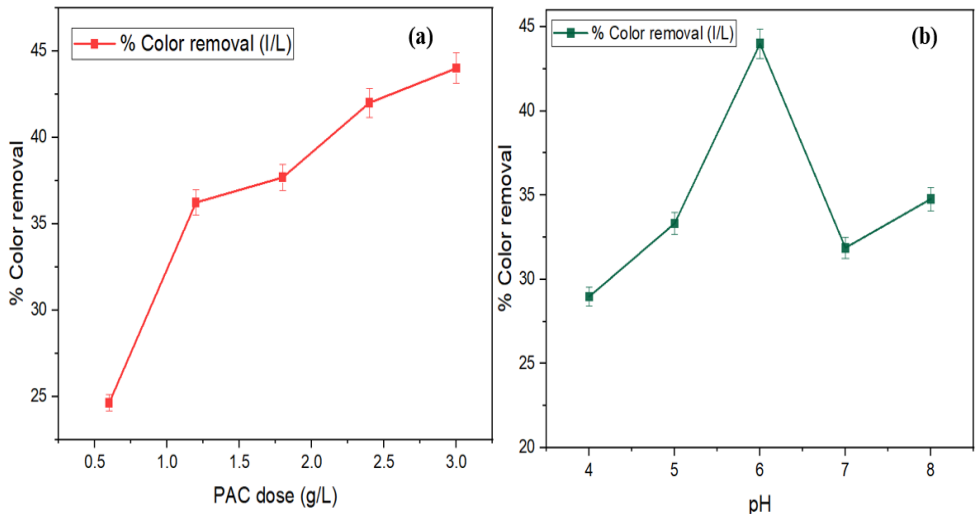

Fig. 4. 28 (a) Effect of PAC dose on % color removal (t=20 min., pH = 5.5) (b) Effect of pH on % color removal (t=20 min., PAC dose = 3g/l)

4.4.5 Dual Process Optimization at Batch scale

In order to optimize the dual process, we took into account several important aspects, such as the oxidant, catalyst dose, time and pH were considered to improve the efficiency and efficacy of the dual process and enhance the quality of the treated streams. The findings of this study emphasize the substantial influence of the first coagulation and flocculation phase on the effectiveness of the dual process, underscoring the significance of taking these aspects into account in wastewater treatment.

4.4.5.1 Effect of oxidant dose on dual process

The use of hydrogen peroxide (H_2O_2) in photo-Fenton and photocatalysis is effective for increasing hydroxyl radical ($OH^{\bullet}$) production. In this study, H_2O_2 serves a dual role in both processes, as shown in Eqs. 4.1-4.3, reacting with conduction band electrons to prevent electron-hole recombination, thus enhancing ROS and $OH^{\bullet}$ production. H_2O_2 concentration was varied from 0.2 to 0.6 g/L. Results show that pigment removal increased with H_2O_2 concentration, peaking at 0.35 g/L for the I/L stream (Fig. 4.29 a). Beyond this concentration, efficiency declined due to H_2O_2 scavenging effect, which consumes $OH^{\bullet}$ (Eqs.4.1-4.3). Our study identified an optimal H_2O_2 dose lower than those reported in similar studies (Ginni et al. 2014a; Grötzner et al. 2018a; Yuliani et al. 2018).

4.4.5.2 Effect of catalyst dose on dual process

As the catalyst is coated on the composite beads, the catalyst dose in this study is expressed as the percentage of surface area covered by catalyst-coated beads for the treatment of wastewater using a dual process. To determine the optimal catalyst dosage, the number of beads were varied taking into consideration the area of the reactor while keeping the H_2O_2 dose constant as mentioned in the previous section. The results indicate that a low catalyst dosage, as indicated by 50% surface area coverage, resulted in less effective removal of color from the effluent. However, increasing the percentage of surface area covered by beads from 50% to 100% led to a substantial increase in removal efficiency, which was confirmed by an incrementing trend in the % color removal graph. Beyond 100% coverage, a negative trend was observed, which was attributed to bead overlap that capped active sites, hampered light penetration, and hindered binding of pollutants to the composite, ultimately resulting in a decrease in the % color removal. Both streams exhibited a similar trend in the results, with the best outcome being achieved when the surface area coverage was 100% for both as shown in

Fig. 4.29 b. These findings are consistent with previous studies that have emphasized the importance of sufficient active sites for effective catalyst performance (Thakur et al. 2020a; Puri et al. 2021; Puri and Verma 2023). Effect of time i.e., % color removal at different time intervals which gave a decent color removal of 87.17% in 120 min. as given in Fig. 4.29 c.

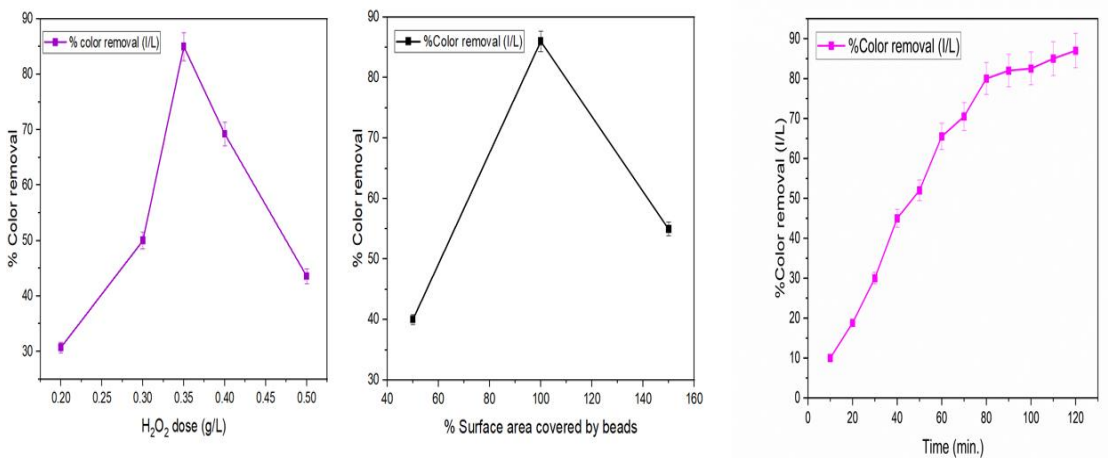

Fig. 4. 29 (a) Effect of H_2O_2 dosage on % color removal (t= 140 min., pH= 4.5, % S.A covered= 100) (b) Effect of change in % color removal at different no. of beads (t= 140 min., pH= 4.5, H_2O_2 dose= 0.35 g/L) (c) Effect of time on % color removal (pH= 4.5, H_2O_2 dose= 0.35 g/L, % S.A covered= 100)

4.4.5.3 Scavenging study for I/L stream

An extensive investigation was undertaken to identify and scavenge various radicals such as $OH^{\bullet}$, h^{+}, and $O^{2\bullet-}$, with $OH^{\bullet}$ being confirmed as the predominant radical. Several experiments were meticulously designed to pinpoint the specific radicals involved and to assess their impact on the process's efficacy. A variety of radical-neutralizing agents were utilized in this study. Specifically, 0.01M p-benzoquinone (BQ) was employed to counteract $O2^{\bullet-}$, disodium ethylene diamine tetra acetic acid (EDTA) was used to neutralize h^{+}, and tert-butyl alcohol (TBA) was selected as the quencher for $OH^{\bullet}$ radicals. These quenching agents were systematically introduced into different reactors, and the reactions were carried out under optimized conditions. The results demonstrated that the effluent's color removal efficiency decreased in all instances; however, the presence of TBA notably reduced activity by approximately 70-75%, as shown in **Table 4.4**. This significant reduction indicates that the inhibition of $OH^{\bullet}$ activity plays a crucial role in the process, highlighting the importance of $OH^{\bullet}$ radicals.

Table 4. 4 Scavenging study for I/L using various quenchers

% Color removal without scavenger (I/L)	*% Color removal with BQ (I/L)*	*% Color removal with EDTA (I/L)*	*% Color removal with TBA (I/L)*
87.17%	*60%*	*85.5%*	*26%*

4.4.5.4 Mineralization study

To validate the oxidation process, a mineralization study was performed by measuring COD reduction. The results of the study revealed that the dual effect approach, which combined photocatalysis and photo-Fenton processes, was more effective at reducing COD than either the isolated photocatalysis or photo-Fenton process. The superior performance of the dual effect approach was attributed to its ability to generate a significantly larger quantity of $OH^{\bullet}$, which are instrumental in breaking down the organic pollutants in wastewater. The dual process achieved a COD removal of 68 % for the I/L stream, while the isolated photocatalysis and photo-Fenton processes achieved 15 % and 5 % COD removal for I/L stream, respectively as shown in Fig. 4.30.

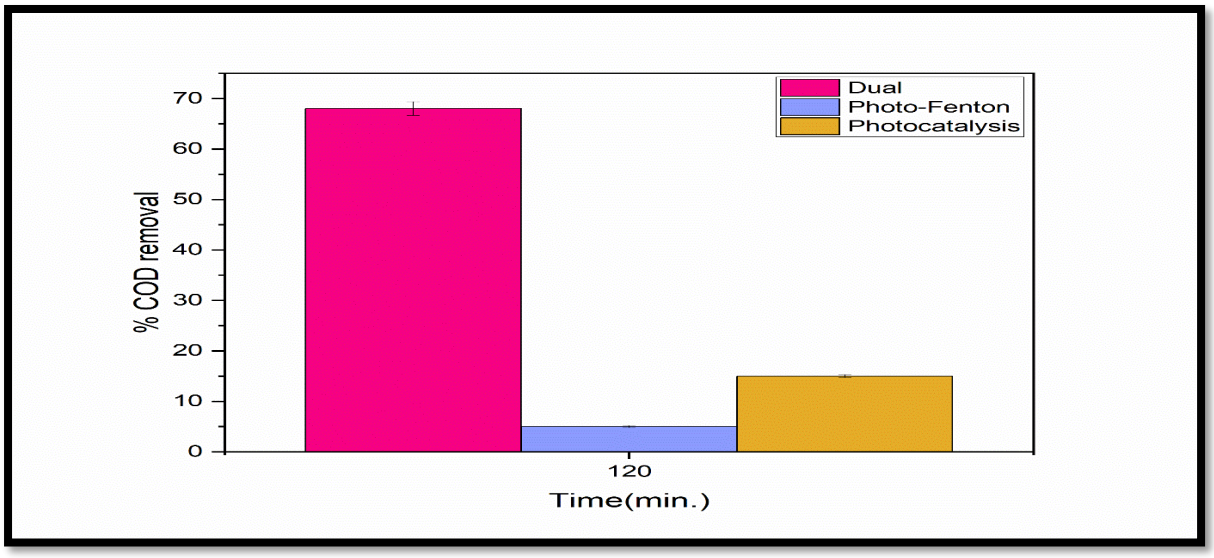

Fig. 4. 30 COD removal by different processes in I/L stream (pH= 4.5, H_2O_2 dose= 0.35 g/L, % S.A covered= 100)

4.4.6 I/L stream (Recirculation study)

This steam is alternatively referred to as the alkali stream or the stream mostly originating from the paper manufacturing sector. This too exhibits a highly concentrated color, although slightly lower than the UASB stream, yet possesses a greater volume. A similar approach was followed here as well i.e., Pretreatment (coagulation/flocculation) followed by AOP (Dual technique) as explained in section 4.4.4.

4.4.6.1 Coagulation/Flocculation as a pretreatment

It followed the similar method as explained in earlier sections. It was an important step to be performed due to stout color of the I/L stream, this included optimization of the pH and coagulant dose. Optimal results were achieved at pH 6 for the I/L effluent, maintaining this level throughout the study (as shown in Fig. 4.28 b). The pH optimization at 6 resulted in a significant 43.47% color removal. The most effective color removal in the I/L stream was identified at a PAC dosage of 3 g/L, leading to a significant color removal rate of approximately 45%. Despite obtaining superior results with a concentration of 3 g/L, a practical decision was made to designate 2.5 g/L as the optimized dosage. This choice was grounded in the negligible difference observed in outcomes between the two PAC volumes tested i.e., hardly 2% difference as shown in Fig. 4.28 a.

4.4.7 Design of Experiment

The Design-Expert software employed RSM, or response surface methodology, to conduct the experiment. This methodology incorporates a variety of statistical and mathematical methodologies to construct and analyse outcomes, especially in cases when the dependent variable is influenced by several factors. The primary objective of this research was to optimize the response through the variation of multiple parameters. RSM facilitates the interpretation of the relationship between regulated input parameters and response variables while conserving time. Numerous trials designed under RSM were conducted to optimize the H_2O_2 dose, % surface area covered, and Flow rate for color removal from the I/L stream of the P&P industry. The study on color removal employed a factorial method to ensure its completion. The RSM design presented in Table 4.5 suggested 17 set of responses with actual and predicted results. The variables were fit with the second-order regression model in the form of a quadratic polynomial Eq. 4.5

$$\boldsymbol{R = \beta_{\circ} + \sum_{i=1}^{k} \beta_i x_i + \sum_{i=1}^{k} \beta_{ii} x_i^2 + \sum_{i,j=1} \sum_{i<j} \beta_{ij} x_i x_j + e} \qquad \textbf{4. 5}$$

Where constant regression coefficients are denoted by β_0, β_i, β_{ii}, and β_{ij}; coded input factors are denoted by x_i and x_j; e is an error function, and R is the response.

Designs such as the first order, 2k factorial, Plackett–Burman, and simplex are commonly used. First-order polynomial models are not very reliable and flexible in predicting variance, and they often show a lack of fit due to the curvature of the response surface and the factors involved. To address these limitations, second-order polynomial models are needed to create a quadratic response surface model. This helps overcome the drawbacks of first-order designs and improves the optimization process. Designs such as the Box-Behnken, Doehlert, central composite, and three-level factorial designs are examples of second-order symmetrical designs. For this study, the Box-Behnken design was selected.

Table 4. 5 Factorial BBD matrix with 3 independent variables for I/L stream

Experiment No.	x_1 **H_2O_2 (mg L^{-1})**	x_2 **% Surface area covered**	x_3 **Flow rate (mL min^{-1})**	**R1 % color removal (min)**	**R2 % COD removal**
1	500	150	4.0	69	40
2	500	100	6.0	80	35.5
3	500	100	6.0	78.9	35
4	500	100	6.0	89	35
5	500	100	6.0	75	35
6	700	100	4.0	64	30.1
7	700	150	6.0	65.9	30
8	500	150	8.0	58.5	29.2

9	500	100	6.0	80.5	25
10	700	100	8.0	48	24.6
11	700	50	6.0	52	20
12	300	100	4.0	60	20
13	500	50	4.0	59	19.5
14	300	150	6.0	34.5	12
15	500	50	8.0	40.5	12
16	300	50	6.0	17.2	10
17	300	100	8.0	20	5

4.4.7.1 Response Study and Elucidation Using Box-Behnken Design (BBD)

The study used Response Surface Methodology (RSM) with Box-Behnken Design (BBD) in the Design-Expert software to design the experiments. It aimed to understand how dual technology affects the removal of color from P&P industry wastewater. Several parameters were optimized to investigate the best process variables for color and COD removal, focusing on the response to these variables i.e., % color and % COD removal. The experimental design involved three different process variables i.e., design included three diverse process variables, i.e., H_2O_2 dose (A) (300-600 mgL^{-1}), (B) % surface area covered by beads (50–150%), and (C) flow rate (4-8 Lh^{-1}). The construction of the BBD matrix involved seventeen iterations of experiments. The outcomes correlated to the predicted and actual results, as illustrated in Table 4.6. The research revealed that the maximum achievable level of color removal was between 85 and 87 percent, with an error of less than 5 % in comparison to the predicted values. Analysis of variance (ANOVA) was employed to evaluate the reliability and significance of the quadratic model fitted to the experimental data.

Table 4. 6 Predicted versus Experimental values of the I/L stream study

Responses	Predicted value	Experimental value
% Color removal	84.13%	84.5%
% COD removal	38.30%	40%

4.4.7.2 Analysis of variance (ANOVA)

The model Robustness was determined by R^2 values in case of both % color and % COD removal. The acceptable value of R^2 has to be greater than or equivalent to 0.8; it becomes increasingly significant as it approaches near to 1. Both responses had R^2 value greater than 0.8 i.e., 0.95 and 0.90 for % color and % COD removal respectively. The results of an analysis of variance (ANOVA) indicate that p-values less than 0.05 provide further evidence that the model is appropriate for the intended investigation as shown in Table 4.7. Statistical analysis of the percentage of color and COD removal from wastewater was carried out using ANOVA and the model was found to be non-significant with an F-value of 3.03 and 1.35 for % color and % COD removal respectively confirming the model to be sufficiently valid.

Table 4. 7 Analysis of variance for the response rate of color removal study of I/L stream

Source	Sum of Squares	df	Mean Square	F-value	p-value	
Model	6658.98	9	739.89	15.07	0.0009	significant
A-H_2O_2	1205.41	1	1205.41	24.55	0.0016	
B-% surface area covered	438.08	1	438.08	8.92	0.0203	

C-Flow rate	903.13	1	903.13	18.39	0.0036	
AB	2.89	1	2.89	0.0588	0.8153	
AC	144.00	1	144.00	2.93	0.1306	
BC	16.00	1	16.00	0.3258	0.5860	
A^2	2328.23	1	2328.23	47.41	0.0002	
B^2	917.92	1	917.92	18.69	0.0035	
C^2	353.67	1	353.67	7.20	0.0314	
Residual	343.76	7	49.11			
Lack of Fit	238.61	3	79.54	3.03	0.1564	not significant
Pure Error	105.15	4	26.29			
Cor Total	7002.74	16				

4.4.7.3 The influence of several variables on the color and COD removal

To analyse the interplay between the factors and the outcome, individual modifications were made to each factor, while the two process variables remains unchanged. Fig 4.31 a-c and 4.32 a-c shows the effect of each variable (A, B, C) on response (Y_1, i.e., color removal and Y_2, i.e., COD removal respectively) i.e., effect of oxidant dose, % surface area covered by the beads, and flow rate. Each factor was determined to be extremely significant in the investigation, but H_2O_2 was the most substantial factor in this study. Besides photo-Fenton it also reacts with conduction band e^- in photocatalysis and add extra amount of $OH^\bullet$ in the system. Hydrogen peroxide (H_2O_2) is employed simultaneously in the photocatalytic and photo-Fenton processes in the present study. By reacting with the electrons of the conduction band (e^-_{CB}), it prevents the recombination of holes (h^+) and electrons (e^-). The research investigates the effects of H_2O_2 concentrations ranging from 300 to 700 mg L^{-1}. As illustrated

in the Fig. 4.31 a, a progressive increase in color and COD removal was observed as the oxidant dose was augmented from 300 to 600 mg L^{-1}. However, as the oxidant dose continued to be increased, the efficacy of color and COD removal commenced to deteriorate. This drop can be attributed to the H_2O_2 scavenging effect when used at higher concentrations, as it starts to consume the $OH^{\bullet}$ as given in Eqs. 4.6-4.7

$$\boldsymbol{Oxygen + OH^{\bullet} \rightarrow Hydroperoxyl^{\bullet} + H_2O} \quad \textbf{4.6}$$

$$\boldsymbol{Hydroperoxyl^{\bullet} + OH^{\bullet} \rightarrow +H_2O + Oxygen} \quad \textbf{4.7}$$

A significant challenge in implementing AOPs on a large scale is the development of a durable catalyst that can be easily managed and provides an efficient surface area for wastewater treatment. This study addresses this challenge by using a spherical support to immobilize the catalyst, which enhances the surface area available for the reaction. During the experiment, it was observed that the efficiency of color removal was lower when 50% of the reactor area was covered with beads. However, as more surface area was covered, there was a noticeable increase in color removal according to the graph. The study revealed that the optimal coverage of beads for the reactor area was 91.4%. This coverage increased the catalyst's reaction space, resulting in the production of more $OH^{\bullet}$ radicals, which deteriorate color and COD more rapidly. However, adding more beads beyond this point would cause them to overlap. This overlapping would reduce the amount of light getting through and the number of active sites available for the reaction, making color and COD removal less effective.

The analysis of the three-dimensional (3D) surface responses, as illustrated by the model reveals that the color removal efficiency can be forecasted by maintaining a constant reaction time. As shown in Fig. 4.31 a-c and 4.32 a-c the interactions (AB, AC, BC) are manifestly more influential than the individual (A, B, C) and quadratic (A^2, B^2, C^2) effects. This discovery is consistent with previous investigations (Bansal et al. 2018; Puri et al. 2021), which have consistently shown that all three criteria have a significant influence on the efficacy of color removal.

Flow rate was another factor varied from 4.0-8.0 Lh^{-1} for the optimization. Fig. 4.31 b and 4.32 b shows that when flow rate was increased from 4 to 8 the % color and % COD removal started declining attributing to the fact that when flow rate increases the contact time of wastewater pollutants and the composite decreases. It leaves the reactor without any

significant contact with the catalytic particles, thus decreasing the efficacy. The best reduction of color and COD was seen at the lowest flow rate i.e., 4.23 Lh^{-1}.

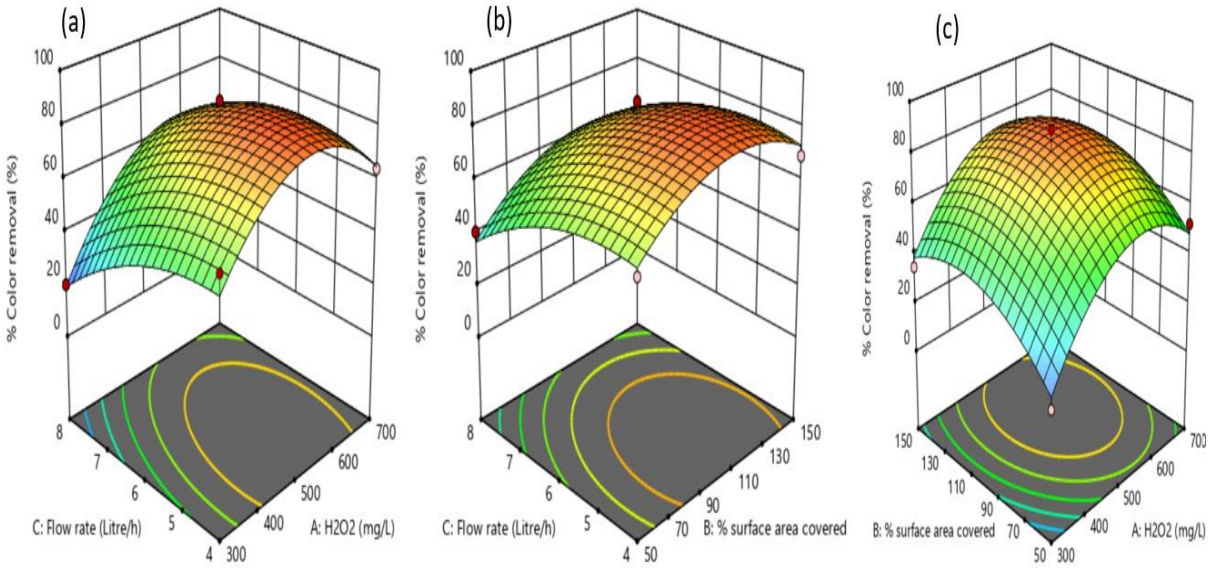

Fig. 4. 31 3D response surface plot of the effect of different factors and their interactions on % color removal (a) Flow rate and H_2O_2 (b) Flow rate and % Surface area covered (c) % Surface area covered and H_2O_2

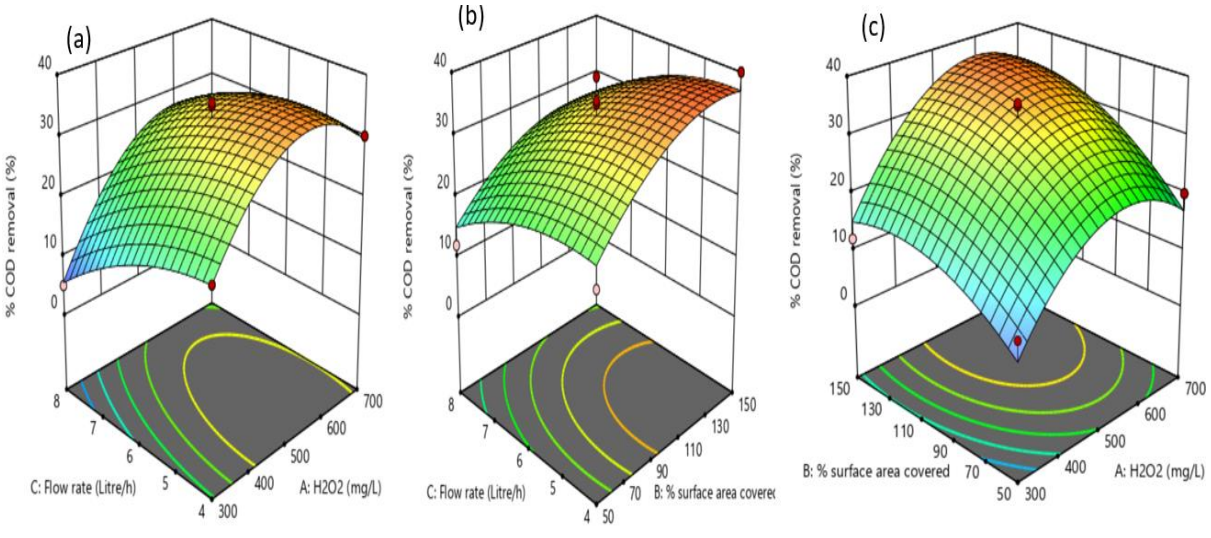

Fig. 4. 32 3D response surface plot of the effect of different factors and their interactions on % COD removal (a) Flow rate and H_2O_2 (b) Flow rate and % Surface area covered (c) % Surface area covered and H_2O_2

4.4.7.4 Numerical optimization

To optimize the eradication of color, specific ranges were established for individual factors A, B, and C using numerical optimization in the Design-Expert software. The optimized parameters, which were determined using a desirability function approach. One hundred sets of solutions were generated, and the optimal condition was determined by selecting the most preferable set are illustrated in Fig 4.33.

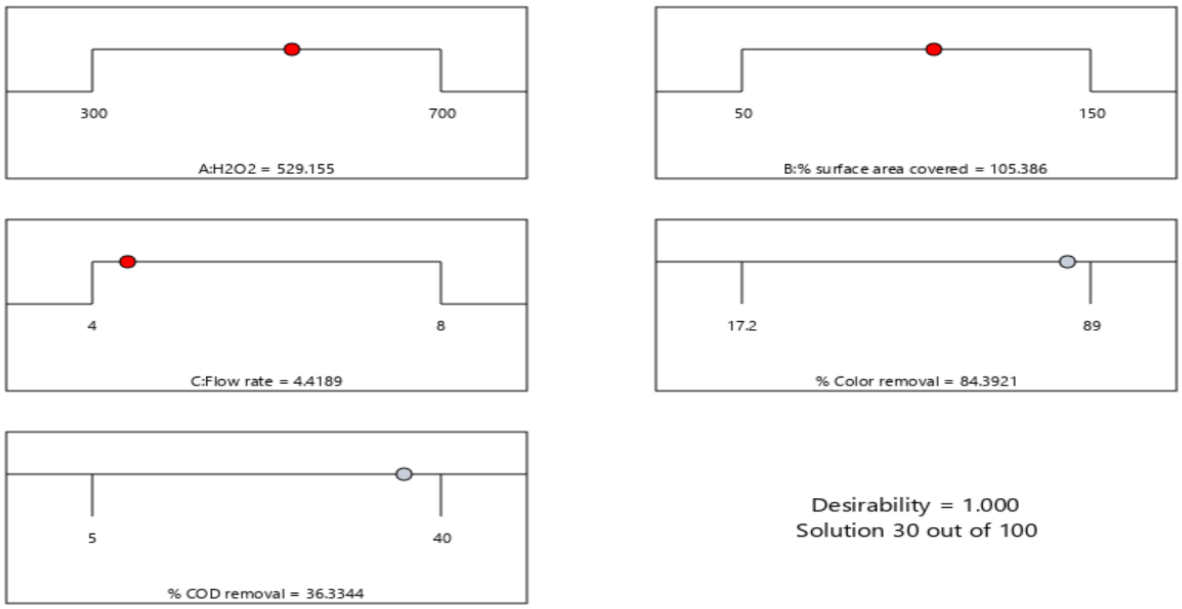

Fig. 4. 33 Numerically optimized conditions in ramp plots

4.5 Treatment of I/L stream in once through mode

4.5.1 Experimental test results for coagulation/flocculation (I/L stream)

Prior to further treatment of the intensely colored I/L stream, preliminary coagulation/flocculation was used to initially reduce the color. This step enhances the efficiency of subsequent photocatalytic treatment by improving light penetration. Various parameters were optimized to achieve the best conditions for the coagulation and flocculation of the selected stream.

4.5.1.1 Coagulation/Flocculation as a pretreatment

Following the previously described method, an essential step was conducted due to the intense color of the I/L stream. This involved optimizing the pH and coagulant dosage. Optimal results were obtained at a pH level of 6 for the I/L effluent, which was maintained throughout

the study (as shown in Fig. 4.34b). At this pH, a significant 43.47% reduction in color was achieved. The most effective color removal was observed with a PAC dosage of 3 g/L, resulting in approximately 45% color removal. However, it was practically decided to use a dosage of 2.5 g/L, as the difference in effectiveness between the two doses was minimal (around 2%), as shown in Fig. 4.34 a.

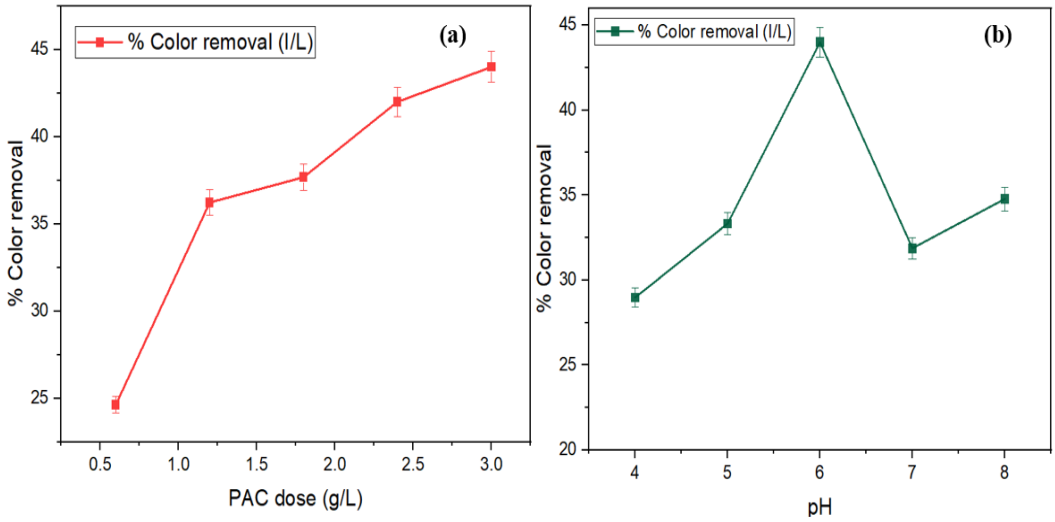

Fig. 4. 34 (a) Effect of PAC dose on % color removal (t=20 min., pH = 5.5) (b) Effect of pH on % color removal (t=20 min., PAC dose= 3 g/L)

4.5.2 Process optimization for dual process

Different factors like number of reactors, number of baffles, flow rate, % surface area covered and role of different quenchers were varied to obtain the best-optimized results for the color removal of the given streams provided by the agro-based P & P industry using dual study.

4.5.2.1 Effect of % surface area covered by beads

Fig. 4.35 a shows the optimal number of composite beads required for effective color removal by varying the % surface area (S.A) covered by the beads was determined. We evaluated coverage percentages ranging from 50% to 100%, and observed a significant improvement in color removal with greater surface area coverage i.e., 100%. By increasing the number of composite beads, the exposed surface area and the amount of catalyst increased correspondingly. This augmented catalyst presence accelerated the rate of color removal across the I/L stream. As the stream progressed through consecutive reactors, it encountered newly introduced fixed-bed composite catalysts in each reactor. This arrangement extended the active sites and facilitated the generation of more active radicals, which substantially enhanced color

removal efficiency. However, when the surface area coverage was increased to 110%, no further improvement or decline in the percentage of color removal was observed. Consequently, it was determined that the optimal configuration involved a 100% exposed surface area, which resulted in an 89% color removal efficiency for the I/L stream. This setup provided the most effective balance between the percentage of surface area covered by the beads and the efficiency of color removal, indicating that maximizing surface area exposure up to 100% is essential for improving treatment efficacy.

4.5.2.2 Effect of the number of reactors

In this study, we used a series of three reactors to investigate the effects of various treatment configurations on the color removal efficiency of I/L effluent. Our experimental apparatus treated 10 L of this stream containing H_2O_2 under natural solar light, aiming to assess the system's practical application and sustainability. The results, illustrated in the accompanying Fig. 4.35 b show that the color of the streams decreased as they passed through each successive reactor. The series of three reactors plays a significant role in determining the residence time of pollutants with the active sites of the composite material, which in turn affects the color removal rate. Specifically, after passing through the first reactor, with an approximate residence time of 15 min., there was a 35.5% reduction in color in the I/L stream. When the second reactor was added, the color removal increased to 62.2%. Upon introducing a third reactor, the color removal efficiency reached 88.88%. Beyond this, further reactors were not taken into consideration because the ideal number of reactors depends on a variety of criteria, not just the percentage of color removal, but also operational efficiency and economic viability. The entire procedure was conducted in a once-through mode at a consistent flow rate, ensuring uniform treatment conditions. This study found that increasing the number of reactors in series can greatly improve color removal efficiency. However, the choice of reactors must balance economic and operational aspects to ensure viability. Achieving this balance is crucial for the practical implementation of wastewater treatment technologies.

4.5.2.3 Effect of different scavengers

To determine the primary oxidative species or radicals (such as $OH^{\bullet}$, $O^{2\bullet-}$, and h^{+}) responsible for the color removal from I/L stream using the Fe-TiO_2 composite, a series of experiments were conducted under optimal conditions. As depicted in Fig. 4.35 c, various quenching agents were utilized, including tert-butyl alcohol (TBA) for $OH^{\bullet}$, disodium ethylenediaminetetraacetic acid (EDTA) for h^{+}, and p-benzoquinone (BQ) for $O^{2\bullet-}$. The results

indicated that the % color removal was diminished in the presence of each quenching agent. This suggests that each of the previously mentioned oxidative species plays a role in the color removal process. A significant reduction of approximately 40-50% in color removal was observed for the I/L stream when TBA quencher was used, highlighting the crucial role of $OH^{\bullet}$ radicals in the color removal process. This indicates that $OH^{\bullet}$ radicals are the primary active species in the dual process of color removal.

4.5.2.4 Effect of flow rate

The flow rate also plays a major role in study as it decides the time of contact between the pollutant and the active site. In this study we varied the flow rate between 4.0 ± 1.0 L h^{-1} to 12.0 ± 1.0 L h^{-1}. Fig. 4.35 d shows that the best color removal for all three streams occurred at the minimum flow rate i.e., with increasing flow rate from 4.0 ± 1.0 L h^{-1} towards 12.0 ± 1.0 L h^{-1} the color removal efficiency started declining. The reason might me the less contact time between pollutant and the composite material. Whereas further decreasing may increase the color removal efficiency but it will hinder in commercial viability due to increased time and higher electricity consumption the overall cost of process will increase. But there was only marginal difference in % color removal between 4.0 and 6.0 ± 1.0 L h^{-1} so in study the best flow rate chosen was 6.0 ± 1.0 L h^{-1} with a % color removal of 88% was seen in I/L stream.

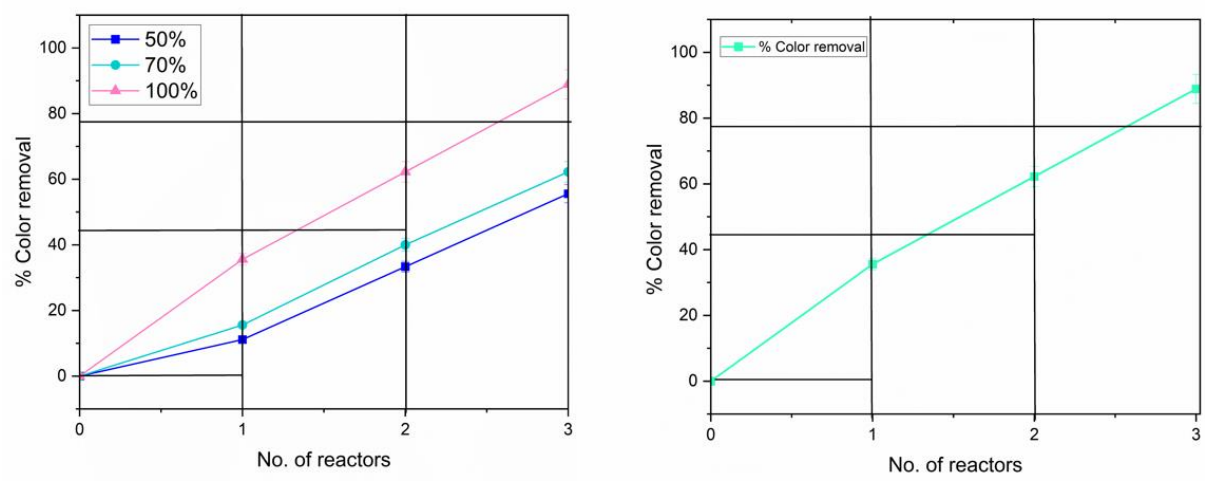

Fig. 4. 35 Change in the % color removal with (a) variation in the % surface area covered by the beads (t=45 min., No. of reactors= 3, Flow rate= 7.0 Lh^{-1}) (b) variation in the number of reactors (t=45 min., % S.A covered= 100, Flow rate= 7.0 Lh^{-1})

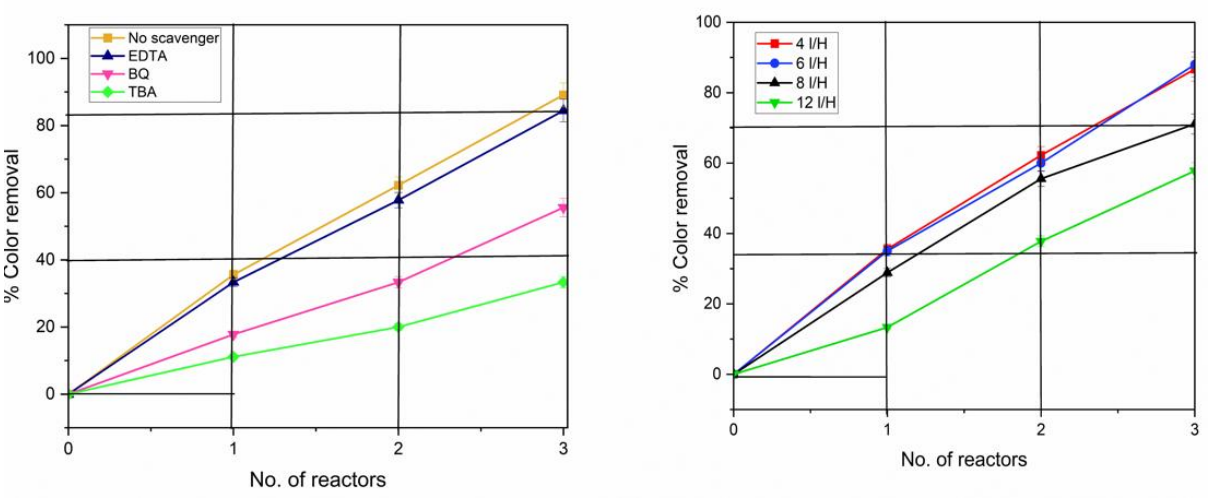

Fig. 4. 36 Change in the % color removal with (a) variation in different scavengers used rate (t=45 min., No. of reactors= 3, % S.A covered= 100, flow rate= 7.0 Lh^{-1}) (b) variation in flow rate (t=45 min., No. of reactors= 3, % S.A covered= 100)

4.5.3 Cost analysis

In dual scale-up studies, accurate cost estimation is essential for evaluating the financial feasibility of process integration. Building on the detailed explanation provided in section 4.3.8, this study combines the estimated cost of raw materials and process factors to assess wastewater treatment economics. For this estimate, assuming 10,000 L of wastewater, the 0.6 scaling-up rule was applied, as shown in Eq. 4.4. Table 4.8 presents the estimated costs, which may be adjusted based on the design elements of industrial-scale reactors.

The main advantage of this study is the beads' reusability, significantly reducing catalyst recovery and production costs, making it a viable option for commercial application. The scale-up cost estimation is provided in Table 4.8.

Table 4. 8 Cost analysis for the complete Dual-process and scale-up study for I/L stream

Capital Cost	**Energy consumption**
Cost of Reactor fabrication= 35 US$ Buffering of tank =2 US$ The cost of fittings and piping= 10 US$	Cost of energy consumption=0.81 $/kwh

Any pre-treatment required = 1.2 US$ The total cost involved in fabrication = 48.2 US$	
Catalyst and raw material The cost involved in catalyst Raw material cost (FS, FA, and clay) = 0US$ Cost of TiO_2 catalyst (36 gm) = 1.152US$ Electricity consumption using muffle=0.75 kwh×0.064 $/kwh= 0.048$ Total Price = 1.2 US$	**Other costs involved** Various controls involved = 1US$ Various other costs = 7US$ Contingency cost = 2US$
Cost of the oxidant involved H_2O_2 usage For 100 runs= 300 ×100=30000 mL The total cost of H_2O_2 used= 2.5 US$	**Total cost** Overall Total cost involved = 62.71 US$ for 100 recycles for 10 L Cost of 1 cycle for handling 10 L = 0.62 US$ Treatment cost/ L per cycle = 0.062 US$
Scale-up cost analysis (10,000L) Scale-up cost of raw material = 70.39 US$ Scale-up cost of energy consumption = 55.60 US$ Scale-up cost of oxidant = 109.33 US$ Scale-up cost of reactor fabrication = 532.64 US$ Other miscellaneous cost and contingency = 416.19 US$	

Total cost = 1184.15 US$ (for 100 reactions handling

10,000L Volume)

Cost for 1 reaction per cycle = 0.00118 US$

The cost analysis for treating effluent using the once-through technique indicates a total expenditure of 62.71 US$ for 100 recycles handling 10 L, leading to a treatment cost of 0.062 US$ per litre per cycle. Scaling up to a 10,000 L capacity results in an overall cost of 1184.15 US$ for 100 reactions, equating to 0.00118 US$ per cycle. Although the capital costs for reactor fabrication, energy consumption, and oxidant usage, particularly H_2O_2, contribute significantly to the total expense, there are opportunities for cost reduction. In the pulp and paper industry, reusing treated effluent and optimizing the recovery of catalysts and materials, such as TiO_2, can help minimize costs. Furthermore, enhancing process efficiency and reducing energy consumption by improving system design or using renewable energy sources can contribute to further cost savings. The reusable nature of certain process components, combined with these optimizations, can significantly impact long-term cost reductions, making the treatment process more economically viable.

4.5.4 Characterization

While the composite's detailed characterization was previously conducted and discussed, we repeated the analysis to determine if the different effluent had any impact on the characterization.

4.5.4.1 FESEM/EDS analysis

The results confirm the uniform distribution of TiO_2 on the surface, as seen in Fig. 4.37 a-b. Using field emission scanning electron microscopy (FESEM) and energy-dispersive X-ray spectroscopy (EDS), we analysed the morphology and elemental composition of TiO_2-coated beads before and after exposure to different effluents, including the I/L stream. The FESEM images revealed a consistent, glossy surface, while EDS confirmed the presence of titanium (Ti), iron (Fe), and oxygen (O). Notably, the characterization of the beads exposed to the I/L stream was similar to that of the other effluents, indicating that the I/L stream did not exert

additional strain. The composite beads maintained their integrity and potential for industrial applications even after exposure to the I/L stream.

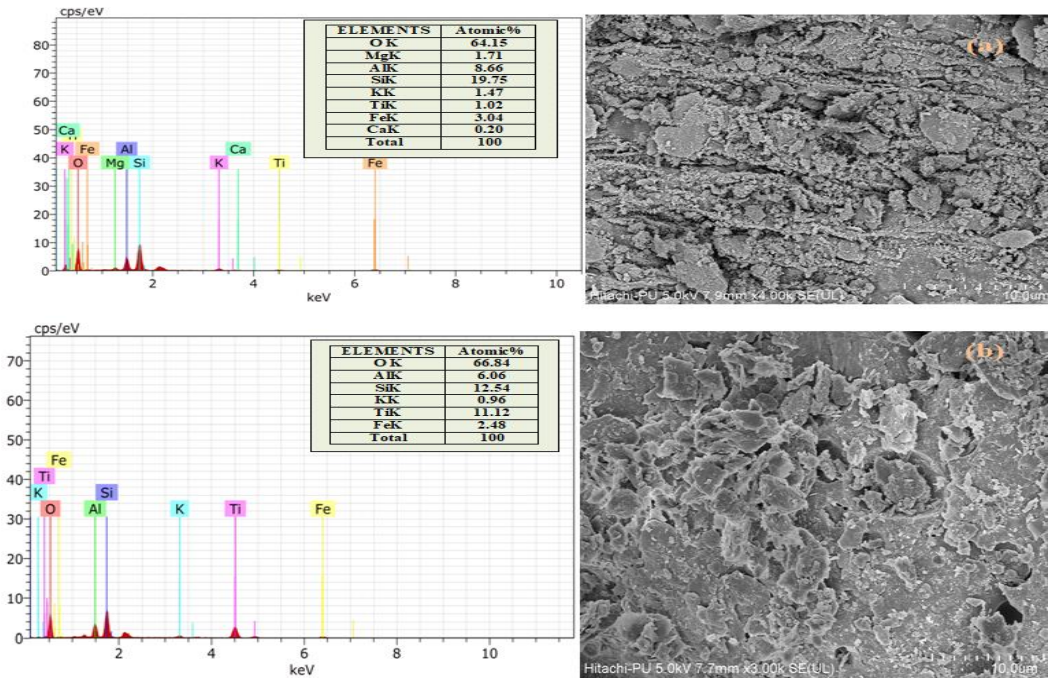

Fig. 4. 37 FESEM/EDS analysis of (a) Fresh composite (b) Recycled composite

4.5.4.2 XRD analysis

XRD analysis confirmed the formation of the Fe-TiO_2 composite and identified its crystalline phases as shown in Fig. 4.38 a-c. The XRD patterns displayed characteristic peaks for the anatase (25.4◦, 37.8◦, 48◦, 55◦, 62.6◦) and rutile (26◦, 36◦, 55◦) phases in both raw TiO_2 and the Fe-TiO_2 composite, with no changes observed after 100 recycling cycles or exposure to the I/L stream, indicating structural stability. The presence of ITO peaks confirmed the successful formation of the Fe-TiO_2 composite, with ITO peaks at 70.3◦ and 75.28◦ supporting enhanced photocatalytic activity through photo-Fenton reactions. These results, corroborated by UV-DRS analysis, underscore the composite's efficiency and durability under visible light, even after exposure to the I/L stream.

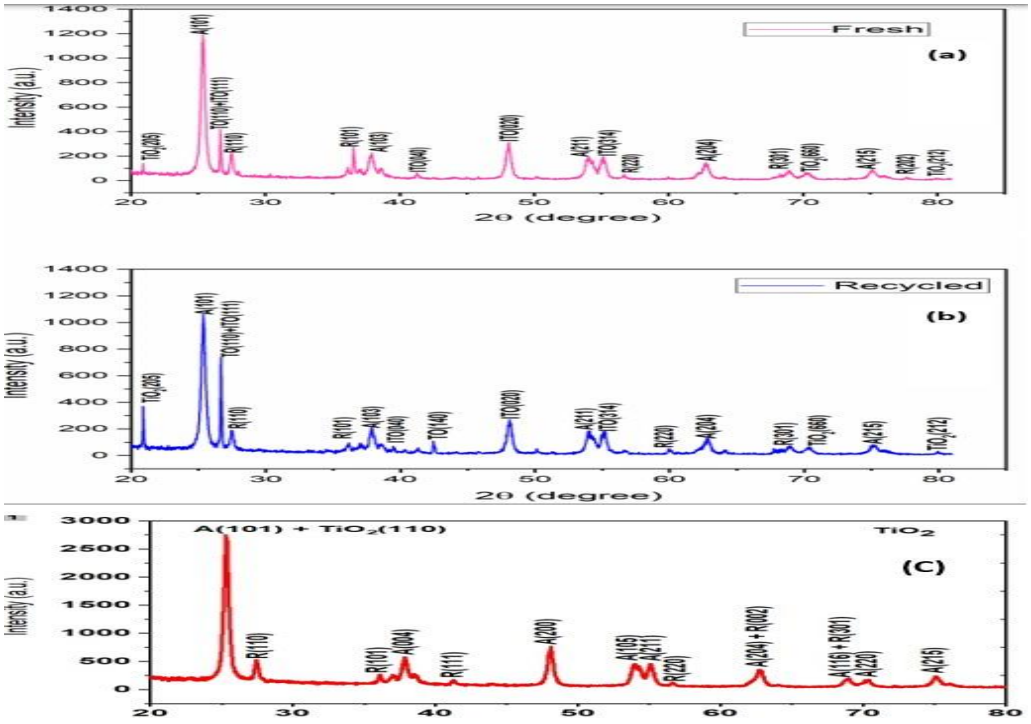

Fig. 4. 38 XRD Analysis of Composite Material: Crystal Structure and Phase Identification: (a) Fresh Composite Material (b) Recycled Composite Material (c) TiO_2 P25 Degussa

4.5.4.3 UVDRS analysis

UV-DRS analysis confirmed the catalyst's visible light activity, highlighting the presence of Fe-TiO_2 complexes shown in Fig. 4.39. The bandgap of raw TiO_2 (P25 Degussa) was 3.2 eV, while both the fresh and recycled Fe-TiO_2 composites exhibited a reduced bandgap of 2.9 eV and 2.8 eV respectively. Absorbance values increased from 415 nm for raw TiO_2 to 430 nm for the fresh composite and 452 nm for the recycled composite. These results indicate enhanced visible light absorption and improved photocatalytic performance of the Fe-TiO_2 composite, consistent with the findings from XRD analysis. The energy band gap was calculated using Tauc Eq. 4.8 (Tumuluri et al. 2014):

$$(\alpha h\upsilon)^{\frac{1}{n}} = A(h\upsilon - Eg) \qquad \textbf{4. 8}$$

Where E_g is the energy band gap in eV, h is Planck's constant in joule seconds, υ is photon frequency in Hz, A is proportionality constant. The energy bandgap of TiO_2 was 3.24 eV and reduced to 2.9 eV for fresh and 2.8 eV for recycled composite beads, respectively.

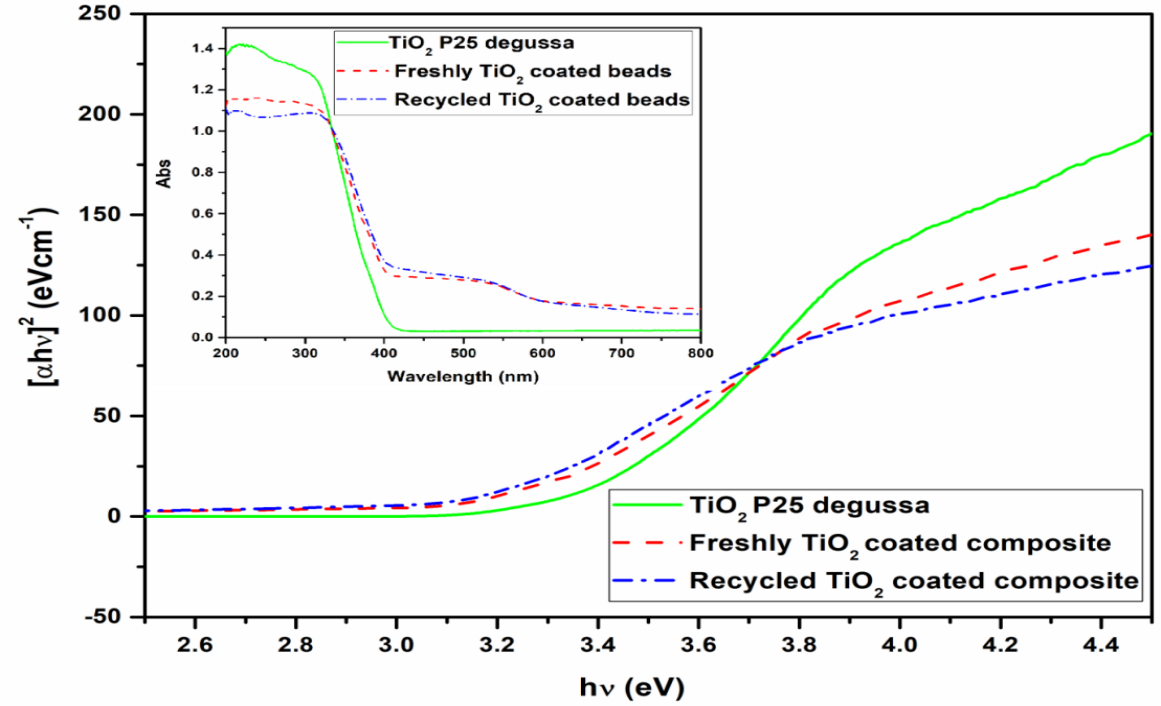

Fig. 4. 39 UVDRS image of fresh and recycled composite bead

4.5.5 Durability study for I/L stream

Ensuring the catalytic activity of the composite for multiple recycles in terms of the efficacy of coated TiO_2 for photocatalysis and the steady leaching of iron to sustain photo-Fenton was the toughest task for this study. While there are limited studies in the literature on the durability of the hybrid approach (Ganiyu et al. 2018; John et al. 2020), it is a noteworthy technique because it addresses the individual limitations of photocatalysis and photo-Fenton while maintaining catalyst activity over multiple recycles. This study compared the durability and iron leaching of the reused catalyst and found that it maintained its effectiveness for more than 100 recycles. The results showed a slight reduction of 5-10% in catalytic activity for color removal, as illustrated in Fig. 4.40 a. This marginal decrease in the surface-coated catalyst's activity may be attributed to its partial removal during continuous washing after each cycle.

In addition, an examination of iron leaching was conducted after 100 recycling processes. The results, depicted in Fig. 4.40 b demonstrated remarkably positive outcomes, with only a marginal reduction in activity of 1-2%. It is noteworthy to mention that there have been only a few studies thus far that have reported such exceptional durability of the catalyst,

particularly when considering its application in real waste scenarios. This outstanding performance makes the catalyst highly viable for commercial-scale applications.

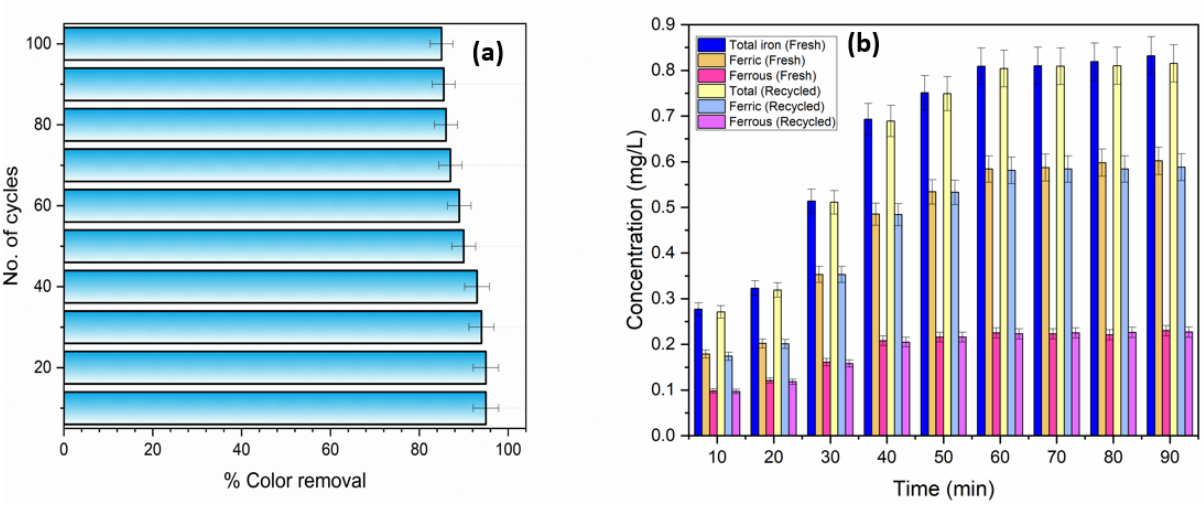

Fig. 4. 40 (a) Durability study of I/L stream using 100 times recycled beads (b) Durability study in terms of iron leaching for freshly coated and recycled beads

4.6 Batch study for O/L stream

O/L is the final treated stream from the P & P industry which still persists color even after the treatment. The color was not as dense as that of the other two steams i.e., UASB, and I/L but the major challenge here was to apply the dual technique as the wastewater volume was much higher than that of other streams.

4.6.1 Kinetic models in wastewater color removal for O/L stream

To investigate color removal, three distinct kinetic models namely, log-linear, Weibull, and biphasic shoulder were employed, as elaborated below. Non-linear regression analysis was applied to derive the kinetic coefficients from the experimental data. The software GInaFiT, developed by (Geeraerd et al. 2005), and integrated with Microsoft Excel Solver, was utilized for fitting the experimental values. Assessment of the discoloration results' fitting accuracy was conducted through RMSD and R^2. Additionally, a comprehensive comparison and graphical representation of both mathematical and experimental outcomes were performed to ensure the robustness of the selected models.

4.6.1.1 Log-linear model

It is a modified form of Chick's equation which administers the relationship between the amount of color removal and the amount of catalyst used for color removal as given in Eq. 4.9

$$\boldsymbol{logC = log\, C_0 - \frac{K_{MAX}.t}{ln\,10}} \qquad \textbf{4. 9}$$

Where K_{MAX} = Rate of color removal and t = Time

4.6.1.2 Weibull model

It is a continuous probability-based model which describes the variability in system behaviour. This model describes the amount of the pollutant as heterogeneous. Furthermore, pollutant removal depends on the amount of time a pollutant remains under stress conditions also the contact time needed by each pollutant molecule to mineralize. The Weibull model is given in Eq. 4.10

$$logC = logC_0 - \left(\frac{t}{\delta}\right)^m \quad \textbf{4. 10}$$

Where, C = change in the concentration with time, C_0 = initial concentration of the pollutant, C_{res} = % residual concentration, δ = initial decimal reduction time (min), k_{max} = decrement in first order rate constant (min^{-1}), m = curve shape factor

4.6.1.3 The biphasic model with the shoulder

This is a modified form of the biphasic equation. This model describes curves of the biphasic model with a previous shoulder phenomenon. The biphasic shoulder model is given in Eq. 4.11

$$log\frac{N_t}{N_0} = log\left\{fe^{-K_1 t}\frac{e^{Ks_1}}{\left(e^{Ks_1-1}\right)e^{-K_1 t}} + (1-f)e^{-K_2 t}\left\{\frac{e^{Ks_1}}{1+e\,K_{s_1}{}^{-1}e^{-K_1 t}}\right\}^{\frac{K_1}{K_1}}\right. \quad \textbf{4. 11}$$

Where N is the total amount of pollutants, and N_1 and N_2 are the numbers of pollutants that are not mineralized. The parameter f is defined as $N_1(0)/N_2(0)$ and K_1 = First kinetic rate constant.

4.6.1.4 Tentative mechanism of dual process

In this novel dual process, photocatalysis and the photo-Fenton method coexist within a single system. Specifically, composite beads made from rich waste materials promote iron extraction in acidic wastewater by promoting the photo-Fenton reaction in conjunction with TiO_2 photocatalysis in the presence of H_2O_2. The systematic iron leaching in the reactor serves the dual purpose of preventing the formation of iron sludge by photo-reducing Fe^{3+} to Fe^{2+}. The intriguing aspect of this process is the participation of e^-_{CB} in the photoreduction of Fe^{3+} to Fe^{2+} and the combined use of H_2O_2 and sunlight, which increases the production of $OH^{\bullet}$. This synergy, known as the hybrid/dual effect, can be conceptualized using the hypothesis that TiO_2 photocatalysis, a well-established technique, entails the coordinated action of e^-_{CB} and h^+_{VB} (valence band hole) in generating oxidative radicals (as per Eqs. 4.12-4.14).

Simultaneously, the lixiviation of iron from the catalytic beads after the reaction with H_2O_2 resulted in photo-Fenton, as demonstrated by Eqs. 4.15-4.17. Tentative mechanism is illustrated in Fig. 4.41. The dual approach effectively curtails the recombination of electron-hole pairs (e^-h^+) by integrating the e^-_{CB} with Fe^{3+} to regenerate Fe^{2+}, as illustrated in Eq. 4.18. Additionally, the concurrent presence of H_2O_2 serves a dual-purpose interacting with iron in the photo-Fenton process, as previously highlighted, and engaging in the photocatalysis process, as depicted in Eq. 4.19. Consequently, this intricate interplay results in an elevated

production of OH• as shown in Fig. 4.42. For quantification and verification of the difference in kinetics of three different processes, their kinetic rate constants were compared for the final treated stream i.e. (O/L) as shown in Table 4.9.

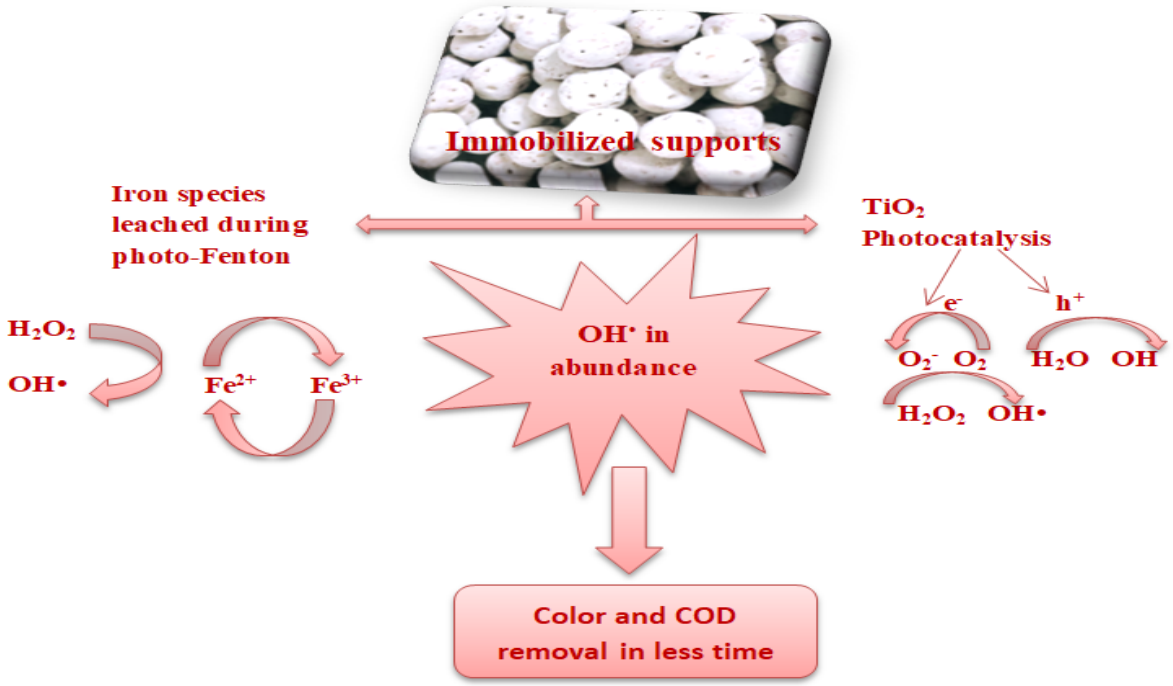

Fig. 4. 41 Tentative mechanism of dual process

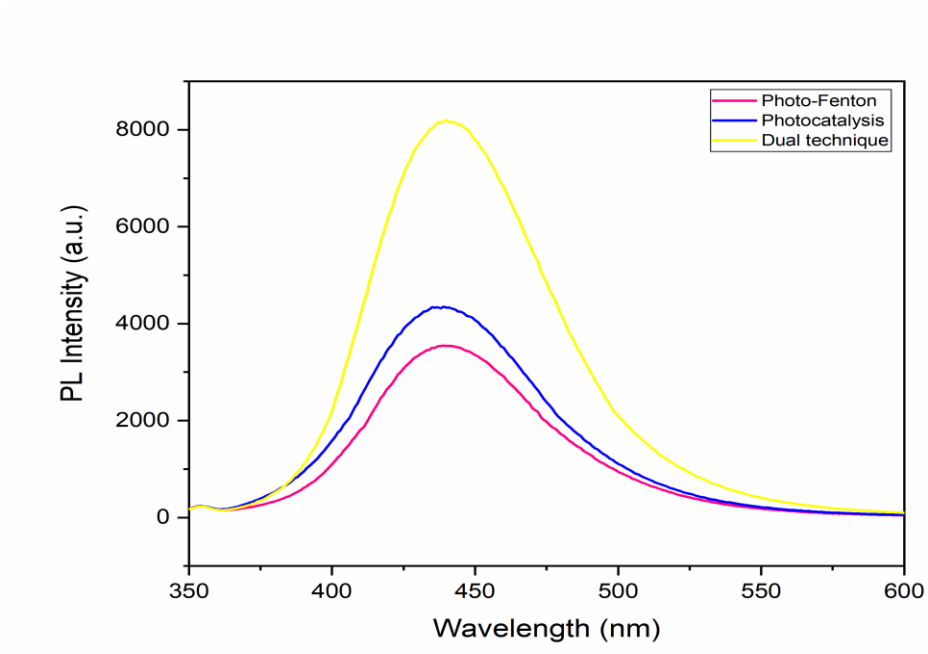

Fig. 4. 42 Illustrated enhanced prominence of OH• in Dual Photoluminescence Spectroscopy compared to isolated processes

Table 4. 9 First order rate constant values for color removal from O/L stream using different processes

Type of process	k value(min^{-1})
Photocatalysis	0.002
Photo-Fenton	0.003
Dual Process (Photo-Fenton + Photocatalysis)	0.049

$$TiO_2 + uv \rightarrow TiO_2(e^- + h^+) \quad \textbf{4. 12}$$

$$e^-_{CB} + O_2 \rightarrow O_2^- \quad \textbf{4. 13}$$

$$h^+_{(TiO_2)} + H_2O_2 \rightarrow OH^o + H^+ \quad \textbf{4. 14}$$

$$Fe^{2+}_{(aquous)} + H_2O_2 \rightarrow Fe^{3+}_{(aquous)} + OH^o + OH^- \quad \textbf{4. 15}$$

$$Fe^{3+}_{(aquous)} + H_2O_2 \rightarrow Fe^{2+}_{(aquous)} + H_3O^+ + HO_2^- \quad \textbf{4. 16}$$

$$Fe^{3+}_{(aquous)} + H_2O \xrightarrow{uv} Fe^{2+}_{(aquous)} + OH^o + H^+ \quad \textbf{4. 17}$$

$$Fe^{3+}_{(aquous)} + e^-_{(CB)} + H_2O \rightarrow Fe^{2+}_{(aquous)} + OH^o + H^+ \quad \textbf{4. 18}$$

$$e^-_{(CB)} + H_2O_2 \rightarrow OH^o + OH^- \quad \textbf{4. 19}$$

4.6.2 Preliminary study of O/L effluent

To establish the necessary boundary conditions, a series of preliminary reactions were conducted within a batch reactor. The first phase involved an adsorption study in a dark environment, employing only blank beads. However, this approach yielded no observable reduction in the color of the effluent. The absence of significant color change was hypothesized to result from the formation of a monolayer of effluent over the beads, hindering any substantive reduction in color. Subsequently, photolysis experiments were undertaken under

solar irradiation, utilizing blank beads to cover the reactor's surface. Despite the addition of waste effluent to the reactor, there was no noticeable alteration in effluent color under solar light. This outcome underscored that solar light alone lacked the potency to influence the concentration of effluent color significantly.

The impact of oxidant dose on color removal was investigated under both dark and solar irradiation conditions. Surprisingly, the results indicated a lack of substantial color reduction. Fig. 4.43 a, visually encapsulates all the preliminary reactions conducted in both dark and sunlight for color removal from O/L effluent. Fig. 4.43 b gives the confirmation of increasing $OH^{\bullet}$ with increasing time. Delving into the statistical evaluation for selecting the most fitting model under varied experimental conditions, Table 4.10, Table 4.11, and Table 4.12 present detailed insights into the relevant factors. Notably, Table 4.10-4.12 reveals that all models attained commendable R^2 values, each exceeding 0.8, affirming their effectiveness in describing the experimental data.

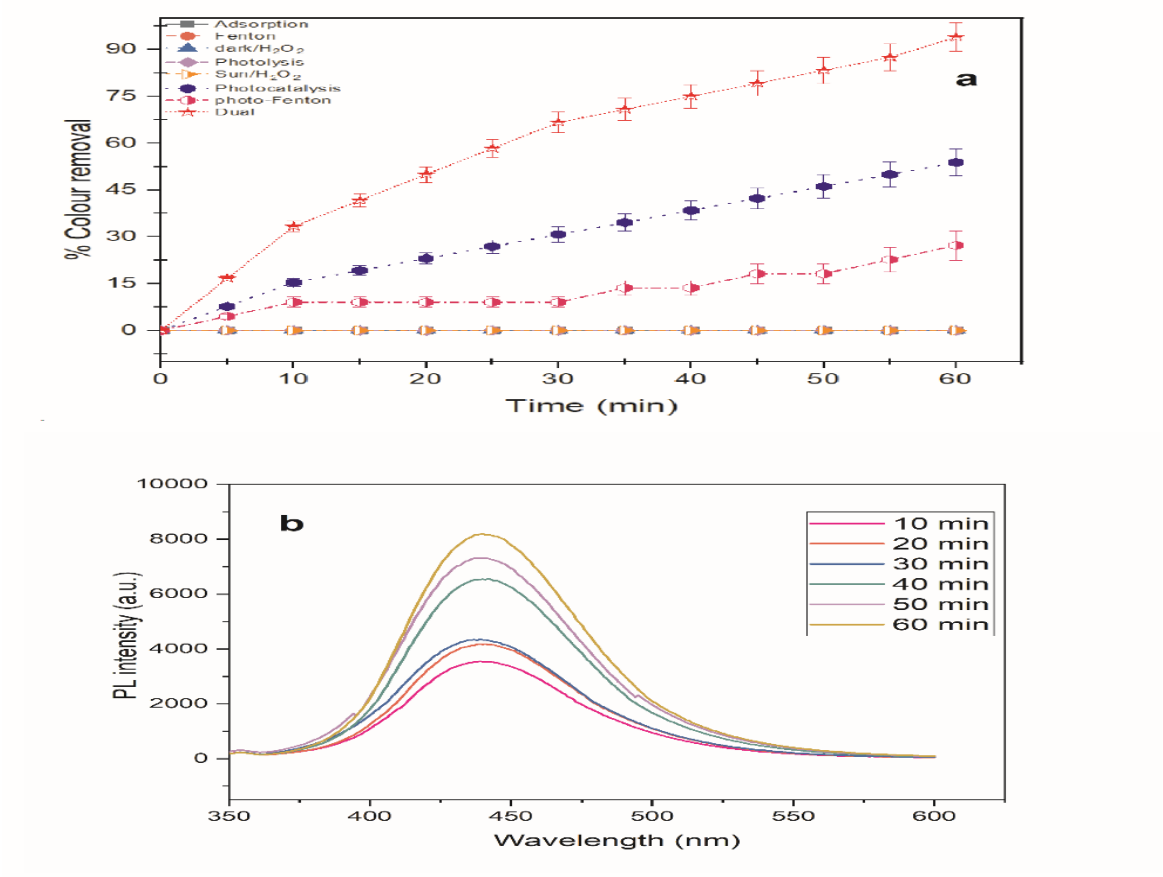

Fig. 4. 43 (a) Dark and solar irradiated experiments (b) Confirmation of $OH^{\bullet}$ production by photo luminance spectroscopy

4.6.3 Sunlight assisted isolated and dual experiments

After completing a comprehensive analysis of the preliminary experiments, we proceeded to carry out processes i.e., photocatalysis, photo-Fenton and dual in the solar light results of which are illustrated in Fig. 4.43 a, which describes the solar-driven experiments under an irradiance of 553 Wm^{-2}, specifically focusing on solar/Fe/H_2O_2 (photo-Fenton), TiO_2-photocatalysis, and dual-process.

The photo-Fenton technique occurred in a fixed-bed maintaining an acidic environment deliberately with a pH value set at 4.5. Uncoated beads were systematically exposed to solar irradiation., ensuring 100% surface area coverage, employing a total of 80 beads in the process. Additionally, the H_2O_2 dosage was precisely set at 525 mg L^{-1}. However, the noteworthy outcome was the observed color removal, amounting to a modest 27.27%, as intricately depicted in Fig. 4.43 a.

In the case of the photo-Fenton process, Fig. 4.44 a, provides a visually compelling demonstration of the alignment achieved across various mathematical models. Notably, the R2 values for both the Log-linear and Weibull models converge at 0.935, signifying a consistent fit, while the Biphasic with shoulder model surpasses with an impressive R_2 value of 0.998. This comprehensive analysis is further encapsulated in Table 4.10, where the Weibull model takes centre stage, with the parameter δ set at 72 min. for the photo-Fenton process.

In sunlight, the utilization of TiO_2-coated beads in photocatalysis resulted in a notable 53.84% reduction in color, as demonstrated in Fig. 4.44 b within a brief 60 min., treatment period. The effectiveness of the photocatalysis process was further validated by the correlation between mathematical modelling and experimental outcomes. Notably, both Log-linear and Biphasic models with a shoulder exhibited an identical R^2 value of 0.950. Meanwhile, the Weibull model demonstrated a higher R^2 value of 0.984. The photocatalysis process, characterized by a δ value of 64 min., is detailed in Table 4.11.

Various studies have addressed the treatment of colored wastewater, particularly utilizing methodologies such as Fenton. However, the prevalent challenges associated with high chemical consumption and sludge generation have hindered their practical implementation. Attempts to employ hybrid techniques combining chemical treatments with processes like UV irradiation or electro-coagulation have encountered issues such as prolonged treatment duration, increased operational costs, and unresolved practical challenges.

Our current work presents a new dual process that addresses the mentioned restrictions by reducing treatment time, eliminating sludge creation, and minimizing chemical usage. The dual technique incorporates Log-linear, Weibull, and Biphasic with shoulder models, demonstrating robust fits with R^2 values of 0.874, 0.981, and 0.998, respectively (refer to Table 5). Fig. 4.44 c further confirms the efficacy of all three models in the dual process.

The in-situ dual approach involved the use of Fe-TiO_2 beads, which combined sequential iron percolation and surface-coated TiO_2. The proposed methodology involves the simultaneous implementation of TiO_2 photocatalytic and photo-Fenton processes. The dual technique has a significant color elimination efficacy of 91.6%, outperforming separate procedures such as photo-Fenton and TiO_2 photocatalysis (as depicted in Fig. 4.43 a).

The dual technique mitigates electron-hole recombination by facilitating the reaction of ferric ions with e^-_{cb} for ferrous ion production, thereby promoting the reoccurring photo-Fenton process. Simultaneously, the addition of H_2O_2 plays a dual role, reacting with both TiO_2 and iron to enhance $OH^{\bullet}$ production in the treatment system. Evaluation of rate constants, considering Log-linear and Weibull δ values, demonstrates the superior efficiency of the dual-process over other techniques, requiring less time for color removal ($k = 0.049$ min-1, $\delta = 38$ min.), compared to photo-Fenton ($k = 0.002$ min-1, $\delta = 72$ min.) and photocatalysis ($k = 0.003$ min-1, $\delta = 64$ min.). In summary, our dual process emerges as a superior solution for efficient colored wastewater treatment than other two isolated processes as shown in Table 4.12.

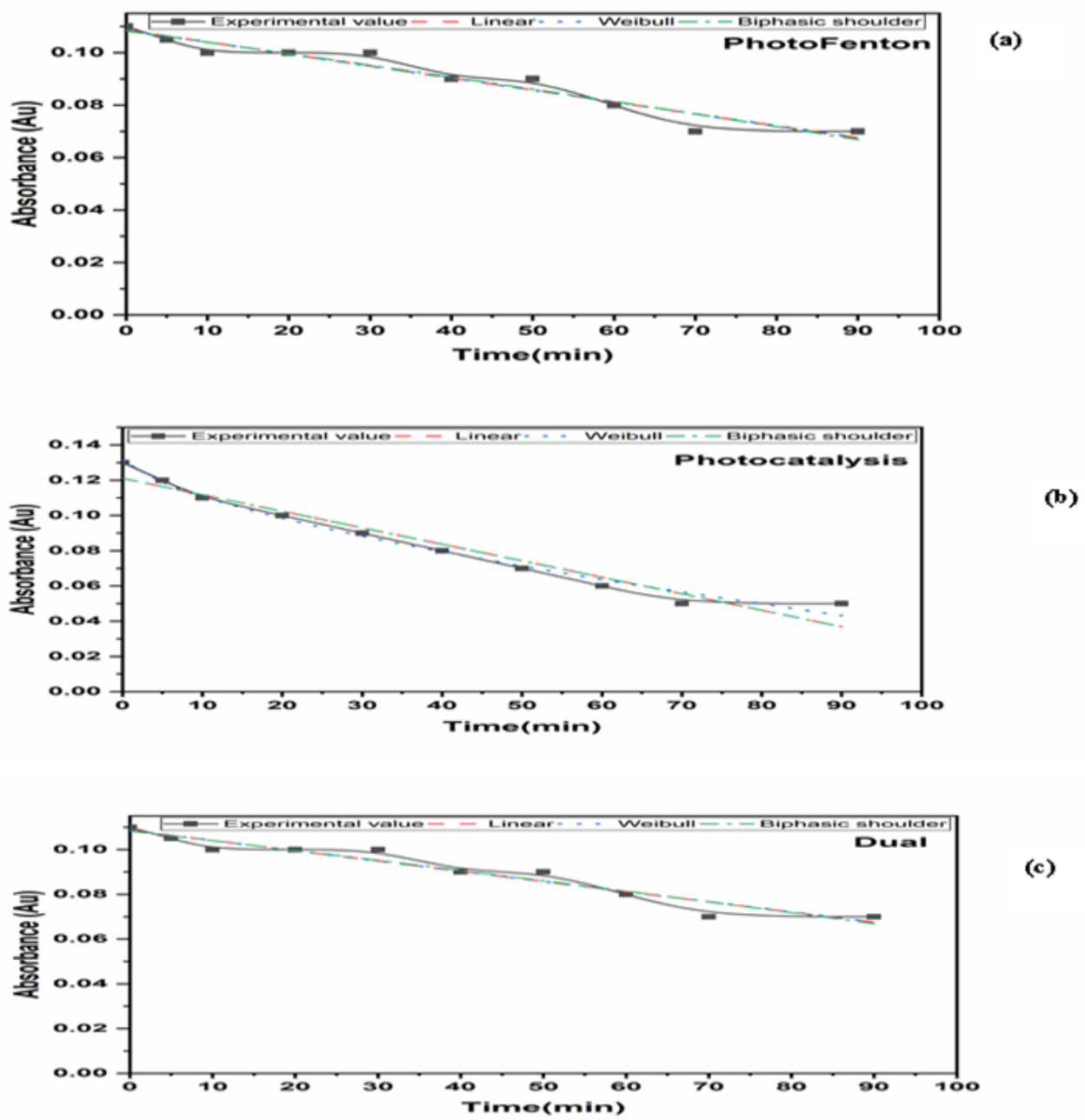

Fig. 4. 44 (a) Fitting of modelling graphs in color removal of the industrial effluent by photo-Fenton (b) Fitting of modelling graphs in color removal of the industrial effluent by photocatalysis (c) Fitting of modelling graphs in color removal of the industrial effluent by dual technique

Table 4. 10 Different kinetic parameters used for color removal by the photo-Fenton method in various mathematical models

Treatment process	Models	K(min^{-1})	δ (min.)	$\left(\frac{R^2}{RMSD}\right)$
photo-Fenton	Log-linear	-	-	0.935/0.003
	Weibull	-	72	0.935/0.004
	Biphasic with shoulder	0.002	-	0.936/0.004

Table 4. 11 Different kinetic parameters used for color removal by the Photocatalysis method in various mathematical models

Treatment process	Models	K(min^{-1})	δ (min.)	$\left(\frac{R^2}{RMSD}\right)$
Photocatalysis	Log-linear	-	-	0.950/0.006
	Weibull	-	64	0.984/0.004
	Biphasic with shoulder	0.003	-	0.950/0.008

Table 4. 12 Different kinetic parameters used for color removal by the Dual method in various mathematical models

Treatment process	Models	K(min^{-1})	δ (min.)	$\left(\frac{R^2}{RMSD}\right)$
Dual	Log-linear	-	-	0.874/0.015
	Weibull	-	38	0.981/0.006
	Biphasic with shoulder	0.049	-	0.998/0.002

4.6.4 Optimization of dual-process

4.6.4.1 H_2O_2 dose-effect study

Numerous studies have investigated the influence of H_2O_2 on photo-Fenton and photocatalysis, as it is a well-established method for increasing the $OH^{\bullet}$ amount in the system. The current study involves simultaneous H_2O_2 consumption by both processes in a single system. In photocatalysis, the addition of an oxidant prevents the electron-hole recombination by reacting with electrons in the conduction band as given in Eq. 4.20. Optimization of the oxidant dose was a chief factor for the dual in-situ process. The dual-process helps in increasing the $OH^{\bullet}$ production and oxidizing species. In the present work, the concentration of H_2O_2 was optimized by varying it between the ranges of 225 mg L^{-1}-750 mg L^{-1} and the optimized concentration value of H_2O_2 came to be 525 mg L^{-1} at a pH 4.5. After H_2O_2 dose optimization maximum color removal was observed between 60 min as shown in Fig. 4.45 a. It was detected that with increased H_2O_2 concentration to 525 mg L^{-1} the color removal efficiency was increased constantly but started to decline when the dose was increased from 525 mg L^{-1}-750 mg L^{-1}. The decrease in % color removal was mainly due to the scavenging effect of H_2O_2 i.e. H_2O_2 itself starts consuming $OH^{\bullet}$ as shown in Eqs. 4.20-4.22.

$$e^{-}_{(CB)} + H_2O_2 \rightarrow OH^{\bullet} + OH^{-} \quad \textbf{4. 20}$$

$$H_2O_2 + OH^{\bullet} \rightarrow OH^{\bullet}_2 + H_2O \quad \textbf{4. 21}$$

$$OH_2^{\bullet} + OH^{\bullet} \rightarrow H_2O + O_2 \qquad \textbf{4. 22}$$

4.6.4.2 pH effect study

In the current study of dual-process, one of the techniques is the photo-Fenton. This photo-Fenton technique requires iron leaching from beads in acidic conditions for the process to be executed so hereby pH plays a significant part in dual-process execution (Bansal et al. 2018; Thakur et al. 2020a; Puri et al. 2021). For pH optimization, experiments were carried out in between the range of 3.5-6.5 at optimized H_2O_2 concentration as shown in Fig 4.45 b. When pH was less than 4.5, the % color removal was decreased which owed to the $OH^{\bullet}$ scavenging effect. Whereas when pH was augmented from 4.5-6.5 the % color removal again decreased. The hydrolysis of Fe^{3+} and FeO (OH) complexion precipitation could be the reason behind this reduction in color removal. This might be due to precipitation of and Fe^{3+} hydrolysis which leads to lesser $OH^{\bullet}$, ultimately leading to the decrement of % color removal. It is visible from Fig. 4.45 b that maximum color removal was accomplished at pH 4.5 in 60 min. which then was used for the rest of the study. At alkaline pH, HO_2^- starts to form which is sparsely active so this leads to the consecutive formation of O_2 and H_2O when reacted with H_2O_2. But for the present study, $OH^{\bullet}$ formation is very important rather than the formation of O_2 and H_2O. Hence it signifies the importance of optimizing the pH for the whole process.

4.6.4.3 Catalyst dose

Here catalyst dose refers to number of beads coated by the catalyst. The impact of the surface area covered for wastewater treatment was examined in this study by altering the number of composite beads on the surface of the reactor. The optimum number of catalytic beads required for effluent color removal is investigated in this effect. As a result, the analysis was depicted as a % area covered by changing the number of beads. The present study varies the number of beads in the range of 40-120 i.e. 80 beads covered 100% area of the reactor. The best % color removal (91.6%) was attained with 80 beads (100 % surface area covered) as shown in Fig. 4.45 c. This might be due to the availability of free active sites without any overlapping of beads for pollutant mineralization. When no. of beads was reduced to 40 and increased to 120, a reduction in color removal was observed due to decreased no. of active sites

and overlapping of beads respectively. The explanation for this may be the reduction in the active site in either of the case leads to insufficient pollutant-catalyst interaction hence decreasing the % color removal.

4.6.4.4 Synergy

Synergy is the method that proves the prominence of dual effect over isolated photocatalysis and photo-Fenton processes. The synergistic effect of dual technique over other techniques i.e. photocatalysis and photo-Fenton were checked which implies that the combined effect of both (photocatalysis + photo-Fenton) above the processes individually is better for discoloration of industrial wastewater. This can be calculated using the kinetic value as given in the aforementioned tables 4.10-4.12. Here the rate constant (k) of dual (0.049 min^{-1}) is much higher than the other two processes (0.002 min^{-1} for photocatalysis and 0.003 min^{-1} for photo-Fenton) when performed individually. The synergy of dual over both individual processes was found to be 10.82% as given in Eq. (4.23-4.24) and Fig. 4.45 d.

Synergy of modified dual over photo-Fenton technique:

$$\% \text{ Synergy} = 100\times \{(k_{dual} - k_{photocatalysis} \text{ or } k_{photo\text{-}Fenton})\}/ k_{dual} \quad \textbf{4. 23}$$

% Synergy =95.91% over photocatalysis and 93.87% over photo-Fenton

Overall synergy was calculated using following equation:

$$\% \text{ Synergy} = 100\times \{(k_{dual} - (k_{photocatalysis} + k_{photo\text{-}Fenton})\}/ k_{dual} \quad \textbf{4. 24}$$

% Synergy =10.82%

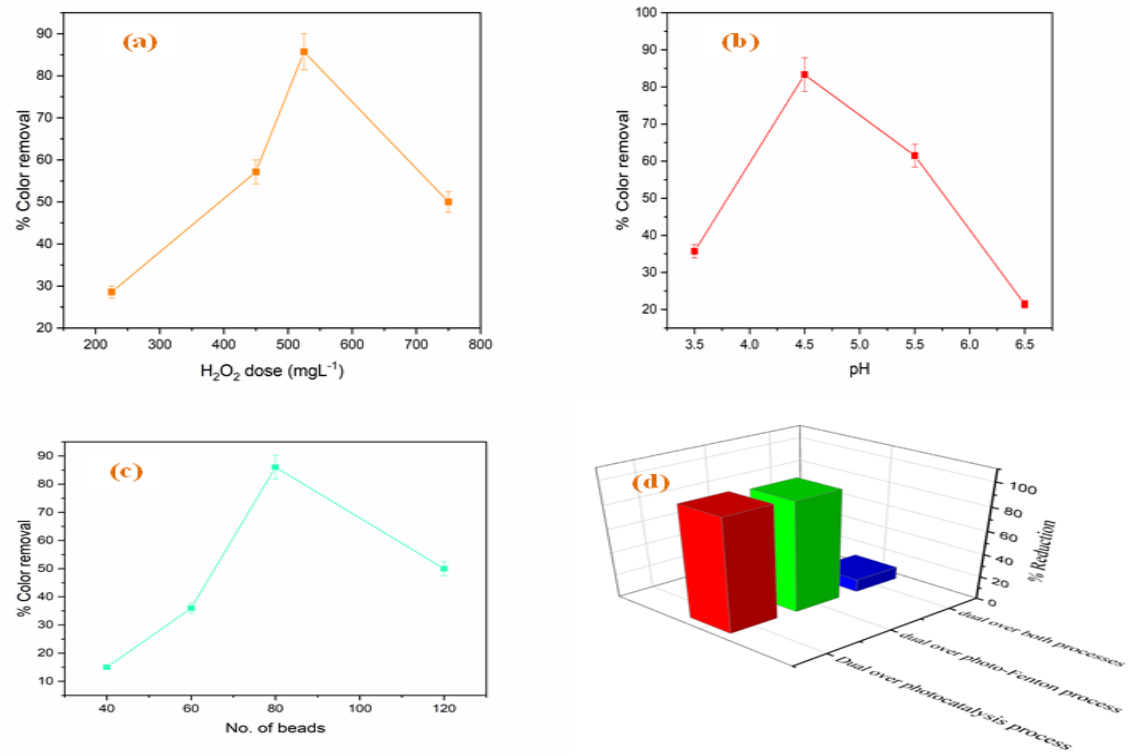

Fig. 4. 45 (a) Effect of H_2O_2 dose (t= 60 min., pH= 4, No. of beads = 100) (b) Effect of pH (t= 60 min., H_2O_2 dose= 545 mgL^{-1} No. of beads = 100) (c) Effect of Catalyst dose (t= 60 min., pH= 4, H_2O_2 dose= 545 mgL^{-1}) (d) Synergy of Dual over photocatalysis, photo-Fenton, and both the processes

4.6.4.5 Mineralization study

The mineralization study was executed by % COD removal. COD reduction of 18%, 27%, and 60% was observed for photo-Fenton, photocatalysis, and dual technique respectively using optimized parameters as shown in Fig. 4.46 To further confirm the breakdown of complex compounds in the real effluent, LCMS analysis was performed at different intervals of the treatment. Initial, intermediate, and finally treated effluent was subjected to LCMS which showed the pattern of different peaks as given in Fig. 4.47 a-c.

❖ **Initial Effluent (a):**

- Typically, the initial effluent stream will show a complex set of peaks, indicating the presence of multiple compounds, often in high concentrations. Peaks might be broader and more intense, reflecting the untreated or raw effluent, rich in organic and inorganic pollutants.

❖ **Intermediate Effluent (b):**

- The intermediate stage may show fewer peaks or reduced intensity for certain compounds. This suggests partial degradation or removal of some pollutants. New peaks might also appear, corresponding to intermediate breakdown products formed during the treatment process.

❖ **Final Treated Effluent (c):**

- In the final treated effluent, the chromatogram should show significantly reduced peaks, indicating the removal or substantial reduction of contaminants. The peaks that remain might be smaller or less complex, reflecting residual compounds that are either non-toxic or present in very low concentrations.

There was a significant reduction in the peaks in the treated effluent as compared to raw effluent which showed several crowded peaks. The diminishing peaks during treatment might be due to the formation of aliphatic from aromatic compounds.

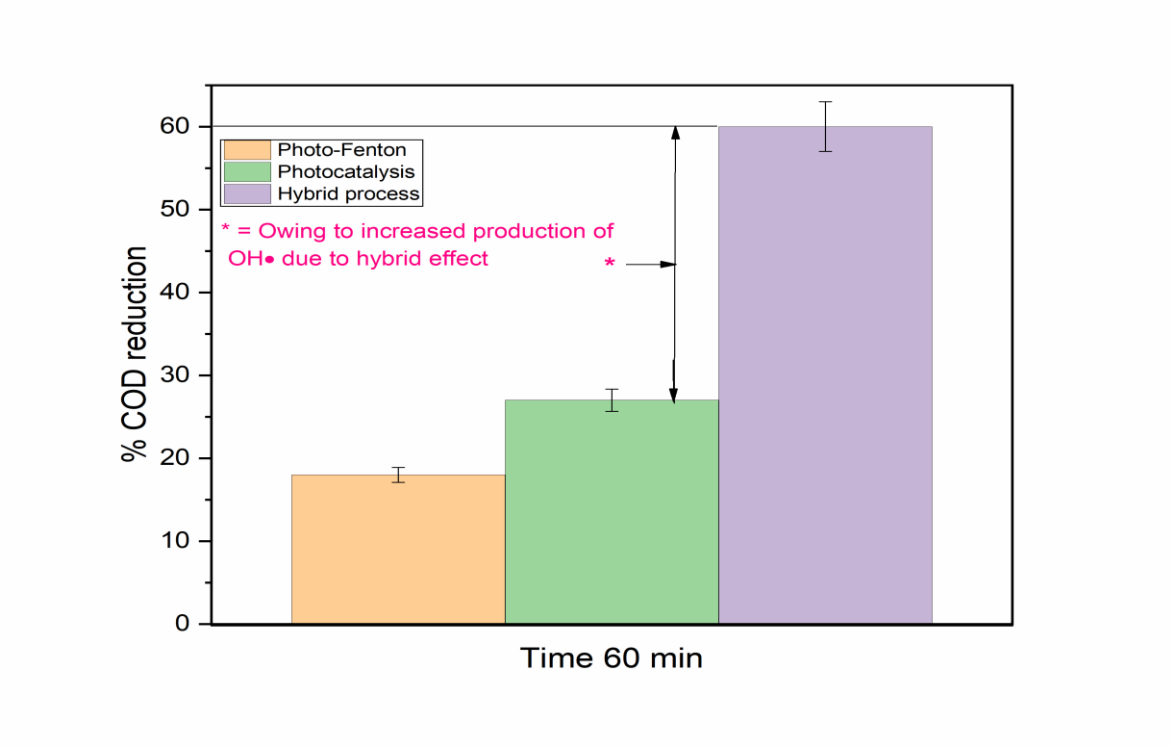

Fig. 4. 46 % COD reduction in three different processes with hybrid process owing to more OH• production than the other two processes

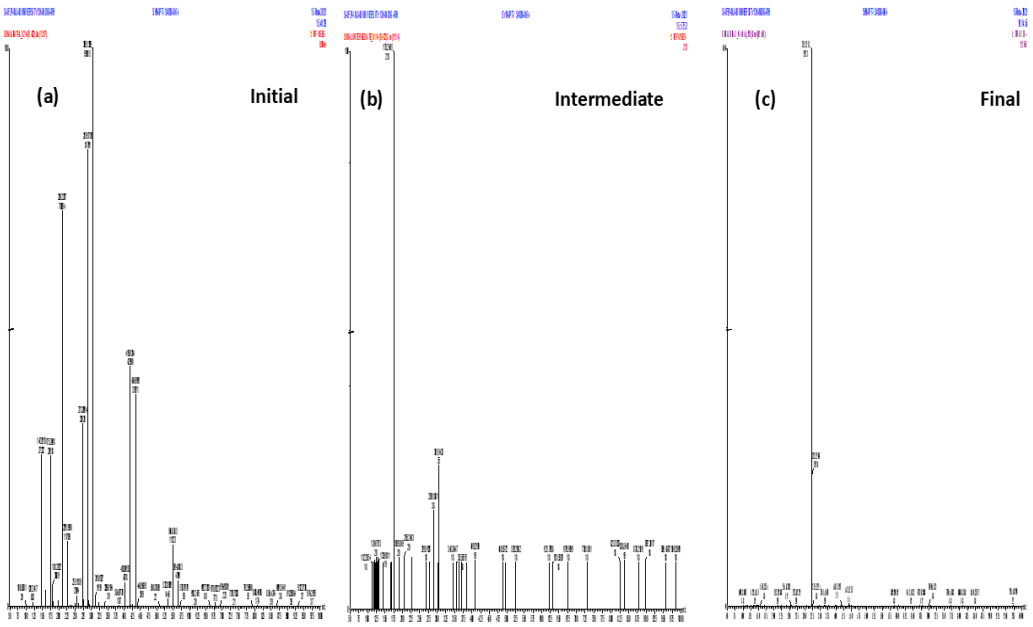

Fig. 4. 47 LCMS analysis for (a) Initial (b) Intermediate and (c) Final treated effluent

4.7 O/L (outlet) stream recirculation study

O/L is the final treated stream from the P & P industry which still persists color even after the treatment. The color was not as dense as that of the other two steams i.e., UASB, and I/L but the major challenge here was to apply the dual technique as the wastewater volume was much higher than that of other streams.

4.7.1 Design of Experiment

To set up experiment, Design-Expert software was used which employs RSM. This approach provides a diverse set of statistical and mathematical techniques for predicting and evaluating outcomes when multiple factors influence the outcome of our interest. Our main aim in this study was to fine-tune the response by optimizing the variables involved. RSM is efficient because it saves time and facilitates the analysis of the relationship between controlled input parameters and response variables. A series of tests were conducted using the RSM to optimize the dosage of H_2O_2, the percentage of surface area covered, and flow rate of the effluent. To complete the study on color removal, a factorial technique was employed. The RSM design outlined in Table 4.13. suggested an alternative set of 17 responses with actual and predicted results. Furthermore, the residual plot for color removal exhibited good characteristics, as it displayed a normal distribution and closely resembled a straight line. The

variables were fitted using a second-order regression model, which took the shape of a quadratic polynomial.

$$\boldsymbol{R = \beta_{\circ} + \sum_{i=1}^{k} \beta_i x_i + \sum_{i=1}^{k} \beta_{ii} x_i^2 + \sum_{i,j=1} \sum_{i<j} \beta_{ij} x_i x_j \ + e} \qquad \textbf{4. 25}$$

Table 4. 13 Factorial BBD matrix with 3 independent variables for O/L stream

Experiment No.	x_1 H_2O_2 (mg L^{-1})	x_2 % Surface area covered	x_3 Flow rate (mL min^{-1})	Y1 % color removal (min)
1	450	50	8.0	45
2	450	100	6.0	70
3	450	100	6.0	71
4	600	50	6.0	40
5	300	150	6.0	50
6	600	100	8.0	37
7	600	100	4.0	57
8	450	150	8.0	55
9	450	50	4.0	65
10	600	150	6.0	51
11	450	100	6.0	70
12	450	150	4.0	75

13	300	50	6.0	40
14	450	100	6.0	68
15	450	100	6.0	65
16	300	100	4.0	55
17	300	100	8.0	35

4.7.1.1 Response study using BBD

To study the effects of different input parameters on the % color removal (response Y1) in wastewater treatment, we employed a Box-Behnken Design (BBD) with Analysis of Variance (ANOVA). The input parameters considered were A (H_2O_2 dose), B (% surface area covered), and C (flow rate), along with their interactions (AB, AC) and quadratic effects (A^2, B^2, C^2). The BBD was chosen for its ability to handle multiple variables efficiently. It allowed us to select three levels for each factor (low, medium, high) to capture potential nonlinear relationships. The design consisted of a total of 17 experimental runs, including 3 replicates at the center point to estimate experimental error. Each run was conducted with a unique combination of the input parameters, varying A, B, and C according to the BBD matrix. The % color removal (Y1) was measured after each run and used as the response variable for the ANOVA analysis. This approach enabled us to assess the individual and combined effects of A, B, and C on the efficiency of color removal, providing valuable insights into the optimal conditions for wastewater treatment. Table 4.14 shows predicted versus actual value for Y1 response which shows a very marginal difference indicating that the model is substantial.

Table 4. 14 Predicted versus Experimental values of the O/L stream study

Responses	**Predicted value**	**Experimental value**
% Color removal	74.45%	75%

4.7.1.2 ANOVA

The model's robustness was evaluated by considering both the coefficient of determination R^2 and the adjusted R^2. The slight difference of 0.1 between these two metrics suggests that the model has a decent level of predictability. The statistical fit of the model is presented in Table 4.15, which displays the R^2 and adjusted R^2 values of 0.99 and 0.98, respectively. These values indicate a very small difference of 0.1, demonstrating that the model has a high level of predictability. A satisfactory R^2 value is generally considered to be 0.8 or higher, with increasing significance as it approaches 1.

An analysis of variance (ANOVA) was performed, which showed that the p-values were less than 0.05. This suggests that the model is appropriate for the planned inquiry. The R^2 value of 0.99 for the % color removal response indicates a strong correlation between the expected and observed data (Probability > F = 0.0001). Furthermore, the lack of fit value is 0.15, which surpasses the minimum fit threshold of 0.05. Additionally, the F value is 3.11, suggesting that the lack of fit is not statistically significant. Table 4.15 provides evidence supporting the validity of the concept.

Table 4. 15 Analysis of variance for the response rate of color removal from O/L stream

Source	Sum of Squares	df	Mean Square	F-value	p-value	Significance
Model	2758.42	9	306.49	89.21	< 0.0001	significant
A-H_2O_2 dose	3.13	1	3.13	0.9096	0.3720	-
B-% Surface area covered	210.13	1	210.13	61.16	0.0001	-
C-Flow rate	800.00	1	800.00	232.85	< 0.0001	-
AB	0.2500	1	0.2500	0.0728	0.7951	-
AC	0.0000	1	0.0000	0.0000	1.0000	-
BC	0.0000	1	0.0000	0.0000	1.0000	-
A^2	1484.21	1	1484.21	432.00	< 0.0001	-
B^2	96.00	1	96.00	27.94	0.0011	-
C^2	68.21	1	68.21	19.85	0.0030	-
Residual	24.05	7	3.44	-	-	-
Lack of Fit	1.25	3	0.4167	0.0731	0.9713	not significant
Pure Error	22.80	4	5.70	-	-	-
Cor Total	2782.47	16	-	-	-	-

4.7.1.3 Parametric Optimization

The study examined the effects of various parameters, including the dose of H_2O_2 as an oxidant, the % surface area covered by the beads, and the flow rate. The amount of H_2O_2 is critical for enhancing color reduction by increasing the presence of hydroxyl radicals ($OH^{\bullet}$) in the system. The analysis, illustrated in Fig. 4.48 a reveals that with H_2O_2 concentrations below 300 mg L^{-1}, only a minor reduction in color was observed. As the H_2O_2 dose increased from 300 to 500 mg L^{-1}, there was a notable enhancement in color reduction, which coincided with an increase in the percentage of surface area covered by the beads. However, when the H_2O_2 concentration exceeded 500 mg L^{-1} and approached 600 mg L^{-1}, a decline in color removal efficiency was observed. This decline can be explained by a scavenging effect that occurs at higher H_2O_2 concentrations. Specifically, excessive H_2O_2 begins to consume the hydroxyl radicals ($OH^{\bullet}$) through various side reactions, reducing the availability of these radicals for effective color degradation. This effect, therefore, diminishes the overall efficiency of the color removal process at higher oxidant doses.

The BBD results clearly demonstrate the importance of optimizing H_2O_2 concentration to balance between sufficient oxidant availability and minimizing the scavenging effect, thereby achieving the best possible outcomes in the color reduction process. This consumption happens due to various reactions, including the following simplified Eq. 4.26:

$$\boldsymbol{2H_2O_2 + 2OH^{\cdot} \rightarrow 2H_2O + O_2} \qquad \textbf{4. 26}$$

In this reaction, two molecules of H_2O_2 react with two hydroxyl radicals to form two molecules of water and one molecule of oxygen. As a result, the availability of hydroxyl radicals decreases, which can reduce the effectiveness of the oxidative processes, such as photocatalysis or Fenton-like reactions, leading to a decrease in color removal efficiency at higher H_2O_2 concentrations.

A significant technical challenge hindering the widespread application of AOPs is the development of an efficient, long-lasting catalyst that can be easily handled and provides a high surface area for wastewater treatment. Addressing this challenge, the current study explores the use of spherical supports to immobilize the catalyst, offering an optimal surface area for reactions. Regarding catalyst dose i.e., the % surface area covered, initial results showed lower color removal when 50% of the reactor area was covered with beads. However, as more surface area was covered, the graph indicated a notable increase in color removal. The optimum value

was found to be 100% surface area coverage. This is because a larger surface area implies a greater amount of catalyst available for the reaction, leading to increased $OH^{\bullet}$ generation and faster color removal, as depicted in Fig. 4.48 b.

In addition to the technical challenges, the practical aspects of catalyst immobilization are crucial for real-scale application. Effective immobilization not only ensures the catalyst's stability and longevity but also facilitates easy handling and maintenance. The choice of support material, such as spherical shapes, plays a pivotal role in providing an optimal surface area for catalytic reactions.

Furthermore, the relationship between catalyst dose and surface area coverage is critical. While increasing the surface area coverage beyond a certain point can enhance catalytic activity, exceeding the optimal coverage may lead to diminishing results. This is due to the overlapping of beads, which can reduce light penetration and limit the availability of active sites for reactions. The study's findings highlight the delicate balance required in catalyst immobilization for ATTs, where maximizing surface area coverage must be balanced with ensuring sufficient light penetration and active site availability. Achieving this balance is essential for optimizing the efficiency and effectiveness of wastewater treatment processes.

Another crucial parameter considered for optimization was the flow rate, which was systematically varied from 4 to 8 Lh^{-1}. The results demonstrated a clear trend: as the flow rate increased from 4 to 8 Lh^{-1}, the percentage of color removal decreased. This decline can be attributed to the reduced contact time between the wastewater pollutants and the catalytic composite at higher flow rates. When the flow rate is increased, the wastewater spends less time in contact with the catalytic particles within the reactor. This shorter contact time reduces the opportunity for the catalytic particles to effectively interact with and reduces the color-removing efficiency of the composite from the wastewater. Consequently, the overall treatment efficiency decreases as the flow rate increases beyond an optimal point (Fig. 4.48 a-b).

Interestingly, the most significant reduction in color was observed at the lowest flow rate tested, i.e., 4 Lh^{-1}. At this lower flow rate, the wastewater had a longer residence time within the reactor, allowing for more extensive and effective contact between the pollutants and the catalytic particles. This prolonged contact facilitated greater color removal, underscoring the importance of optimizing flow rates for efficient wastewater treatment processes.

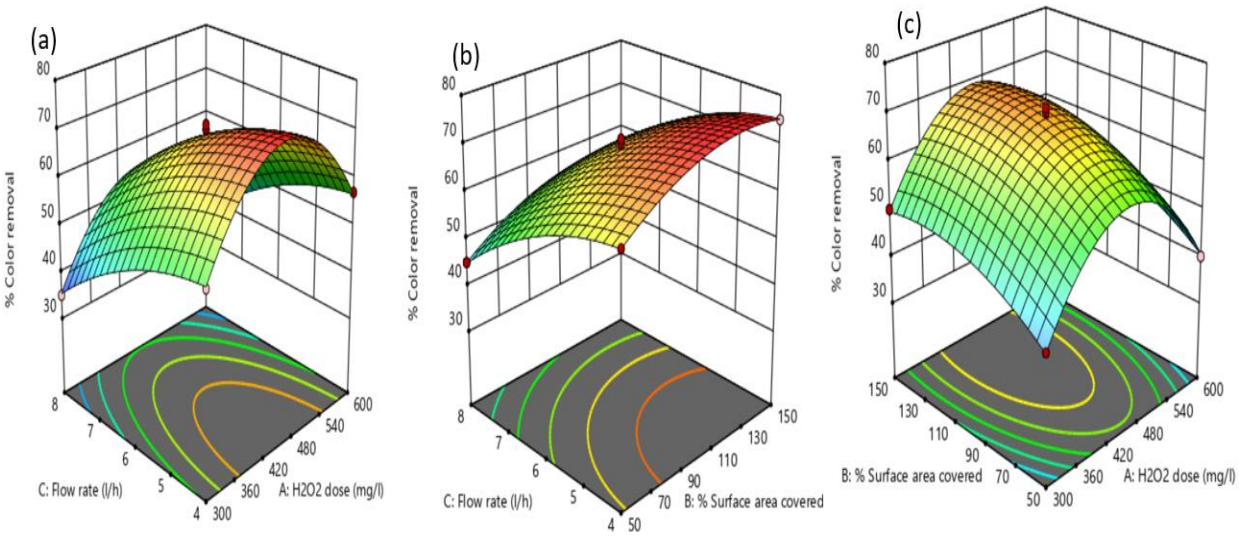

Fig. 4. 48 3D response surface plot of the effect of different factors and their interactions on % color removal (a) Flow rate and H_2O_2 (b) Flow rate and % Surface area covered (c) % Surface area covered and H_2O_2

4.7.1.4 Numerical optimization

Using numerical optimization in Design-Expert software, the parameters A, B, and C were systematically changed within predetermined limits to increase color removal efficacy. There was a strong 90% confidence level in the adjustments that were made. The parameters were changed using a desirability function technique, producing a more accurate set of values, as seen in Fig.4.49. The most ideal design was found among the 100 sets of solutions that were developed, demonstrating the effectiveness of the optimization procedure.

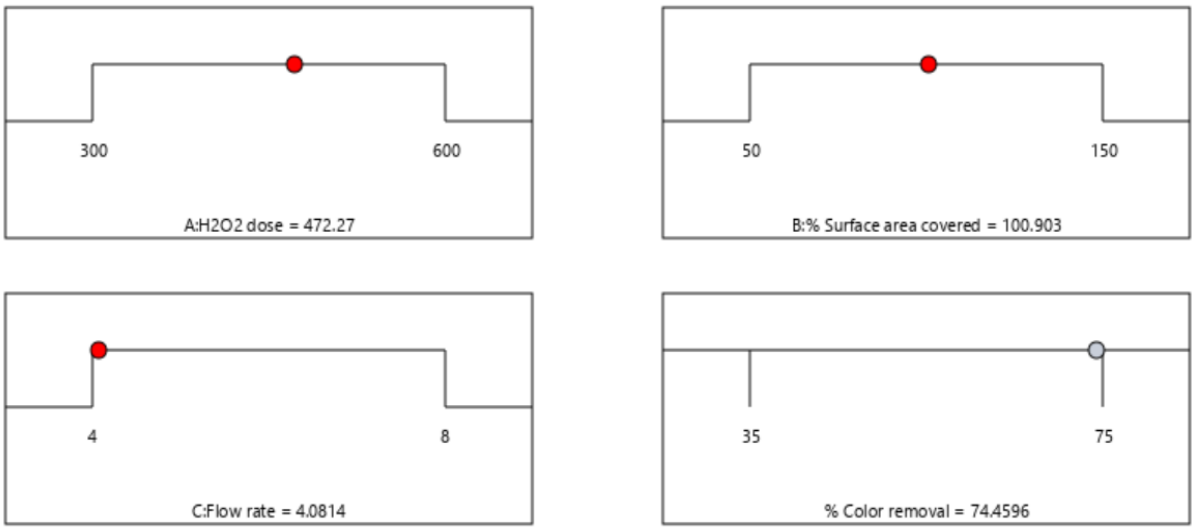

Fig. 4. 49 Numerically optimized conditions in ramp plots for O/L stream

4.7.1.5 Evaluation of catalyst efficiency

The main objective of this study was to evaluate the catalytic efficiency of three distinct processes (hybrid process, isolated photocatalysis, and photo-Fenton) in removing effluent color. Quantum yields (QY) for these processes were calculated using Eq. 4.27, providing insights into their catalytic capabilities under solar irradiation using the same catalyst.

$$\textbf{Quantum yield (QY)} = \frac{decay\ rate\ (per\ second)}{photon\ flux\ (photon\ per\ second)} \qquad \textbf{4. 27}$$

The QY values obtained for the three processes were as follows: 0.00071 $\times 10^{-15}$ for photocatalysis, 0.00044 $\times 10^{-15}$ for photo-Fenton, and significantly higher at 0.184 $\times 10^{-15}$ for the dual process (photocatalysis + photo-Fenton). This significant increase in QY for the dual technique can be attributed to its enhanced production of hydroxyl radicals ($OH^{\bullet}$), as discussed earlier.

4.8 Study of O/L stream in Once through mode

4.8.1 Process optimization for dual process of O/L stream (once through)

Different factors like number of reactors, number of baffles, flow rate, % surface area covered and role of different quenchers were varied to obtain the best-optimized results for the color removal of the given streams provided by the agro-based P & P industry using dual study.

4.8.1.1 Effect of % surface area covered by beads

Fig. 4.50 a, shows the optimal number of composite beads required for effective color removal by varying the % surface area (S.A) covered by the beads was determined. We tested coverage percentages from 50% to 100% and found that color removal improved significantly with greater surface area coverage, particularly at 100%. Increasing the number of beads increased the exposed surface area and the amount of catalyst, speeding up the color removal rate in the O/L stream. As the stream moved through each reactor, it encountered new fixed-bed composite catalysts, increasing the active sites and generating more active radicals, which enhanced color removal. When the surface area coverage was increased to 110%, there was no additional improvement or decline in color removal efficiency. Therefore, we concluded that the optimal configuration was 100% surface area coverage, achieving an 94.4% color removal efficiency for the O/L stream. This setup provided the best balance between bead surface area

and color removal efficiency, showing that maximizing surface area exposure up to 100% is crucial for effective treatment.

4.8.1.2 Effect of the number of reactors

In this study, we employed a sequence of three reactors to investigate the influence of various treatment setups on the effectiveness of removing color from O/L effluent. The experimental configuration processed a volume of 10L of this solution, containing H_2O_2, utilizing natural solar light as the energy source, in order to assess the feasibility and long-term viability of the system. The results, illustrated in the accompanying Fig. 4.50 b, show a gradual reduction in the color of the stream as it passed through each reactor in the sequence. The utilization of three reactors played a crucial role in defining the duration of the pollutants' presence on the active sites of the composite material, hence directly impacting the rate at which the color was eliminated. Specifically, after passing through the first reactor with an approximate residence time of 15 min., the O/L stream exhibited a 44% reduction in color. The addition of a second reactor increased the color removal to 77%. When a third reactor was introduced, the color removal efficiency peaked at 94%. Further reactors were not considered as the optimal number depends on various factors, including operational efficiency and economic viability, not just the percentage of color removal.

The process was conducted in a once-through mode at a constant flow rate, ensuring consistent treatment conditions. The study shows that increasing the number of reactors in series significantly enhances color removal efficiency. However, practical implementation requires balancing the number of reactors with economic and operational considerations to ensure the technology's viability.

4.8.1.3 Effect of flow rate

The flow rate significantly impacts this study as it determines the contact time between the pollutant and the active site. In our investigation, we varied the flow rate between 4.0 ± 1.0 L h^{-1} and 12.0 ± 1.0 L h^{-1}. The results, depicted in the Fig. 4.50 c indicate that the optimal color removal for all three streams was achieved at the lowest flow rate. As the flow rate increased from 4.0 ± 1.0 L h^{-1} to 12.0 ± 1.0 L h^{-1}, the color removal efficiency decreased, likely due to reduced contact time between the pollutant and the composite material. Although further reducing the flow rate could potentially enhance color removal efficiency, it would negatively affect commercial viability by increasing processing time and electricity consumption, thus

raising the overall cost. Since the difference in color removal efficiency between flow rates of 4.0 and 6.0 ± 1 L h^{-1} was minimal, we selected 6.0 ± 1.0 L h^{-1} as the optimal flow rate for this study. At this rate, the O/L stream exhibited an 88% color removal efficiency.

4.8.1.4 Effect of different scavengers

To determine the primary oxidative species or radicals (such as $OH^{\bullet}$, $O2^{\bullet-}$, and h^{+}) responsible for the color removal from O/L stream using the Fe-TiO_2 composite, a series of experiments were conducted under optimal conditions. As depicted in Fig. 4.50 d various quenching agents were utilized, including TBA for $OH^{\bullet}$, EDTA for h^{+}, and BQ for $O^{2\bullet-}$. The results indicated that the % color removal was diminished in the presence of each quenching agent. This suggests that each of the previously mentioned oxidative species plays a role in the color removal process. A significant reduction of approximately 45-50% in color removal was observed for the O/L stream when TBA quencher was used, highlighting the crucial role of $OH^{\bullet}$ radicals in the color removal process. This indicates that $OH^{\bullet}$ radicals are the primary active species in the dual process of color removal.

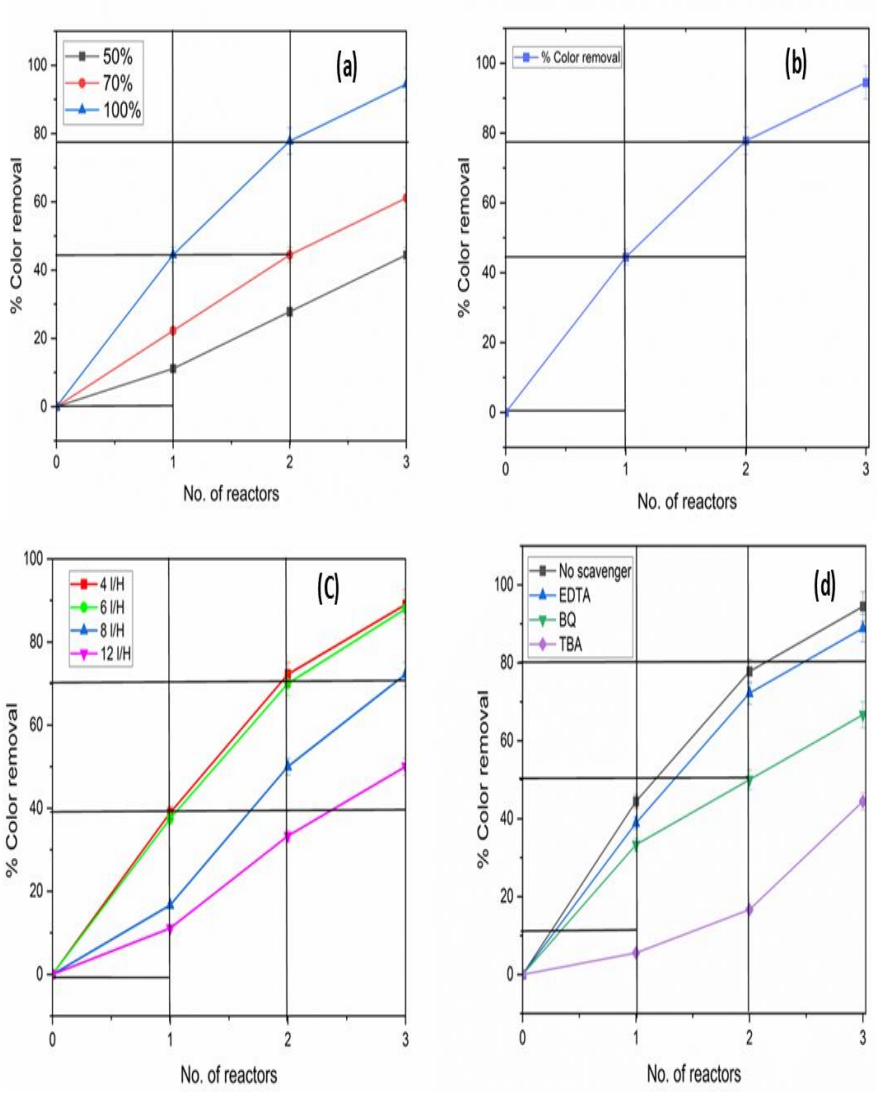

Fig. 4. 50 Change in the % color removal with (a) variation in the % surface area covered by the beads (t=45 min., No. of reactors= 3, %, flow rate= 7.0 Lh^{-1}) (b) variation in the number of reactors Change in the % color removal with (t=45 min., % S.A covered= 100, flow rate= 7.0 Lh^{-1}) (c) variation in flow rate (t=45 min., No. of reactors= 3, % S.A covered= 100, flow rate= 7.0 Lh^{-1}) (d) variation in different scavengers used (t=45 min., No. of reactors= 3, % S.A covered= 100, flow rate= 6.0 Lh^{-1})

4.8.2 Characterization

The characterization was repeated for the O/L stream because it differs significantly from the UASB and I/L wastewater streams. This additional characterization was essential to ensure that the differences in the O/L stream did not affect the performance of the composite. Repeating the characterization also allowed for a more thorough understanding of how the

composite interacts with each type of P&P wastewater stream, ensuring consistent treatment efficacy across all streams.

4.8.2.1 XRD analysis

XRD analysis confirmed the formation of the Fe-TiO_2 composite and identified its crystalline phases (Fig. 4.51 a-c). The patterns displayed characteristic peaks for the anatase (25.4°, 37.8°, 48°, 55°, 62.6°) and rutile (26°, 36°, 55°) phases in both the raw TiO_2 and the Fe-TiO_2 composite, with no changes observed after 100 recycling cycles or exposure to the O/L stream, indicating strong structural stability. The presence of ITO peaks at 70.3° and 75.28° confirmed the successful formation of the Fe-TiO_2 composite, suggesting enhanced photocatalytic activity through photo-Fenton reactions. These findings, supported by UV-DRS analysis, highlight the composite's efficiency and durability under visible light, even after exposure to the O/L stream.

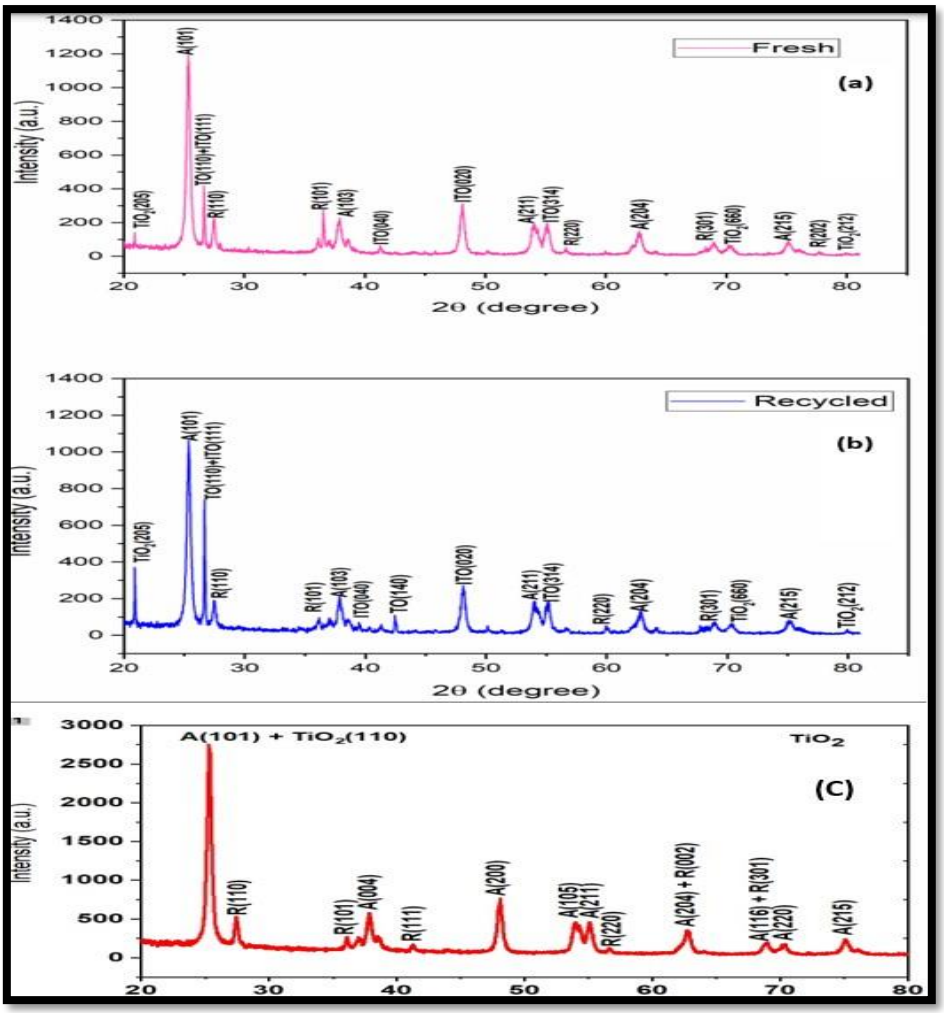

Fig. 4. 51 XRD Analysis of Composite Material: Crystal Structure and Phase Identification: (a) Fresh Composite Material (b) Recycled Composite Material (c) TiO_2 P25 Degussa

4.8.2.2 UVRDS analysis

To further confirm our claim, we performed UVDRS which confirmed the presence of Fe and TiO_2 along with the importance of Fe in the composite. Before and after recycling, the bandgap energy of the catalyst was measured in the visible spectrum between 200 and 800 nm. $BiSo_4$ was used as a standard compound. When iron was added, the energy gap between the beads and TiO_2 got smaller, as shown in Fig. 4.52. This decrease shows that the hybrid beads are better at absorbing light in the visible spectrum. At first, TiO_2 had an absorption peak at 450 nm. This changed to 470 nm before catalytic bead recycling and to 490 nm after recycling. Pure TiO_2 had a bandgap energy of 3.1 eV, but this number dropped to 2.9 eV for the newly

coated composite and then to 2.8 eV for the recycled composite beads. Tauc's plot was used to figure out the bandgap energy of the synthesised catalyst.

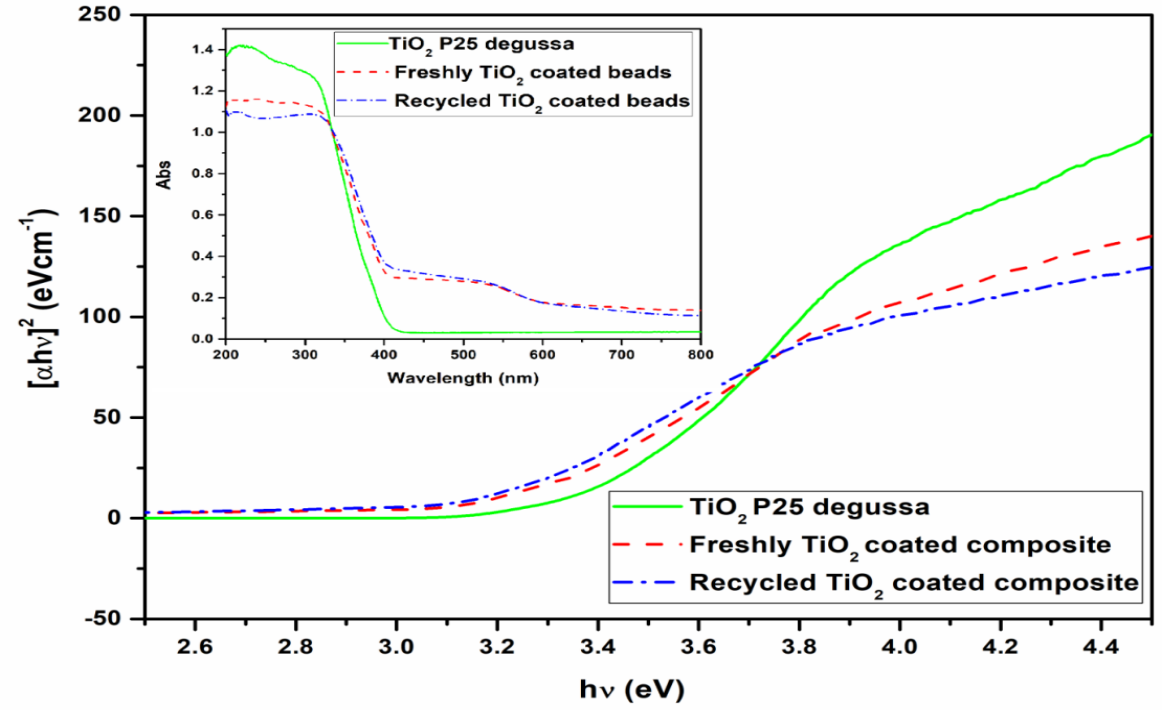

Fig. 4. 52 UVDRS image of TiO_2 Degussa p25, fresh and recycled composite beads

4.8.2.3 HRTEM analysis

In Fig. 4.53 high-resolution transmission electron microscopy (HRTEM) was employed to meticulously examine the morphology and lattice spacing of both fresh and recycled Fe-TiO_2 composites. The HRTEM images revealed well-defined lattice patterns, corresponding to the crystal plane of the TiO_2 anatase (101) phase, with observed lattice spacings ranging from 0.35 to 0.36 nm. This consistent lattice spacing indicates a high degree of crystallinity in the anatase phase of TiO_2 within the composite. The analysis also demonstrated a uniform distribution of Fe within the TiO_2 matrix, confirming the effective incorporation of Fe into the TiO_2 structure. Notably, the comparison between fresh and recycled samples revealed minimal structural degradation, underscoring the robustness and stability of the Fe-TiO_2 composite. This stability is vital for practical applications, as it ensures the composite's reusability and sustained effectiveness in various catalytic processes.

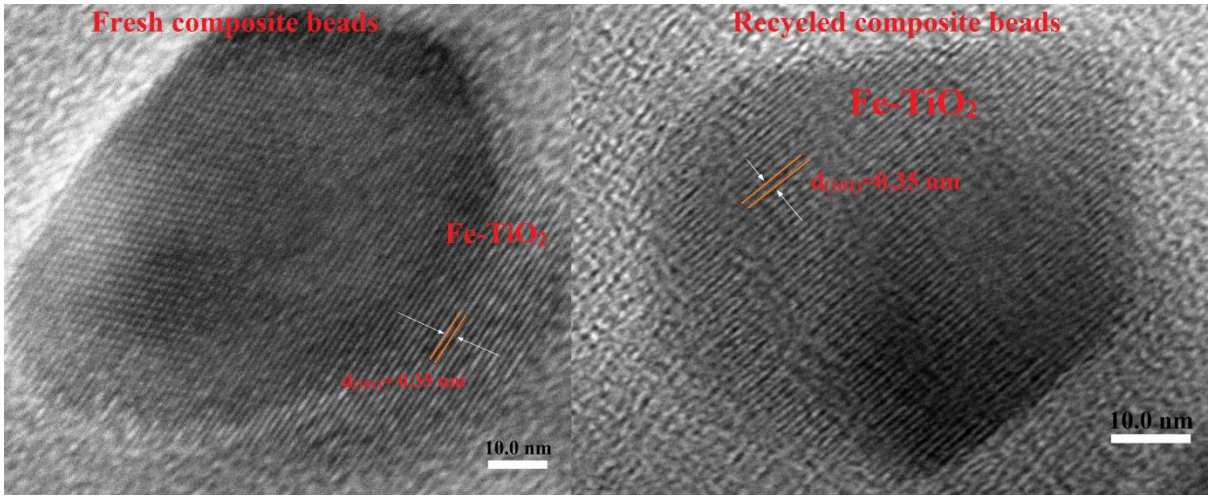

Fig. 4. 53 HRTEM analysis of fresh and recycled beads

4.8.2.4 XPS analysis

The chemical composition of the Fe-TiO_2 composite was investigated using X-ray photoelectron spectroscopy (XPS). The technique of XPS was utilized to analyse the elemental composition and chemical states of the composite. By employing XPS, valuable insights into the chemical composition of Fe-TiO_2 were obtained, allowing for a comprehensive understanding of its molecular structure and elemental constituents. The results obtained from XPS analysis provided crucial information regarding the presence and distribution of iron (Fe) within the TiO_2 matrix. Fig. 4.54 a, illustrates the binding energy spectrum of the Ti2p region for an $FeTiO_2$ composite, with binding energies ranging from 450 eV to 470 eV. The y-axis represents the intensity of the signals, indicating the presence and concentration of various chemical states of titanium. The graph includes raw data and several fitted peaks (Fit Peak 1, Fit Peak 2, and Fit Peak 3), each corresponding to different oxidation states or chemical environments of titanium in the composite. The cumulative fit curve represents the combined contribution of these individual peaks, providing a comprehensive model that accurately reflects the raw experimental data. Analysing these peaks helps identify the electronic structure and oxidation states of titanium, which are crucial for understanding the material's properties and performance. Fig. 4.54 b, represents the binding energy spectrum for the Fe2p3 region, with binding energies ranging approximately from 705 eV to 740 eV. The y-axis shows the intensity, which reflects the concentration of different iron states. The raw data curve is decomposed into multiple fitted peaks (Peak 1 through Peak 5), each representing different chemical states or environments of iron in the composite. The cumulative fit peak is the aggregate of these individual peaks, providing a comprehensive model of the iron's electronic

structure in the composite. Fig. 4.54 c, depicts the binding energy spectrum for the O1s region, with binding energies ranging from approximately 525 eV to 540 eV. The y-axis represents the intensity in arbitrary units. Similar to the Fe2p3 graph, the raw data is decomposed into fitted peaks (Peak 1 and Peak 2) representing different chemical states of oxygen. The cumulative fit peak combines these individual peaks to accurately model the oxygen states in the composite.

Analysing the Fe2p3 and O1s graphs is critical for understanding the interaction of iron, titanium, and oxygen in the $FeTiO_2$ composite. The Fe2p3 spectrum exposes iron's multiple oxidation states, which affect the composite's magnetic and catalytic capabilities. The O1s spectrum displays the many chemical states of oxygen, which is critical for understanding the material's bonding and structural integrity. These evaluations help to improve the composite for applications like as photocatalysis, where element interactions have a substantial impact on efficiency and performance.

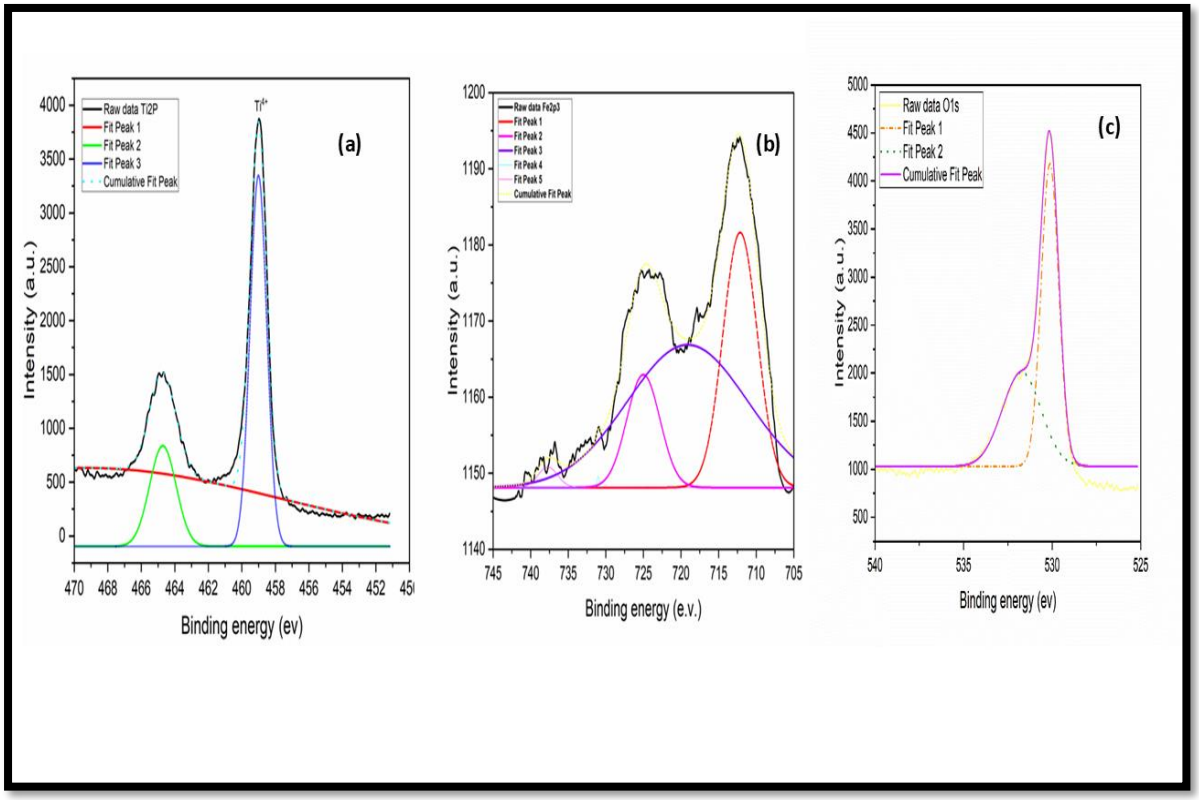

Fig. 4. 54 XPS analysis of $FeTiO_2$ having various contents (a) Ti2p (b) Fe2p3 (c) O1s

4.8.3 Reusability study

One of the key findings of this study is the extended durability of the Fe-TiO_2 composite beads, which effectively maintain their dual in-situ effect over multiple recycles. Few studies have reported such high reusability for wastewater treatment composites. The main goal was to ensure that the TiO_2 catalyst retained its dual functionality even after numerous recycling cycles, which was confirmed through various characterization techniques comparing fresh and recycled beads. Maintaining the original structure of TiO_2 after repeated use was crucial. The catalyst's durability was assessed by its consistent effectiveness in removing color from industrial wastewater over many recycles. As shown in Fig. 4.55, the efficiency of the recycled beads was measured up to 100 recycles. The beads were thoroughly dried after each cycle to preserve their catalytic activity. Remarkably, even after 100 recycles, there was only a slight reduction in catalyst activity, around 10-12%, likely due to minimal surface wear during the process.

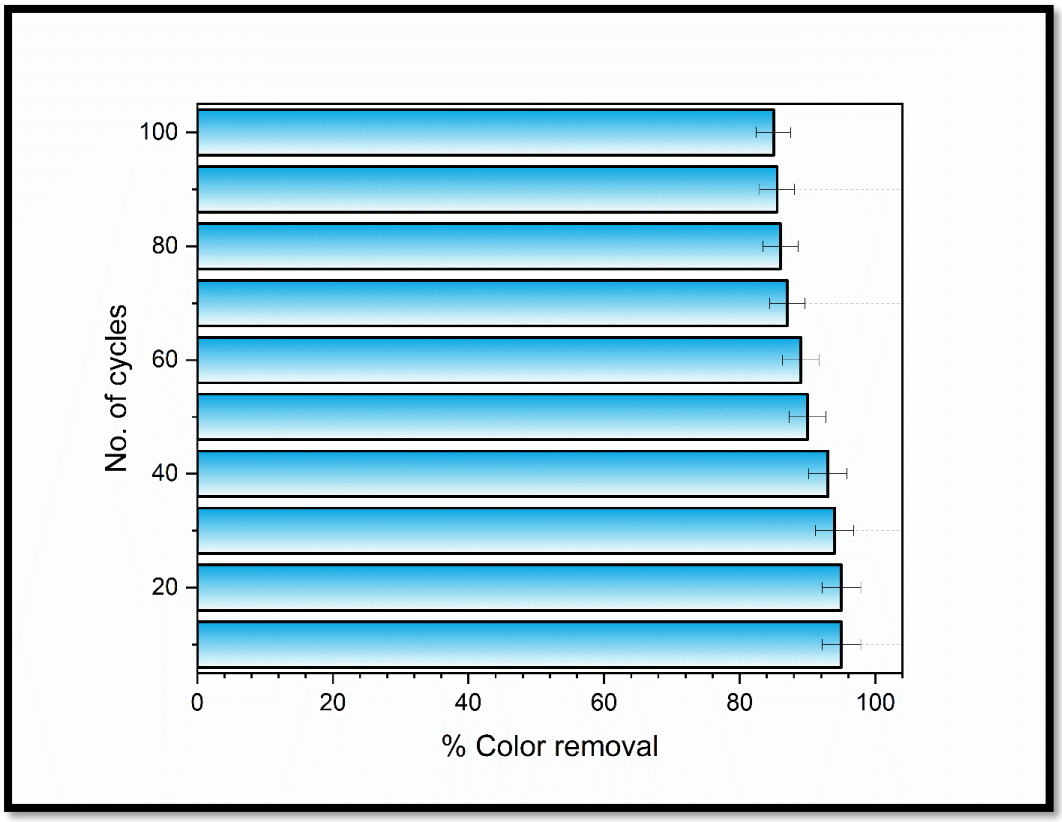

Fig. 4. 55 Reusability study of O/L stream in terms of % color removal for 100 recycles

4.8.4 Cost analysis

Accurate cost estimation is pivotal in dual scale-up studies to determine the financial viability of process integration. Building upon the insights detailed earlier, this research integrates the projected costs of raw materials with process parameters to evaluate the economics of wastewater treatment. For this assessment, considering a wastewater volume of 10,000 L, the 0.6 scaling-up principle was employed, as illustrated in Eq. 4.4 The estimated costs are summarized in Table 4.16, with potential adjustments based on the specific design features of large-scale industrial reactors. The primary advantage of this study lies in the multiple reusability of the beads, significantly reducing the catalyst recovery and production costs for each cycle. This makes it a promising option for commercial applications. The cost estimation for the scale-up study is provided in Table 4.16.

Table 4. 16 Cost analysis for the complete Dual-process and scale-up study for O/L stream

Capital Cost	**Energy consumption**
Cost of Reactor fabrication= 35 US$ Buffering of tank =2 US$ The cost of fittings and piping= 10 US$ The total cost involved in fabrication = 47 US$	Cost of energy consumption=0.81 $/kwh
Catalyst and raw material	**Other costs involved**
The cost involved in catalyst Raw material cost (FS, FA, and clay) = 0US$ Cost of TiO_2 catalyst (36 gm) = 1.152US$ Electricity consumption using muffle=0.75 kwh×0.064 $/kwh= 0.048$	Various controls involved = 1US$ Various other costs = 7US$ Contingency cost = 2US$

Total Price = 1.2 US$	
Cost of the oxidant involved H_2O_2 usage for 100 runs= 300 ×100=35000 mL The total cost of H_2O_2 used= 2.5 US$	**Total cost** Overall Total cost involved = 61.51 US$ for 100 recycles for 10 L Cost of 1 cycle for handling 10 L = 0.61 US$ Treatment cost/ L per cycle = 0.061 US$
Scale-up cost analysis (10,000L) Scale-up cost of raw material = 70.39 US$ Scale-up cost of energy consumption = 55.60 US$ Scale-up cost of oxidant = 109.33 US$ Scale-up cost of reactor fabrication = 532.64 US$ Other miscellaneous cost and contingency = 403.13 US$ Total cost = 1171.09 US$ (for 100 reactions handling 10,000L Volume) Cost for 1 reaction per cycle = 0.00117 US$	

The cost analysis for treating effluent using the once-through technique shows a total expense of 61.51 US$ for 100 recycles handling 10 L, resulting in a treatment cost of 0.061 US$ per litres per cycle. Scaling up to 10,000 L incurs a total cost of 1171.09 US$ for 100

reactions, equating to 0.00117 US$ per cycle. While initial costs such as reactor fabrication, energy consumption, and oxidant usage are significant, cost reduction is achievable through process optimization and reusing materials like catalysts. The potential for long-term savings increases as process efficiency improves and reusable components contribute to further cost reductions in large-scale operations.

Chapter 5

Conclusion and Recommendations

5.1. Conclusion

In conclusion, the study explored an innovative, cost-effective approach to decolorize wastewater from the P&P industry, which is notoriously difficult to treat due to its high content of lignin derivatives and other persistent organic compounds. By utilizing a dual process that combines photocatalysis and photo-Fenton reactions within a single system, the real wastewater streams using a composite material composed of furnace blast sand (FBS) and foundry sand (FS) was treated successfully. The $FeTiO_2$ composite facilitated both photocatalytic and photo-Fenton reactions simultaneously in a single reaction system, capitalizing on the iron's ability to lixiviate under acidic conditions and the photocatalytic properties of TiO_2. The study also highlighted the importance of a systematic equilibrium study to manage iron leaching, prevent the formation of iron sludge, and ensure effective treatment. By employing a two-step process that included coagulation/flocculation as a pretreatment, followed by the dual process, the researchers were able to treat wastewater from various stages of the P&P process. The pretreatment step was crucial for enhancing light penetration and tackling stubborn organics that hindered direct application of the dual process in UASB and I/L streams.

5.1.1. Color removal study under sunlight using Batch scale reactor.

- The innovative concept of incorporating the in-situ dual effect of photocatalysis and photo-Fenton has been applied to remove color from real P&P industry wastewater streams.
- The composite support was made from discard i.e. FS and FBS which turned out to be good substitutes for Fe.
- Three different selected streams i.e., UASB, I/L, and O/L were treated using different reactors i.e., Batch, Recirculation, and Once through.
- A combined approach was adopted for the treatment of UASB and I/L streams, which involved coagulation-flocculation followed by the dual technique of simultaneous photocatalysis and photo-Fenton process.
- UASB and I/L were given coagulation/flocculation as a pretreatment at optimized pH (4 and 6) and coagulant dose (4.84 g/L and 2.42 g/L) which gave a % color removal of 64.1%

and 43.47% respectively. For dual study optimized conditions for were pH (4.5 and 4), H_2O_2 dose (0.4 and 0.35 g/L), and 100% surface area covered by the beads which gave a good color removal of 90.62% and 87.17% for UASB and I/L stream respectively.

- The optimized conditions for O/L stream were pH (4.5), 100% surface area coverage, and H_2O_2 dose (525 mg/L) which gave best color removal of 91.6%.

- The batch scale study was carried out at different time for UASB, I/L, and O/L i.e., 90 min., 120 min., and 60 min.

5.1.2. Color removal study under sunlight using recirculation reactor.

- Scale-up studies were also conducted with the development of pilot-scale fixed-bed reactors using Fe-TiO_2 composite beads incorporating an in-situ dual effect.

- UASB and I/L were given coagulation/flocculation as a pretreatment as explained earlier.

- For dual study BBD was used to design the experiment which obtained the optimized variables i.e. 100% surface area coverage, and H_2O_2 dose (600 mg/L) and bead size (12 mm) which gave the best % color and % COD removal of 89.74% and 53.12% respectively for UASB stream.

- For I/L the optimized variables were H_2O_2 dose (A) (529.155 mgL^{-1}), (B) % surface area covered by beads (105.386 %), and (C) flow rate (4.418 Lh^{-1}) which gave the best % color and % COD removal of 84.5% and 40% respectively.

- For O/L the optimized variables were H_2O_2 dose (A) (427.27 mgL^{-1}), (B) % surface area covered by beads (100.903 %), and (C) flow rate (4.081 Lh^{-1}) which gave the best % color removal of 75% in just 45 min.

- The model was found to be non-significant with an F-value of 3.03 and 3.11 for % color removal of I/L and O/L respectively confirming the model to be sufficiently valid.

5.1.3. Color removal study under sunlight using a once-through reactor. (Scale-up study)

- Finally, once-through study was employed for all the streams handling 10 L volume for treatment in fixed mode under sunlight.

- This effective result was obtained when the 3 reactors in series having a flow rate of 6 L h^{-1}, and 100% surface area covered with beads were employed for all the streams.
- Tentative cost was calculated for all the streams.
- Scale-up cost analysis was also performed which came out to be 0.00120 US$, 0.00118US$, and 0.00117 US$ for UASB, I/L, and O/L respectively.
- The treatment was performed in a very short time of 45 min. for all the streams which gave a good color removal.
- Also, the total cost of the process assessed in this study is substantially lower than other AOPs-related studies found in the literature.
- Hence, the extended applications of the novel composite for color removal from actual pulp and paper industry wastewater even at a large scale confirm the commercial-scale viability of the in-situ hybrid effect.

5.1.4. Durability studies of the composite beads

- The Fe-TiO_2 composite portrayed an exceptional extended durability/recyclability efficacy (>100 recycles) under this entire study as confirmed from analysis including XRD, SEM, EDS FTIR, UVDRS, HRTEM, and XPS.
- Thus, the extended durability and stability of the composite further highlight its commercial applications.

5.2. Recommendations

5.2.1. Utilization of Alternative Waste Materials:

Future research should explore additional waste materials from the environment as alternative sources of iron or as efficient binding agents. This approach can help create more durable and effective catalyst-immobilized supports while promoting environmental sustainability.

5.2.2. Techno-Economic Analysis:

Conduct a detailed techno-economic analysis to assess the feasibility of scaling up the in-situ dual process. This analysis should consider the costs, material efficiency, and potential benefits of large-scale applications in actual wastewater treatment scenarios.

5.2.3. Development of Durable Composite Materials:

Focus on creating more durable and efficient composite materials that can be used in large-scale reactors. This will help improve the longevity and effectiveness of the process in industrial applications.

5.2.4. Scale-Up and Reactor Design:

Further research should prioritize the design and implementation of reactors capable of handling larger wastewater volumes. These reactors should be optimized to maximize the efficiency of the dual process, especially in industrial sectors.

5.2.5. Field Trials and Validation:

Conduct real-world field trials to validate the efficacy of the dual process in various wastewater treatment setups. These trials are essential to ensure that the process performs effectively outside of controlled laboratory conditions.

5.2.6. Expansion to Other Industries:

Explore the application of this dual process in treating wastewater from other industries, such as textiles and pharmaceuticals. These industries face similar challenges with organic pollutants and color removal, and the dual process could offer a viable solution.

Both recirculation and once-through reactors were effective in the studies, but once-through reactors showed better performance, achieving higher efficiency in a shorter time. Therefore, it is recommended to use the once-through reactor configuration for improved results. The dual treatment technique (photocatalysis and photo-Fenton) can be applied either as a pre-treatment or post-treatment depending on the specific needs of the wastewater stream. For example, applying the dual process after the UASB (Up-flow Anaerobic Sludge Blanket) reactor, along with coagulation and flocculation as pre-treatments, is likely the most beneficial approach. In P&P industries, the UASB stream generally handles a lower volume of wastewater compared to the secondary treated O/L stream. This smaller volume makes the use of advanced oxidation processes (AOP) more practical and cost-effective when applied after UASB treatment. By adopting this method, industries can enhance the efficiency of their wastewater treatment systems while reducing costs due to the lower volume of effluent. However, the specific application of the process will depend on the type of wastewater stream and the specific treatment requirements of the industry.

References

Aba-Guevara CG, Medina-Ramírez IE, Hernández-Ramírez A, et al (2017) Comparison of two synthesis methods on the preparation of Fe, N-Co-doped TiO2 materials for degradation of pharmaceutical compounds under visible light. Ceram Int 43:5068–5079. https://doi.org/10.1016/j.ceramint.2017.01.018

Abd El-Sayed ES, El-Sakhawy M, El-Sakhawy MAM (2020) Non-wood fibers as raw material for pulp and paper industry. Nord Pulp Paper Res J 35:215–230. https://doi.org/10.1515/npprj-2019-0064

Abdul Khalil HPS, Davoudpour Y, Islam MN, et al (2014) Production and modification of nanofibrillated cellulose using various mechanical processes: A review. Carbohydr Polym 99:649–665

Abhishek A, Dwivedi A, Tandan N, Kumar U (2017) Comparative bacterial degradation and detoxification of model and kraft lignin from pulp paper wastewater and its metabolites. Appl Water Sci 7:757–767. https://doi.org/10.1007/s13201-015-0288-9

Agulló-Barceló M, Polo-López MI, Lucena F, et al (2013) Solar Advanced Oxidation Processes as disinfection tertiary treatments for real wastewater: Implications for water reclamation. Appl Catal B 136–137:341–350. https://doi.org/10.1016/j.apcatb.2013.01.069

Ahmad N, Gondal MA, Sheikh AK (2016) Comparative study of different solar-based photo catalytic reactors for disinfection of contaminated water. Desalination Water Treat 57:213–220. https://doi.org/10.1080/19443994.2015.1012340

Akach J, Kabuba J, Ochieng A (2020) Simulation of the Light Distribution in a Solar Photocatalytic Bubble Column Reactor Using the Monte Carlo Method. Ind Eng Chem Res 59:17708–17719. https://doi.org/10.1021/acs.iecr.0c02124

Alhaji MH, Sanaullah K, Khan A, et al (2017) Recent developments in immobilizing titanium dioxide on supports for degradation of organic pollutants in wastewater- A review. International Journal of Environmental Science and Technology 14:2039–2052

Ali M, Sreekrishnan TR (2001) Aquatic toxicity from pulp and paper mill effluents: a review

Ali N, Said A, Ali F, et al (2020) Photocatalytic Degradation of Congo Red Dye from Aqueous Environment Using Cobalt Ferrite Nanostructures: Development, Characterization, and Photocatalytic Performance. Water Air Soil Pollut 231:. https://doi.org/10.1007/s11270-020-4410-8

Alinsafi A, Evenou F, Abdulkarim EM, et al (2007) Treatment of textile industry wastewater by supported photocatalysis. Dyes and Pigments 74:439–445. https://doi.org/10.1016/j.dyepig.2006.02.024

Aljuboury DADA, Palaniandy P, Aziz HBA, Feroz S (2015) Treatment of petroleum wastewater using combination of solar photo-two catalyst TiO2 and photo-Fenton process. J Environ Chem Eng 3:1117–1124. https://doi.org/10.1016/j.jece.2015.04.012

Alrousan DMA, Polo-López MI, Dunlop PSM, et al (2012) Solar photocatalytic disinfection of water with immobilised titanium dioxide in re-circulating flow CPC reactors. Appl Catal B 128:126–134. https://doi.org/10.1016/j.apcatb.2012.07.038

Alvarado-Camacho C, Castillo-Araiza CO, Ruiz-Martínez RS (2022) Degradation of Rhodamine B in water alone or as part of a mixture by advanced oxidation processes. Chem Eng Commun 209:69–82. https://doi.org/10.1080/00986445.2020.1835874

Amadi AA, Osu AS (2018) Effect of curing time on strength development in black cotton soil – Quarry fines composite stabilized with cement kiln dust (CKD). Journal of King Saud University - Engineering Sciences 30:305–312. https://doi.org/10.1016/j.jksues.2016.04.001

Amândio MST, Pereira JM, Rocha JMS, et al (2022) Getting Value from Pulp and Paper Industry Wastes: On the Way to Sustainability and Circular Economy. Energies (Basel) 15

Amaral-Silva N, Martins RC, Castro-Silva S, Quinta Ferreira RM (2016) Fenton's treatment as an effective treatment for elderberry effluents: Economical evaluation. Environmental Technology (United Kingdom) 37:1208–1219. https://doi.org/10.1080/09593330.2015.1107624

Amat AM, Arques A, García-Ripoll A, et al (2009) A reliable monitoring of the biocompatibility of an effluent along an oxidative pre-treatment by sequential bioassays and chemical analyses. Water Res 43:784–792. https://doi.org/10.1016/j.watres.2008.11.017

Ananpattarachai J, Seraphin S, Kajitvichyanukul P (2016) Formation of hydroxyl radicals and kinetic study of 2-chlorophenol photocatalytic oxidation using C-doped TiO2, N-doped TiO2, and C,N Co-doped TiO2 under visible light. Environmental Science and Pollution Research 23:3884–3896. https://doi.org/10.1007/s11356-015-5570-8

And RV, Madras G Environmental remediation by photocatalysis

Aragaw TA (2021) Functions of various bacteria for specific pollutants degradation and their application in wastewater treatment: a review. International Journal of Environmental Science and Technology 18:2063–2076

Arslan-Alaton I, Caglayan AE (2006) Toxicity and biodegradability assessment of raw and ozonated procaine penicillin G formulation effluent. In: Ecotoxicology and Environmental Safety. pp 131–140

Asaithambi P (2016) Studies on various operating parameters for the removal of COD from pulp and paper industry using electrocoagulation process. Desalination Water Treat 57:11746–11755. https://doi.org/10.1080/19443994.2015.1046149

Asgari E, Mohammadi F, Nourmoradi H, et al (2022) Heterogeneous catalytic degradation of nonylphenol using persulphate activated by natural pyrite: response surface methodology modelling and optimisation. Int J Environ Anal Chem 102:6041–6060. https://doi.org/10.1080/03067319.2020.1807528

Ashrafi O, Yerushalmi L, Haghighat F (2015) Wastewater treatment in the pulp-and-paper industry: A review of treatment processes and the associated greenhouse gas emission. J Environ Manage 158:146–157

Assalin MR, Almeida EDS, Duran N (2009) Combined system of activated sludge and ozonation for the treatment of Kraft e1 effluent. Int J Environ Res Public Health 6:1145–1154. https://doi.org/10.3390/ijerph6031145

Bajpai P, Bajpai PK (1994) journal of biotechnology Minireview Biological colour removal of pulp and paper mill wastewaters

Banerjee T, Sharma P, Pradhan S (2020) Consensus based Data Aggregation for Energy Conservation in Wireless Sensor Network. International Journal of Distributed and Parallel systems 11:11–26. https://doi.org/10.5121/ijdps.2020.11502

Banerjee T, Singh MK, Khanna A (2006) Prediction of binary VLE for imidazolium based ionic liquid systems using COSMO-RS. Ind Eng Chem Res 45:3207–3219. https://doi.org/10.1021/ie051116c

Bansal A, Wanchoo RK, Sharma SK (2007) Modeling of trickle bed reactors involving beds of different configurations under low and high interaction regimes. Ind Eng Chem Res 46:677–683. https://doi.org/10.1021/ie060671r

Bansal P, Verma A (2017) Novel Fe-TiO2 composite driven dual effect for reduction in treatment time of pentoxifylline: Slurry to immobilized approach. Mater Des 125:135–145. https://doi.org/10.1016/j.matdes.2017.03.083

Bansal P, Verma A, Mehta C, et al (2018) Assessment of integrated binary process by coupling photocatalysis and photo-Fenton for the removal of cephalexin from aqueous solution. J Mater Sci 53:7326–7343. https://doi.org/10.1007/s10853-018-2094-x

Baresel C, Malmborg J, Ek M, Sehlén R (2016) Removal of pharmaceutical residues using ozonation as intermediate process step at Linköping WWTP, Sweden. Water Science and Technology 73:2017–2024. https://doi.org/10.2166/wst.2016.045

Bautitz IR, Nogueira RFP (2010) Photodegradation of lincomycin and diazepam in sewage treatment plant effluent by photo-Fenton process. Catal Today 151:94–99. https://doi.org/10.1016/j.cattod.2010.02.018

Bayraktar OY (2019) The possibility of fly ash and blast furnace slag disposal by using these environmental wastes as substitutes in portland cement. Environ Monit Assess 191:. https://doi.org/10.1007/s10661-019-7741-4

Behravesh S, Mirghaffari N, Alemrajabi AA, et al (2020) Photocatalytic degradation of acetaminophen and codeine medicines using a novel zeolite-supported TiO2 and ZnO under UV and sunlight irradiation. Environmental Science and Pollution Research 27:26929–26942. https://doi.org/10.1007/s11356-020-09038-y

Beltran De Heredia J, Torregrosa J, Dominguez JR, Peres JA Kinetic model for phenolic compound oxidation by Fenton's reagent

Bezerra MA, Santelli RE, Oliveira EP, et al (2008) Response surface methodology (RSM) as a tool for optimization in analytical chemistry. Talanta 76:965–977

Biń AK, Sobera-Madej S (2012) Comparison of the Advanced Oxidation Processes (UV, UV/H 2O 2 and O 3) for the Removal of Antibiotic Substances during Wastewater Treatment. Ozone Sci Eng 34:136–139. https://doi.org/10.1080/01919512.2012.650130

Blanco-Vega MP, Guzmán-Mar JL, Villanueva-Rodríguez M, et al (2017) Photocatalytic elimination of bisphenol A under visible light using Ni-doped TiO2 synthesized by microwave assisted sol-gel method. Mater Sci Semicond Process 71:275–282. https://doi.org/10.1016/j.mssp.2017.08.013

Boguniewicz-Zablocka J, Klosok-Bazan I, Naddeo V, Mozejko CA (2020) Cost-effective removal of COD in the pre-treatment of wastewater from the paper industry. Water Science and Technology 81:1345–1353. https://doi.org/10.2166/wst.2019.328

Borges R, Kai KC, Lima CA, et al (2021) Bioactive glass/poloxamer 407 hydrogel composite as a drug delivery system: The interplay between glass dissolution and drug release kinetics. Colloids Surf B Biointerfaces 206:. https://doi.org/10.1016/j.colsurfb.2021.111934

Cagide C, Castro-Sowinski S (2020) Technological and biochemical features of lignin-degrading enzymes: a brief review. Environmental Sustainability 3:371–389. https://doi.org/10.1007/s42398-020-00140-y

Cai QQ, Lee BCY, Ong SL, Hu JY (2021) Fluidized-bed Fenton technologies for recalcitrant industrial wastewater treatment–Recent advances, challenges and perspective. Water Res 190

Can N, Ömür BC, Altındal A (2016) Modeling of heavy metal ion adsorption isotherms onto metallophthalocyanine film. Sens Actuators B Chem 237:953–961. https://doi.org/10.1016/j.snb.2016.07.026

Carey RO, Migliaccio KW (2009) Contribution of wastewater treatment plant effluents to nutrient dynamics in aquatic systems. Environ Manage 44:205–217

Carolin CF, Kumar PS, Saravanan A, et al (2017) Efficient techniques for the removal of toxic heavy metals from aquatic environment: A review. J Environ Chem Eng 5:2782–2799

Chakrabarti S, Dutta BK (2004) Photocatalytic degradation of model textile dyes in wastewater using ZnO as semiconductor catalyst. J Hazard Mater 112:269–278. https://doi.org/10.1016/j.jhazmat.2004.05.013

Chamorro S, Hernández V, Matamoros V, et al (2013) Chemical characterization of organic microcontaminant sources and biological effects in riverine sediments impacted by urban sewage and pulp mill discharges. Chemosphere 90:611–619. https://doi.org/10.1016/j.chemosphere.2012.08.053

Chan AHC, Chan CK, Barford JP, Porter JF (2003) Solar photocatalytic thin film cascade reactor for treatment of benzoic acid containing wastewater

Chan SHS, Wu TY, Juan JC, Teh CY (2011) Recent developments of metal oxide semiconductors as photocatalysts in advanced oxidation processes (AOPs) for treatment of dye waste-water. Journal of Chemical Technology and Biotechnology 86:1130–1158

Chan YJ, Chong MF, Law CL, Hassell DG (2009) A review on anaerobic-aerobic treatment of industrial and municipal wastewater. Chemical Engineering Journal 155:1–18

Changotra R, Rajput H, Dhir A (2019) Treatment of real pharmaceutical wastewater using combined approach of Fenton applications and aerobic biological treatment. J Photochem Photobiol A Chem 376:175–184. https://doi.org/10.1016/j.jphotochem.2019.02.029

Chatterjee D, Dasgupta S (2005) Visible light induced photocatalytic degradation of organic pollutants. Journal of Photochemistry and Photobiology C: Photochemistry Reviews 6:186–205. https://doi.org/10.13140/RG.2.1.3848.1364

Chauhan S, Meena BL Introduction to pulp and paper industry: Global scenario. https://doi.org/10.1515/b_psr-2020-0014

Cheng X, Yu X, Xing Z, Yang L (2016) Synthesis and characterization of N-doped TiO2 and its enhanced visible-light photocatalytic activity. Arabian Journal of Chemistry 9:S1706–S1711. https://doi.org/10.1016/j.arabjc.2012.04.052

Chkirida S, Zari N, Achour R, et al (2021) Highly synergic adsorption/photocatalytic efficiency of Alginate/Bentonite impregnated TiO2 beads for wastewater treatment. J Photochem Photobiol A Chem 412:. https://doi.org/10.1016/j.jphotochem.2021.113215

Chong MN, Cho YJ, Poh PE, Jin B (2015) Evaluation of Titanium dioxide photocatalytic technology for the treatment of reactive Black 5 dye in synthetic and real greywater effluents. J Clean Prod 89:196–202. https://doi.org/10.1016/j.jclepro.2014.11.014

Chong MN, Jin B, Chow CWK, Saint C (2010) Recent developments in photocatalytic water treatment technology: A review. Water Res 44:2997–3027

Claes T, Fransen S, Degrève J, et al (2021) Kinetic optimization of multilayered photocatalytic reactors. Chemical Engineering Journal 421:. https://doi.org/10.1016/j.cej.2020.127794

Cleveland V, Bingham JP, Kan E (2014) Heterogeneous Fenton degradation of bisphenol A by carbon nanotube-supported Fe3O4. Sep Purif Technol 133:388–395. https://doi.org/10.1016/j.seppur.2014.06.061

Collivignarelli MC, Cillari G, Ricciardi P, et al (2020) The production of sustainable concrete with the use of alternative aggregates: A review. Sustainability (Switzerland) 12

Colmenares JC, Magdziarz A, Chernyayeva O, et al (2013) Sonication-assisted low-temperature routes for the synthesis of supported Fe-TiO2 econanomaterials: Partial photooxidation of glucose and phenol aqueous degradation. ChemCatChem 5:2270–2277. https://doi.org/10.1002/cctc.201300025

Comninellis C, Kapalka A, Malato S, et al (2008) Advanced oxidation processes for water treatment: Advances and trends for R&D. Journal of Chemical Technology and Biotechnology 83:769–776. https://doi.org/10.1002/jctb.1873

Dahm A, Lucia LA (2004) Titanium dioxide catalyzed photodegradation of lignin in industrial effluents. Ind Eng Chem Res 43:7996–8000. https://doi.org/10.1021/ie0498302

Davarnejad R, Nasiri S (2017) Slaughterhouse wastewater treatment using an advanced oxidation process: Optimization study. Environmental Pollution 223:1–10. https://doi.org/10.1016/j.envpol.2016.11.008

De Torres-Socías E, Prieto-Rodríguez L, Zapata A, et al (2015) Detailed treatment line for a specific landfill leachate remediation. Brief economic assessment. Chemical Engineering Journal 261:60–66. https://doi.org/10.1016/j.cej.2014.02.103

Delnavaz A, Ramezanianpour AA (2012) The assessment of carbonation effect on chloride diffusion in concrete based on artificial neural network model. Magazine of Concrete Research 64:877–884. https://doi.org/10.1680/macr.11.00059

Deng L, Wang S, Liu D, et al (2009) Synthesis, characterization of Fe-doped TiO2 nanotubes with high photocatalytic activity. Catal Letters 129:513–518. https://doi.org/10.1007/s10562-008-9834-5

Deng Y, Zhao R (2015) Advanced Oxidation Processes (AOPs) in Wastewater Treatment. Curr Pollut Rep 1:167–176. https://doi.org/10.1007/s40726-015-0015-z

Dixit M, Gupta GK, Shukla P (2019) Insights into the resources generation from pulp and paper industry wastes: challenges, perspectives and innovations. Elsevier Ltd

Doll TE, Frimmel FH (2005) Removal of selected persistent organic pollutants by heterogeneous photocatalysis in water. In: Catalysis Today. pp 195–202

Dong S, Zhou D, Bi X (2010) Liquid phase heterogeneous photocatalytic ozonation of phenol in liquid-solid fluidized bed: Simplified kinetic modeling. Particuology 8:60–66. https://doi.org/10.1016/j.partic.2009.04.011

Ebele AJ, Abou-Elwafa Abdallah M, Harrad S (2017) Pharmaceuticals and personal care products (PPCPs) in the freshwater aquatic environment. Emerg Contam 3:1–16

El-Naas MH, Surkatti R, Al-Zuhair S (2016) Petroleum refinery wastewater treatment: A pilot scale study. Journal of Water Process Engineering 14:71–76. https://doi.org/10.1016/j.jwpe.2016.10.005

Esplugas S, Gim! Enez J, Contreras S, et al (2002) Comparison of different advanced oxidation processes for phenol degradation

Fabiyi ME, Skelton RL (2000) Photocatalytic mineralisation of methylene blue using buoyant TiO 2-coated polystyrene beads

Fallmann H, Krutzler T, Bauer R, et al (1999) Applicability of the Photo-Fenton method for treating water containing pesticides

Feitz AJ, Boyden BH, Waite TD EVALUATION OF TWO SOLAR PILOT SCALE FIXED-BED PHOTOCATALYTIC REACTORS

Fernández-Ibáñez P, Polo-López MI, Malato S, et al (2015) Solar photocatalytic disinfection of water using titanium dioxide graphene composites. Chemical Engineering Journal 261:36–44. https://doi.org/10.1016/j.cej.2014.06.089

Ferreira SLC, Bruns RE, Ferreira HS, et al (2007) Box-Behnken design: An alternative for the optimization of analytical methods. Anal Chim Acta 597:179–186

Gadipelly C, Pérez-González A, Yadav GD, et al (2014) Pharmaceutical industry wastewater: Review of the technologies for water treatment and reuse. Ind Eng Chem Res 53:11571–11592

Ganiyu SO, Zhou M, Martínez-Huitle CA (2018) Heterogeneous electro-Fenton and photoelectro-Fenton processes: A critical review of fundamental principles and application for water/wastewater treatment. Appl Catal B 235:103–129. https://doi.org/10.1016/j.apcatb.2018.04.044

Ganzenko O, Huguenot D, van Hullebusch ED, et al (2014) Electrochemical advanced oxidation and biological processes for wastewater treatment: A review of the combined approaches. Environmental Science and Pollution Research 21:8493–8524

Gao B, Yap PS, Lim TM, Lim TT (2011) Adsorption-photocatalytic degradation of Acid Red 88 by supported TiO2: Effect of activated carbon support and aqueous anions. Chemical Engineering Journal 171:1098–1107. https://doi.org/10.1016/j.cej.2011.05.006

García-Montaño J, Pérez-Estrada L, Oller I, et al (2008) Pilot plant scale reactive dyes degradation by solar photo-Fenton and biological processes. J Photochem Photobiol A Chem 195:205–214. https://doi.org/10.1016/j.jphotochem.2007.10.004

Gaur RZ, Khoury O, Zohar M, et al (2020) Hydrothermal carbonization of sewage sludge coupled with anaerobic digestion: Integrated approach for sludge management and energy recycling. Energy Convers Manag 224:. https://doi.org/10.1016/j.enconman.2020.113353

Gavrilescu M, Teodosiu C, Gavrilescu D, Lupu L (2008) Strategies and practices for sustainable use of water in industrial papermaking processes. Eng Life Sci 8:99–124

Gaya UI, Abdullah AH (2008) Heterogeneous photocatalytic degradation of organic contaminants over titanium dioxide: A review of fundamentals, progress and problems. Journal of Photochemistry and Photobiology C: Photochemistry Reviews 9:1–12

Geeraerd AH, Valdramidis VP, Van Impe JF (2005) GInaFiT, a freeware tool to assess non-log-linear microbial survivor curves. Int J Food Microbiol 102:95–105. https://doi.org/10.1016/j.ijfoodmicro.2004.11.038

Gerber Van Doren L, Posmanik R, Bicalho FA, et al (2017) Prospects for energy recovery during hydrothermal and biological processing of waste biomass. Bioresour Technol 225:67–74. https://doi.org/10.1016/j.biortech.2016.11.030

Gernjak W, Maldonado ML, Malato S, et al (2004) Pilot-plant treatment of olive mill wastewater (OMW) by solar TiO 2 photocatalysis and solar photo-Fenton. Solar Energy 77:567–572. https://doi.org/10.1016/j.solener.2004.03.030

Gholami M, Abbasi Souraki B, Pendashteh A, Bagherian Marzouni M (2017) Efficiency evaluation of the membrane/AOPs for paper mill wastewater treatment. Environmental Technology (United Kingdom) 38:1127–1138. https://doi.org/10.1080/09593330.2016.1218553

GilPavas E, Dobrosz-Gómez I, Gómez-García MÁ (2017) Coagulation-flocculation sequential with Fenton or Photo-Fenton processes as an alternative for the industrial textile wastewater treatment. J Environ Manage 191:189–197. https://doi.org/10.1016/j.jenvman.2017.01.015

Ginni G, Adishkumar S, Rajesh Banu J, Yogalakshmi N (2014a) Treatment of pulp and paper mill wastewater by solar photo-Fenton process. Desalination Water Treat 52:2457–2464. https://doi.org/10.1080/19443994.2013.794114

Ginni G, Adishkumar S, Rajesh Banu J, Yogalakshmi N (2014b) Treatment of pulp and paper mill wastewater by solar photo-Fenton process. Desalination Water Treat 52:2457–2464. https://doi.org/10.1080/19443994.2013.794114

Giri AS, Golder AK (2014) Fenton, photo-fenton, H2O2 Photolysis, and TiO 2 Photocatalysis for Dipyrone Oxidation: Drug Removal, Mineralization, Biodegradability, and Degradation Mechanism. Ind Eng Chem Res 53:1351–1358. https://doi.org/10.1021/ie402279q

Giri S (2021) Water quality prospective in Twenty First Century: Status of water quality in major river basins, contemporary strategies and impediments: A review. Environmental Pollution 271

Glaze WH, Kang JW, Chapin DH (1987) The chemistry of water treatment processes involving ozone, hydrogen peroxide and ultraviolet radiation. Ozone Sci Eng 9:335–352. https://doi.org/10.1080/01919518708552148

Gomec CY (2010) High-rate anaerobic treatment of domestic wastewater at ambient operating temperatures: A review on benefits and drawbacks. J Environ Sci Health A Tox Hazard Subst Environ Eng 45:1169–1184

Gonçalves NPF, Varga Z, Nicol E, et al (2021) Comparison of advanced oxidation processes for the degradation of maprotiline in water—kinetics, degradation products and potential ecotoxicity. Catalysts 11:1–15. https://doi.org/10.3390/catal11020240

Grötzner M, Melchiors E, Schroeder LH, et al (2018a) Pulp and Paper Mill Effluent Treated by Combining Coagulation-Flocculation-Sedimentation and Fenton Processes

Grötzner M, Melchiors E, Schroeder LH, et al (2018b) Pulp and Paper Mill Effluent Treated by Combining Coagulation-Flocculation-Sedimentation and Fenton Processes. Water Air Soil Pollut 229:. https://doi.org/10.1007/s11270-018-4017-5

Guo HG, Gao NY, Chu WH, et al (2013) Photochemical degradation of ciprofloxacin in UV and UV/H2O2 process: Kinetics, parameters, and products. Environmental Science and Pollution Research 20:3202–3213. https://doi.org/10.1007/s11356-012-1229-x

Guo S, Wang Q, Luo C, et al (2020) Hydroxyl radical-based and sulfate radical-based photocatalytic advanced oxidation processes for treatment of refractory organic matter in semi-aerobic aged refuse biofilter effluent arising from treating landfill leachate. Chemosphere 243:. https://doi.org/10.1016/j.chemosphere.2019.125390

Gupta N, Mahur BK, Izrayeel AMD, et al (2022) Biomass conversion of agricultural waste residues for different applications: a comprehensive review. Environmental Science and Pollution Research 29:73622–73647

Gutierrez-Mata AG, Velazquez-Martínez S, Álvarez-Gallegos A, et al (2017) Recent Overview of Solar Photocatalysis and Solar Photo-Fenton Processes for Wastewater Treatment. International Journal of Photoenergy 2017

Haile A, Gelebo GG, Tesfaye T, et al (2021) Pulp and paper mill wastes: utilizations and prospects for high value-added biomaterials. Bioresour Bioprocess 8

Han N, Zhang J, Hoang M, et al (2021) A review of process and wastewater reuse in the recycled paper industry. Environ Technol Innov 24

Hanrahan G, Lu K (2006) Application of factorial and response surface methodology in modern experimental design and optimization. Crit Rev Anal Chem 36:141–151. https://doi.org/10.1080/10408340600969478

Haq BU, Ahmed R, Abdellatif G, et al (2016) Dominant ferromagnetic coupling over antiferromagnetic in Ni doped ZnO: First-principles calculations. Front Phys (Beijing) 11:1–7. https://doi.org/10.1007/s11467-015-0542-5

Haq I, Mazumder P, Kalamdhad AS (2020) Recent advances in removal of lignin from paper industry wastewater and its industrial applications – A review. Bioresour Technol 312

Haranaka-Funai D, Didier F, Giménez J, et al (2017) Photocatalytic treatment of valproic acid sodium salt with TiO2 in different experimental devices: An economic and energetic comparison. Chemical Engineering Journal 327:656–665. https://doi.org/10.1016/j.cej.2017.06.148

Haroune L, Salaun M, Ménard A, et al (2014) Photocatalytic degradation of carbamazepine and three derivatives using TiO2 and ZnO: Effect of pH, ionic strength, and natural organic matter. Science of the Total Environment 475:16–22. https://doi.org/10.1016/j.scitotenv.2013.12.104

Harrelkas F, Paulo A, Alves MM, et al (2008) Photocatalytic and combined anaerobic-photocatalytic treatment of textile dyes. Chemosphere 72:1816–1822. https://doi.org/10.1016/j.chemosphere.2008.05.026

Hashimoto K, Irie H, Fujishima A (2005) TiO 2 photocatalysis: A historical overview and future prospects. Japanese Journal of Applied Physics, Part 1: Regular Papers and Short Notes and Review Papers 44:8269–8285. https://doi.org/10.1143/JJAP.44.8269

Hermosilla D, Merayo N, Gascó A (2015) The application of advanced oxidation technologies to the treatment of effluents from the pulp and paper industry : a review. 168–191. https://doi.org/10.1007/s11356-014-3516-1

Hermosilla D, Merayo N, Ordóñez R, Blanco Á (2012) Optimization of conventional Fenton and ultraviolet-assisted oxidation processes for the treatment of reverse osmosis retentate from a paper mill. Waste Management 32:1236–1243. https://doi.org/10.1016/j.wasman.2011.12.011

Holkar CR, Jadhav AJ, Pinjari D V., et al (2016) A critical review on textile wastewater treatments: Possible approaches. J Environ Manage 182:351–366

Huang C, Hu J, Cong S, et al (2015) Hierarchical BiOCl microflowers with improved visible-light-driven photocatalytic activity by Fe(III) modification. Appl Catal B 174–175:105–112. https://doi.org/10.1016/j.apcatb.2015.03.001

Hubbe B, Hubbe MA, Bowden C (2009) Handmade paper, review

Hubbe MA, Metts JR, Hermosilla D, et al (2016a) Pulp & paper effluent

Hubbe MA, Metts JR, Hermosilla D, et al (2016b) Pulp & paper effluent

Idris A, Misran E, Hassan N, et al (2012) Modified PVA-alginate encapsulated photocatalyst ferro photo gels for Cr(VI) reduction. J Hazard Mater 227–228:309–316. https://doi.org/10.1016/j.jhazmat.2012.05.065

Ioannidou O, Zabaniotou A, Antonakou E V., et al (2009) Investigating the potential for energy, fuel, materials and chemicals production from corn residues (cobs and stalks) by non-catalytic and catalytic pyrolysis in two reactor configurations. Renewable and Sustainable Energy Reviews 13:750–762

Irfan M, Butt T, Imtiaz N, et al (2013) The removal of COD , TSS and colour of black liquor by coagulation – flocculation process at optimized pH , settling and dosing rate. ARABIAN JOURNAL OF CHEMISTRY. https://doi.org/10.1016/j.arabjc.2013.08.007

Islam MR, Mostafa MG (2018) Textile Dyeing Effluents and Environment Concerns-A Review. J Environ Sci & Natural Resources 11:131–144

Ismail AA (2012) Mesoporous PdO-TiO 2 nanocomposites with enhanced photocatalytic activity. Appl Catal B 117–118:67–72. https://doi.org/10.1016/j.apcatb.2012.01.006

Ji Y, Zhou L, Ferronato C, et al (2013) Photocatalytic degradation of atenolol in aqueous titanium dioxide suspensions: Kinetics, intermediates and degradation pathways. J Photochem Photobiol A Chem 254:35–44. https://doi.org/10.1016/j.jphotochem.2013.01.003

John D, Yesodharan S, Sivanandan Achari V (2020) Integration of Coagulation-Flocculation and Heterogeneous Photocatalysis for the Treatment of Pulp and Paper Mill Effluent. Environmental Technology (United Kingdom) 0:1–35. https://doi.org/10.1080/09593330.2020.1791972

Kabra K, Chaudhary R, Sawhney RL (2004) Treatment of hazardous organic and inorganic compounds through aqueous-phase photocatalysis: A review. Ind Eng Chem Res 43:7683–7696

Kamali M, Alavi-Borazjani SA, Khodaparast Z, et al (2019) Additive and additive-free treatment technologies for pulp and paper mill effluents: Advances, challenges and opportunities. Water Resour Ind 21

Kamali M, Khodaparast Z (2015) Review on recent developments on pulp and paper mill wastewater treatment. Ecotoxicol Environ Saf 114:326–342

Kandananond K (2010) Using the response surface method to optimize the turning process of AISI 12L14 steel. Advances in Mechanical Engineering 2010:. https://doi.org/10.1155/2010/362406

Kansal SK, Singh M, Sud D (2007) Optimization of photocatalytic process parameters for the degradation of 2,4,6-trichlorophenol in aqueous solutions. Chem Eng Commun 194:787–802. https://doi.org/10.1080/00986440701193803

Kansal SK, Singh M, Sud D (2008) Effluent quality at kraft/soda agro-based paper mills and its treatment using a heterogeneous photocatalytic system. Desalination 228:183–190. https://doi.org/10.1016/j.desal.2007.10.007

Kaur D, Bhardwaj NK, Lohchab RK (2017) Prospects of rice straw as a raw material for paper making. Waste Management 60:127–139

Kesari KK, Soni R, Jamal QMS, et al (2021) Wastewater Treatment and Reuse: a Review of its Applications and Health Implications. Water Air Soil Pollut 232

Khalid S, Shahid M, Natasha, et al (2018) A review of environmental contamination and health risk assessment of wastewater use for crop irrigation with a focus on low and high-income countries. Int J Environ Res Public Health 15

Khan SJ, Reed RH, Rasul MG (2012) Thin-film fixed-bed reactor for solar photocatalytic inactivation of Aeromonas hydrophila: influence of water quality

Khuri AI, Mukhopadhyay S (2010) Response surface methodology. Wiley Interdiscip Rev Comput Stat 2:128–149

Kim S (2016) Journal of Industrial and Engineering Chemistry Application of response surface method as an experimental design to optimize coagulation – flocculation process for pre-treating paper wastewater. Journal of Industrial and Engineering Chemistry. https://doi.org/10.1016/j.jiec.2016.04.010

Kim S, Hwang SJ, Choi W (2005) Visible light active platinum-ion-doped TiO2 photocatalyst. Journal of Physical Chemistry B 109:24260–24267. https://doi.org/10.1021/jp055278y

Kishor R, Purchase D, Saratale GD, et al (2021) Ecotoxicological and health concerns of persistent coloring pollutants of textile industry wastewater and treatment approaches for environmental safety. J Environ Chem Eng 9:. https://doi.org/10.1016/j.jece.2020.105012

Kong L, Hasanbeigi A, Price L (2016) Assessment of emerging energy-efficiency technologies for the pulp and paper industry: A technical review. J Clean Prod 122:5–28

Ksibi M, Amor S Ben, Cherif S, et al (2003) Photodegradation of lignin from black liquor using a UV/TiO 2 system

Ksibi M, Rossignol S, Tatibouët JM, Trapalis C (2008) Synthesis and solid characterization of nitrogen and sulfur-doped TiO2 photocatalysts active under near visible light. Mater Lett 62:4204–4206. https://doi.org/10.1016/j.matlet.2008.06.026

Kujur SK, Kumar Kujur S 0)

Kumar M, Puri A (2012) A review of permissible limits of drinking water. Indian J Occup Environ Med 16:40–44

Kumar P, Srivastava VC, Štangar UL, et al (2021) Recent progress in dimethyl carbonate synthesis using different feedstock and techniques in the presence of heterogeneous catalysts. Catal Rev Sci Eng 63:363–421. https://doi.org/10.1080/01614940.2019.1696609

Kumar V, Bansal A, Gupta R (2019) Synthesis of rGO/TiO2 Nanocomposite for the Efficient Photocatalytic Degradation of RhB Dye. In: Lecture Notes in Civil Engineering. Springer, pp 265–280

Lakshminarasimhan N, Varadaraju U V. (2008) Role of crystallite size on the photoluminescence properties of SrIn2O4:Eu3+ phosphor synthesized by different methods. J Solid State Chem 181:2418–2423. https://doi.org/10.1016/j.jssc.2008.06.005

Lee H, Shoda M (2008) Removal of COD and color from livestock wastewater by the Fenton method. J Hazard Mater 153:1314–1319. https://doi.org/10.1016/j.jhazmat.2007.09.097

Lee SY, Park SJ (2013) TiO2 photocatalyst for water treatment applications. Journal of Industrial and Engineering Chemistry 19:1761–1769

Li D, Zhu Q, Han C, et al (2015a) Photocatalytic degradation of recalcitrant organic pollutants in water using a novel cylindrical multi-column photoreactor packed with TiO2-coated silica gel beads. J Hazard Mater 285:398–408. https://doi.org/10.1016/j.jhazmat.2014.12.024

Li H, Sang Y, Chang S, et al (2015b) Enhanced Ferroelectric-Nanocrystal-Based Hybrid Photocatalysis by Ultrasonic-Wave-Generated Piezophototronic Effect. Nano Lett 15:2372–2379. https://doi.org/10.1021/nl504630j

Li L, Yang Y, Liu X, et al (2013) A direct synthesis of B-doped TiO 2 and its photocatalytic performance on degradation of RhB. Appl Surf Sci 265:36–40. https://doi.org/10.1016/j.apsusc.2012.10.075

Lieder M, Rashid A (2016) Towards circular economy implementation: A comprehensive review in context of manufacturing industry. J Clean Prod 115:36–51

Lin B, Yang G, Yang B, Zhao Y (2016) Construction of novel three dimensionally ordered macroporous carbon nitride for highly efficient photocatalytic activity. Appl Catal B 198:276–285. https://doi.org/10.1016/j.apcatb.2016.05.069

Liu B, Nakata K, Liu S, et al (2012) Theoretical kinetic analysis of heterogeneous photocatalysis by TiO 2 nanotube arrays: The effects of nanotube geometry on photocatalytic activity. Journal of Physical Chemistry C 116:7471–7479. https://doi.org/10.1021/jp300481a

Liu Y, Chen L, Hu J, et al (2010) TiO2 nanoflakes modified with gold nanoparticles as photocatalysts with high activity and durability under near UV irradiation. Journal of Physical Chemistry C 114:1641–1645. https://doi.org/10.1021/jp910500c

Liu Y, Li Z, Green M, et al (2017) Titanium dioxide nanomaterials for photocatalysis. J Phys D Appl Phys 50

Loh YR, Sujan D, Rahman ME, Das CA (2013) Review Sugarcane bagasse - The future composite material: A literature review. Resour Conserv Recycl 75:14–22

Luo H, Zeng Y, He D, Pan X (2021) Application of iron-based materials in heterogeneous advanced oxidation processes for wastewater treatment: A review. Chemical Engineering Journal 407

Luo X, Wang J, Dooner M, Clarke J (2015) Overview of current development in electrical energy storage technologies and the application potential in power system operation. Appl Energy 137:511–536. https://doi.org/10.1016/j.apenergy.2014.09.081

Mahboob S, Nivetha R, Gopinath K, et al (2021) Facile synthesis of gold and platinum doped titanium oxide nanoparticles for antibacterial and photocatalytic activity: A photodynamic approach. Photodiagnosis Photodyn Ther 33:. https://doi.org/10.1016/j.pdpdt.2020.102148

Mainardis M, Ferrara C, Cantoni B, et al (2024) How to choose the best tertiary treatment for pulp and paper wastewater? Life cycle assessment and economic analysis as guidance tools. Science of the Total Environment 906:. https://doi.org/10.1016/j.scitotenv.2023.167598

Malato S, Blanco J, Richter C, et al (1997) Low-concentration CPC collectors for photocatalytic water detoxification: Comparison with a medium concentrating solar collector. In: Water Science and Technology. pp 157–164

Maniakova G, Kowalska K, Murgolo S, et al (2020) Comparison between heterogeneous and homogeneous solar driven advanced oxidation processes for urban wastewater treatment: Pharmaceuticals removal and toxicity. Sep Purif Technol 236:. https://doi.org/10.1016/j.seppur.2019.116249

Martínez-Huitle CA, Brillas E (2009) Decontamination of wastewaters containing synthetic organic dyes by electrochemical methods: A general review. Appl Catal B 87:105–145

Mau V, Quance J, Posmanik R, Gross A (2016) Phases' characteristics of poultry litter hydrothermal carbonization under a range of process parameters. Bioresour Technol 219:632–642. https://doi.org/10.1016/j.biortech.2016.08.027

Mecha AC, Onyango MS, Ochieng A, Momba MNB (2017) Ultraviolet and solar photocatalytic ozonation of municipal wastewater: Catalyst reuse, energy requirements and toxicity assessment. Chemosphere 186:669–676. https://doi.org/10.1016/j.chemosphere.2017.08.041

Mehrjouei M, Müller S, Möller D (2013) Design and characterization of a multi-phase annular falling-film reactor for water treatment using advanced oxidation processes. J Environ Manage 120:68–74. https://doi.org/10.1016/j.jenvman.2013.02.021

Mehta CM, Khunjar WO, Nguyen V, et al (2015) Technologies to recover nutrients from waste streams: A critical review. Crit Rev Environ Sci Technol 45:385–427

Merayo N, Hermosilla D, Blanco L, et al (2013) Assessing the application of advanced oxidation processes, and their combination with biological treatment, to effluents from pulp and paper industry. J Hazard Mater 262:420–427. https://doi.org/10.1016/j.jhazmat.2013.09.005

Miyawaki A, Taira S, Shiraishi F (2016) Performance of continuous stirred-tank reactors connected in series as a photocatalytic reactor system. Chemical Engineering Journal 286:594–601. https://doi.org/10.1016/j.cej.2015.11.007

Mohammed AS, El-Gendi A, El-Khatib K, Hassan SH (2021) Treatment of Textile Wastewater by Electrocoagulation Method: Case Study; Odiba Textile, Dyeing & Finishing Company. Water, Energy, Food and Environment Journal An International Journal 2:41. https://doi.org/10.18576/wefej/020105

Mohapatra T, Kumar V, Sharma M, Ghosh P (2021) Hybrid Fenton Oxidation Processes with Packed Bed or Fluidized Bed Reactor for the Treatment of Organic Pollutants in Wastewater: A Review. Environ Eng Sci 38:443–457

Monte MC, Fuente E, Blanco A, Negro C (2009) Waste management from pulp and paper production in the European Union. Waste Management 29:293–308. https://doi.org/10.1016/j.wasman.2008.02.002

Moradi V, Ahmed F, Jun MBG, et al (2019) Acid-treated Fe-doped TiO2 as a high performance photocatalyst used for degradation of phenol under visible light irradiation. J Environ Sci (China) 83:183–194. https://doi.org/10.1016/j.jes.2019.04.002

Morikawa T, Asahi R, Ohwaki T, et al (2001) Band-Gap Narrowing of Titanium Dioxide by Nitrogen Doping

Motegh M, Van Ommen JR, Appel PW, Kreutzer MT (2014) Scale-up study of a multiphase photocatalytic reactor - Degradation of cyanide in water over TiO2. Environ Sci Technol 48:1574–1581. https://doi.org/10.1021/es403378e

Mozia S, Brozek P, Przepiórski J, et al (2012) Immobilized TiO2 for phenol degradation in a pilot-scale photocatalytic reactor. J Nanomater 2012:. https://doi.org/10.1155/2012/949764

Nakata K, Fujishima A (2012) TiO 2 photocatalysis: Design and applications. Journal of Photochemistry and Photobiology C: Photochemistry Reviews 13:169–189

Navalon S, Dhakshinamoorthy A, Alvaro M, Garcia H (2011) Heterogeneous Fenton catalysts based on activated carbon and related materials. ChemSusChem 4:1712–1730

Neha, Prasad R, Singh SV (2020) A review on catalytic oxidation of soot emitted from diesel fuelled engines. J Environ Chem Eng 8:. https://doi.org/10.1016/j.jece.2020.103945

Neoh CH, Noor ZZ, Mutamim NSA, Lim CK (2016) Green technology in wastewater treatment technologies: Integration of membrane bioreactor with various wastewater treatment systems. Chemical Engineering Journal 283:582–594

Nogueira RFP, Jardim WF (1996) TiO2-FIXED-BED REACTOR FOR WATER DECONTAMINATION USING SOLAR LIGHT

Ochiai T, Fujishima A (2012) Photoelectrochemical properties of TiO2 photocatalyst and its applications for environmental purification. Journal of Photochemistry and Photobiology C: Photochemistry Reviews 13:247–262

Ogundele OD, Oyegoke DA, Anaun TE (2023) Exploring the Potential and Challenges of Electrochemical Processes for Sustainable Waste Water Remediation and Treatment. Acadlore Transactions on Geosciences 2:80–93. https://doi.org/10.56578/atg020203

Okoro HK, Orosun MM, Oriade FA, et al (2023) Potentially Toxic Elements in Pharmaceutical Industrial Effluents: A Review on Risk Assessment, Treatment, and Management for Human Health. Sustainability (Switzerland) 15

Ola O, Maroto-Valer MM (2015) Review of material design and reactor engineering on TiO2 photocatalysis for CO2 reduction. Journal of Photochemistry and Photobiology C: Photochemistry Reviews 24:16–42

Olejnik K (2011) Water Consumption in Paper Industry – Reduction Capabilities and the Consequences. In: NATO Science for Peace and Security Series C: Environmental Security. Springer Science and Business Media B.V., pp 113–129

Oliveira DVM de (2014) Evaluation of a MBBR (Moving Bed Biofilm Reactor) Pilot Plant for Treatment of Pulp and Paper Mill Wastewater. International Journal of Environmental Monitoring and Analysis 2:220. https://doi.org/10.11648/j.ijema.20140204.15

Oller I, Malato S, Sánchez-Pérez JA (2011) Combination of Advanced Oxidation Processes and biological treatments for wastewater decontamination-A review. Science of the Total Environment 409:4141–4166

Oller I, Polo-López I, Miralles-Cuevas S, et al (2014) Advanced Technologies for Emerging Contaminants Removal in Urban Wastewater. pp 145–169

Özgen S, Yildiz A (2010) Application of box-behnken design to modeling the effect of smectite content on swelling to hydrocyclone processing of bentonites with various geologic properties. Clays Clay Miner 58:431–448. https://doi.org/10.1346/CCMN.2010.0580312

P Ravichandran (2018) Biodegradability Studies on Pulp and Paper Mill Wastewater: A Review. Int J Res Appl Sci Eng Technol 6:1956–1965. https://doi.org/10.22214/ijraset.2018.4335

Pan Z, Song C, Li L, et al (2019) Membrane technology coupled with electrochemical advanced oxidation processes for organic wastewater treatment: Recent advances and future prospects. Chemical Engineering Journal 376:120909. https://doi.org/10.1016/j.cej.2019.01.188

Pang YL, Abdullah AZ (2013) Current status of textile industry wastewater management and research progress in malaysia: A review. Clean (Weinh) 41:751–764

Pareek V, Chong S, Tadé M, Adesina AA (2008) Light intensity distribution in heterogenous photocatalytic reactors. Asia-Pacific Journal of Chemical Engineering 3:171–201. https://doi.org/10.1002/apj.129

Pariente MI, Martínez F, Melero JA, et al (2008) Heterogeneous photo-Fenton oxidation of benzoic acid in water: Effect of operating conditions, reaction by-products and coupling with biological treatment. Appl Catal B 85:24–32. https://doi.org/10.1016/j.apcatb.2008.06.019

Park JA, Yang B, Park C, et al (2017) Oxidation of microcystin-LR by the Fenton process: Kinetics, degradation intermediates, water quality and toxicity assessment. Chemical Engineering Journal 309:339–348. https://doi.org/10.1016/j.cej.2016.10.083

Parra S, Malato S, Blanco J, et al (2001) Concentrating versus non-concentrating reactors for solar photocatalytic degradation of p-nitrotoluene-o-sulfonic acid

Paździor K, Bilińska L, Ledakowicz S (2019) A review of the existing and emerging technologies in the combination of AOPs and biological processes in industrial textile wastewater treatment. Chemical Engineering Journal 376:. https://doi.org/10.1016/j.cej.2018.12.057

Pérez-Estrada LA, Maldonado MI, Gernjak W, et al (2005) Decomposition of diclofenac by solar driven photocatalysis at pilot plant scale. In: Catalysis Today. pp 219–226

Pokhrel D, Viraraghavan T (2004) Treatment of pulp and paper mill wastewater - A review. Science of the Total Environment 333:37–58. https://doi.org/10.1016/j.scitotenv.2004.05.017

Prieto-Rodríguez L, Oller I, Klamerth N, et al (2013) Application of solar AOPs and ozonation for elimination of micropollutants in municipal wastewater treatment plant effluents. Water Res 47:1521–1528. https://doi.org/10.1016/j.watres.2012.11.002

Primo A, Corma A, García H (2011) Titania supported gold nanoparticles as photocatalyst. Physical Chemistry Chemical Physics 13:886–910

Prokop R, Dostál P, Prokopová Z (1997) Robust PID Control: Application to a Continuous-Stirred Tank Reactor. IFAC Proceedings Volumes 30:81–86. https://doi.org/10.1016/s1474-6670(17)41420-0

Pronina N, Klauson D, Moiseev A, et al (2015) Titanium dioxide sol–gel-coated expanded clay granules for use in photocatalytic fluidized-bed reactor. Appl Catal B 178:117–123. https://doi.org/10.1016/j.apcatb.2014.10.006

Puri S, Thakur I, Verma A, Barman S (2021) Degradation of pharmaceutical drug paracetamol via UV irradiation using Fe-TiO2 composite photocatalyst: statistical analysis and parametric

optimization. Environmental Science and Pollution Research 28:47327–47341. https://doi.org/10.1007/s11356-021-13895-6

Puri S, Verma A (2023) Potential use of foundry sand and furnace blast sand for fabrication of visibly active composite to promote circular economy/waste management for treating real agro-industrial wastewater. Water Environment Research 95:. https://doi.org/10.1002/wer.10844

Qamar M, Yoon CR, Oh HJ, et al (2008) Preparation and photocatalytic activity of nanotubes obtained from titanium dioxide. Catal Today 131:3–14. https://doi.org/10.1016/j.cattod.2007.10.015

Quereshi S, Naiya TK, Mandal A, Dutta S (2022) Residual sugarcane bagasse conversion in India: current status, technologies, and policies. Biomass Convers Biorefin 12:3687–3709

Rahim Pouran S, Abdul Aziz AR, Wan Daud WMA (2015) Review on the main advances in photo-Fenton oxidation system for recalcitrant wastewaters. Journal of Industrial and Engineering Chemistry 21:53–69

Rahimi S, Poormohammadi A, Salmani B, et al (2016) Comparing the photocatalytic process efficiency using batch and tubular reactors in removal of methylene blue dye and COD from simulated textile wastewater. Journal of Water Reuse and Desalination 6:574–582. https://doi.org/10.2166/wrd.2016.190

Rajput H, Kwon EE, Younis SA, et al (2021) Photoelectrocatalysis as a high-efficiency platform for pulping wastewater treatment and energy production. Chemical Engineering Journal 412

Rajput H, Verma A, Kaur M, et al (2016) Heterogeneous solar photo-fenton degradation of reactive black 5 using foundry sand and fly ash: value addition to waste. Journal of Environmental Engineering and Landscape Management 24:124–132. https://doi.org/10.3846/16486897.2015.1109517

Ram C, Rani P, Gebru KA, Abrha MGM (2020) Pulp and paper industry wastewater treatment: Use of microbes and their enzymes. Physical Sciences Reviews 5:. https://doi.org/10.1515/psr-2019-0050

Ramírez J, Godínez LA, Méndez M, et al (2010) Heterogeneous photo-electro-Fenton process using different iron supporting materials. J Appl Electrochem 40:1729–1736. https://doi.org/10.1007/s10800-010-0157-z

Rao NN, Chaturvedi V, Li Puma G (2012) Novel pebble bed photocatalytic reactor for solar treatment of textile wastewater. Chemical Engineering Journal 184:90–97. https://doi.org/10.1016/j.cej.2012.01.004

Rashid R, Shafiq I, Akhter P, et al A state-of-the-art review on wastewater treatment techniques: the effectiveness of adsorption method. https://doi.org/10.1007/s11356-021-12395-x/Published

Rebelo A, Ferra I, Gonçalves I, Marques AM (2014) A risk assessment model for water resources: Releases of dangerous and hazardous substances. J Environ Manage 140:51–59. https://doi.org/10.1016/j.jenvman.2014.02.025

Rey A, Quiñones DH, Álvarez PM, et al (2012) Simulated solar-light assisted photocatalytic ozonation of metoprolol over titania-coated magnetic activated carbon. Appl Catal B 111–112:246–253. https://doi.org/10.1016/j.apcatb.2011.10.005

Ribeiro JP, Marques CC, Portugal I, Nunes MI (2020) Fenton processes for AOX removal from a kraft pulp bleaching industrial wastewater: Optimisation of operating conditions and cost assessment. J Environ Chem Eng 8:. https://doi.org/10.1016/j.jece.2020.104032

Rimoldi L, Meroni D, Cappelletti G, Ardizzone S (2017) Green and low cost tetracycline degradation processes by nanometric and immobilized TiO2 systems. Catal Today 281:38–44. https://doi.org/10.1016/j.cattod.2016.08.015

Rincón AG, Pulgarin C (2007) Fe3+ and TiO2 solar-light-assisted inactivation of E. coli at field scale. Implications in solar disinfection at low temperature of large quantities of water. Catal Today 122:128–136. https://doi.org/10.1016/j.cattod.2007.01.028

Rincón GJ, la Motta EJ (2019) A fluidized-bed reactor for the photocatalytic mineralization of phenol on TiO2-coated silica gel. Heliyon 5:. https://doi.org/10.1016/j.heliyon.2019.e01966

Rodriguez-Narvaez OM, Peralta-Hernandez JM, Goonetilleke A, Bandala ER (2017) Treatment technologies for emerging contaminants in water: A review. Chemical Engineering Journal 323:361–380

Rogers JG, Cooper SJ, Norman JB (2018) Uses of industrial energy benchmarking with reference to the pulp and paper industries. Renewable and Sustainable Energy Reviews 95:23–37

Romay M, Diban N, Rivero MJ, et al (2020) Critical issues and guidelines to improve the performance of photocatalytic polymeric membranes. Catalysts 10

Ruales-Lonfat C, Barona JF, Sienkiewicz A, et al (2015) Iron oxides semiconductors are efficients for solar water disinfection: A comparison with photo-Fenton processes at neutral pH. Appl Catal B 166–167:497–508. https://doi.org/10.1016/j.apcatb.2014.12.007

Sacco O, Vaiano V, Sannino D (2020) Main parameters influencing the design of photocatalytic reactors for wastewater treatment: a mini review. Journal of Chemical Technology and Biotechnology 95:2608–2618

Saghafi S, Ebrahimi A, Mehrdadi N, Bidhendy GN (2019) Evaluation of aerobic/anaerobic industrial wastewater treatment processes: The application of multi-criteria decision analysis. Environ Prog Sustain Energy 38:. https://doi.org/10.1002/ep.13166

Saien J, Asgari M, Soleymani AR, Taghavinia N (2009) Photocatalytic decomposition of direct red 16 and kinetics analysis in a conic body packed bed reactor with nanostructure titania coated Raschig rings. Chemical Engineering Journal 151:295–301. https://doi.org/10.1016/j.cej.2009.03.011

Saran S, Arunkumar P, Devipriya SP (2018) Disinfection of roof harvested rainwater for potable purpose using pilot-scale solar photocatalytic fixed bed tubular reactor. Water Sci Technol Water Supply 18:49–59. https://doi.org/10.2166/ws.2017.097

Saraswathi R, Saseetharan MK (2012) Simultaneous optimization of multiple performance characteristics in coagulation-flocculation process for Indian paper industry wastewater. Water Science and Technology 66:1231–1238. https://doi.org/10.2166/wst.2012.304

Saravanan A, Kumar PS, Carolin CF, Sivanesan S (2017) Enhanced Adsorption Capacity of Biomass through Ultrasonication for the Removal of Toxic Cadmium Ions from Aquatic System: Temperature Influence on Isotherms and Kinetics. J Hazard Toxic Radioact Waste 21:. https://doi.org/10.1061/(asce)hz.2153-5515.0000355

Saroj S, Singh L, Singh SV (2020) Solution-combustion synthesis of anion (iodine) doped TiO2 nanoparticles for photocatalytic degradation of Direct Blue 199 dye and regeneration of used photocatalyst. J Photochem Photobiol A Chem 396:. https://doi.org/10.1016/j.jphotochem.2020.112532

Sattler C, Funken K-H, De Oliveira L, et al (2004) Paper mill wastewater detoxification by solar photocatalysis

Schneider OM, Liang R, Bragg L, et al (2019) Photocatalytic degradation of microcystins by TiO2 using UV-LED controlled periodic illumination. Catalysts 9:. https://doi.org/10.3390/catal9020181

Schwegmann H, Ruppert J, Frimmel FH (2013) Influence of the pH-value on the photocatalytic disinfection of bacteria with TiO2 - Explanation by DLVO and XDLVO theory. Water Res 47:1503–1511. https://doi.org/10.1016/j.watres.2012.11.030

Scott JP, Ollis DF Integration of Chemical and Biological Oxidation Processes for Water Treatment: Review and Recommendations

Shet A, Shetty KV (2016) Photocatalytic degradation of phenol using Ag core-TiO2 shell (Ag@TiO2) nanoparticles under UV light irradiation. Environmental Science and Pollution Research 23:20055–20064. https://doi.org/10.1007/s11356-015-5579-z

Sidhu JPS, Ahmed W, Gernjak W, et al (2013) Sewage pollution in urban stormwater runoff as evident from the widespread presence of multiple microbial and chemical source tracking markers. Science of the Total Environment 463–464:488–496. https://doi.org/10.1016/j.scitotenv.2013.06.020

Sigoillot JC, Berrin JG, Bey M, et al (2012) Fungal Strategies for Lignin Degradation. In: Advances in Botanical Research. Academic Press Inc., pp 263–308

Silva M, Baltrusaitis J (2021) Destruction of emerging organophosphate contaminants in wastewater using the heterogeneous iron-based photo-Fenton-like process. Journal of Hazardous Materials Letters 2

Sood S, Umar A, Mehta SK, Kansal SK (2015) Highly effective Fe-doped TiO2 nanoparticles photocatalysts for visible-light driven photocatalytic degradation of toxic organic compounds. J Colloid Interface Sci 450:213–223. https://doi.org/10.1016/j.jcis.2015.03.018

Sophia A. C, Lima EC (2018) Removal of emerging contaminants from the environment by adsorption. Ecotoxicol Environ Saf 150:1–17. https://doi.org/10.1016/j.ecoenv.2017.12.026

Sordo C, Van Grieken R, Marugán J, Fernández-Ibáñez P (2010) Solar photocatalytic disinfection with immobilised TiO2 at pilot-plant scale. Water Science and Technology 61:507–512. https://doi.org/10.2166/wst.2010.876

Sridhar R, Sivakumar V, Prince Immanuel V, Prakash Maran J (2011) Treatment of pulp and paper industry bleaching effluent by electrocoagulant process. J Hazard Mater 186:1495–1502. https://doi.org/10.1016/j.jhazmat.2010.12.028

Stasinakis AS, Elia I, Petalas A V., Halvadakis CP (2008) Removal of total phenols from olive-mill wastewater using an agricultural by-product, olive pomace. J Hazard Mater 160:408–413. https://doi.org/10.1016/j.jhazmat.2008.03.012

Stephan B, Ludovic L, Dominique W (2011) Modelling of a falling thin film deposited photocatalytic step reactor for water purification: Pesticide treatment. Chemical Engineering Journal 169:216–225. https://doi.org/10.1016/j.cej.2011.03.016

Su S, Xing Z, Zhang S, et al (2021) Ultrathin mesoporous g-C3N4/NH2-MIL-101(Fe) octahedron heterojunctions as efficient photo-Fenton-like system for enhanced photo-thermal effect and

promoted visible-light-driven photocatalytic performance. Appl Surf Sci 537:. https://doi.org/10.1016/j.apsusc.2020.147890

Suwanchawalit C, Wongnawa S, Sriprang P, Meanha P (2012) Enhancement of the photocatalytic performance of Ag-modified TiO 2 photocatalyst under visible light. Ceram Int 38:5201–5207. https://doi.org/10.1016/j.ceramint.2012.03.027

Tan YH, Abdullah MO, Nolasco-Hipolito C, Ahmad Zauzi NS (2017) Application of RSM and Taguchi methods for optimizing the transesterification of waste cooking oil catalyzed by solid ostrich and chicken-eggshell derived CaO. Renew Energy 114:437–447. https://doi.org/10.1016/j.renene.2017.07.024

Tanaka K, Padermpole K, Hisanaga T PHOTOCATALYTIC DEGRADATION OF COMMERCIAL AZO DYES

Tanaka Y, Ohnuma' N, Katsunami K, Ohki Y (1991) Effects of Crystallinity and Electron Mean-free-path on Dielectric Strength of Low-density Polyethylene

Tarlan E, Dilek FB, Yetis U Effectiveness of algae in the treatment of a wood-based pulp and paper industry wastewater

Taylor P, Choudhary AK, Kumar S, Sharma C (2013) Desalination and Water Treatment Removal of chloro-organics and color from pulp and paper mill wastewater by polyaluminium chloride as coagulant. Desalination Water Treat 1–12. https://doi.org/10.1080/19443994.2013.848670

Temmink H, Grolle K (2005) Tertiary activated carbon treatment of paper and board industry wastewater. Bioresour Technol 96:1683–1689. https://doi.org/10.1016/j.biortech.2004.12.035

Thakur I, Örmeci B, verma A (2020a) Inactivation of E. coli in water employing Fe-TiO2 composite incorporating in-situ dual process of photocatalysis and photo-Fenton in fixed-mode. Journal of Water Process Engineering 33:101085. https://doi.org/10.1016/j.jwpe.2019.101085

Thakur I, Örmeci B, verma A (2020b) Inactivation of E. coli in water employing Fe-TiO2 composite incorporating in-situ dual process of photocatalysis and photo-Fenton in fixed-mode. Journal of Water Process Engineering 33:. https://doi.org/10.1016/j.jwpe.2019.101085

Thakur I, Verma A, Örmeci B (2021) Fe-TiO2Composite Mediated the Hybrid Effect of Photocatalysis and Photo-Fenton for the Inactivation of Escherichia coli Using a Continuous Flow Recirculation Reactor. Ind Eng Chem Res 60:7558–7571. https://doi.org/10.1021/acs.iecr.1c00628

Thompson G, Swain J, Kay M, Forster CF The treatment of pulp and paper mill e□uent: a review

Toczyłowska-Mamińska R (2017) Limits and perspectives of pulp and paper industry wastewater treatment – A review. Renewable and Sustainable Energy Reviews 78:764–772

Tong T, Elimelech M (2016) The Global Rise of Zero Liquid Discharge for Wastewater Management: Drivers, Technologies, and Future Directions. Environ Sci Technol 50:6846–6855

Tribe MA, Alpine RLW (1986) SCALE ECONOMIES AND THE "'0.6 RULE"

Tumuluri A, Naidu KL, Raju KCJ (2014) Band gap determination using Tauc ' s plot for LiNbO 3 thin films. 6:3353–3356

ul Pala seg, Tokat E (2002) Color removal from cotton textile industry wastewater in an activated sludge system with various additives

Veluchamy C, Kalamdhad AS (2017) Influence of pretreatment techniques on anaerobic digestion of pulp and paper mill sludge: A review. Bioresour Technol 245:1206–1219

Verma S, Kumar P, Lavrenčič Štangar U (2023) A Perspective on Removal of Cyanotoxins from Water Through Advanced Oxidation Processes. Global Challenges 7:. https://doi.org/10.1002/gch2.202300125

Wallender EK, Ailes EC, Yoder JS, et al (2014) Contributing Factors to Disease Outbreaks Associated with Untreated Groundwater. Groundwater 52:886–897. https://doi.org/10.1111/gwat.12121

Wang B, Gu L, Ma H (2007) Electrochemical oxidation of pulp and paper making wastewater assisted by transition metal modified kaolin. J Hazard Mater 143:198–205. https://doi.org/10.1016/j.jhazmat.2006.09.013

Wang J, Chen H (2020) Catalytic ozonation for water and wastewater treatment: Recent advances and perspective. Science of the Total Environment 704:135249. https://doi.org/10.1016/j.scitotenv.2019.135249

Wang P, Zhou T, Wang R, Lim TT (2011) Carbon-sensitized and nitrogen-doped TiO2 for photocatalytic degradation of sulfanilamide under visible-light irradiation. Water Res 45:5015–5026. https://doi.org/10.1016/j.watres.2011.07.002

Yabalak E, Gizir AM (2020) Treatment of agrochemical wastewater by subcritical water oxidation method: chemical composition and ion analysis of treated and untreated samples. J Environ Sci Health A Tox Hazard Subst Environ Eng 55:1424–1435. https://doi.org/10.1080/10934529.2020.1805249

Yang S, Guo X, Wang Z, et al (2019) Significance of B-site cobalt on bisphenol A degradation by MOFs-templated CoxFe3−xO4 catalysts and its severe attenuation by excessive cobalt-rich phase. Chemical Engineering Journal 359:552–563. https://doi.org/10.1016/j.cej.2018.11.187

Yang X, Cao C, Erickson L, et al (2009) Photo-catalytic degradation of Rhodamine B on C-, S-, N-, and Fe-doped TiO2 under visible-light irradiation. Appl Catal B 91:657–662. https://doi.org/10.1016/j.apcatb.2009.07.006

Yoon M, Oh Y, Hong S, et al (2017) Synergistically enhanced photocatalytic activity of graphitic carbon nitride and WO3 nanohybrids mediated by photo-Fenton reaction and H2O2. Appl Catal B 206:263–270. https://doi.org/10.1016/j.apcatb.2017.01.038

Younger PL, Wolkersdorfer C Mining Impacts on the Fresh Water Environment: Technical and Managerial Guidelines for Catchment Scale Management ERMITE-Consortium

Yousefi M, Gholami M, Oskoei V, et al (2021) Comparison of LSSVM and RSM in simulating the removal of ciprofloxacin from aqueous solutions using magnetization of functionalized multi-walled carbon nanotubes: Process optimization using GA and RSM techniques. J Environ Chem Eng 9:. https://doi.org/10.1016/j.jece.2021.105677

Yu D, Li L, Wu M, Crittenden JC (2019) Enhanced photocatalytic ozonation of organic pollutants using an iron-based metal-organic framework. Appl Catal B 251:66–75. https://doi.org/10.1016/j.apcatb.2019.03.050

Yu X, Somoza-Tornos A, Graells M, Pérez-Moya M (2020) An experimental approach to the optimization of the dosage of hydrogen peroxide for Fenton and photo-Fenton processes. Science of the Total Environment 743:. https://doi.org/10.1016/j.scitotenv.2020.140402

Yuliani G, Agustiningsih R, Munawaroh HSH, Rahmi NF (2018) The use of coagulation-uv irradiation/h2o2 and electrocoagulation methods on pulp and paper mill wastewater treatment. Solid State Phenomena 280 SSP:393–398. https://doi.org/10.4028/www.scientific.net/SSP.280.393

Zayani G, Bousselmi L, Mhenni F, Ghrabi A (2009) Solar photocatalytic degradation of commercial textile azo dyes: Performance of pilot plant scale thin film fixed-bed reactor. Desalination 246:344–352. https://doi.org/10.1016/j.desal.2008.03.059

Zhang B, He X, Yu C, et al (2022) Degradation of tetracycline hydrochloride by ultrafine TiO2 nanoparticles modified g-C3N4 heterojunction photocatalyst: Influencing factors, products and mechanism insight. Chinese Chemical Letters 33:1337–1342. https://doi.org/10.1016/j.cclet.2021.08.008

Zhang S, Zhang J, Sun J, Tang Z (2020a) Capillary microphotoreactor packed with TiO2-coated glass beads: An efficient tool for photocatalytic reaction. Chemical Engineering and Processing - Process Intensification 147:. https://doi.org/10.1016/j.cep.2019.107746

Zhang S, Zhang J, Sun J, Tang Z (2020b) Capillary microphotoreactor packed with TiO2-coated glass beads: An efficient tool for photocatalytic reaction. Chemical Engineering and Processing - Process Intensification 147:. https://doi.org/10.1016/j.cep.2019.107746

Zhang T, Wang X, Zhang X (2014) Recent progress in TiO2-mediated solar photocatalysis for industrial wastewater treatment. International Journal of Photoenergy 2014

Zhang W, Liu Y, Yu B, et al (2015) Effects of silver substrates on the visible light photocatalytic activities of copper-doped titanium dioxide thin films. Mater Sci Semicond Process 30:527–534. https://doi.org/10.1016/j.mssp.2014.10.030

Zhang Y (2020) Wet Oxidation Technology Based on Organic Wastewater Treatment. In: Journal of Physics: Conference Series. Institute of Physics Publishing

Zhao W, Ma W, Chen C, et al (2004) Efficient Degradation of Toxic Organic Pollutants with Ni2O 3/TiO2-xBx under Visible Irradiation. J Am Chem Soc 126:4782–4783. https://doi.org/10.1021/ja0396753

Zhu J, Zheng W, He B, et al (2004) Characterization of Fe-TiO2 photocatalysts synthesized by hydrothermal method and their photocatalytic reactivity for photodegradation of XRG dye diluted in water. J Mol Catal A Chem 216:35–43. https://doi.org/10.1016/j.molcata.2004.01.008

Zhu Q, Hinkle M, Kim DJ, Kim JH (2021) Modular Hydrogen Peroxide Electrosynthesis Cell with Anthraquinone-Modified Polyaniline Electrocatalyst. ACS ES and T Engineering 1:446–455. https://doi.org/10.1021/acsestengg.0c00173

LIST OF CONTRIBUTIONS

Published Articles

- **Puri, S.**, & Verma, A. (2022). Color removal from secondary treated pulp & paper industry effluent using waste-driven Fe–TiO_2 composite. ***Chemosphere*****, 135143.**

  (Indexed in SCI, Impact factor- 8.8)

- **Puri, S.**, & Verma, A. (2023). Potential use of Foundry sand and Furnace blast sand for fabrication of visibly active composite to promote circular economy/waste management for treating real agro-industrial wastewater. ***Water Environment Research*****, e10844. (Indexed in SCI, Impact factor- 3.1)**

- **Puri, S**., & Verma, A. (2023). Detoxification of real Pulp and Paper industry wastewater via sunlight assisted dual technology employing waste driven composite: A parametric optimization and statistical analysis. ***Water, Air, and Soil pollution*** **(Indexed in SCI, Impact factor- 2.9)**

Submitted Articles

- **Puri, S.,** & Verma, A. (2024). Synergistic Application of Fe-TiO_2 Composite-based Dual Photocatalysis and Photo-Fenton for Sustainable Remediation of Color-impacting Streams in the Pulp and Paper Industry. ***Journal of Water Environmental Management***

Articles with multiple authors

- **S. Puri**, I. Thakur, A. Verma, & S. Barman (2021). Degradation of pharmaceutical drug paracetamol via UV irradiation using Fe-TiO_2 composite photocatalyst: statistical analysis and parametric optimization. ***Environmental Science and Pollution Research, 1-15*****. (I. F.: 5.8 Springer)**

Conference Presentations

- Participated in Oral Presentation in international conference on "**Advances and Innovations in Recycling Engineering"** (AIR2021), held at UPES, Dehradun on October 21-22,2021